



Advancement of covalent and noncovalent nitroxide spin-labeling of RNA

Subham Saha



**Faculty of Physical Sciences
School of Engineering and Natural Sciences
University of Iceland
2017**

Advancement of covalent and noncovalent nitroxide spin-labeling of RNA

Subham Saha

Dissertation submitted in partial fulfillment of a
Philosophiae Doctor degree in Chemistry

Advisor

Prof. Snorri Th. Sigurdsson

PhD Committee

Prof. Guðmundur G. Haraldsson

Dr. Stefán Jónsson

Opponents

Prof. Ronald Micura

Prof. Poul Nielsen

Faculty of Physical Sciences
School of Engineering and Natural Sciences
University of Iceland
Reykjavík, June 2017

Advancement of covalent and noncovalent nitroxide spin-labeling of RNA

Dissertation submitted in partial fulfillment of a *Philosophiae Doctor* degree in Chemistry

Copyright © 2017 Subham Saha
All rights reserved

Faculty of Physical Sciences
School of Engineering and Natural Sciences
University of Iceland
Dunhagi 3
107 Reykjavik
Iceland

Telephone: 525 4000

Bibliographic information:

Subham Saha, 2017, *Advancement of covalent and noncovalent nitroxide spin-labeling of RNA*, PhD dissertation, Faculty of Physical Sciences, University of Iceland.

Printing: Háskólaprent Ehf.
Reykjavík, Iceland, June 2017

Abstract

Electron paramagnetic resonance (EPR) spectroscopy is routinely used to study the structure and dynamics of nucleic acids, to obtain information about their functions. A prerequisite for most EPR studies of nucleic acids is the incorporation of paramagnetic centers called “spin labels” at specific positions and this technique is known as site-directed spin-labeling (SDSL).

This doctoral dissertation describes the development of two new methods of site-directed spin-labeling of RNA, the first of which focuses on utilizing noncovalent interactions between an RNA aptamer and a ligand connected to a paramagnetic spin label. The malachite green (MG) aptamer is known to bind to dyestuffs MG and tetramethylrosamine (TMR). In this study, spin-labeled derivatives of MG and TMR were prepared and their binding affinity to the aptamer was investigated by using EPR spectroscopy. A pyrrolidine-based nitroxide derivative of TMR was found to bind completely to the aptamer at 25 °C with a dissociation constant (KD) of 66 nM, as determined by fluorescence titration studies. This spin-labeling approach is the first example of noncovalent and site-directed spin-labeling that involves a native (unmodified) RNA. Pulsed electron-electron double resonance (PELDOR) was used to measure a distance of 3.3 nm between the spin-labeled ligand and an isoindoline-based spin label that was covalently attached to the aptamer. In a related study, the noncovalent binding of a new class of benzimidazole-fused isoindoline nitroxides to bind to abasic sites in duplex DNA and RNA was explored. Five spin-labeled nitroxides were screened using an in-house devised “combinatorial approach”, out of which binding affinity of two spin labels were studied in detail.

A post-synthetic spin-labeling approach was also developed, where a nucleophilic 2'-amino group in RNA was reacted with two aromatic isoindoline nitroxides having an isothiocyanate modification, thereby forming a thiourea bond upon conjugation to RNA. The isothiocyanate spin-labels were found to have a minor effect on RNA duplex stability. Furthermore, they showed limited mobility after incorporation into RNA, as judged by continuous wave EPR, which enhances their usefulness for distance measurement studies using pulsed-EPR techniques. A tetraethyl isoindoline derivative was found to be substantially resistant towards reduction by ascorbic acid, which makes this label a promising candidate to perform in-cell distance measurements using PELDOR.

Útdráttur

Rafeindasegullitrófsgreiningu (e. electron paramagnetic resonance (EPR) spectroscopy) er beitt reglubundið í rannsóknum á byggingu og hreyfingu kjarnsýra, til að varpa ljósi á starfsemi þeirra og hlutverk. EPR rannsóknir á kjarnsýrum krefjast innleiðingar meðseglandi kjarna (spunamerkja) á ákveðinn stað, en sú aðferð kallast staðbundin spunamerking (e. site-directed spin-labeling, SDSL).

Þessi doktorsritgerð lýsir þróun tveggja nýrra aðferða til staðbundinnar spunamerkingar á ribósakjarnsýrum (e. ribonucleic acid, RNA). Fyrri aðferðin byggir á myndun ósamgildra tengja milli RNA aptamers og tengils sem ber spunamerki. Malachite green (MG) aptamerinn er þekktur fyrir að bindast litarefnunum MG og tetrametýlrósamíni (TMR). Smíðaðar voru spunamerktar afleiður af MG og TMR og bindisækni þeirra í aptamerinn rannsökuð með EPR. Flúrljómunarmælingar við 25 °C sýndu að TMR-afleitt pyrrólídín nítroxíð bast að fullu við aptamerinn, með klofningsfastann (KD) 66 nM. Þessi spunamerkingaraðferð er fyrsta dæmið um staðbundna spunamerkingu á óbreyttu RNA. PELDOR (e. pulsed electron-electron double resonance) var notað til þess að mæla 3,3 nm fjarlægð á milli spuna-merkta tengilsins og ísóindólín-afleidds spunamerks, sem bundið var samgildum tengjum við aptamerinn. Í tengdri rannsókn var bindisækni bensímídasól-ísóindólín nítroxíða í basalaust kirni í tvístrendu DNA og RNA rannsökuð. Tenging fimm nítroxíða var rannsökuð með skimun á bindisækni þeirra í blöndu af DNA og RNA tvístrendingum. Bindisækni tveggja þeirra var svo rannsökuð nánar.

Einnig var þróuð aðferð til að spunamerkja RNA eftir smíði þess (e. post-synthetic spin labeling), þar sem kjarnsækinn 2'-amínó hópur á RNA var hvarfaður við tvö arómatísk ísóindólín nítroxíð sem innihéldu ísóþíósýanat virkniþóp og mynda því þíóúrea tengi við RNA. Þessi nýju spunamerki hafa lítil áhrif á stöðugleika RNA tvístrendinga. Ennfremur sýndi EPR greining að þessi spunamerki höfðu takmarkaðan hreyfanleika eftir innleiðingu í RNA, sem eykur notagildi þeirra til fjarlægðamælinga með PELDOR. Tetraetýlísóindólínafleiðan var fremur stöðug í viðurvist askorbínsýru sem lofar góðu fyrir notkun þess sem spunamerkis með EPR mælingum í frumum.

Table of Contents

List of Figures	vii
List of Schemes.....	x
List of Tables	xi
List of Original Publications	xiii
Abbreviations.....	xv
Acknowledgements.....	xvii
1 Objective and Scope of the PhD Thesis	1
2 Introduction	3
2.1 Techniques for Structure Determination of Nucleic Acids	4
2.2 EPR Spectroscopy	5
2.3 Site-Directed Spin-Labeling (SDSL).....	7
2.3.1 The Phosphoramidite Approach	8
2.3.2 The Post-Synthetic Spin-Labeling Approach.....	9
2.3.3 The Noncovalent Spin-Labeling Approach	9
3 Noncovalent Spin-Labeling of Unmodified RNA: The Aptamer Approach	13
3.1 Nucleic Acid Aptamers	13
3.1.1 The Malachite Green Aptamer.....	15
3.2 Design of Spin Labels for the MG Aptamer	17
3.2.1 Synthesis of Spin-Labeled Derivatives of Malachite Green.....	19
3.2.2 EPR Studies of the Binding of MG-derivatives with the Aptamer.....	20
3.2.3 Spin-Labeled Derivatives of Tetramethylrosamine (TMR).....	22
3.2.4 Synthesis of Spin-Labeled Derivatives of Tetramethylrosamine	23
3.2.5 EPR Studies for the Binding of TMR-Derived Spin Labels.....	24
3.2.6 Determination of Dissociation Constants (K_D) for 26 , 27 and 28 by Fluorescence Titration.....	26
3.3 Distance Measurements by PELDOR on the Malachite Green Aptamer	28
3.4 Conclusion.....	30

4 Noncovalent Spin-Labeling with Benzimidazole-Isoindoline Nitroxides	31
4.1 Introduction	31
4.2 Results and Discussion	32
4.2.1 Synthesis of the Benzimidazole-Based Isoindoline Nitroxides	32
4.2.2 The “Combinatorial Approach” for Screening Promising Candidates	33
4.2.3 Binding Studies of Nitroxides 35 and 36 using EPR spectroscopy	34
4.3 Conclusion	36
5 Post-Synthetic Spin-Labeling of 2'-Amino Groups in RNA with Aromatic Isoindolines	37
5.1 Background	37
5.2 Spin-Labeling at 2'-Amino Position Using Aromatic Isothiocyanates	38
5.2.1 Stability of the Spin Labels 51 and 52 in Reducing Environment	43
5.3 Conclusion	45
6 Conclusions.....	47
References	49
Publications	57
Paper I	139
Paper II.....	171
Paper III	193
Paper IV	213

List of Figures

- Figure 2.1.** (A) A piperidine-based nitroxide radical TEMPO ((2,2,6,6-Tetramethylpiperidin-1-yl)oxyl). (B) CW-EPR spectrum of a nitroxide radical.....6
- Figure 2.2.** Strategies for site-directed spin labeling (SDSL). (A) The “classical” phosphoramidite approach. (B) Post-synthetic spin-labeling. (C) Noncovalent spin-labeling. A pyrrolidine-based spin label has been used to represent a nitroxide spin label. Nucleotides are represented by links that form oligonucleotide chains.^[62] This figure has been reproduced with permission from *Methods Enzymol.*, **2015**, 563, 397-414.7
- Figure 2.3.** A phosphoramidite building block for an RNA oligonucleotide. PG is a protecting group for the 2'-hydroxy group and B is a nucleobase.8
- Figure 2.4.** (A) Structure of ζ and its base-pairing scheme with guanine (G) (left) and an abasic site in DNA (right). (B) A molecular model of the noncovalent spin-labeling approach based on the nitroxide ζ (bold) and a duplex DNA (light) containing an abasic site. The EPR spectra shown are of the unbound spin label (left) and of the bound spin label (right) in duplex DNA containing an abasic site at $-30\text{ }^{\circ}\text{C}$. This figure has been reproduced with permission from *Eur. J. Org. Chem.*, **2012**, 2291-2301.10
- Figure 2.5.** (A) Structure of \hat{G} (B) CW EPR data of \hat{G} (left) and \hat{G} bound to a RNA duplex containing an abasic site at $-20\text{ }^{\circ}\text{C}$ (right).....11
- Figure 3.1.** A general scheme for the systematic evolution of ligands by exponential (SELEX) enrichment process. Figure courtesy of Integrated DNA Technologies Inc.14
- Figure 3.2.** Structures of dyes that are known to bind to the MG aptamer.15
- Figure 3.3.** (A) Secondary structure of the RNA aptamer-TMR complex showing the position of the ligand in red, (B) X-ray structure of TMR (red) bound to the aptamer (grey).....16
- Figure 3.4.** Arrows indicating possible sites of modifications in MG **1**. Structures and dissociation constants (K_D) of m-methoxy derivative of TMR **5**, p-methoxy derivative of TMR **6**, MG substituted by long-chain alkyl groups in both the meta- and para-positions **7**, 4-methoxystyryl derivatives of MG at para-position **8** and meta-position **9**.17
- Figure 3.5.** (A) A molecular model of the crystal structure of the MG aptamer bound to TMR, showing possible sites of modifications in TMR. (B) A piperidine-

based acetylene-linked nitroxide (10) and spin-labeled derivatives of malachite green (11 , 12 and 13) that were planned to be synthesized.	18
Figure 3.6. Attack of a hydroxide ion into the central carbon of MG to form colorless MG-OH.	21
Figure 3.7. EPR data for the isoindoline-derived MG 13 bound to the aptamer (left column), mutant RNA (middle column) and without any RNA (right column). EPR spectra were recorded as a function of temperature. All data were recorded in 10 mM phosphate, 100 mM NaCl, 0.1 mM Na ₂ EDTA, pH 7.0.	22
Figure 3.8. Spin-labeled derivatives of tetramethylrosamine that were proposed to be synthesized.	23
Figure 3.9. EPR data of the spin labels 26 , 27 and 28 without any RNA (left), when bound to the MG aptamer (centre) and mutant RNA (right, negative control). All data were recorded at +20 °C in 10 mM phosphate, 100 mM NaCl, 0.1 mM Na ₂ EDTA, pH 7.0.	25
Figure 3.10. EPR data for the spin-labeled TMR 27 bound to the aptamer (left column), control RNA (middle column) and without any RNA (right column). EPR spectra were recorded as a function of temperature. All data were recorded in 10 mM phosphate, 100 mM NaCl, 0.1 mM Na ₂ EDTA, pH 7.0.	26
Figure 3.11. Dissociation constants (K_D) by fluorescence titration for the TMR-derived spin labels (A) 27 , $K_D = 66$ nM, (B) 28 , $K_D = 95$ nM and (C) 26 , $K_D = 101$ nM. θ denotes the fraction of ligand binding sites in the aptamer that are occupied by the spin label, the dotted line indicates the experimentally obtained data points and the solid line represents the fitted curve. Data were recorded in 10 mM phosphate, 100 mM NaCl, 0.1 mM Na ₂ EDTA, pH 7.0 at 20 °C.	27
Figure 3.12. (A) Secondary structure of the malachite green aptamer bound to TMR (red) showing the position of covalently modified U36 (blue) with a 2'-amino uridine. (B) A molecular model showing the positions of the two spin labels (covalent label: blue, TMR core: red, pyrrolidine nitroxide modification on TMR: green); the structure of the covalently attached label is shown (blue) in a box. (C) PELDOR data with the time trace and distance distribution (inset) indicating a mean inter-spin distance of 3.3 nm (33 Å).	29
Figure 4.1. Structures of the benzimidazole-based isoindoline nitroxides 35 , 36 , 37 , 38 and 39 that were analyzed in this investigation.	32
Figure 4.2. DNA and RNA duplex sequences and EPR data for nitroxides 35 , 36 , 37 , 38 and 39 screened as per the "combinatorial approach". All data were recorded at -10 °C. Binding studies were performed in phosphate buffer (10 mM phosphate, 100 mM NaCl, 0.1 mM Na ₂ EDTA, pH = 7.0) containing 2% DMSO and 30% ethylene glycol.	34

Figure 4.3. (a) DNA and RNA duplexes used for EPR binding studies where “_” denotes an abasic site and X the complementary base. The EPR spectra show the extent of binding of 35 and 36 to duplex DNA (b) and RNA (c), respectively. Letters above each spectrum denote the base opposite to the abasic site. For unmodified duplexes, “_” and X stand for C and G, respectively. Binding studies were performed in phosphate buffer (10 mM phosphate, 100 mM NaCl, 0.1 mM Na ₂ EDTA, pH = 7.0) containing 2% DMSO and 30% ethylene glycol at -30 °C. The red arrow indicates the slow moving (bound) component and the circle shows signs of aggregation.....	35
Figure 5.1. Time-courses of spin-labeling reactions of RNA IX with (A) 51 and (B) 52	40
Figure 5.2. DPAGE analysis showing the different time-points of sample collection of reaction of isothiocyanate 51 with the unmodified oligonucleotide XII (5'-GAC CUC GUA UCG UG). Lane B contains spin-labeled RNA X and lane A is a mixture of the spin-labeled RNA X and an aliquot after running the reaction for 48 h.	40
Figure 5.3. EPR spectra of the spin-labeled oligonucleotides in phosphate buffer, recorded at 10 °C.....	42
Figure 5.4. Molecular models of the RNA duplex 51 (grey) shown in entirety (A) and as close-ups from two different dimensions (B) and (C). Conjugated spin label 51 has been shown in red except for the sulfur atom that has been colored yellow.....	43
Figure 5.5. Ascorbate reduction data for RNA duplexes labeled with spin labels 45 (circle), 51 (triangle) and 52 (square) in 5 mM ascorbic acid, 10 mM phosphate, 100 mM NaCl, 0.1 mM Na ₂ EDTA, pH 7.0. Inset shows a longer time course (12 h) for duplex containing 52	44

List of Schemes

Scheme 3.1. Synthetic scheme used to obtain the meta- and para-substituted spin-labeled malachite greens 11 and 12 , respectively.....	19
Scheme 3.2. Synthetic scheme used to obtain the isoindoline-based spin-labeled derivative of MG (13).	20
Scheme 3.3. Synthetic scheme for synthesizing the spin-labeled derivatives of TMR 26 , 27 and 28	24
Scheme 3.4. An in-house developed post-synthetic spin labeling scheme used to covalently label the malachite green aptamer for inter-spin distance measurement studies using PELDOR.....	28
Scheme 4.1. Synthetic scheme for obtaining benzimidazole-based isoindoline nitroxide 35 . The syntheses were carried out by Dr. Kye-Simeon Masters' research group based at the Queensland University of Technology, Brisbane, Australia.....	32
Scheme 5.1. Spin-labeling of 2'-amino position in RNA by amide modification 48 (lower), and by urea modification 46 (higher).....	38
Scheme 5.2. Preparation of spin-labeling reagents 51 and 52 from their respective precursors 49 and 50 , respectively (performed by Dr. Anil P. Jagtap); and their reaction with the 2'-amino modified RNA oligonucleotide IX [5'-GAC CUC G(2'-NH ₂ U)A UCG UG] to yield spin-labeled oligonucleotides X and XI	39

List of Tables

Table 5.1. RNA duplexes prepared for in-cell PELDOR measurements. Nucleotides in blue indicate overhangs that were introduced to prevent end-to-end stacking of the duplexes, X represents uridine labeled post-synthetically with tetraethyl isothiocyanate 52	45
---	----

List of Original Publications

- I. Benjamin A Chalmers, Subham Saha, Tri Nguyen, John McMurtrie, Snorri Th Sigurdsson, Steven E Bottle, and Kye-Simeon Masters. "TMIO-PyrImid Hybrids Are Profluorescent, Site-Directed Spin Labels for Nucleic Acids", *Org. Lett.* (2014), 16 (21), 5528-31.
- II. Subham Saha, Anil P Jagtap, and Snorri Th Sigurdsson. "Site-Directed Spin Labeling of 2'-Amino Groups in RNA with Isoindoline Nitroxides That Are Resistant to Reduction", *Chem. Commun.* (2015), 51 (66), 13142-45.
- III. Subham Saha, Anil P Jagtap, and Snorri Th Sigurdsson. "Chapter Fifteen-Site-Directed Spin Labeling of RNA by Postsynthetic Modification of 2'-Amino Groups." (Editors: Peter Z. Qin and Kurt Warncke), *Methods Enzymol.* (2015), 563, 397-414.
- IV. Subham Saha, Thilo Hetzke, Thomas F Prisner and Snorri Th Sigurdsson. "Noncovalent Spin-Labeling of Unmodified RNA: The Aptamer Approach", (*Manuscript in preparation*).

Abbreviations

A	adenine
<i>m</i> -CPBA	<i>meta</i> -chloroperbenzoic acid
C	cytosine
CD	circular dichroism
CW	continuous wave
DEER	double electron-electron resonance
DMF	<i>N,N</i> -dimethylformamide
DMSO	dimethylsulfoxide
DNA	deoxyribonucleic acid
DPAGE	denatured polyacrylamide gel electrophoresis
EDTA	ethylenediaminetetracarboxylic acid
EPR	electron paramagnetic resonance
ESR	electron spin resonance
FRET	förster resonance energy transfer
G	guanine
K_D	dissociation constant
kDa	kilodalton
MALDI-TOF	matrix-assisted laser desorption/ionization-time of flight
MG	malachite green
PELDOR	pulsed electron-electron double resonance
ppm	parts per million
RNA	ribonucleic acid
SDSL	site-directed spin labeling
SELEX	systematic evolution of ligands by exponential enrichment
T	thymine
TEMPO	(2,2,6,6-tetramethylpiperidin-1-yl)oxy
TLC	thin layer chromatography
T_M	melting temperature
TMR	tetramethylrosamine
U	uracil

Acknowledgements

The Almighty has been very kind to me because never did I imagine during my growing up years that eventually, I would be one of the privileged few that get an opportunity to write the final dissertation for a PhD degree. The one person whom I shall remain forever indebted to, without whom this day would never have come in my life, is my doctoral supervisor Prof. Snorri. Th. Sigurdsson. I thank him wholeheartedly for offering me this once-in-a-lifetime opportunity to be a part his research group which has been a tremendously enriching professional and personal experience. I truly appreciate his scientific acumen and his impeccable problem-solving abilities. I thank him for training me to stay composed during pressurized and demanding situations. He has been extremely generous to me over the years, at times going beyond his professional capacity. I will feel myself utmost fortunate if I manage to imbibe even a fraction of his qualities as a researcher.

I take this opportunity to thank my doctoral committee members, Prof. Guðmundur G. Haraldsson and Dr. Stefán Jónsson for scrutinizing my work and finding me worthy of this doctorate degree. I would also like to thank my distinguished opponents, Prof. Ronald Micura and Prof. Poul Nielsen for kindly willing to review this dissertation and my work.

This work would not have been possible without the help of my international collaborators, Dr. Kye-Simeon Masters, Markus Gränz, Thilo Hetzke, Nicole Erlenbach, Dr. Alberto Collauto, Dr. Burkhard Endeward and Prof. Thomas Prisner. Also, I am highly grateful to Dr. Anil Jagtap for a fruitful in-house collaboration.

I would like to thank the present members of the Sigurdsson research group, Dr. Anil Jagtap, Nilesh Kamble, Sucharita Mandal, Haraldur Y. Júlíusson and Anna-Lena Johanna Segler, for their friendship and support. Also, I am thankful to the past members, Dr. Sandip Shelke, Dr. Kristmann Gíslason, Dr. Dnyaneshwar Gophane, Dr. Marco Körner, Gunnar Sandholt, Snaedis Björgvinsdóttir and Hörður Kári Harðarson. Very special thanks to Dr. Nitin Kunjir who has helped me immensely during my initial days in Iceland.

My sincere thanks go to all my friends and professors at Raunvísindastofnun with special gratitude to Kristinn Ragnar Óskarsson for teaching me CD and fluorescence spectroscopic techniques. Thanks to my compatriots at the university, Prof. Krishna Kumar

Damodaran, Dipankar Ghosh, Ragesh Kumar and former members Dr. Vivek Gaware and Dr. Erika Das. My sincere thanks also go to the office staff and support staff at Raunvísindastofnun. I am highly grateful to the University of Iceland Research Fund and Prof. Sigurdsson, once again, for financial assistance. I would also like to thank the Student Housing for allowing me to have a very comfortable stay over the years.

I am also indebted to my former mentors, Dr. Ajay Soni and Prof. Sampak Samanta for inspiring me to pursue a doctoral degree. My friends during my work experience in the industry, Dr. Appaso Jadhav, Dr. Vinayak Pagar, Rakesh Patil and Dr. Sabir Ahammed have also played major roles in driving my inclination towards pursuing doctoral studies. I convey my deepest thanks to my best friend Sumeet Anand for advising me to opt for organic chemistry during our undergraduate days at college.

My biggest strength has been my parents, who have always believed in me, despite my numerous flaws and failures. I have no words to thank them for everything that they have done for me, even going beyond their capabilities, just to see this day when their son would make them proud. I am indebted for their patience and endless wait, despite turning old over the years, just to see me hold a PhD. Also, I profusely thank my brother, Rupam, and his wife, Ria, for inspiring me on a daily basis and to carry on during the toughest of times. I also thank my parents-in-law for their patience and for believing in me by entrusting me with their daughter. I would like to convey a very special 'thank you' to my nonagenarian grandmother, who bought me hundreds of books during my childhood days, which inculcated my reading habit. Biggest inspiration has come from my late grandfather, who has been my greatest teacher, philosopher and guide; the person who always believed that education comes before everything else and who would have been the happiest person if he were alive today.

Most importantly, the person that I am most thankful to is my wife, Bristi, who has been my biggest pillar of support during the past years. I have no words to thank her for standing by my side during all highs and lows, for her unconditional love and support, especially during my sleepless nights, long evenings and weekends in the lab. It fills my heart with guilt to realize that she sacrificed her own promising career just to make sure that I complete my degree successfully. I am blessed to have her in my life and I dedicate this degree to my wife because she is the one that deserves this honor more than me, and more than anyone else.

*Dedicated to
my wife, Bristi,
my parents,
and my late grandfather*

1 Objective and Scope of the PhD Thesis

To understand functions of biopolymers, it is essential to investigate their structure and dynamics. In this regard, electron paramagnetic resonance (EPR) spectroscopy has emerged as a valuable technique that is routinely used to study structure and dynamics of nucleic acids. A prerequisite for most EPR studies of nucleic acids is the technique of incorporation of paramagnetic entities called “spin labels” at chosen positions, known as site-directed spin labeling (SDSL). Although several methods of SDSL have been already developed, most of them are tedious and involve substantial effort. Therefore, it is of interest to develop simpler approaches for SDSL.

This doctoral dissertation is primarily based on development of two new methods of spin-labeling of nucleic acids. The first, delineated in **Chapter 3**, focuses on utilizing noncovalent interactions between an RNA and a paramagnetic spin label. Moreover, **Chapter 4** deals with further investigation of an already established noncovalent spin-labeling approach which involves spin labels that bind noncovalently to abasic sites in duplex nucleic acids. The other newly-developed method, described in **Chapter 5**, is based on the development of a post-synthetic spin-labeling strategy where the RNA and the paramagnetic spin label are connected covalently.

The noncovalent spin-labeling approach described in **Chapter 3** utilizes an RNA aptamer which is known to bind to small molecule dyes of the malachite green family. The basic concept of this strategy relies on modifying the dyes paramagnetically and allowing them to bind to the RNA aptamer, thereby forming an RNA-ligand complex that involves a noncovalent association and possesses properties that permit investigation using EPR spectroscopy. This noncovalent spin-labeling approach is the first example of spin-labeling where a completely unmodified RNA has been used. Moreover, once the spin label has been prepared, this method potentially becomes an effortless “mix and measure” approach which can be used by researchers that require highly simplified spin-labeling techniques. Also, this method presents the first example of noncovalent spin-labeling where the spin-labeled ligand binds to the nucleic acid at room temperature, thereby enhancing the practical usability of this

approach. Additionally, in collaboration with Prof. Thomas Prisner at Goethe University in Frankfurt, Germany; distance measurement between the spin-labeled ligand and a spin label that was covalently linked to the aptamer was carried out. It can be speculated that this approach of spin-labeling has the potential to be very useful in the future to spin-label long RNAs that are predominantly prepared by enzymatic methods.

In a related study, delineated in **Chapter 4**, the approach of noncovalent spin-labeling was further explored where a new class of benzimidazole-isoindoline nitroxides was evaluated as spin labels that were found to bind to abasic sites in duplex DNA and RNA. This project was run in collaboration with Dr. Kye-Simeon Masters based at Queensland University of Technology, Brisbane, Australia. In this study, binding of two spin labels were studied in detail that displayed enhanced binding affinity to abasic sites, albeit at low temperatures.

Finally, **Chapter 5** describes another new approach for spin-labeling that was developed during the course of this doctoral study. This technique was based on a post-synthetic spin-labeling strategy. In this approach, nucleophilic 2'-amino groups in RNA were reacted with two aromatic isoindoline nitroxides having an isothiocyanate modification to form a rigid thiourea linkage between the RNA and the spin labels. The aromatic isothiocyanate spin labels were synthesized by Dr. Anil P. Jagtap in the Sigurdsson group. This new method is perhaps the quickest method of covalent spin-labeling, where spin-labeled RNAs can potentially be obtained in just a few hours. Moreover, the isothiocyanate spin-labels were found to have limited mobility in the RNA that would render them as interesting and useful candidates for measurements of distance and orientation using pulsed-EPR studies. Also, one of the spin labels was found to be highly resistant towards reduction, which makes this label a very promising candidate to perform in-cell distance measurement experiments.

2 Introduction

Nucleic acids belong to the category of biomolecules that play major roles in sustaining all forms of life. Delving into history, it was the Swiss scientist Friedrich Miescher who isolated a few unknown phosphate-rich chemicals way back in 1869 and named them “nucleons”, that later came to be known as nucleic acids.^[1-4] In 1938, William Astbury and Florence Bell attempted to study the first X-ray diffraction pattern of DNA, but they were unable to propose its naturally-existing structure.^[5] Rosalind Franklin, came very close to elucidating the correct structure of DNA in 1952, by producing the first ever high-resolution crystallographic photographs of DNA fibers.^[6,7] However, the most significant and well-known discovery in this field was done by James Watson and Francis Crick, who in 1953, discovered the first double helical structure of DNA that has been hailed as one of the most path-breaking scientific discoveries in the previous century.^[8]

Nucleic acids comprise of deoxyribonucleic acid (DNA) and ribonucleic acid (RNA). They are mainly known to play the classical roles of storage and transfer of genetic information in all known living organisms. DNA functions as a long-term storage unit for genetic information that are passed from one generation into subsequent generations. RNA functions in converting genetic information from genes into the amino acid sequences of proteins.^[9] Initially, RNA was sub-divided into three main types according to their functions, viz., transfer RNA (tRNA), messenger RNA (mRNA), and ribosomal RNA (rRNA). Messenger RNA functions as carriers of genetic sequence information between DNA and ribosomes, directing protein synthesis; ribosomal RNA is a major component of the ribosome and transfer RNA serves as the carrier module for amino acids to be used in protein synthesis, and is responsible for decoding the mRNA.^[10,11]

However, it has been revealed in recent decades that nucleic acids have several other cellular functions in addition to facilitating genetic information storage and transfer. RNA is known to have a broader functional range; for example, it is a major component of nucleoprotein complexes involved with translation and processing of mRNA.^[12,13] Some RNAs catalyze reactions, referred to as ribozymes, for example peptide bond formation in a

ribosome.^[14] Additionally, some specific regulatory segments of mRNA have been found to be responsible for controlling gene expression. These components came to be known as riboswitches that are capable of targeting and capturing small target molecules.^[15-17] Also, similar to naturally-occurring riboswitches, some artificial nucleic acids called aptamers were identified that bind a variety of targets. An in-depth account of aptamers has been included in chapter 3 of this doctoral thesis. It has also been brought to light that RNA is capable of blocking the expression of certain genes referred to as “gene silencing” and the RNAs that are involved in such functions are known as small interfering RNA (siRNA) and micro RNA (miRNA).^[18,19]

2.1 Techniques for Structure Determination of Nucleic Acids

Due to the great importance of nucleic acids today, it has become essential to study their structure and dynamics because these are the properties that help us to gain insight into their complete range of functions. Over the last few decades, a variety of biochemical and biophysical techniques have been developed that are routinely used to study the structure and dynamics of nucleic acids. Amongst them, the most powerful and sophisticated technique is X-ray crystallography, which is capable of providing “photographical” information about the three-dimensional molecular structure and precise arrangements of atoms in space.^[20] Although this technique is highly informative and widely used, it comes with some disadvantages. Firstly, it is a prerequisite to obtain a sufficiently large and regular single crystal of the sample to be studied by X-ray. It is often a daunting and time-consuming task to obtain a single crystal for large biomolecules like nucleic acids. Secondly, biomolecules cannot be studied in their preferred solution state by this technique. Thirdly, the conformation of a nucleic acid in a crystal might not be a biologically-active one.^[21] And finally, as X-ray provides a static view, conformational changes that govern and affect functions, cannot be studied by X-ray.

Nuclear magnetic resonance (NMR) spectroscopy is another widely used high-resolution technique that is used to study nucleic acids. NMR provides structural information of the nucleic acids in solution, thus revealing their conformation under their innate biologically relevant conditions.^[22-25] However, NMR also has a few limitations. For example,

NMR of nucleic acids often requires relatively large amounts of isotopically-labeled samples. Furthermore, NMR studies are usually restricted to nucleic acids that are smaller than 50 kDa.^[26] This is because the increased anisotropy associated with slower tumbling of large molecules in solution causes broadening of the NMR peaks. Moreover, NMR is a time-consuming process. For example, it might take up to a few months to analyze an entire set of experimental data necessary to estimate a three-dimensional structure for a mid-sized nucleic acid or protein.

Another common technique for studying structure of nucleic acids is Förster resonance energy transfer (FRET), also known as fluorescence resonance energy transfer, which is capable of measuring distances between two or more fluorophores in the nanometer range.^[27] In addition to enabling single-molecule studies,^[28,29] this technique can also be used to study nucleic acids under biologically-relevant conditions. Although not a very high-resolution technique, FRET is widely used owing to its sensitivity. Unlike NMR, FRET requires a very little amount of sample for analysis or structure determination. Moreover, it is less time-consuming than NMR. However, it has demerits too. For example, FRET requires incorporation of at least a pair of rather bulky chromophores, that can be difficult to incorporate and can alter the native structure of the biomolecule that is to be studied.

Another useful technique to investigate the structure and dynamics of nucleic acids is electron paramagnetic resonance (EPR) spectroscopy, which will be described in the following sections.

2.2 EPR Spectroscopy

EPR spectroscopy, also known as electron spin resonance (ESR), was first reported by Zavoisky in 1945.^[30,31] EPR is applicable for the study of the local environments of paramagnetic centers, and is a highly useful technique to study structure and dynamics of biomolecules like nucleic acid and proteins.^[32] Similar to NMR, EPR is based on the principles of magnetic resonance that involves spins of unpaired electrons, such as those present in free radicals. As NMR involves nuclear spins, EPR detects transitions of electron spins from a lower to a higher energy level, induced by absorption of microwave electromagnetic radiation in the presence of an applied external magnetic field. Some transition metals are paramagnetic and have been used for EPR studies.^[33-35] However, free unpaired electrons like nitroxides

(Figure 2.1 A) are paramagnetic, and thus, EPR-active too (Figure 2.1 B) and are more widely used for EPR-based investigations.^[36,37] Most of the paramagnetic reporter groups are usually smaller as compared to the exogenous fluorophores used for FRET, thus making them less perturbing to the native structure of biopolymers. EPR provides structural information by measuring distances between two paramagnetic centers incorporated within nucleic acids.^[38] Also, information about dynamics can be obtained from line-broadening of the EPR spectra and from orientation studies using pulsed-EPR.^[39-43]

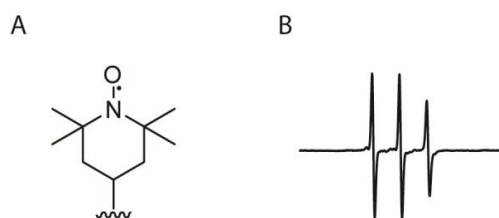


Figure 2.1. (A) A piperidine-based nitroxide radical TEMPO ((2,2,6,6-Tetramethylpiperidin-1-yl)oxyl). (B) CW-EPR spectrum of a nitroxide radical.

The technique of EPR can be classified into two main types, continuous wave- (CW) and pulsed-EPR. CW-EPR spectra are recorded by putting a paramagnetic sample into a microwave-irradiated field having a constant frequency and sweeping the external magnetic field until the resonance condition is fulfilled. CW-EPR can be used to measure distances of up to 25 Å through analysis of peak broadening.^[44,45] In pulsed EPR, the spectrum is recorded by exciting a large frequency range simultaneously with a single high-power microwave pulse of given frequency at a constant magnetic field.^[46] One of the most commonly used pulsed EPR techniques is called pulsed electron-electron double resonance (PELDOR), which sometimes, is also referred to as double electron-electron resonance (DEER).^[47,48] PELDOR is capable of measuring longer-range distances between 15-100 Å^[38,49-53] and has been extensively used to measure distances between two paramagnetic centers in nucleic acids.^[43,54,55]

Nucleic acids are not inherently paramagnetic and, therefore, it is necessary to modify them with paramagnetic atoms or groups, referred to as spin labels. As mentioned before, although there are some examples of paramagnetic metal ions like Gd (III) and Mn (II) that have been used as spin probes,^[34,35] bench-stable nitroxides are the most commonly used spin labels.^[56] Many of these nitroxide radicals are commercially available or can be readily

synthesized using standard techniques of synthetic organic chemistry, which helped them in gaining popularity as spin labels for EPR studies.

2.3 Site-Directed Spin-Labeling (SDSL)

From the perspective of EPR-based studies, the spin labels need to be incorporated at specific sites of interest within nucleic acids, referred to as site-directed spin-labeling (SDSL).^[36,41,57-61] While performing SDSL, spin labels can be attached to nucleic acids either covalently or noncovalently (**Figure 2.2**). Moreover, there are two main strategies that have been applied for covalent SDSL. The first one utilizes spin-labeled phosphoramidites that are incorporated at specific positions during automated chemical synthesis of the nucleic acid, shown schematically in **Figure 2.2 A**, and sometimes referred to as the “classical” phosphoramidite method.

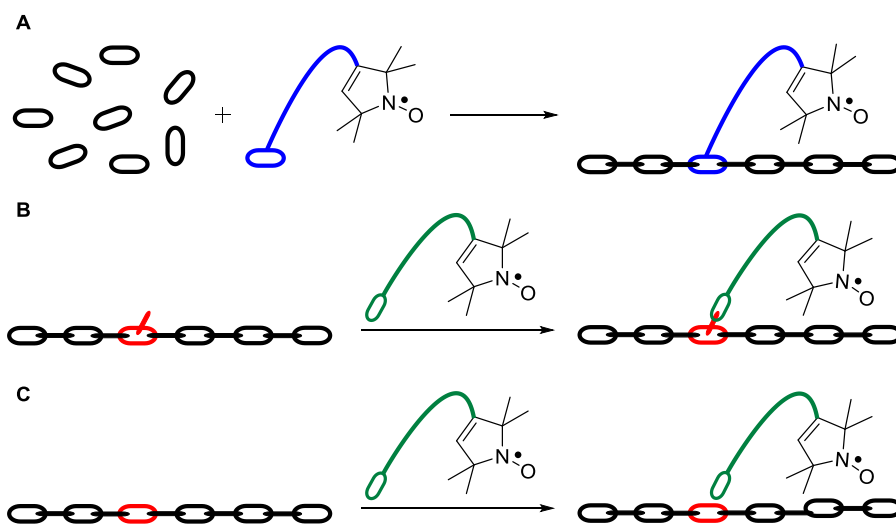


Figure 2.2. Strategies for site-directed spin labeling (SDSL). (A) The “classical” phosphoramidite approach. (B) Post-synthetic spin-labeling. (C) Noncovalent spin-labeling. A pyrrolidine-based spin label has been used to represent a nitroxide spin label. Nucleotides are represented by links that form oligonucleotide chains.^[62] This figure has been reproduced with permission from *Methods Enzymol.*, 2015, 563, 397-414.

The second SDSL strategy is post-synthetic spin labeling, where spin labels are incorporated after either chemical or enzymatic synthesis of the oligonucleotide (**Figure 2.2 B**). The third strategy of SDSL relies on noncovalent interactions like hydrogen bonding and π -stacking between the spin label and the nucleic acid (**Figure 2.2 C**). The three techniques are described briefly in the following sections.

2.3.1 The Phosphoramidite Approach

Nucleoside phosphoramidites are derivatives of nucleosides and act as the key building blocks in solid-phase synthesis of nucleic acids. A generic structure of an RNA phosphoramidite is shown in **Figure 2.3**, where the 5'- and the 2'-hydroxyl groups are protected, while the phosphoramidite group is at the 3'-position. After synthesis of the RNA using the solid-phase synthesis method, the oligonucleotide is deprotected to obtain the desired unprotected RNA. The main advantage of the phosphoramidite method is that spin labels with specific and desired structural features can be inserted at chosen sites, which might not be possible using post-synthetic labeling.^[63]

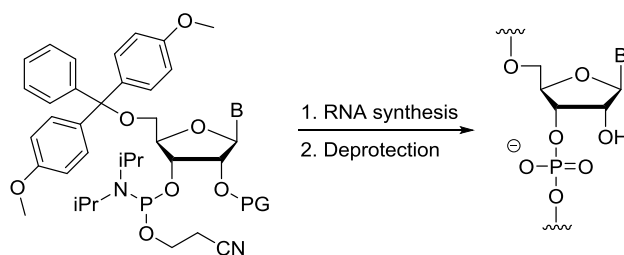


Figure 2.3. A phosphoramidite building block for an RNA oligonucleotide. PG is a protecting group for the 2'-hydroxy group and B is a nucleobase.

However, this particular approach is a laborious method of spin-labeling that involves substantial prowess in synthetic organic chemistry, which might be a challenge for researchers that have expertise predominantly in biochemistry or molecular biology. Another drawback of this method is that the spin labels get exposed to the reagents used during the oligonucleotide synthesis, which sometimes result in partial reduction of the nitroxide radicals.^[64,65]

2.3.2 The Post-Synthetic Spin-Labeling Approach

Post-synthetic spin-labeling is another important and widely-used method for covalent incorporation of spin labels at specific sites for SDSL (**Figure 2.2 B**). This strategy requires oligonucleotides that have uniquely reactive groups at specific sites where the spin label can be incorporated after undergoing a chemical reaction.^[62,66-71] Such modified oligonucleotides are usually prepared by the classical phosphoramidite method, often using commercially available reagents. This makes this method especially appealing to a broader range of researchers, because both the modified oligonucleotide and a suitable spin label can often be either purchased or readily prepared. The other merit of this method is that the spin label does not get exposed to the reagents used in the chemical synthesis of oligonucleotides, as is the case with the phosphoramidite approach. However, although this approach is usually very specific, a drawback of this method is the possibility of non-specific labeling due to the nucleophilic groups present in the nucleic acids, such as the exocyclic amino groups of the nucleobases, the N7 of purines, and non-bridging oxygen atoms of the phosphodiester. Moreover, incomplete spin labeling is also a well-known drawback of this method.

2.3.3 The Noncovalent Spin-Labeling Approach

Attaching a spin label noncovalently to a nucleic acid avoids the various challenges faced while connecting via a covalent bond. Although some examples of noncovalent spin labels that bind non-specifically to nucleic acids have previously been known,^[72-75] our research group has developed some useful techniques that involve highly specific noncovalent association of spin labels with nucleic acids. These techniques are based on the ligand-receptor interactions where the spin label acts as a ligand and an abasic site in a DNA/RNA acts as a receptor. Notably, in one of the studies, this abasic site in the DNA provided a binding site for the spin labeled ligand ζ , a derivative of cytosine, which bound a guanine on the complementary strand through hydrogen bonding and π -stacking (**Figure 2.4**).^[76] The binding

of the spin label to the DNA duplex was monitored by EPR spectroscopy and it was seen that at $-30\text{ }^{\circ}\text{C}$, the label was fully and specifically bound to the abasic site. This method of noncovalent spin-labeling is considerably simpler than other approaches like the phosphoramidite method and the post-synthetic approach. For one thing, synthesis of the spin-labeled ζ is easier and secondly, sample preparation step is very simple. Merely mixing of the spin label and the modified nucleic acid suffices the sample preparation and enables one to take EPR measurements directly, eliminating the need of any additional purification step.

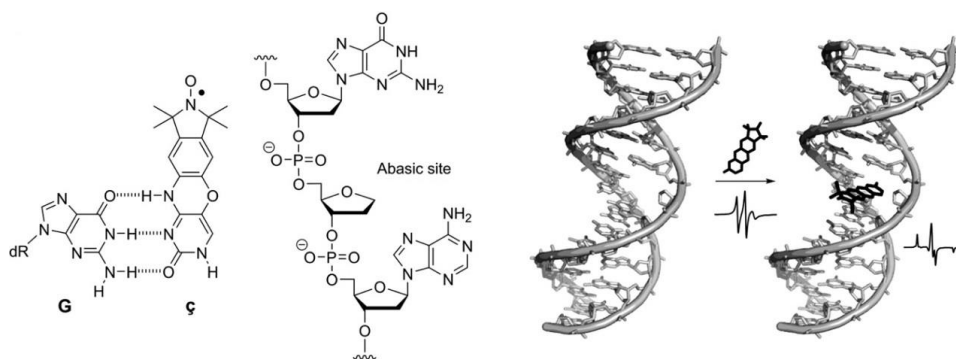


Figure 2.4. (A) Structure of ζ and its base-pairing scheme with guanine (G) (left) and an abasic site in DNA (right). (B) A molecular model of the noncovalent spin-labeling approach based on the nitroxide ζ (bold) and a duplex DNA (light) containing an abasic site. The EPR spectra shown are of the unbound spin label (left) and of the bound spin label (right) in duplex DNA containing an abasic site at $-30\text{ }^{\circ}\text{C}$. This figure has been reproduced with permission from *Eur. J. Org. Chem.*, **2012**, 2291-2301.

This noncovalent spin-labeling strategy has several advantages over the two covalent spin-labeling approaches, namely, the phosphoramidite method and post-synthetic labeling. For example, it is easier to synthesize ζ as compared to similar spin-labeled phosphoramidites. Also, smaller amounts of the spin label are usually required for this approach as compared to the covalent approaches. Another important benefit of this strategy over the phosphoramidite method is that the spin label is not exposed to the chemicals used for the oligonucleotide synthesis. Also, the simplicity of this potentially “mix and measure” spin-labeling method can be easily used by non-chemists.

However, this approach too, has a few disadvantages. For one thing, ζ bound to an abasic site in a DNA duplex only at a very low temperature ($-30\text{ }^{\circ}\text{C}$), limiting its applicability to be used under physiological conditions that involve ambient temperature. Moreover, it failed to bind well to a similar RNA duplex containing an abasic site. Also, it was found that only a few flanking sequences showed complete binding to the abasic site. Additionally, it was

experimentally observed that incorporation of two binding sites into the same duplex resulted in incomplete binding.^[77]

Substantial improvements in the shortcomings of ζ were made by developing \dot{G} (Figure 2.5. A), a spin-labeled derivative of guanine, which was found to bind with high affinity and specificity to abasic sites in duplex RNA (Figure 2.5 B).^[78] ζ required a multistep synthesis, whereas \dot{G} was prepared in a single step from readily available starting materials. Also, it was seen that \dot{G} bound substantially well to nucleic acids containing abasic sites, especially RNA duplexes at higher temperatures.^[78] Another improvement of \dot{G} over ζ was that, flanking sequence for the latter had minor effect on the binding. Additionally, \dot{G} allowed accurate measurement of inter-spin distances between two spin labels using PELDOR.^[78]



Figure 2.5. (A) Structure of \dot{G} (B) CW EPR data of \dot{G} (left) and \dot{G} bound to a RNA duplex containing an abasic site at -20°C (right).

However, all the existing strategies of spin-labeling developed thus far, including formation of an abasic site, involve chemical modification of the nucleic acids, which can be a limiting factor for preparing long spin-labeled oligonucleotides. In the next chapter, a new approach that enables spin labeling of unmodified RNA will be described, which can potentially be applied to spin-label long RNAs that can be prepared by *in vitro* transcription.

3 Noncovalent Spin-Labeling of Unmodified RNA: The Aptamer Approach

Spin-labeling, in combination with EPR, is an efficient method to study structure and dynamics of nucleic acids. However, all the existing spin-labeling techniques developed thus far require modification of the nucleic acids. Therefore, it is important to develop spin-labeling approaches for unmodified nucleic acids, which will enable labeling of long RNAs that are difficult to prepare by chemical methods. To this end, an aptamer-based spin-labeling approach was developed.

3.1 Nucleic Acid Aptamers

Aptamers are short, single-stranded nucleic acids that are known to bind to a wide variety of ligands with high binding affinity and specificity by folding into a well-defined three-dimensional structure.^[79] Two research groups independently discovered aptamers by identifying RNA molecules that bind to small organic dyes^[80] and to the bacteriophage T4 DNA polymerase.^[81] The name “aptamer” came from a word chimera built up from the Latin expression “aptus” (to fit) and the Greek word “meros” (part).^[80] Aptamers have been reported to bind amino acids,^[82] drugs,^[83] proteins^[84] and other small molecules.^[85] Most of the known aptamers known are RNA aptamers, although there are DNA aptamers as well.^[86] Aptamers are also found in nature in the form of riboswitches. A riboswitch is usually a part of an mRNA molecule that can directly bind a small target molecule, and whose binding of the target affects the gene's activity.^[87]

Due to their unique and strong binding properties, aptamers have found a wide range of applications in development of bioanalytical assays,^[88,89] inhibition of enzymes and receptors,^[90,91] target validation,^[92] drug screening,^[93] imaging of cellular organelles,^[94] and development of biosensors^[95] etc. Owing to their huge range of applications, aptamers are considered to be promising candidates for medicinal research and are regarded as one of the major discoveries in nucleic acid science during the past decades.

Aptamers are selected from a random library or “pool” of nucleic acids by an iterative process of adsorption, recovery and re-amplification. This process has been termed systematic evolution of ligands by exponential (SELEX) enrichment (**Figure 3.1**).^[81] This method is also

referred to as “*in vitro* selection” or “*in vitro* evolution”.[96] The SELEX technique selects aptamers with high binding affinity to a variety of target ligands. The classical SELEX method begins with the synthesis of a very large oligonucleotide library composed of random sequences. The library is then incubated with the desired target molecule under conditions suitable for binding. Next, the unbound nucleic acids are partitioned from those bound specifically to the target molecule, which are then eluted from the target molecule and amplified. This selection procedure is reiterated for several rounds until the resulting sequences are highly enriched. The selected nucleic acids are subjected to sequencing and evaluation of their binding to the target.

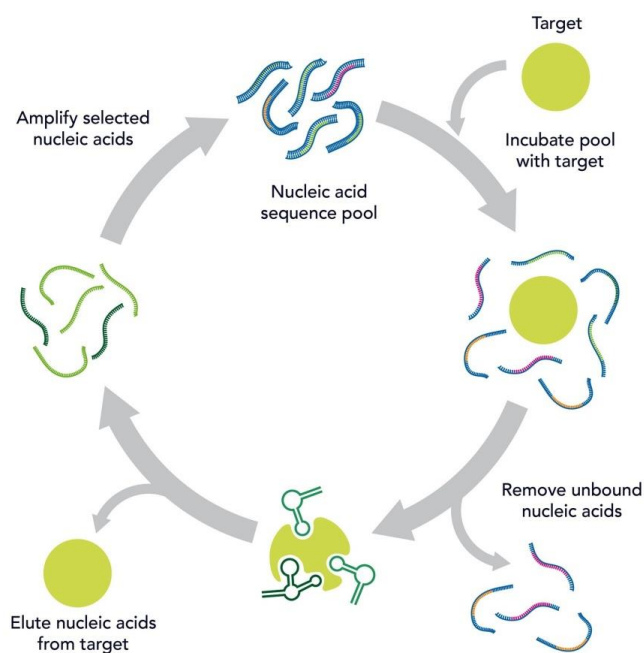


Figure 3.1. A general scheme for the systematic evolution of ligands by exponential (SELEX) enrichment process. Figure courtesy of Integrated DNA Technologies Inc.

3.1.1 The Malachite Green Aptamer

A 38-nucleotide RNA aptamer was discovered by *in vitro* selection that targeted the dyestuff malachite green (MG) (**Figure 3.2, 1**).^[97] The ligand bound the aptamer with substantially strong affinity having a dissociation constant (K_D) of 200 nM.^[98] Ligands structurally similar to malachite green were also found to bind to the MG-binding aptamer, thus highlighting the versatility of this aptamer.^[99] For example, a dye called tetramethylrosamine (TMR) (**Figure 3.2, 2**) was found to have a five-fold higher affinity ($K_D \sim 40$ nM) as compared to malachite green. The structural difference between malachite green and tetramethylrosamine is marked by only a single oxygen atom that bridges two of the aromatic rings to form a partial planar structure. This particular property was hypothesized to attribute to the superior binding of TMR over MG as the aptamer does not need to expend energy to align the two rings in the same plane in space.^[99]

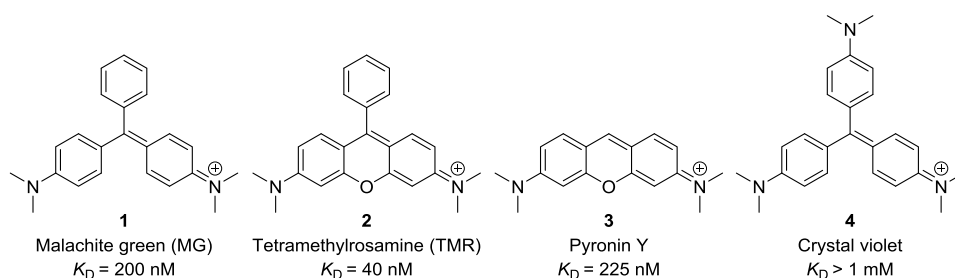


Figure 3.2. Structures of dyes that are known to bind to the MG aptamer.

Pyronin Y (**Figure 3.2, 3**), which is identical to TMR, except that it lacks a free phenyl ring attached to the xanthene moiety, was shown to bind to the aptamer having a K_D of 225 nM. However, crystal violet **4**, that differed from malachite green simply by addition of a dimethylamine to the free phenyl ring, did not show any significant binding to the aptamer ($K_D > 1$ mM). It was hypothesized that as the net positive charge was distributed to the third amine group in crystal violet, favorable electrostatic interactions between the amine and the backbone phosphate groups were reduced, that led to a drop in the binding affinity.^[99] Also the fact that crystal violet shows a significant propeller twist in all the three rings, was attributed to be a likely reason for its inferior binding to the aptamer.

Both X-ray and NMR structures of the TMR- and MG-bound aptamer complexes, respectively, revealed that the ligand binding-site in the aptamer was defined by an

asymmetric internal loop flanked by a pair of helices (**Figure 3.3 A**).^[99,100] Also, it was known from the crystal structure that the binding was mainly stabilized by base-stacking and formation of noncanonical base pairs.^[99] The binding pocket of the aptamer was found to be a series of stacked nucleotide tiers and the ligand was revealed to be intercalated within these tiers and is placed horizontally in the binding pocket (**Figure 3.3 B**). Additionally, electrostatic interactions between the cationic ligand and the anionic RNA contributed to the binding. Strikingly enough, interactions through hydrogen bonds between the heteroatoms on the ligand and the RNA were found to be completely absent.

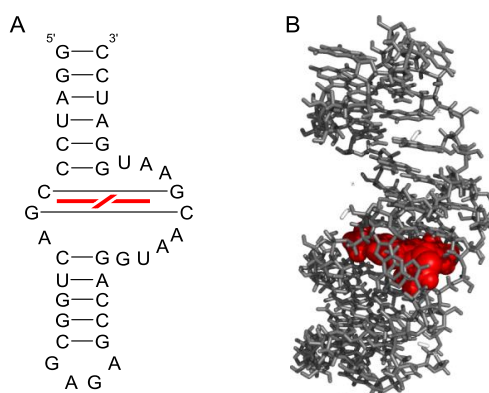


Figure 3.3. (A) Secondary structure of the RNA aptamer-TMR complex showing the position of the ligand in red, (B) X-ray structure of TMR (red) bound to the aptamer (grey).

It was later revealed that not only structurally similar ligands were tolerated by the aptamer, the RNA is versatile enough to endure structural changes in the ligand as well, with respect to various types of substitutions.^[101] However, modifications were found to be possible only in limited areas of MG. The two conjugated aromatic rings containing the dimethylamino-modifications were deeply buried within the binding pocket. Therefore, any kind of modification in those parts of the ligand was speculated to negatively impact the binding. The only region where modifications would be tolerated was either the “para” or the “meta” position of the non-nitrogen bearing aromatic ring of MG (**Figure 3.4, 1**).

Substitutions by small groups like a methoxyl at the para-position of MG (**Figure 3.4, 5**) showed inferior binding to the aptamer and raised the K_D to 1.43 μM . However, the same substitution at the meta-position (**Figure 3.4, 6**) bound substantially strongly to the aptamer ($K_D = 150 \text{ nM}$). Also, another derivative of MG with hexyloxy groups substituted at both the

meta- and para-positions (**Figure 3.4, 7**) gave a modest K_D of 1.82 μM . Additionally, it was known that when a bulky group, such as 4-methoxystyrene, was substituted at the para-position (**Figure 3.4, 8**) modest binding to the aptamer was obtained with a K_D of 540 nM. Interestingly, similar derivatization at the meta-position of MG (**Figure 3.4, 9**) displayed no binding to the aptamer.

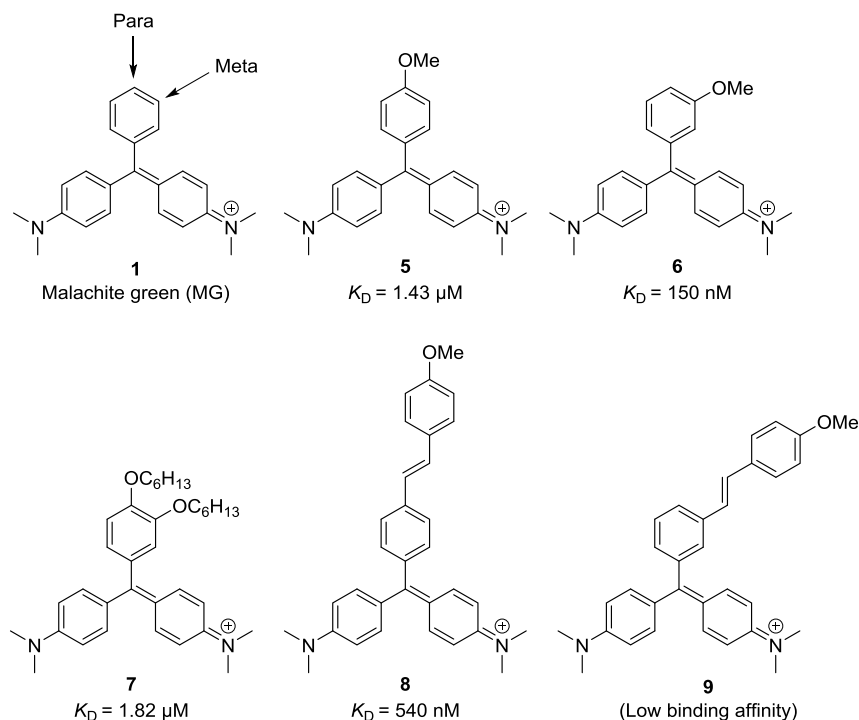


Figure 3.4. Arrows indicating possible sites of modifications in MG **1**. Structures and dissociation constants (K_D) of m-methoxy derivative of TMR **5**, p-methoxy derivative of TMR **6**, MG substituted by long-chain alkyl groups in both the meta- and para-positions **7**, 4-methoxystyryl derivatives of MG at para-position **8** and meta-position **9**.

3.2 Design of Spin Labels for the MG Aptamer

To spin label an RNA like the MG aptamer without chemically modifying the RNA, the only option is to convert the ligand into a nitroxide. In line with previous findings, it was clear that the point of attachment of a nitroxide radical would essentially be either at the meta- or the para-position of the unsubstituted aromatic ring. Simple molecular modeling based on the crystal structure of TMR bound to the MG aptamer revealed that the nitroxide radical essentially had to be connected to MG/TMR with a long and straight tether, such as an

acetylene functional group, that would enable the label to jut out of the narrow gap in the binding pocket into the solution (**Figure 3.5 A**). The initial plan was to identify MG-derived spin label(s) that bind well, and then prepare their TMR derivatives with the aim of increasing their binding affinity further. Another reason behind synthesizing spin labeled derivatives of MG was that the syntheses looked simpler than that for TMR-based spin labels.

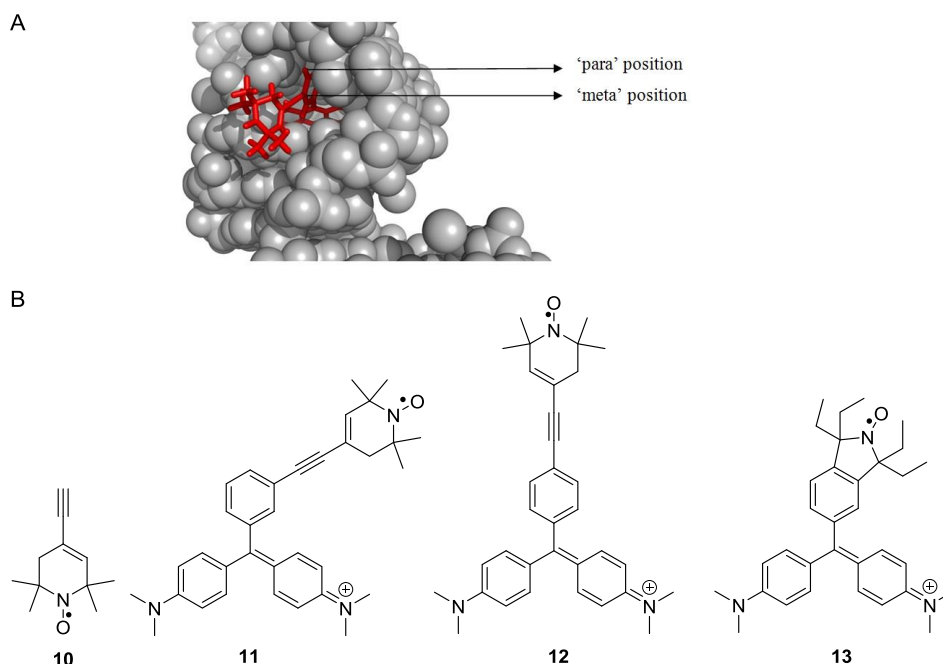


Figure 3.5. (A) A molecular model of the crystal structure of the MG aptamer bound to TMR, showing possible sites of modifications in TMR. (B) A piperidine-based acetylene-linked nitroxide (**10**) and spin-labeled derivatives of malachite green (**11**, **12** and **13**) that were planned to be synthesized.

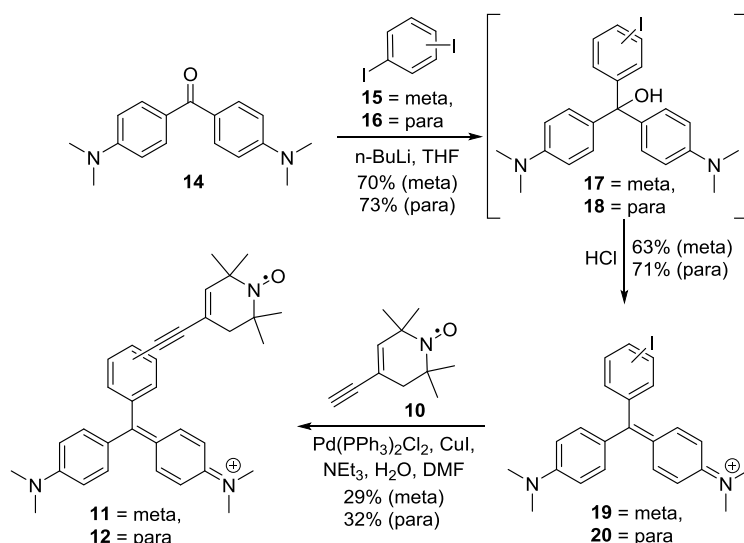
Accordingly, a piperidine-based nitroxide **10** ((4-ethynyl-2,2,6,6-tetramethyl-3,6-dihydropyridin-1-yl)-oxyl)^[102] was proposed to be attached to the meta- and para-positions of MG to afford spin-labeled candidates **11** and **12**, respectively (**Figure 3.5 B**). It was planned to have a halogen at the desired meta- or para-position of the unsubstituted phenyl ring, which would be utilized to perform the Sonogashira reaction at that position to conjugate the acetylene-linked nitroxides. A labile halogen like iodine was the first choice, for the fact that iodine is the best leaving group/atom amongst all the halogens.

In addition to the piperidine-based spin labels, an isoindoline-based nitroxide derivative of malachite green **13** was planned to be synthesized where the unsubstituted aromatic ring

would be replaced by a tetraethyl-isoindoline nitroxide to check how the binding is affected if both the meta- and para-positions of the triaryl dye are blocked, similar to nitroxide 7.

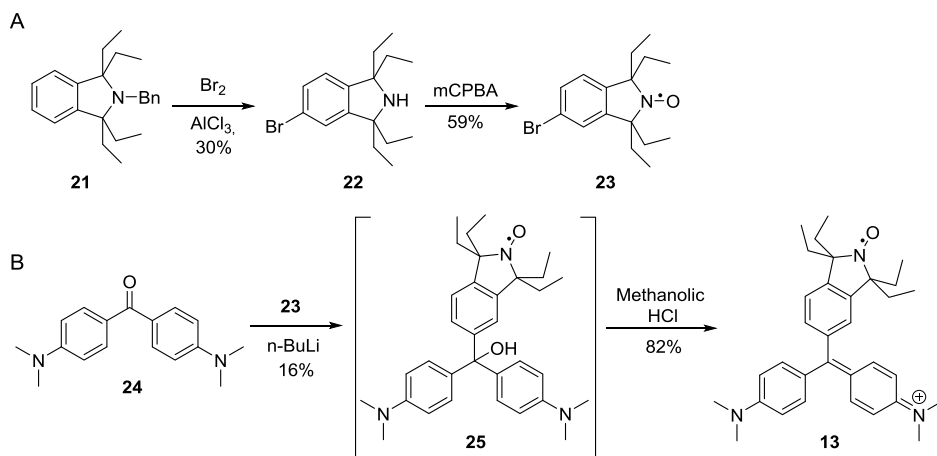
3.2.1 Synthesis of Spin-Labeled Derivatives of Malachite Green

The synthesis of the meta- and para- modified MG **11** and **12** (**Scheme 3.1**) started with lithiating either 1,3- (**15**) or 1,4-diiodo benzene (**16**) that was allowed to react with Michler's ketone **14** to obtain meta- and para-iodo substituted intermediates **17** and **18**, respectively. Those were converted to meta- and para-iodo substituted malachite greens **19** and **20**, respectively, by stirring in hydrochloric acid, which were further subjected under Sonogashira reaction conditions to couple with nitroxide **10**, which was synthesized in-house following a reported protocol,^[102] to obtain spin-labeled malachite greens **11** and **12**.



Scheme 3.1. Synthetic scheme used to obtain the meta- and para-substituted spin-labeled malachite greens **11** and **12**, respectively.

The synthesis of the isoindoline-derived malachite green **13** followed an altogether different route (**Scheme 3.2**). The synthesis began with deprotecting a benzyl-protected isoindoline **21** which was brominated *in situ* to obtain intermediate **22**, which was further oxidized to afford nitroxide **23** (**Scheme 3.2 A**). In the second part, nitroxide **23** was lithiated and reacted with Michler's ketone **24** to obtain intermediate **25** which under acidic conditions yielded the final spin-labeled isoindoline **13** (**Scheme 3.2 B**).



Scheme 3.2. Synthetic scheme used to obtain the isoindoline-based spin-labeled derivative of MG (**13**).

However, purification issues were encountered while executing these synthetic schemes, although they looked simple on paper. Being derivatives of commercial dyes, the lithiation step generated intense green-colored impurities that appeared as overlapping bands on preparative TLC. However, after a lot of hardship, all the three spin labels **11**, **12** and **13** were obtained in workable amounts by performing repeated chromatographic separations.

3.2.2 EPR Studies of the Binding of MG-derivatives with the Aptamer

Unfortunately, the pyrrolidine-based MG-derived spin labels **11** and **12** showed very poor solubility in aqueous medium and the binding studies could not be accomplished. They were found to be insoluble even in a buffered system of 2% DMSO + 30% ethylene glycol + 68% water. No improvements were seen by raising the percentage of DMSO up to 5%. Increasing the content of DMSO any further was not a valid option because DMSO is a known denaturing agent and it was obvious that excess of DMSO would negatively affect the binding. Moreover, stability issues were encountered when suspension of nitroxides **11** in **12** in aqueous buffers even for a couple of hours led to discoloration of the otherwise intensely green-colored solution. It was later learnt that the central carbon atom of MG is highly susceptible to an attack by a base such as a hydroxide ion (OH^-), which oxidizes MG to convert it to a colorless MG-OH form (**Figure 3.6**).^[103]

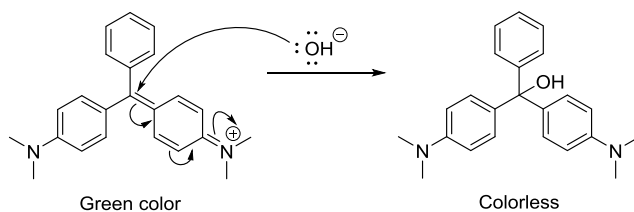


Figure 3.6. Attack of a hydroxide ion into the central carbon of MG to form colorless MG-OH.

The isoindoline-derived MG spin label **13** showed better aqueous solubility and its binding with the MG aptamer was studied by EPR (**Figure 3.7**). However, **13** did not appear to be a promising spin label because first of all, the binding was completely non-specific as similar broadening was observed for the sample containing a non-binding mutant aptamer as the negative control. In other words, it was concluded that although restricted motion of the spin label was observed, it was not due to its binding in the binding pocket. Moreover, aggregation or precipitation of **13** in solution was evident from the noisy baseline of the EPR spectra, even at 10 °C.

Since none of the MG-derived spin labels yielded promising results, either due to stability and solubility issues, or due to binding non-specifically to the aptamer, a series of TMR-derived nitroxides were synthesized to check if better results could be obtained.



Figure 3.7. EPR data for the isoindoline-derived MG **13** bound to the aptamer (left column), mutant RNA (middle column) and without any RNA (right column). EPR spectra were recorded as a function of temperature. All data were recorded in 10 mM phosphate, 100 mM NaCl, 0.1 mM Na₂EDTA, pH 7.0.

3.2.3 Spin-Labeled Derivatives of Tetramethylrosamine (TMR)

Since all attempts to obtain good MG-derived spin labels went futile, it was decided to synthesize a series of spin-labeled derivatives of TMR in anticipation of obtaining better stability and specific binding properties. To begin with, only “meta”-substituted spin-labeled TMR-derivatives were proposed to be synthesized (**Figure 3.8**). In addition to the piperidine-derivative **26**, two more spin-labeled derivatives of TMR having acetylene tethers were designed, one with a pyrrolidine-based spin label **27** ((2,2,5,5-tetramethyl-3-(prop-1-yn-1-yl)-2,5-dihydro-1H-pyrrol-1-yl)-oxyl)^[104] and the other, an isoindoline nitroxide having tetramethyl substituents **28** ((5-ethynyl-1,1,3,3-tetramethylisoindolin-2-yl)-oxyl).^[105,106]

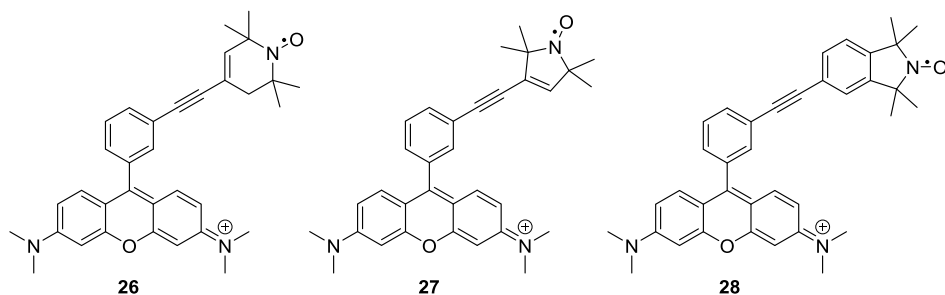
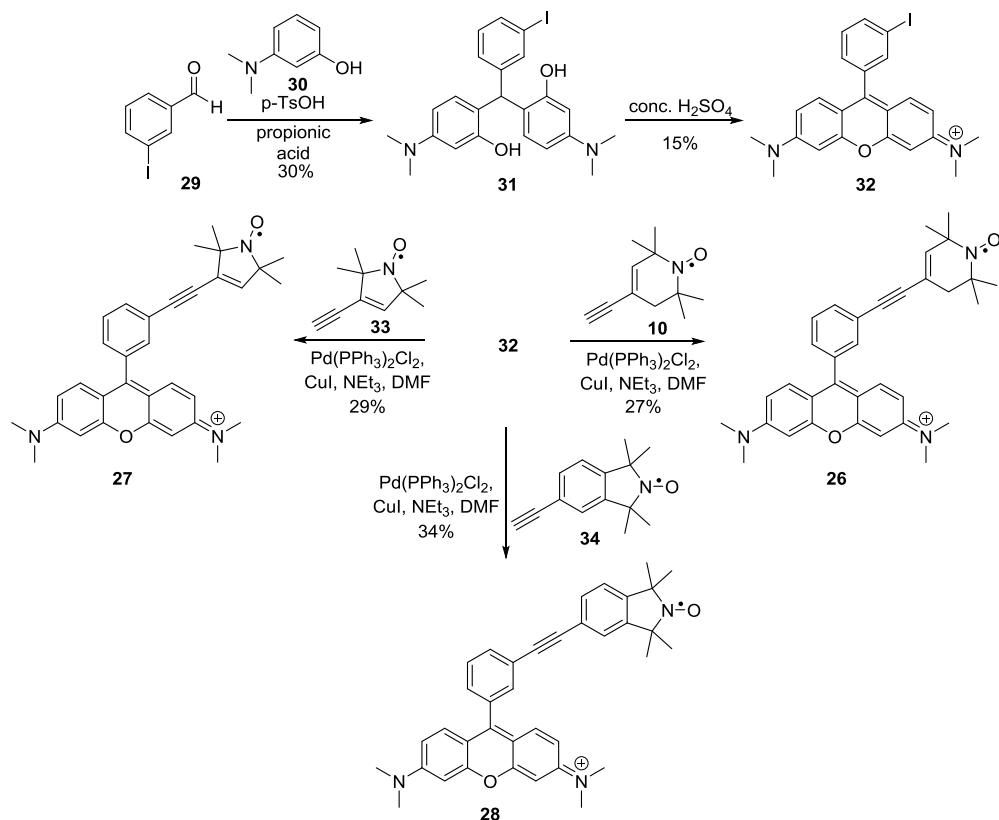


Figure 3.8. Spin-labeled derivatives of tetramethylrosamine that were proposed to be synthesized.

3.2.4 Synthesis of Spin-Labeled Derivatives of Tetramethylrosamine

The syntheses of the spin-labeled TMR derivatives began by reacting 3-iodobenzaldehyde **29** with 3-*N,N*-dimethylaminophenol **30** to obtain ring-opened diol intermediate **31** (Scheme 3.3). The ring-closed iodo-intermediate **32** was obtained by stirring **31** in sulfuric acid, which under Sonogashira cross-coupling conditions with **10**, **33** and **34** afforded the final spin-labeled TMRs **26**, **27** and **28**, respectively.

Although the reactions looked straight-forward, purification was the main issue while executing this scheme, as anticipated beforehand. Because TMR and its derivatives are characterized by an intense red colour, it was extremely difficult to isolate intermediate **32** and final paramagnetic compounds **26**, **27** and **28** from the impurities generated from the reactions that had equally intense characteristic red color. However, repeated chromatographic attempts yielded workable amount of the desired spin-labeled nitroxides.



Scheme 3.3. Synthetic scheme for synthesizing the spin-labeled derivatives of TMR 26, 27 and 28.

3.2.5 EPR Studies for the Binding of TMR-Derived Spin Labels

The binding of the spin-labeled probes **26**, **27** and **28** to the malachite green aptamer was studied by EPR spectroscopy (**Figure 3.9**). As before, the data were recorded in a phosphate buffer dissolved in an aqueous solution containing 2% DMSO and 30% ethylene glycol.^[76] From the EPR data recorded at 20 °C, we could conclude that all the nitroxides bound specifically to the binding pocket of the aptamer, although to varying extent; a slow-moving component emerged in all the samples where the ligand was bound to the aptamer that suggested binding. Absence of a similar broadening with the mutant RNA (negative control) indicated that the binding was specific. It was observed that two of the spin-labeled TMRs, **26** and **28** had only bound partially to the MG aptamer which was concluded by presence of a sharp fast-moving component that usually originates from the rapid tumbling motion of a freely rotating nitroxide in solution. The isoindoline-modified spin label of TMR **28** showed

comparable, albeit slightly better binding profile on EPR as compared to the piperidine-derived **26**. However, the pyrrolidine-based TMR spin label **27** appeared to be the best spin label synthesized in this entire series and exhibited full and specific binding to the MG aptamer, which was inferred by absence of any fast-moving component in the EPR spectra for the sample containing **27** bound to the MG aptamer.

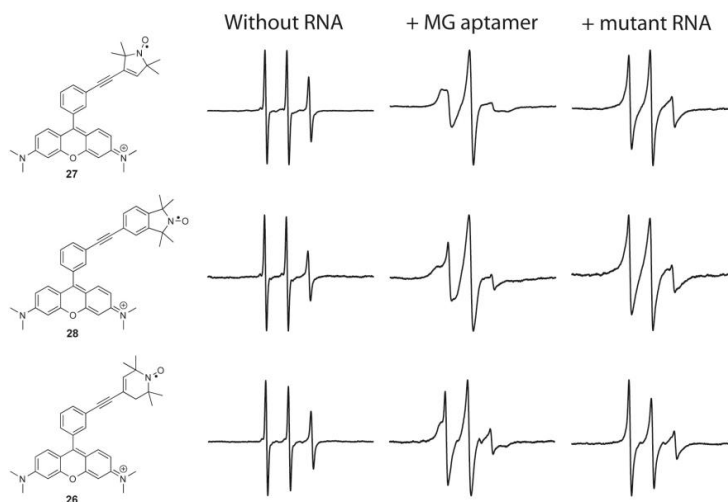


Figure 3.9. EPR data of the spin labels **26**, **27** and **28** without any RNA (left), when bound to the MG aptamer (centre) and mutant RNA (right, negative control). All data were recorded at +20 °C in 10 mM phosphate, 100 mM NaCl, 0.1 mM Na₂EDTA, pH 7.0.

An extensive temperature-dependent EPR spectroscopic study was performed for the pyrrolidine-derived spin label **27** (**Figure 3.10**). No sharp fast-moving component was observed in the sample for the label bound to TMR, not even at +30 °C. A degree of rigidity of the label was evident by the peaks splitting between high and low fields even at +10 °C and no non-specific binding was observed up to this temperature. At -10 °C though, a minute amount of non-specific binding was seen deduced from a slightly broadened EPR spectra for the negative control sample but the label was rigidly bound for the aptamer sample. At lower temperatures, slight aggregation was observed in the sample without RNA, but the extent of aggregation was found to be much lower than that obtained for the previous labels **26** and **28**.

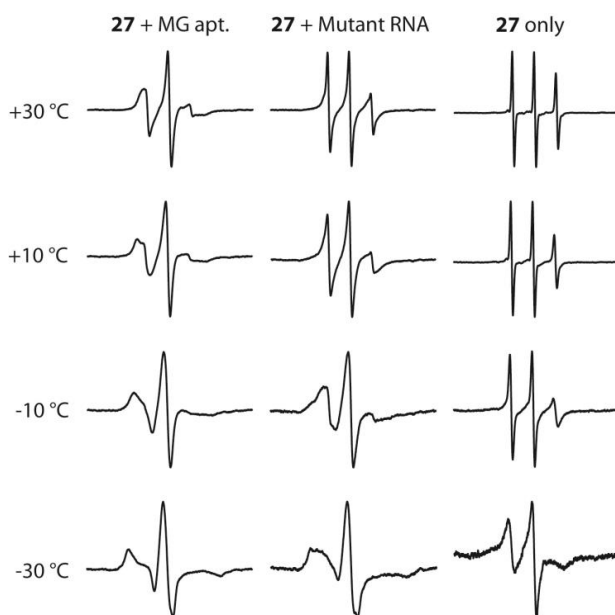


Figure 3.10. EPR data for the spin-labeled TMR 27 bound to the aptamer (left column), control RNA (middle column) and without any RNA (right column). EPR spectra were recorded as a function of temperature. All data were recorded in 10 mM phosphate, 100 mM NaCl, 0.1 mM Na₂EDTA, pH 7.0.

3.2.6 Determination of Dissociation Constants (K_D) for 26, 27 and 28 by Fluorescence Titration

To further characterize binding of the spin-labeled derivatives of TMR bound to the malachite green aptamer, dissociation constants (K_D) for binding of the ligands were determined by performing fluorescence titration experiments. Upon binding to the aptamer, fluorescence intensities of MG 1 and its structurally-related derivatives like TMR 2, pyronin Y 3 and crystal violet 4 are known to increase by more than thousand fold.^[107,108]

Therefore, additive amounts of the aptamer were added to a fixed amount of each of the spin-labeled ligands 26, 27 and 28 until saturation was reached. Fluorescence was found to be quenched upon binding of the ligands to the aptamer. By normalizing and inverting the maximum fluorescence intensity data to fit into a simple ligand binding equation, dissociation constants (K_D) of the spin-labeled ligands were calculated by curve-fitting (**Figure 3.11**). Although perfect fits were not obtained, a rough estimation of the dissociation constants was obtained by this method. The best-binding derivative 27 showed a dissociation constant (K_D) of 66 nM (**Figure 3.11 A**), whereas isoindoline-derived 28 and pyrrolidine-derived 26 showed dissociation constants of 95 nM (**Figure 3.11 B**) and 101 nM (**Figure 3.11 C**), respectively. These

values are in line with the data obtained from EPR in that **27** proved to be the best binder in the series, whereas **26** and **28** had already shown partial binding to the aptamer as judged by EPR, and were expected to show higher K_D values than **27**.

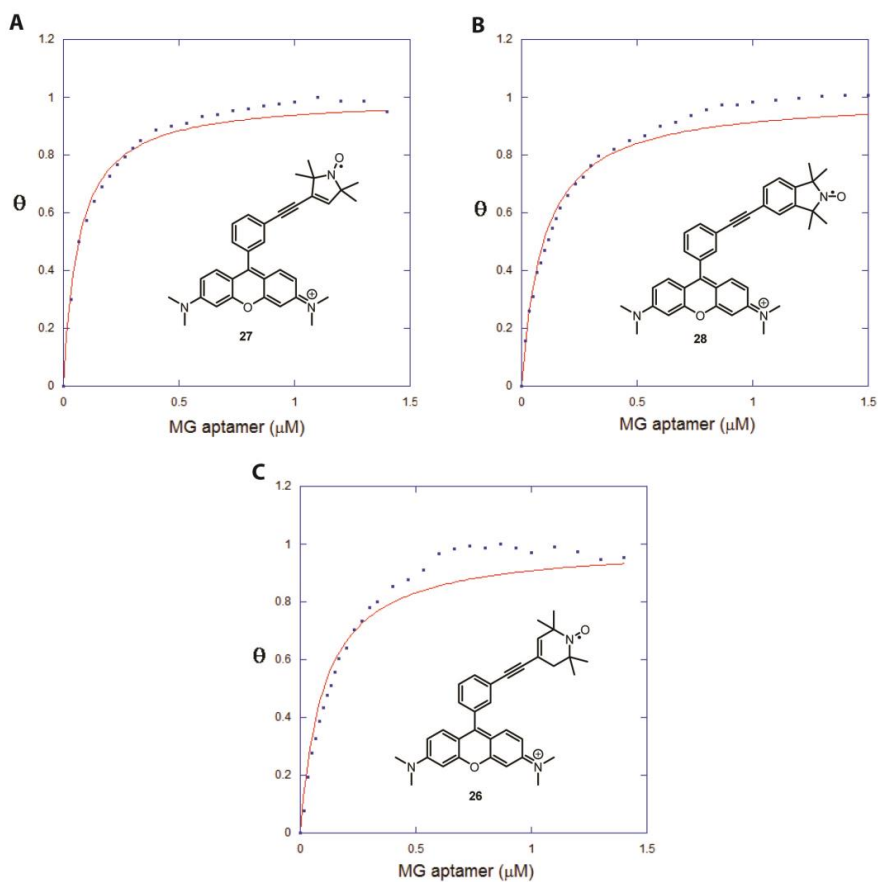
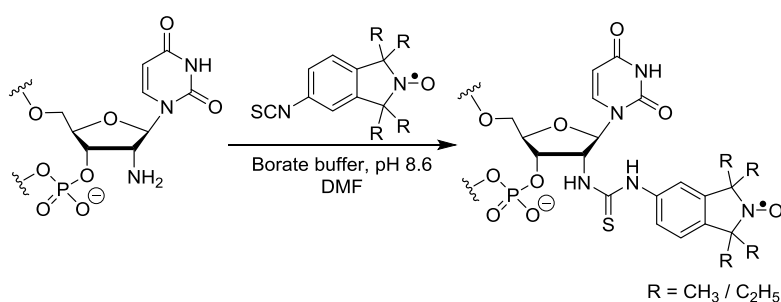


Figure 3.11. Dissociation constants (K_D) by fluorescence titration for the TMR-derived spin labels (A) **27**, $K_D = 66$ nM, (B) **28**, $K_D = 95$ nM and (C) **26**, $K_D = 101$ nM. θ denotes the fraction of ligand binding sites in the aptamer that are occupied by the spin label, the dotted line indicates the experimentally obtained data points and the solid line represents the fitted curve. Data were recorded in 10 mM phosphate, 100 mM NaCl, 0.1 mM Na₂EDTA, pH 7.0 at 20 °C.

3.3 Distance Measurements by PELDOR on the Malachite Green Aptamer

To further confirm that the spin-labeled TMR derivative **27** binds specifically to the malachite green aptamer, distance measurement studies by PELDOR spectroscopy were planned. The prerequisite for any pulsed-EPR based studies is the presence of a biradical system in the sample of interest. In the current aptamer-spin labeled complex, a biradical unit can be generated by two ways. The first option was to prepare an aptamer sequence that would be a dimer possessing two binding pockets, principally binding two equivalents of the spin label. However, this approach was envisioned to be somewhat complicated as placing the two binding domains with a fixed distance and orientation between them might not be trivial.

The other option was to covalently spin label a suitable position in the helical regions of the aptamer. As discussed in chapter 2, there are two possible ways to attach a spin label covalently to a nucleic acid.^[36] The first method is the phosphoramidite approach which is tedious and time-consuming. Moreover, as the label is prone to get reduced, this is not a reliable method to spin label long RNAs like the 38-nucleotide malachite green aptamer. The other method, i.e., the post-synthetic approach is easier and less time-consuming. Therefore, the in-house developed approach for post-synthetic spin-labeling of reactive 2'-amino groups of uridine in RNA described in detail in Chapter 5, was used to covalently attach an isoindoline-based nitroxide to the aptamer (**Scheme 3.4**).^[69]



Scheme 3.4. An in-house developed post-synthetic spin labeling scheme used to covalently label the malachite green aptamer for inter-spin distance measurement studies using PELDOR.

Based on the molecular modeling of the crystal structure, labeling the 2'-amino group of U36 in the MG aptamer at the stem-loop (**Figure 3.12 A**) would separate the two spin labels by a distance of 3.3 nm, which is an optimum distance for PELDOR measurements (**Figure 3.12 B**).^[109,110] The spin label can also exist as another rotamer which is obtained by rotating the single bond connecting the isoindoline and the thiourea by 180°, yielding an inter-spin distance of 3.5 nm. The molecular model showed that a covalently-attached tetraethyl isoindoline spin label located at this position would clearly jut out of the RNA into the solution without hindering the binding (**Figure 3.12 B**).

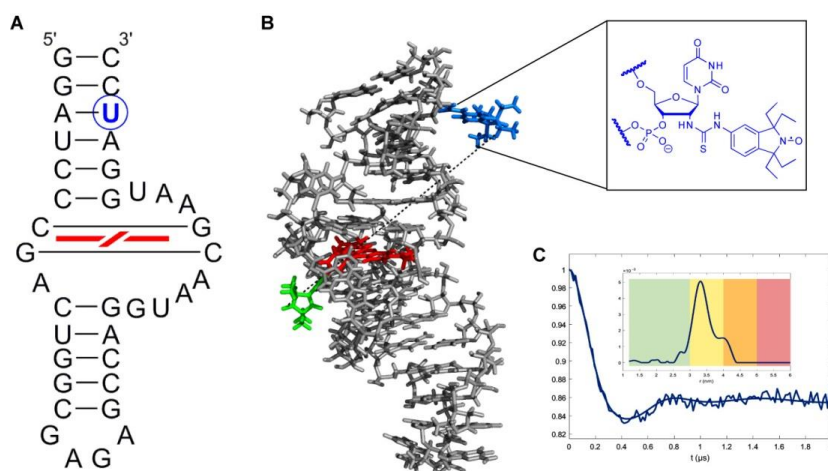


Figure 3.12. (A) Secondary structure of the malachite green aptamer bound to TMR (red) showing the position of covalently modified U36 (blue) with a 2'-amino uridine. (B) A molecular model showing the positions of the two spin labels (covalent label: blue, TMR core: red, pyrrolidine nitroxide modification on TMR: green); the structure of the covalently attached label is shown (blue) in a box. (C) PELDOR data with the time trace and distance distribution (inset) indicating a mean inter-spin distance of 3.3 nm (33 Å).

PELDOR distance measurements, performed at our collaborator Prof. Thomas Prisner's research group based at the University of Frankfurt, showed a clear oscillation that arose due to dipolar coupling between spins from the two spin labels in the aptamer system. Summing up the time traces and performing Tikhonov regularization,^[111] a mean distance of 3.3 nm was obtained (**Figure 3.12 B**), which was in very good agreement with the distances obtained from simple molecular modeling.

3.4 Conclusion

On our quest of noncovalent spin-labeling of unmodified RNA, we prepared a series of malachite green-derived nitroxide spin labels as ligands for the malachite green aptamer. Two spin labels based on malachite green were found to be unstable, whereas a third isoindoline-based MG derivative bound non-specifically to the aptamer. Better results were obtained by preparing spin-labeled derivatives of TMR. Although two TMR-based spin labels bound only partially to the aptamer at ambient temperature, remarkably, a pyrrolidine-based spin label **27** showed full and specific binding even at ambient temperature. By fluorescence titration studies, it was shown that all three TMR-based spin labels had dissociation constants in the sub-micromolar range. Also, an accurate distance obtained by PELDOR between noncovalently bound **27** and a covalently attached spin label within the aptamer system confirmed that **27** was indeed bound to the binding pocket of the aptamer as had been presumed.

There are several merits of this research. Most importantly, this is the first example of spin-labeling of unmodified nucleic acids. Additionally, this is the first example of noncovalent spin labeling at room temperature. Also, for the first time, distance measurement by pulsed EPR between a noncovalent and a covalent label incorporated into the same biopolymer was carried out. In the future, this research will open doors to spin-label long RNAs that can be prepared solely by enzymatic methods.

4 Noncovalent Spin-Labeling with Benzimidazole-Isoindoline Nitroxides

4.1 Introduction

In this project, the technique of noncovalent spin-labeling was further explored by investigating nucleic acid binding properties of a series of novel benzimidazole-based isoindoline nitroxides. This project was pursued in collaboration with Dr. Kye-Simeon Masters' research group based at the Queensland University of Technology, Brisbane, Australia who synthesized this new class of nitroxides. Our role in this initiative was to evaluate these benzimidazole-based isoindoline nitroxides as potential spin labels for noncovalent spin-labeling.

Isoindoline nitroxides have long been established as bench-stable free radicals.^[106,112-115] Additionally, they have found considerable importance as paramagnetic probes for spin-labeling using EPR spectroscopy.^[63,76,78,116] On the other hand, pyrido(1,2-a)benzimidazoles are known to be highly fluorescent ^[117-119]. Therefore, it was envisioned that if isoindoline nitroxides are fused with fluorophores like pyrido(1,2-a)benzimidazoles, they might be useful as bi-functional probes for nucleic acid binding studies. It was hypothesized that, first of all, these nitroxides would retain their key property of detection by EPR, and secondly, their reduced diamagnetic version could be of use as (pro)fluorescent probes, because nitroxides are known to quench fluorescence through an intermolecular electron-exchange interaction between their ground-state and the excited-state fluorophore.^[120,121]

The nitroxides that were investigated in this study are shown in **Figure 4.1**. Nitroxide **35** is the basic benzimidazole-fused isoindoline nitroxide, whereas **36** and **37** are benzannulated derivatives of **35**. Nitroxides **38** and **39** were designed to have a purine-type moiety fused to the isoindoline nitroxide. Since **38** and **39** had more nitrogen atoms on their aromatic ring systems, they were presumed to be more hydrophilic than **35**, **36** and **37**.

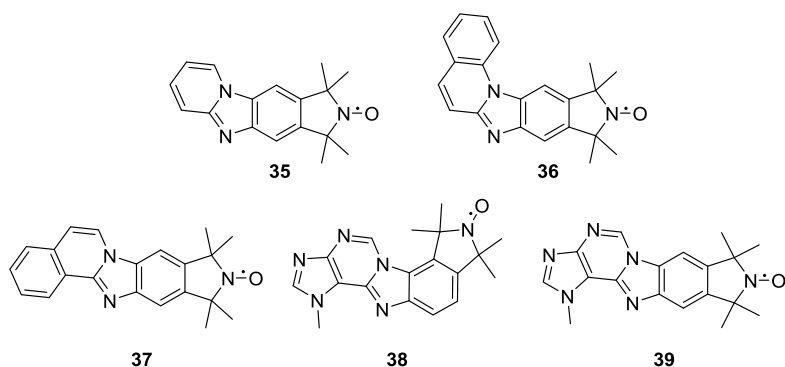
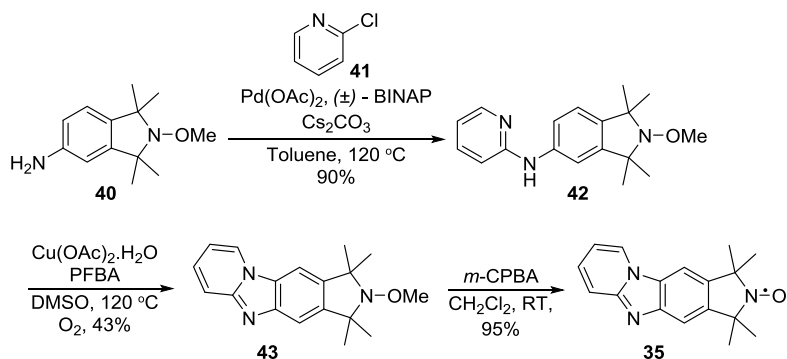


Figure 4.1. Structures of the benzimidazole-based isoindoline nitroxides **35**, **36**, **37**, **38** and **39** that were analyzed in this investigation.

4.2 Results and Discussion

4.2.1 Synthesis of the Benzimidazole-Based Isoindoline Nitroxides

Our collaborators synthesized this new class of spin labels by applying a variation of the Buchwald-Hartwig coupling and copper-catalyzed C–H amination as key steps.^[122] The synthesis of **35** is shown as an example in **Scheme 4.1**. Methoxyamine **40** was coupled with 2-chloropyridine **41** to obtain amidine intermediate **42**.^[123] Cyclization of N-aryl-N-pyridylamine **42** was performed using catalytic amounts of copper(II) acetate and pentafluorobenzoic acid^[124] to afford intermediate **43** with 43% yield. The final nitroxide **35** was obtained in 95% yield by *m*-CPBA oxidation. Compounds **36–39** were prepared by a similar synthetic strategy.



Scheme 4.1. Synthetic scheme for obtaining benzimidazole-based isoindoline nitroxide **35**. The syntheses were carried out by Dr. Kye-Simeon Masters' research group based at the Queensland University of Technology, Brisbane, Australia.

4.2.2 The “Combinatorial Approach” for Screening Promising Candidates

To swiftly assess this new series of nitroxides, a “combinatorial approach” was devised to screen the binding of each spin label to multiple oligonucleotides at once. Each sample contained the spin label with four DNA duplexes (or four RNA duplexes), each of which contained an abasic site placed opposite to four different orphan bases, A, C, G and T/U. Each duplex was in twofold excess relative to the spin label to ensure that the label bound completely to the oligonucleotides. Each of the nitroxides would bind to the duplex to which it had the highest affinity and the extent of binding would be manifested by broadening of the EPR spectra (see below).

The data obtained by this approach showed that all the nitroxides had affinity to abasic sites in duplex DNA and RNA, albeit with varying degrees (**Figure 4.2**). A spin label bound to a large biomolecule like a nucleic acid duplex tumbles slower in solution and results in a broader EPR spectrum that reflects a shorter rotational correlation time, which is usually manifested by generation of a slow-moving component in the EPR spectrum (indicated by a red arrow in **Figure 4.2**).^[76] For both the DNA and the RNA duplexes, nitroxide **39** was found to be the best binder because its ratio between the slow- and fast-moving components was the highest among all the nitroxides. In order to identify the best-suited orphan base for each nitroxide, an extensive evaluation of all the nitroxides was planned, starting with **35** and **36**, which were the first samples we received.

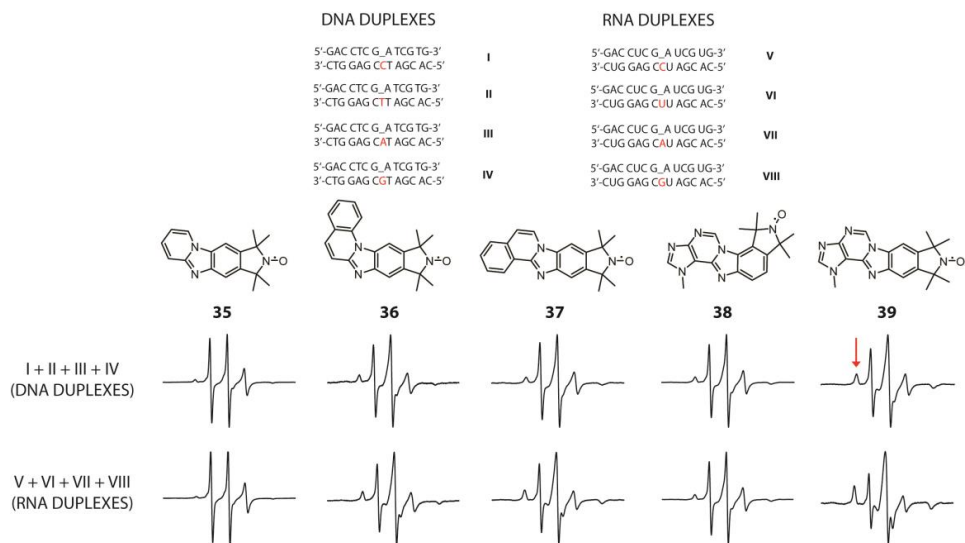


Figure 4.2. DNA and RNA duplex sequences and EPR data for nitroxides **35**, **36**, **37**, **38** and **39** screened as per the “combinatorial approach”. All data were recorded at -10 °C. Binding studies were performed in phosphate buffer (10 mM phosphate, 100 mM NaCl, 0.1 mM Na₂EDTA, pH = 7.0) containing 2% DMSO and 30% ethylene glycol.

4.2.3 Binding Studies of Nitroxides **35** and **36** using EPR spectroscopy

Binding of **35** and **36** to separate DNA and RNA duplexes, each containing an abasic site placed opposite to different orphan bases (**Figure 4.3 a**) was elaborately studied in order to identify the best binding conditions.^[76,78] The EPR data for nitroxide **35** revealed partial binding to the DNA duplexes, especially when the abasic site was placed opposite to G and C, as judged by the emergence of a slow moving component at -30 °C (denoted by a red arrow in **Figure 4.3 b**). However, slight broadening of the EPR spectra was also observed in the control samples having an unmodified DNA duplex, indicating occurrence of some non-specific binding.^[122] Almost no binding for **35** was observed when the abasic site was placed opposite to A and T. On the other hand, much better results were obtained when nitroxide **35** was incubated with an RNA duplex containing an abasic site, in particular opposite C, and modest binding was observed when placed opposite to U (**Figure 4.3 c**). The label did not bind at all when G and A were the orphan bases. In the case of RNA, the binding was clearly specific since the unmodified RNA duplex showed almost no indication of binding to nitroxide **35**.

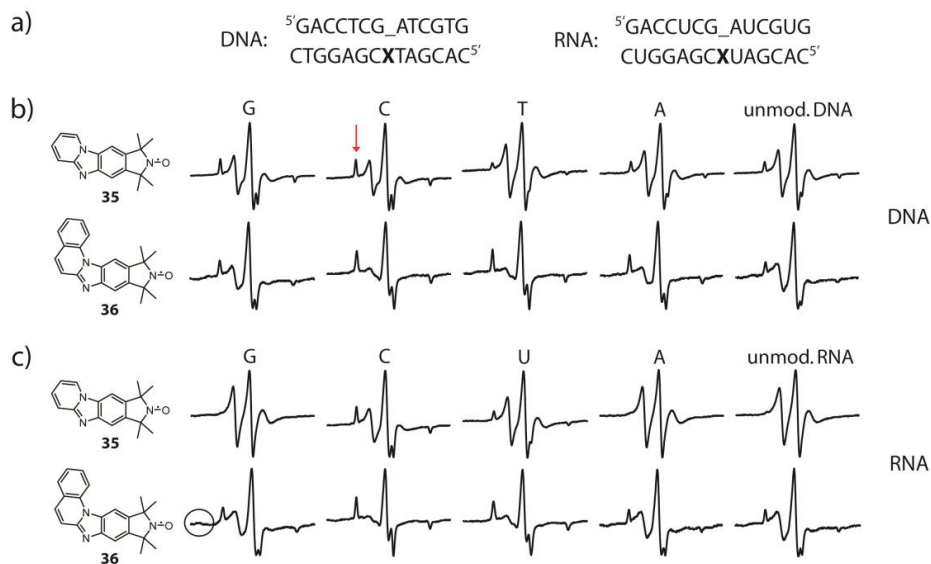


Figure 4.3. (a) DNA and RNA duplexes used for EPR binding studies where “_” denotes an abasic site and X the complementary base. The EPR spectra show the extent of binding of **35** and **36** to duplex DNA (b) and RNA (c), respectively. Letters above each spectrum denote the base opposite to the abasic site. For unmodified duplexes, “_” and X stand for C and G, respectively. Binding studies were performed in phosphate buffer (10 mM phosphate, 100 mM NaCl, 0.1 mM Na₂EDTA, pH = 7.0) containing 2% DMSO and 30% ethylene glycol at -30 °C. The red arrow indicates the slow moving (bound) component and the circle shows signs of aggregation.

In contrast to **35**, the EPR data for nitroxide **36** revealed significant and substantial improvement in binding to abasic sites in both DNA and RNA duplexes, presumably due to the extra aromatic ring that facilitated additional stacking interactions. For DNA, the highest affinity was observed for an abasic site complementary to C or T, where nearly full binding was achieved at -30 °C (**Figure 4.3 b**). However, considerable non-specific binding was also observed which resulted in broadening of the spectra for the sample with unmodified DNA duplex. Although the extra aromatic character of **36** led to better binding, it also showed signs of aggregation in the EPR indicated by an overall noisier baseline (highlighted by a circle in **Figure 4.3 c**), especially for the sequences that had limited affinity for the spin label. This also indicated that binding assisted in solubilizing the labels. The EPR data of nitroxide **36** in the presence of RNA duplexes surprisingly resembled those for DNA (**Figure 4.3 c**). However, close observation revealed less RNA binding, compared with DNA, when the abasic site was placed opposite to A and slightly more binding to C, the latter of which showed almost complete binding. Similar detailed analyses of nitroxides **37**, **38** and **39** are currently underway and will be reported in due course.

4.3 Conclusion

This international collaborative project was aimed at identifying a new class of benzimidazole-isoindoline nitroxide spin labels by fusing EPR-detectable isoindoline nitroxide radicals to a fluorescent pyrido(1,2-a)benzimidazole moiety. Binding of a series of benzimidazole-isoindoline nitroxides to duplex DNA and RNA containing abasic sites were studied by a combinatorial approach. Two of the nitroxides **35** and **36**, were studied in detail and the latter was found to be the better binder especially to RNA duplexes having an abasic site with C and U as the orphan bases.^[122] Three other nitroxides of the same series **37**, **38** and **39** are currently being analyzed in order to identify the best nucleic acid binder in this entire series.

5 Post-Synthetic Spin-Labeling of 2'-Amino Groups in RNA with Aromatic Isoindolines

5.1 Background

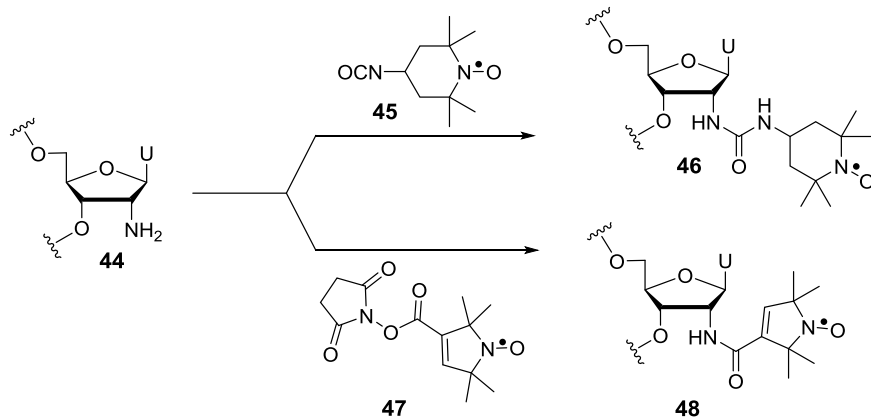
As mentioned in the introductory part in chapter 2, the post-synthetic approach is a particularly appealing method of spin-labeling because, in most cases, both the spin label and the oligonucleotide that contains a uniquely reactive functional group, can be purchased. Moreover, introduction of the spin label after the synthesis of the nucleic acid prevents exposing the label to the variety of strong oligomer-synthesizing reagents, as is the case with the phosphoramidite approach,^[65,125] and thus, partial reduction of the radical is avoided. However, this technique has some drawbacks. First, the reaction can take place at undesired sites, which might lead to non-specific spin-labeling.^[126] Second, this technique sometimes causes incomplete extent of labeling, which may turn out to be a hassle while purifying the end product.

Post-synthetic spin labeling can, in principle, be performed at a number of sites in an RNA oligonucleotide, viz., the nucleobase,^[127] the sugar^[128,129] or at the phosphodiester region.^[130,131] The 2'-position of the sugar is of particular interest because it is the only site in the sugar that is available for internal labeling of a nucleic acid. Furthermore, when attached at the 2'-position, the spin label projects out into the minor groove, thus making it a sterically-comfortable position of attachment.

Post-synthetic labeling of 2'-amino groups is a facile and selective approach for labeling the 2'-position of the sugar, because the aliphatic 2'-amino group is more nucleophilic than the aromatic amines on the nucleobases or the hydroxyl groups on the sugars and the phosphodiester linkages. This facilitates easy conversion of the 2'-amino groups to ureas^[66,67] and amides.^[44] Moreover, RNA oligonucleotides having 2'-amino modifications are commercially available or can be synthesized in-house on an automated synthesizer using 2'-amino-modified phosphoramidites that can be readily purchased. Thus, easy availability of starting materials makes this approach highly attractive.

The 2'-amino group has been spin-labeled through reaction with a succinimidyl ester of a pyrrolidine-derived nitroxide spin label to yield an amide-modified spin label; however, this

modification was found to cause considerable destabilization of RNA duplexes (**Figure 5.1**, lower scheme).^[44] The 2'-amino group in RNA has also been modified to form a urea linkage using 4-isocyanato TEMPO (**45**) (**Figure 5.1**, higher scheme).^[66,67] This spin labeling method has been quite popular among many other research groups and it is particularly useful owing to the fact that both the 2'-amino modified RNA and the spin label, 4-isocyanato TEMPO (**45**), are commercially available.



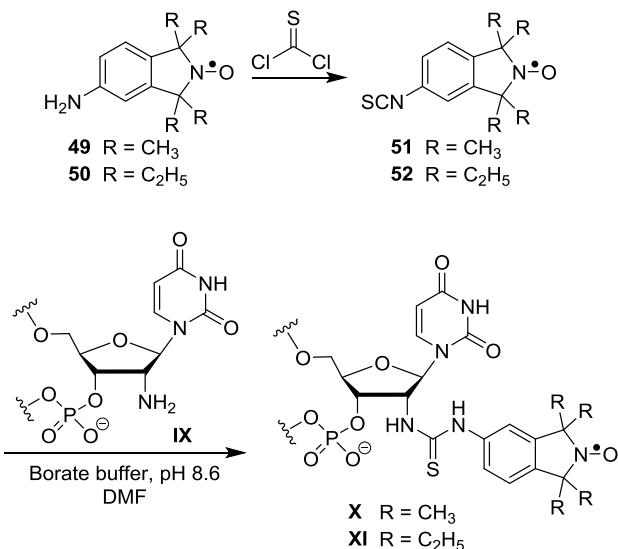
Scheme 5.1. Spin-labeling of 2'-amino position in RNA by amide modification **48** (lower), and by urea modification **46** (higher).

However, despite its usefulness, using aliphatic isocyanates has a few disadvantages. Firstly, 4-isocyanato TEMPO (**45**) is fairly reactive. Therefore, to slow down hydrolysis of the spin label, the reaction has to be performed under controlled conditions, i.e., at a low temperature of $-8\text{ }^{\circ}\text{C}$. Secondly, at this sub-zero temperature, RNA, especially longer ones, are susceptible to forming secondary structures, thus making the reaction sluggish. And thirdly, since TEMPO is a six-membered aliphatic ring, it is known to undergo different conformational changes (viz., chair and boat), which is not a desired property for EPR studies because the more rigid the spin label is, more is the information that can usually be obtained from EPR.

5.2 Spin-Labeling at 2'-Amino Position Using Aromatic Isothiocyanates

As the post-synthetic labeling method of 2'-amino group in RNA with aliphatic isocyanates is associated with the above mentioned problems, we embarked upon trying to improve this

method by introducing new spin-labeling reagents, which are isothiocyanate derivatives of aromatic isoindoline nitroxides. This project was carried out in collaboration with Dr. Anil Jagtap in our research group who prepared both the tetramethyl- (**51**) and tetraethyl- (**52**) derivatives of this isoindoline spin-labeling reagent. These aromatic isothiocyanate spin labels were reacted with a 14-nucleotide 2'-amino modified RNA **IX** (5'-GACCUCG(2'-NH₂U)AUCGUG-3'), forming a highly stable thiourea linkage (**Scheme 5.2**).^[62,69]



Scheme 5.2. Preparation of spin-labeling reagents **51** and **52** from their respective precursors **49** and **50**, respectively (performed by Dr. Anil P. Jagtap); and their reaction with the 2'-amino modified RNA oligonucleotide **IX** [5'-GAC CUC G(2'-NH₂U)A UCG UG] to yield spin-labeled oligonucleotides **X** and **XI**.

By using these new spin labeling reagents, we were able to circumvent all the problems that were associated with the aliphatic isocyanate spin labels. Firstly, the aromatic isoindoline isothiocyanate spin-labeling reagents **51** and **52** are stable nitroxides. Secondly, owing to their stability, the reactions were performed at higher temperatures (37 °C) which prevented the RNA from forming secondary structures. And thirdly, compared to 4-isocyanato TEMPO (**45**), isothiocyanates **51** and **52** have rigid planar structures devoid of any inherent flexibility.

The kinetics and efficiency of the spin labeling reactions of 2'-amino-modified RNA **IX** with aromatic isothiocyanate spin labels **51** and **52** were studied by using denatured polyacrylamide gel electrophoresis (DPAGE) (**Figure 5.1**). Small amounts of reaction mixture were extracted after specific intervals of time and after 8 h, all the samples were run together

on DPAGE. It is evident from both the time-course profiles that reaction of RNA IX with **51** was faster than that of **52**. After 30 min, a prominent new band was seen to have appeared for **51** (**Figure 5.1A**); whereas after the same duration, a faint new band was seen for **52** (**Figure 5.1B**). The new slower-moving band corresponded to an RNA with increased mass which was assumed to be the spin-labeled RNA (**X** or **XI**). It was clear that the reaction of **51** was completed in 2 h whereas the reaction of **52** got over in just over 4 h. No undesired side products could be detected in either reaction.

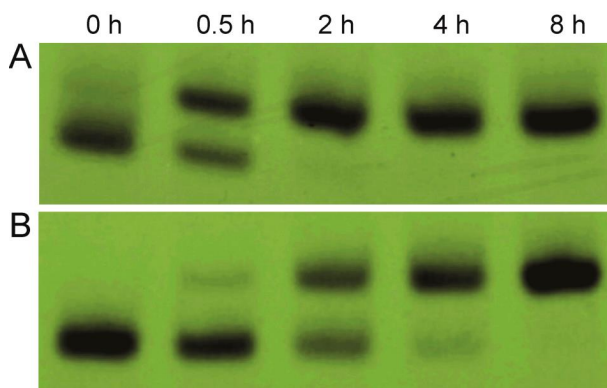


Figure 5.1. Time-courses of spin-labeling reactions of RNA IX with (A) **51** and (B) **52**.

It was also important to know if the reactions were selective to the 2'-amino group in RNA and that the isothiocyanate spin labels were not reacting with other functional groups, such as the exocyclic amines in the bases. Therefore, an unmodified RNA oligonucleotide **XII** (5'-GACCUCGUAUCGUG-3') was subjected to the reaction conditions with **51** and heated at 60 °C. Aliquots were collected at specific time points and analyzed by DPAGE (**Figure 5.2**). No change was observed in the mobility of the unmodified oligonucleotide, even after heating for 48 h, proving that the spin-labeling procedure is highly specific to 2'-amino groups in RNA.

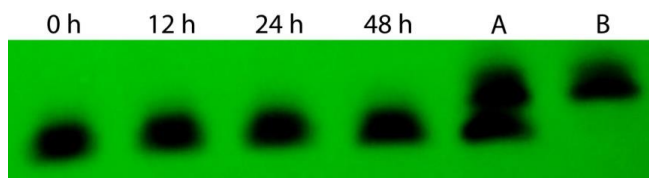


Figure 5.2. DPAGE analysis showing the different time-points of sample collection of reaction of isothiocyanate **51** with the unmodified oligonucleotide **XII** (5'-GAC CUC GUA UCG UG). Lane B contains spin-labeled RNA **X** and lane A is a mixture of the spin-labeled RNA **X** and an aliquot after running the reaction for 48 h.

The purified spin-labeled oligonucleotides **X** and **XI** were analyzed using MALDI-TOF, which verified the incorporation of the spin labels. CD spectra of the duplexes of **X** and **XI** showed negative and positive molar ellipticities at ca. 210 nm and 262-264 nm, respectively, in excellent agreement with the reported values for A-form RNA duplexes.^[132]

It was also important to investigate if the spin labels **51** and **52**, after incorporation into the 2'-amino-modified RNA affected their duplex stability. To gauge their melting temperatures (T_M), thermal denaturation experiments were performed. It was interesting to note that only very minor destabilization of 1.2 °C and 2.0 °C were observed for the duplexes labeled with tetramethyl- (**51**) and the tetraethyl-derivative (**52**), respectively, relative to an unmodified duplex. The corresponding TEMPO-labeled RNA duplex, prepared by reacting 4-isocyanato-TEMPO with oligonucleotide **IX**, was considerably less stable showing a destabilization of 5.3 °C.^[69]

The spin-labeled oligonucleotides were subsequently analyzed by EPR spectroscopy. EPR data, first of all, confirmed successful attachment of the spin labels to the RNA oligonucleotides. Secondly, it was also a final proof that the spin labels were intact, otherwise no EPR signal would have been obtained. And thirdly, EPR data gave valuable information about the mobilities of the spin labels.^[69] **Figure 5.3** shows the EPR spectroscopic data for all the three labels **51**, **52** and **45** in single strands as well as in duplexes. EPR spectra of all the labels were slightly broadened in single-stranded RNAs indicating reduced mobility due to slower tumbling in solution. In duplexes however, the EPR spectra of **51** and **52** were much broader as compared to that of the TEMPO-modified duplex. This was somewhat surprising because although the TEMPO is a flexible label, as mentioned before, the extent of broadening of **51** and **52** implied that the labels were almost fully immobile. Additionally, the data indicated that the isoindoline spin labels were excellent candidates for investigating structure and dynamics of nucleic acids by EPR spectroscopy.

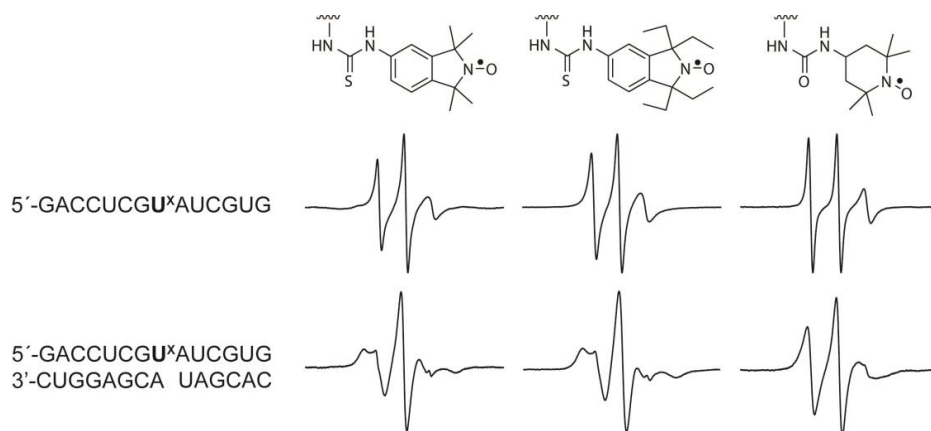


Figure 5.3. EPR spectra of the spin-labeled oligonucleotides in phosphate buffer, recorded at 10 °C.

The reduced mobility of the isoindoline spin labels **51** and **52**, as judged by EPR analysis, was somewhat surprising because rotation along single bonds connecting either ends of the thiourea linker was anticipated to be possible which would have endowed some flexibility to the label. However, careful observation in the molecular model (**Figure 5.4**) yielded a possible explanation for the unexpected rigidity of the labels. The molecular model shows the sulfur atom in yellow, nestled comfortably between the oxygen atom of the 2'-position of uridine and the oxygen belonging to the tetrahydrofuran ring of the following nucleotide towards the 3'-end (**Figure 5.4 B and C**). Due to the resulting snug fit, the sulfur appeared to be “locked” at this particular conformation. Although the spin label can exist as another rotamer which is obtained by rotating the single bond connecting the isoindoline and the thiourea by 180°, rotation of this bond does not alter the position of the sulfur atom. Therefore, molecular modeling concluded and confirmed that the label is indeed fully immobile and the sulfur atom is responsible for endowing the extra rigidity.

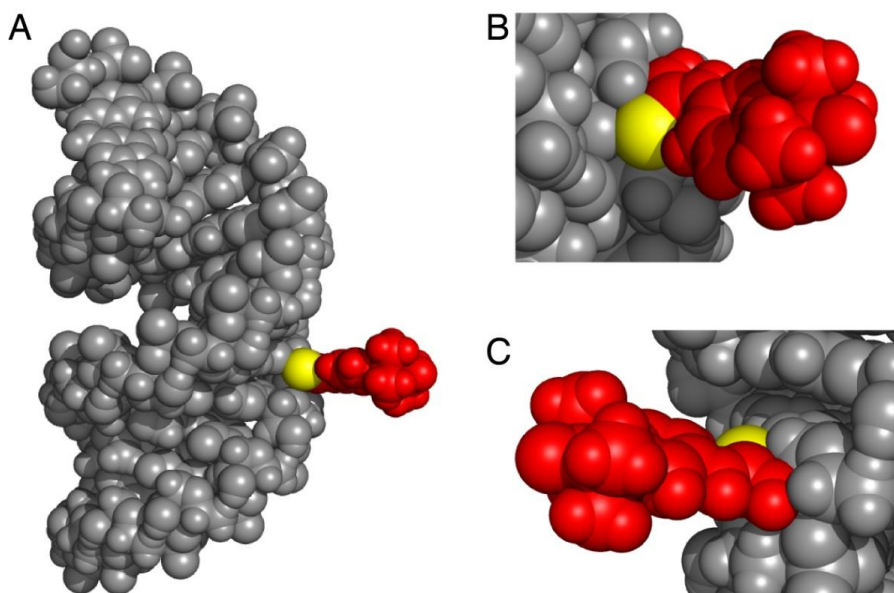


Figure 5.4. Molecular models of the RNA duplex 51 (grey) shown in entirety (A) and as close-ups from two different dimensions (B) and (C). Conjugated spin label 51 has been shown in red except for the sulfur atom that has been colored yellow.

5.2.1 Stability of the Spin Labels 51 and 52 in Reducing Environment

The next step for us was to test the stability of the spin labels in reducing environments. This is because in-cell distance measurement by PELDOR is an important aspect of studying structure and dynamics of nucleic acids by EPR.^[55,133,134] It was therefore, necessary to check the stabilities of the spin labels under cellular conditions, where several reducing agents are present. Ascorbic acid is a known cellular reducing agent and often used to evaluate the stability of nitroxides.^[135-137] Therefore, to check the stability of the spin labels in RNA under reducing conditions, the spin-labeled RNAs were reacted with ascorbic acid in a phosphate buffer and the EPR signal decay was plotted as a function of time (**Figure. 5.5**).

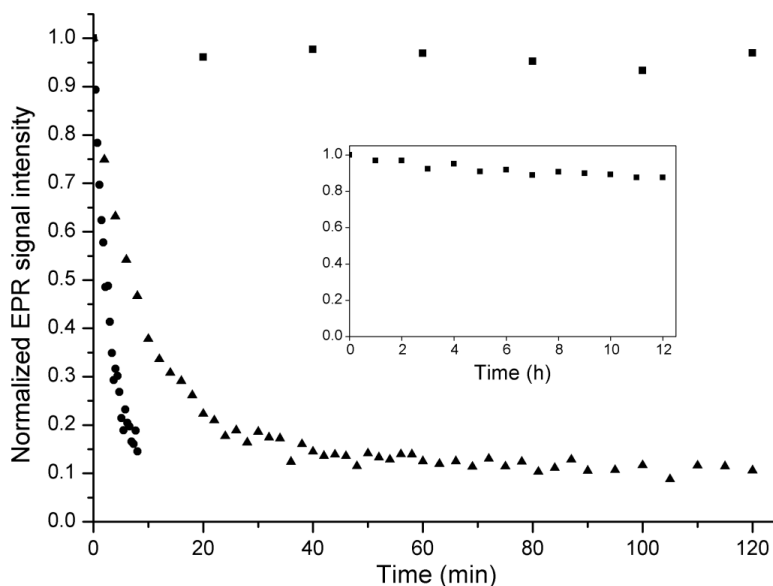


Figure 5.5. Ascorbate reduction data for RNA duplexes labeled with spin labels **45** (circle), **51** (triangle) and **52** (square) in 5 mM ascorbic acid, 10 mM phosphate, 100 mM NaCl, 0.1 mM Na₂EDTA, pH 7.0. Inset shows a longer time course (12 h) for duplex containing **52**.

All the three labels **51**, **52** and **45**, were tested for stability in RNA duplexes (**Figure 5.5**). It was evident that that isocyanato-TEMPO containing duplex was the least stable one under reducing conditions as the EPR signal decayed completely in less than 10 min. The duplex of the tetramethyl isoindoline-modified RNA **X** showed better stability as compared isocyanato-TEMPO containing duplex because the EPR signal survived till 20 min and disintegrated to an equilibrium thereafter. The duplex for the tetraethyl isoindoline-modified RNA **XI** appeared to be highly resistant to reduction as its signal showed very little disintegration after 2 h. This prompted us to study this particular sample for longer duration and ca. 85% of the spin label was found to be intact even after 12 h.^[69] Thus, we could conclude that the tetraethyl spin label **52** is a highly promising candidate for performing in-cell distance measurement experiments using pulsed EPR techniques.

Distance measurement between two paramagnetic centers or spin labels using pulsed EPR techniques such as PELDOR, is an advanced method to study structure and dynamics of biomolecules.^[138,139] Since the tetraethyl isothiocyanate **52** proved to be highly resistant towards reduction, it was decided to use it to label RNA duplex samples and perform in-cell

distance measurement studies. PELDOR is also expected to give further information about the orientation of the spin labels.

For this purpose, three duplex RNA samples (**Table 5.1**) were prepared for inter-spin distance measurements. Overhangs were introduced to prevent end-to-end stacking of duplexes. Distance measurement experiments on these samples are currently underway.

Table 5.1. RNA duplexes prepared for in-cell PELDOR measurements. Nucleotides in blue indicate overhangs that were introduced to prevent end-to-end stacking of the duplexes, X represents uridine labeled post-synthetically with tetraethyl isothiocyanate **52**.

S. No.	Sequence	Modelled Distance (nm)
XIII	5' -A GCG AXG UUA UCU AGA UAA CAU CGC-3' 3' -CGC UAC AAU AGA UCU AUU GXA GCG A-5'	4.7
XIV	5' -GCG AXG UUA UCU AGA UAA CAU CGC A-3' 3' -A CGC UAC AAU AGA UCU AUU GXA GCG-5'	4.7
XV	5' -U GCG AXG UUA UCU AGA UAA CAU CGC-3' 3' -CGC UAC AAU AGA UCU AUU GXA GCG U-5'	4.7

5.3 Conclusion

A new approach for post-synthetic spin labeling of 2'-amino groups in RNA was developed using aromatic isoindoline nitroxides having isothiocyanate functional groups. The reactions were found to be swift with one of the labeling reactions reaching completion in less than 2 h. The nitroxides were well tolerated in RNA duplexes causing minimal destabilization. Moreover, EPR data of these duplexes showed that they were substantially immobile, thus making them excellent candidates for studying structure and dynamics of nucleic acids by pulsed EPR. Finally, the tetraethyl spin label **52** proved to be an exceptional candidate for in-cell PELDOR distance measurements as it demonstrated considerable stability under reductive conditions of ascorbic acid after its incorporation into RNA.

6 Conclusions

In this PhD thesis, development of two new approaches of spin-labeling has been described. One of the new methods is based on an aptamer-ligand binding approach that has been utilized in the context of noncovalent spin-labeling for the first time. Moreover, this method is the first example of spin-labeling that enables one to label unmodified nucleic acids. This approach is based on the adaptive binding of the malachite green aptamer that is known to bind to the dyestuffs malachite green and tetramethyl rosamine. In our study, these ligands have been modified by attaching nitroxide spin labels to them and it was observed that the aptamer was able to bind completely one of the ligands at room temperature which is the first example of noncovalent spin-labeling at ambient conditions. Further, this noncovalent spin-labeling approach was used for determination of a distance between a spin-labeled ligand and a spin label that was covalently attached to the aptamer in collaboration with Prof. Thomas Prisner's research laboratory at the University of Frankfurt. In future, this method can be utilized for spin-labeling of long RNAs that are difficult to synthesize chemically and are mostly prepared by enzymatic methods.

In a related study of noncovalent spin-labeling that was undertaken with our collaborators in Dr. Kye-Simeon Masters' research group based at the Queensland University of Technology in Australia, a new class of benzimidazole-based isoindoline nitroxides was evaluated as spin labels for abasic sites in duplex DNA and RNA. In this study, five such first-in-class benzimidazole-isoindoline hybrids were screened using a combinatorial chemistry-based approach developed in-house, out of which, binding efficiency of two spin labels were analyzed in detail. Additionally, the reduced versions of these nitroxides can be of use as (pro)fluorescent probes because nitroxides are known to quench fluorescence through an intermolecular electron-exchange interaction between their ground-state and the excited-state fluorophore.

Another new method of spin-labeling was developed using a post-synthetic approach, where 2'-amino groups in RNA were reacted with two aromatic isoindoline nitroxides that were modified with isothiocyanate functional groups, thus forming a thiourea linkage with the RNA. This was an in-house collaborative project and the spin labels were prepared by Dr. Anil P. Jagtap. It was observed that the new spin labels caused minimum destabilization of the

RNA duplexes as judged by melting temperature and CD experiments. Also, these spin labels were found to be very rigid, as investigated by CW-EPR spectroscopy, thus making them promising candidates for distance measurement studies using pulsed EPR techniques like PELDOR. Additionally, the tetraethyl-isoindoline derivative was found to be highly resistant towards reduction in presence of ascorbic acid. This particular property of the spin label is expected to be very important as far as in-cell pulsed EPR-based distance measurements studies are concerned, as traditional nitroxides are susceptible towards rapid reduction in the presence of reducing agents in cells.

References

1. Miescher-Rüsch F *Ueber die Chemische Zusammensetzung der Eiterzellen*, 1871.
2. Miescher F *Die Histochemischen und Physiologischen Arbeiten von Friedrich Miescher*; Vogel, 1897.
3. Dahm R, Friedrich Miescher and the discovery of DNA, *Dev. Biol.* 2005, 278, 274-288.
4. Dahm R, Discovering DNA: Friedrich Miescher and the early years of nucleic acid research, *Hum. Genet.* 2008, 122, 565-581.
5. Astbury WT and Bell FO In *Cold Spring Harbor symposia on quantitative biology*; Cold Spring Harbor Laboratory Press: 1938; 6, 109-121.
6. Franklin RE and Gosling RG, The structure of sodium thymonucleate fibres. I. The influence of water content, *Acta Crystallogr.* 1953, 6, 673-677.
7. Franklin RE and Klug A, The splitting of layer lines in X-ray fibre diagrams of helical structures: application to tobacco mosaic virus, *Acta Crystallogr.* 1955, 8, 777-780.
8. Watson JD and Crick F, Molecular structure of nucleic acids: a structure for deoxyribose nucleic acid, *Nature* 1953, 171, 737.
9. Crick F, Central dogma of molecular biology, *Nature* 1970, 227, 561-563.
10. Yusupova GZ, Yusupov MM, Cate J and Noller HF, The path of messenger RNA through the ribosome, *Cell* 2001, 106, 233-241.
11. Ogle JM, Brodersen DE, Clemons WM, Tarry MJ, Carter AP and Ramakrishnan V, Recognition of cognate transfer RNA by the 30S ribosomal subunit, *Science* 2001, 292, 897-902.
12. Oeffinger M, Wei KE, Rogers R, Degrasse JA, Chait BT, Aitchison JD and Rout MP, Comprehensive analysis of diverse ribonucleoprotein complexes, *Nat. Methods* 2007, 4, 951-956.
13. Mamatis T and Reed R, The role of small nuclear ribonucleoprotein particles in pre-mRNA splicing, *Nature* 1987, 325, 673-678.
14. Nissen P, Hansen J, Ban N, Moore PB and Steitz TA, The structural basis of ribosome activity in peptide bond synthesis, *Science* 2000, 289, 920-930.
15. Serganov A and Nudler E, A decade of riboswitches, *Cell* 2013, 152, 17-24.
16. Montange RK and Batey RT, Riboswitches: emerging themes in RNA structure and function, *Annu. Rev. Biophys.* 2008, 37, 117-133.
17. Mandal M and Breaker RR, Gene regulation by riboswitches, *Nat. Rev. Mol. Cell Biol.* 2004, 5, 451-463.
18. Tang G, siRNA and miRNA: an insight into RISCs, *Trends. Biochem. Sci.* 2005, 30, 106-114.
19. Lam JK, Chow MY, Zhang Y and Leung SW, siRNA versus miRNA as therapeutics for gene silencing, *Mol. Ther. Nucleic Acids* 2015, 4, e252.
20. Astbury W In *Symp. Soc. Exp. Biol.* 1947, p 66-76.
21. Holbrook SR, Structural principles from large RNAs, *Annu. Rev. Biophys.* 2008, 37, 445-464.
22. Kim S-G, Lin L-J and Reid BR, Determination of nucleic acid backbone conformation by ¹H NMR, *Biochemistry* 1992, 31, 3564-3574.
23. Wuthrich K *NMR of proteins and nucleic acids*; Wiley, 1986.

24. Sripakdeevong P, Cevce M, Chang AT, Erat MC, Ziegeler M, Zhao Q, Fox GE, Gao X, Kennedy SD and Kierzek R, Structure determination of noncanonical RNA motifs guided by ¹H NMR chemical shifts, *Nat. Methods* 2014, *11*, 413-416.
25. Bermejo GA, Clore GM and Schwieters CD, Improving NMR structures of RNA, *Structure* 2016, *24*, 806-815.
26. Xu Y and Matthews S, TROSY NMR Spectroscopy of Large Soluble Proteins, *Modern NMR Methodology*; Springer, 2011, 97-119.
27. Millar DP, Fluorescence studies of DNA and RNA structure and dynamics, *Curr. Opin. Struct. Biol.* 1996, *6*, 322-326.
28. Sisamakias E, Valeri A, Kalinin S, Rothwell PJ and Seidel CA, Accurate single-molecule FRET studies using multiparameter fluorescence detection, *Methods Enzymol.* 2010, *475*, 455-514.
29. Roy R, Hohng S and Ha T, A practical guide to single-molecule FRET, *Nat. Methods* 2008, *5*, 507-516.
30. Zavoisky E, Paramagnetic relaxation of liquid solutions for perpendicular fields, *J. Phys. USSR* 1945, *9*, 211.
31. Zavoisky E, Spin magnetic resonance in the decimetre-wave region, *J. Phys. USSR* 1946, *10*, 197-198.
32. Berliner LJ *Spin labeling: the next millennium*; Springer Science & Business Media, 2006; Vol. 14.
33. Mabbs FE and Collison D *Electron paramagnetic resonance of d transition metal compounds*; Elsevier, 2013; Vol. 16.
34. Martorana A, Yang Y, Zhao Y, Li Q-F, Su X-C and Goldfarb D, Mn (II) tags for DEER distance measurements in proteins via C-S attachment, *Dalton Trans.* 2015, *44*, 20812-20816.
35. Potapov A, Yagi H, Huber T, Jergic S, Dixon NE, Otting G and Goldfarb D, Nanometer-scale distance measurements in proteins using Gd³⁺ spin labeling, *J. Am. Chem. Soc.* 2010, *132*, 9040-9048.
36. Shelke SA and Sigurdsson ST, Site-Directed Spin Labelling of Nucleic Acids, *Eur. J. Org. Chem.* 2012, *2012*, 2291-2301.
37. Berliner LJ and Reuben J *Spin labeling: theory and applications*; Springer Science & Business Media, 2012; Vol. 8.
38. Jeschke G, Distance measurements in the nanometer range by pulse EPR, *ChemPhysChem* 2002, *3*, 927-932.
39. Marko A, Denysenkov V, Margraf D, Cekan P, Schiemann O, Sigurdsson ST and Prisner TF, Conformational flexibility of DNA, *J. Am. Chem. Soc.* 2011, *133*, 13375-13379.
40. Nguyen P and Qin PZ, RNA dynamics: perspectives from spin labels, *Wiley Interdisciplinary Reviews: RNA* 2012, *3*, 62-72.
41. Sowa GZ and Qin PZ, Site-directed spin labeling studies on nucleic acid structure and dynamics, *Prog. Nucleic Acid Res. Mol. Biol.* 2008, *82*, 147-197.
42. Endeward B, Marko A, Denysenkov V, Sigurdsson ST and Prisner T, Chapter Fourteen-Advanced EPR Methods for Studying Conformational Dynamics of Nucleic Acids, *Methods. Enzymol.* 2015, *564*, 403-425.
43. Prisner T, Marko A and Sigurdsson ST, Conformational dynamics of nucleic acid molecules studied by PELDOR spectroscopy with rigid spin labels, *J. Magn. Reson.* 2015, *252*, 187-198.

44. Kim N-K, Murali A and Deroose VJ, A distance ruler for RNA using EPR and site-directed spin labeling, *Chem. Biol.* 2004, 11, 939-948.
45. Macosko J, Pio M, Tinoco I and Shin Y, A novel 5 displacement spin-labeling technique for electron paramagnetic resonance spectroscopy of RNA, *RNA* 1999, 5, 1158-1166.
46. Prisner T, Rohrer M and Macmillan F, Pulsed EPR spectroscopy: biological applications, *Annu. Rev. Phys. Chem.* 2001, 52, 279-313.
47. Tsvetkov YD, Milov AD and Maryasov AG, Pulsed electron–electron double resonance (PELDOR) as EPR spectroscopy in nanometre range, *Russ. Chem. Rev.* 2008, 77, 487-520.
48. Bode BE, Dastvan R and Prisner TF, Pulsed electron–electron double resonance (PELDOR) distance measurements in detergent micelles, *J. Magn. Reson.* 2011, 211, 11-17.
49. Duss O, Yulikov M, Jeschke G and Allain FH-T, EPR-aided approach for solution structure determination of large RNAs or protein–RNA complexes, *Nat. Commun.* 2014, 5.
50. Jeschke G, DEER distance measurements on proteins, *Annu. Rev. Phys. Chem.* 2012, 63, 419-446.
51. Milov A, Salikhov K and Shirov M, Application of the double resonance method to electron spin echo in a study of the spatial distribution of paramagnetic centers in solids, *Sov. Phys. Solid State* 1981, 23, 565-569.
52. Reginsson GW and Schiemann O, Pulsed electron–electron double resonance: beyond nanometre distance measurements on biomacromolecules, Portland Press Limited, 2011, 434 (3), 353-363.
53. Schiemann O and Prisner TF, Long-range distance determinations in biomacromolecules by EPR spectroscopy, *Quarterly reviews of biophysics* 2007, 40, 1-53.
54. Schiemann O, Cekan P, Margraf D, Prisner TF and Sigurdsson ST, Relative orientation of rigid nitroxides by PELDOR: beyond distance measurements in nucleic acids, *Angew. Chem. Int. Ed.* 2009, 48, 3292-3295.
55. Krstić I, Hänsel R, Romainczyk O, Engels JW, Dötsch V and Prisner TF, Long-range distance measurements on nucleic acids in cells by pulsed EPR spectroscopy, *Angew. Chem. Int. Ed.* 2011, 50, 5070-5074.
56. Kocherginsky N and Swartz HM, *Nitroxide spin labels: reactions in biology and chemistry*; CRC Press, 1995.
57. Fanucci GE and Cafiso DS, Recent advances and applications of site-directed spin labeling, *Curr. Opin. Struct. Biol.* 2006, 16, 644-653.
58. Hubbell WL and Altenbach C, Investigation of structure and dynamics in membrane proteins using site-directed spin labeling, *Curr. Opin. Struct. Biol.* 1994, 4, 566-573.
59. Hubbell WL, Cafiso DS and Altenbach C, Identifying conformational changes with site-directed spin labeling, *Nat. Struct. Mol. Biol.* 2000, 7, 735-739.
60. Shelke SA and Sigurdsson ST, Site-Directed Spin Labeling for EPR Studies of Nucleic Acids, *Modified Nucleic Acids*; Springer: 2016, p 159-187.
61. Shelke SA and Sigurdsson ST In *Structural information from spin-labels and intrinsic paramagnetic centres in the biosciences*; Springer: 2011, p 121-162.
62. Saha S, Jagtap AP and Sigurdsson ST, Chapter Fifteen-Site-Directed Spin Labeling of RNA by Postsynthetic Modification of 2'-Amino Groups, *Methods. Enzymol.* 2015, 563, 397-414.

63. Barhate N, Cekan P, Massey AP and Sigurdsson ST, A nucleoside that contains a rigid nitroxide spin label: a fluorophore in disguise, *Angew. Chem. Int. Ed.* 2007, *119*, 2709-2712.
64. Giotta GJ and Wang HH, Reduction of nitroxide free radicals by biological materials, *Biochem. Biophys. Res. Commun.* 1972, *46*, 1576-1580.
65. Piton N, Mu Y, Stock G, Prisner TF, Schiemann O and Engels JW, Base-specific spin-labeling of RNA for structure determination, *Nucleic Acids Res.* 2007, *35*, 3128-3143.
66. Edwards TE and Sigurdsson ST, Site-specific incorporation of nitroxide spin-labels into 2'-positions of nucleic acids, *Nat. Protoc.* 2007, *2*, 1954-1962.
67. Edwards TE, Okonogi TM, Robinson BH and Sigurdsson ST, Site-specific incorporation of nitroxide spin-labels into internal sites of the TAR RNA; structure-dependent dynamics of RNA by EPR spectroscopy, *J. Am. Chem. Soc.* 2001, *123*, 1527-1528.
68. Büttner L, Javadi-Zarnaghi F and Höbartner C, Site-specific labeling of RNA at internal ribose hydroxyl groups: terbium-assisted deoxyribozymes at work, *J. Am. Chem. Soc.* 2014, *136*, 8131-8137.
69. Saha S, Jagtap AP and Sigurdsson ST, Site-directed spin labeling of 2'-amino groups in RNA with isoindoline nitroxides that are resistant to reduction, *Chem. Commun.* 2015, *51*, 13142-13145.
70. Qin PZ, Iseri J and Oki A, A model system for investigating lineshape/structure correlations in RNA site-directed spin labeling, *Biochem. Biophys. Res. Commun.* 2006, *343*, 117-124.
71. Sicoli G, Wachowius F, Bennati M and Höbartner C, Probing secondary structures of spin-labeled RNA by pulsed EPR spectroscopy, *Angew. Chem. Int. Ed.* 2010, *49*, 6443-6447.
72. Ohnishi S-I and McConnell HM, Interaction of the radical ion of chlorpromazine with deoxyribonucleic acid, *J. Am. Chem. Soc.* 1965, *87*, 2293-2293.
73. Hong S-J and Piette LH, Electron spin resonance spin-label studies of intercalation of ethidium bromide and aromatic amine carcinogens in DNA, *Cancer Res.* 1976, *36*, 1159-1171.
74. Ottaviani MF, Ghatlia ND, Bossmann SH, Barton JK, Duerr H and Turro NJ, Nitroxide-labeled ruthenium (II)-polypyridyl complexes as EPR probes to study organized systems. 2. Combined photophysical and EPR investigations of B-DNA, *J. Am. Chem. Soc.* 1992, *114*, 8946-8952.
75. Sinha BK and Chignell CF, Acridine spin labels as probes for nucleic acids, *Life Sci.* 1975, *17*, 1829-1836.
76. Shelke SA and Sigurdsson ST, Noncovalent and Site-Directed Spin Labeling of Nucleic Acids, *Angew. Chem. Int. Ed.* 2010, *49*, 7984-7986.
77. Reginsson GW, Shelke SA, Rouillon C, White MF, Sigurdsson ST and Schiemann O, Protein-induced changes in DNA structure and dynamics observed with noncovalent site-directed spin labeling and PELDOR, *Nucleic Acids Res.* 2013, *41*, e11.
78. Kamble NR, Gränz M, Prisner TF and Sigurdsson ST, Noncovalent and site-directed spin labeling of duplex RNA, *Chem. Commun.* 2016, *52*, 14442-14445.
79. Hermann T and Patel DJ, Adaptive recognition by nucleic acid aptamers, *Science* 2000, *287*, 820-825.
80. Ellington AD and Szostak JW, In vitro selection of RNA molecules that bind specific ligands, *Nature* 1990, *346*, 818.

81. Tuerk C and Gold L, Systematic evolution of ligands by exponential enrichment: RNA ligands to bacteriophage T4 DNA polymerase, *Science* 1990, 249, 505-510.
82. Yarus M, Widmann JJ and Knight R, RNA–amino acid binding: a stereochemical era for the genetic code, *J. Mol. Evol.* 2009, 69, 406.
83. Rimmle M, Nucleic acid aptamers as tools and drugs: recent developments, *Chembiochem* 2003, 4, 963-971.
84. Hamaguchi N, Ellington A and Stanton M, Aptamer beacons for the direct detection of proteins, *Anal. Biochem.* 2001, 294, 126-131.
85. Famulok M, Oligonucleotide aptamers that recognize small molecules, *Curr. Opin. Struct. Biol.* 1999, 9, 324-329.
86. Bunka DH and Stockley PG, Aptamers come of age—at last, *Nature Rev. Microbiol.* 2006, 4, 588-596.
87. Nahvi A, Sudarsan N, Ebert MS, Zou X, Brown KL and Breaker RR, Genetic control by a metabolite binding mRNA, *Chem. Biol.* 2002, 9, 1043-1049.
88. Mascini M *Aptamers in bioanalysis*; John Wiley & Sons, 2009.
89. Tombelli S and Mascini M, Aptamers as molecular tools for bioanalytical methods, *Curr. Opin. Mol. Ther.* 2009, 11, 179-188.
90. Conrad R, Keranen LM, Ellington AD and Newton AC, Isozyme-specific inhibition of protein kinase C by RNA aptamers, *J. Biol. Chem.* 1994, 269, 32051-32054.
91. Ruckman J, Green LS, Beeson J, Waugh S, Gillette WL, Henninger DD, Claesson-Welsh L and Janjic N, 2'-Fluoropyrimidine RNA-based aptamers to the 165-amino acid form of vascular endothelial growth factor (VEGF165) Inhibition of receptor binding and VEGF-induced vascular permeability through interactions requiring the exon 7-encoded domain, *J. Biol. Chem.* 1998, 273, 20556-20567.
92. Pendergrast PS, Marsh HN, Grate D, Healy JM and Stanton M, Nucleic acid aptamers for target validation and therapeutic applications, *J Biomol. Tech.* 2005, 16, 224.
93. Mayer G and Jenne A, Aptamers in research and drug development, *BioDrugs* 2004, 18, 351-359.
94. Li J, Zhong X, Cheng F, Zhang J-R, Jiang L-P and Zhu J-J, One-pot synthesis of aptamer-functionalized silver nanoclusters for cell-type-specific imaging, *Anal. Chem.* 2012, 84, 4140-4146.
95. Song S, Wang L, Li J, Fan C and Zhao J, Aptamer-based biosensors, *Trends Anal. Chem.* 2008, 27, 108-117.
96. Wilson DS and Szostak JW, In vitro selection of functional nucleic acids, *Annu. Rev. Biochem.* 1999, 68, 611-647.
97. Grate D and Wilson C, Laser-mediated, site-specific inactivation of RNA transcripts, *Proc. Natl. Acad. Sci.* 1999, 96, 6131-6136.
98. Da Costa JB, Andreiev AI and Dieckmann T, Thermodynamics and kinetics of adaptive binding in the malachite green RNA aptamer, *Biochemistry* 2013, 52, 6575-6583.
99. Baugh C, Grate D and Wilson C, 2.8 Å crystal structure of the malachite green aptamer, *J. Mol. Biol.* 2000, 301, 117-128.
100. Flinders J, Defina SC, Brackett DM, Baugh C, Wilson C and Dieckmann T, Recognition of planar and nonplanar ligands in the malachite green–RNA aptamer complex, *ChembioChem* 2004, 5, 62-72.
101. Lux J, Peña EJ, Bolze F, Heinlein M and Nicoud JF, Malachite Green Derivatives for Two-Photon RNA Detection, *ChembioChem* 2012, 13, 1206-1213.

102. Gannett PM, Darian E, Powell JH and Johnson EM, A short procedure for synthesis of 4-ethynyl-2, 2, 6, 6-tetramethyl-3, 4-dehydro-piperidine-1-oxyl nitroxide, *Synth. Commun.* 2001, 31, 2137-2141.
103. Wang T, Hoy JA, Lamm MH and Nilsen-Hamilton M, Computational and experimental analyses converge to reveal a coherent yet malleable aptamer structure that controls chemical reactivity, *J. Am. Chem. Soc.* 2009, 131, 14747-14755.
104. Schiemann O, Piton N, Plackmeyer J, Bode BE, Prisner TF and Engels JW, Spin labeling of oligonucleotides with the nitroxide TPA and use of PELDOR, a pulse EPR method, to measure intramolecular distances, *Nat. Protoc.* 2007, 2, 904-923.
105. Blinco JP, Hodgson JL, Morrow BJ, Walker JR, Will GD, Cooté ML and Bottle SE, Experimental and theoretical studies of the redox potentials of cyclic nitroxides, *J. Org. Chem.* 2008, 73, 6763-6771.
106. Keddie DJ, Fairfull-Smith KE and Bottle SE, The palladium-catalysed copper-free Sonogashira coupling of isoindoline nitroxides: a convenient route to robust profluorescent carbon-carbon frameworks, *Org. Biomol. Chem.* 2008, 6, 3135-3143.
107. Babendure JR, Adams SR and Tsien RY, Aptamers switch on fluorescence of triphenylmethane dyes, *J. Am. Chem. Soc.* 2003, 125, 14716-14717.
108. Zhou Y, Chi H, Wu Y, Marks RS and Steele TW, Organic additives stabilize RNA aptamer binding of malachite green, *Talanta* 2016, 160, 172-182.
109. Milov A, Maryasov A and Tsvetkov YD, Pulsed electron double resonance (PELDOR) and its applications in free-radicals research, *Appl. Magn. Reson.* 1998, 15, 107-143.
110. Schiemann O, Piton N, Mu Y, Stock G, Engels JW and Prisner TF, A PELDOR-based nanometer distance ruler for oligonucleotides, *J. Am. Chem. Soc.* 2004, 126, 5722-5729.
111. Chiang Y-W, Borbat PP and Freed JH, The determination of pair distance distributions by pulsed ESR using Tikhonov regularization, *J. Magn. Reson.* 2005, 172, 279-295.
112. Morris JC, McMurtrie JC, Bottle SE and Fairfull-Smith KE, Generation of profluorescent isoindoline nitroxides using click chemistry, *J. Org. Chem.* 2011, 76, 4964-4972.
113. Fairfull-Smith KE, Brackmann F and Bottle SE, The Synthesis of Novel Isoindoline Nitroxides Bearing Water-Solubilising Functionality, *Eur. J. Org. Chem.* 2009, 1902-1915.
114. Fairfull-Smith KE and Bottle SE, The synthesis and physical properties of novel polyaromatic profluorescent isoindoline nitroxide probes, *Eur. J. Org. Chem.* 2008, 5391-5400.
115. Keddie DJ, Johnson TE, Arnold DP and Bottle SE, Synthesis of profluorescent isoindoline nitroxides via palladium-catalysed Heck alkenylation, *Org. Biomol. Chem.* 2005, 3, 2593-2598.
116. Gophane DB and Sigurdsson ST, Hydrogen-bonding controlled rigidity of an isoindoline-derived nitroxide spin label for nucleic acids, *Chem. Commun.* 2013, 49, 999-1001.
117. Knölker HJ, Hitzemann R and Boese R, Imidazole Derivatives, III. Regiospecific Synthesis, Structure, and Fluorescence Properties of Highly substituted Imidazo [1, 2-a] pyridines and Pyrido [1, 2-a] benzimidazoles, *Eur. J. Inorg. Chem.* 1990, 123, 327-339.
118. Ge YQ, Jia J, Yang H, Tao XT and Wang JW, The synthesis, characterization and optical properties of novel pyrido [1, 2-a] benzimidazole derivatives, *Dyes and pigments* 2011, 88, 344-349.

119. Dhamnaskar S and Rangnekar D, Synthesis of triazoflo [4, 5-b] pyrido [1', 2'-a] benzimidazole derivatives as fluorescent disperse dyes and whiteners for polyester fibre, *Dyes and pigments* 1988, 9, 467-473.
120. Blough NV and Simpson DJ, Chemically mediated fluorescence yield switching in nitroxide-fluorophore adducts: optical sensors of radical/redox reactions, *J. Am. Chem. Soc.* 1988, 110, 1915-1917.
121. London E, Investigation of membrane structure using fluorescence quenching by spin-labels, *Mol. Cell. Biochem.* 1982, 45, 181-188.
122. Chalmers BA, Saha S, Nguyen T, Mcurtrie J, Sigurdsson ST, Bottle SE and Masters K-S, TMIO-PyrImid hybrids are profluorescent, site-directed spin labels for nucleic acids, *Org. Lett.* 2014, 16, 5528-5531.
123. Altman RA, Koval ED and Buchwald SL, Copper-catalyzed N-arylation of imidazoles and benzimidazoles, *J. Org. Chem.* 2007, 72, 6190-6199.
124. Masters KS, Rauws TR, Yadav AK, Herrebout WA, Van Der Veken B and Maes BU, On the Importance of an Acid Additive in the Synthesis of Pyrido [1, 2-a] benzimidazoles by Direct Copper-Catalyzed Amination, *Chem. Eur. J.* 2011, 17, 6315-6320.
125. Cekan P, Smith AL, Barhate N, Robinson BH and Sigurdsson ST, Rigid spin-labeled nucleoside C: a nonperturbing EPR probe of nucleic acid conformation, *Nucleic Acids Res.* 2008, 36, 5946-5954.
126. Sigurdsson ST and Eckstein F, Site specific labelling of sugar residues in oligoribonucleotides: reactions of aliphatic isocyanates with 2' amino groups, *Nucleic Acids Res.* 1996, 24, 3129-3133.
127. Ramos A and Varani G, A New Method To Detect Long-Range Protein- RNA Contacts: NMR Detection of Electron- Proton Relaxation Induced by Nitroxide Spin-Labeled RNA, *J. Am. Chem. Soc.* 1998, 120, 10992-10993.
128. Caron M and Dugas H, Specific spin-labeling of transfer ribonucleic acid molecules, *Nucleic Acids Res.* 1976, 3, 19-34.
129. Pscheidt RH and Wells BD, Different conformations of the 3'termini of initiator and elongator transfer ribonucleic acids. An EPR study, *J. Biol. Chem.* 1986, 261, 7253-7256.
130. Grant GPG and Qin PZ, A facile method for attaching nitroxide spin labels at the 5' terminus of nucleic acids, *Nucleic Acids Res.* 2007, 35, e77.
131. Fidanza JA and Mclaughlin LW, Introduction of reporter groups at specific sites in DNA containing phosphorothioate diesters, *J. Am. Chem. Soc.* 1989, 111, 9117-9119.
132. Steely HT, Gray DM, Lang D and Maestre MF, Circular dichroism of double-stranded RNA in the presence of salt and ethanol, *Biopolymers* 1986, 25, 91-117.
133. Milov A, Samoilova R, Tsvetkov YD, Gusev V, Formaggio F, Crisma M, Toniolo C and Raap J, Spatial distribution of spin-labeled trichogin GA IV in the gram-positive bacterial cell membrane determined from PELDOR data, *Appl. Magn. Reson.* 2002, 23, 81-95.
134. Hänsel R, Luh LM, Corbeski I, Trantirek L and Doetsch V, In-cell NMR and EPR spectroscopy of biomacromolecules, *Angew. Chem. Int. Ed.* 2014, 53, 10300-10314.
135. Jagtap AP, Krstic I, Kunjir NC, Hänsel R, Prisner TF and Sigurdsson ST, Sterically shielded spin labels for in-cell EPR spectroscopy: analysis of stability in reducing environment, *Free Radic. Res.* 2015, 49, 78-85.
136. Kinoshita Y, Yamada K-I, Yamasaki T, Sadasue H, Sakai K and Utsumi H, Development of novel nitroxyl radicals for controlling reactivity with ascorbic acid, *Free Radic. Res.* 2009, 43, 565-571.

137. Kinoshita Y, Yamada K-I, Yamasaki T, Mito F, Yamato M, Kosem N, Deguchi H, Shirahama C, Ito Y and Kitagawa K, In vivo evaluation of novel nitroxyl radicals with reduction stability, *Free Radic. Biol. Med.* 2010, 49, 1703-1709.
138. Schiemann O, Weber A, Edwards TE, Prisner TF and Sigurdsson ST, Nanometer distance measurements on RNA using PELDOR, *J. Am. Chem. Soc.* 2003, 125, 3434-3435.
139. Tsvetkov YD and Grishin YA, Techniques for EPR spectroscopy of pulsed electron double resonance (PELDOR): a review, *Instrum. Exp. Tech.* 2009, 52, 615-636.

Publications

- I. Benjamin A Chalmers, Subham Saha, Tri Nguyen, John McMurtrie, Snorri Th Sigurdsson, Steven E Bottle, and Kye-Simeon Masters. "TMIO-Pyrimid Hybrids Are Profluorescent, Site-Directed Spin Labels for Nucleic Acids", *Org. Lett.* (2014), 16 (21), 5528-31.
- II. Subham Saha, Anil P Jagtap, and Snorri Th Sigurdsson. "Site-Directed Spin Labeling of 2'-Amino Groups in RNA with Isoindoline Nitroxides That Are Resistant to Reduction", *Chem. Commun.* (2015), 51 (66), 13142-45.
- III. Subham Saha, Anil P Jagtap, and Snorri Th Sigurdsson. "Chapter Fifteen-Site-Directed Spin Labeling of RNA by Postsynthetic Modification of 2'-Amino Groups." (Editors: Peter Z. Qin and Kurt Warncke), *Methods Enzymol.* (2015), 563, 397-414
- IV. Subham Saha, Thilo Hetzke, Thomas F Prisner and Snorri Th Sigurdsson. "Noncovalent Spin-Labeling of Unmodified RNA: The Aptamer Approach", (*Manuscript in preparation*).

Paper I

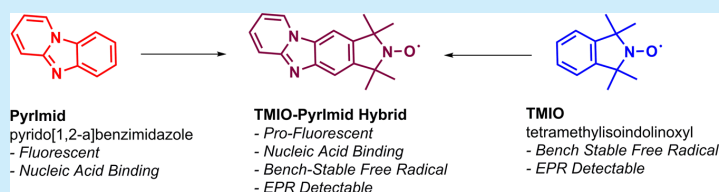
TMIO-PyrImid Hybrids are Profluorescent, Site-Directed Spin Labels for Nucleic Acids

Benjamin A. Chalmers,[†] Subham Saha,[‡] Tri Nguyen, John McMurtrie, Snorri Th. Sigurdsson,^{*,‡} Steven E. Bottle,^{*,†} and Kye-Simeon Masters^{*,†}

[†]Faculty of Science and Engineering, Queensland University of Technology, P.O. Box 2434, 2 George Street, Brisbane, QLD 4001, Australia

[‡]University of Iceland, Department of Chemistry, Science Institute, Dunhaga 3, 107 Reykjavík, Iceland

S Supporting Information



ABSTRACT: We report the synthesis of a new class of molecules which are hybrids of long-lived tetramethylisoidolinoxyl (TMIO) radicals and the pyrido[1,2-*a*]benzimidazole (PyrImid) scaffold. These compounds represent a new lead for noncovalently binding nucleic acid probes, as they interact with nucleic acids with previously unreported C (DNA) and C/U (RNA) complementarity, which can be detected by electron paramagnetic resonance (EPR) techniques. They also have promising properties for fluorimetric analysis, as their fluorescent spin-quenched derivatives exhibit a significant shift.

Research has established nitroxides¹ as the most prominent class of bench-stable free radicals,² and they have therefore been adapted to a diverse array of applications.³ Ongoing efforts have capitalized upon opportunities for the application of structurally diverse nitroxide compounds as antioxidants (free-radical scavengers of superoxides),⁴ stabilizers in the materials industry,⁵ and both chemical (radical clocks⁶) and biological (cellular redox⁷) probes. Recent examples of these include biologically active agents, including roles that can be considered as both metabolically “active” (e.g., chemotherapeutic antioxidant⁸) and “passive” (e.g., electron paramagnetic resonance probes⁹). A prime example of the latter is the use of nitroxides as site-directed spin labels in the analysis of the structure and dynamics of nucleic acids,¹⁰ thereby providing information about their function.¹¹ This involves EPR studies upon a probe molecule bound to RNA or DNA. As the spin label becomes more constrained (by binding to a nucleotide), the EPR spectrum becomes increasingly anisotropic,^{12,11b} which gives information about local structure and orientations in distance measurements.⁵ Binding is also flanking-sequence dependent, providing information about neighboring nucleotides.¹³

Introduction of the requisite spin label is usually achieved by either covalent incorporation of a nitroxide-bearing nucleobase analogue into the nucleic acid sequence¹⁴ or by postsynthetic covalent linkage of the spin label to a functionality of the nucleic acid.¹⁵ More recently, Sigurdsson and co-workers have pioneered noncovalent binding of ζ (“c-spin”), which is the nucleobase of the nucleoside ζ (Figure 1).¹⁶ This site-directed

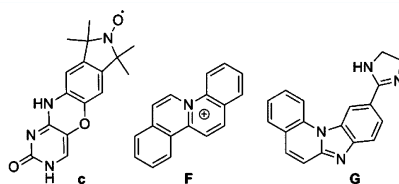


Figure 1. Nitroxide ζ (EPR detection),¹⁶ quinizolinium F (spectrophotometric titration),¹⁷ and DNA intercalator G (anti-cancer).²¹

spin label is a nucleobase isostere of cytidine. It forms stable Watson–Crick pairing with guanine residues and π – π interactions with adjacent base pairs, enabling it to be added to a variety of preformed nucleic acid polymers. A contrasting method for analysis of nucleic acids is with the use of fluorescent noncovalent binders for spectrophotometric titration. In a recent example, Ihmels and co-workers have described the application of quinizolinium scaffolds such as “F” as new probes for abasic DNA.¹⁷ Despite these recent advances in nucleic acid probe technology, noncovalently binding spin labels with complementarity for cytidine (C), thymine (T), adenine (A), and uracil (U) await discovery.

A compound class that may provide an opportunity to achieve this goal are pyrido[1,2-*a*]benzimidazoles, or “PyrImids”.

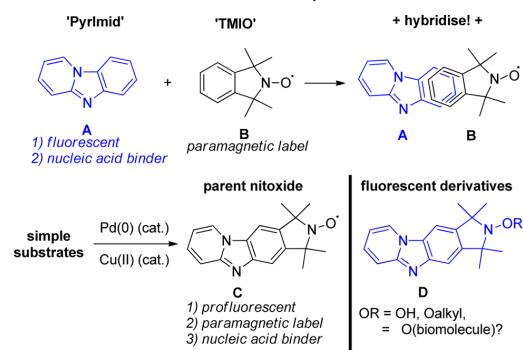
Received: July 20, 2014

Published: October 28, 2014

These interesting imidazole-containing heterocycles are known to possess biological activities, including antipyretic,¹⁸ anti-biotic,¹⁹ and anticancer effects.²⁰ The latter property arises through the isosterism of PyrImid derivatives such as benzimidazo[1,2-*a*]quinazoline, **G**, with purines, which enables their nucleic acid intercalation. Hranjec, Kralj, Zamola, and co-workers found²¹ that derivatives such as **G** (Figure 1) arrest cellular mitosis through their interaction with topoisomerase II, thereby inhibiting growth of human colorectal and other cancer cells. PyrImids are furthermore highly fluorescent²² and possess a remarkable Stokes shift.

Isoindolinoyl radicals based upon “TMIO”, or 1,1,3,3-tetramethylisoindolin-2-oxyl, are one of the most rigid and stable nitroxide classes commonly prepared. Importantly, these nitroxides have a moiety that strongly suppresses fluorescence²³ when in conjugation with a fluorophore; the fluorescence can be (re)generated by “spin-deletion” via one of several methods. It seemed that the marriage of the key features of both PyrImid “A” and TMIO “B” cores may result from simply superimposing the C₆ aryl ring of the core in each to create a hybrid molecular probe, “C” (Scheme 1). It was hypothesized that the

Scheme 1. Fusion of TMIO and PyrImid

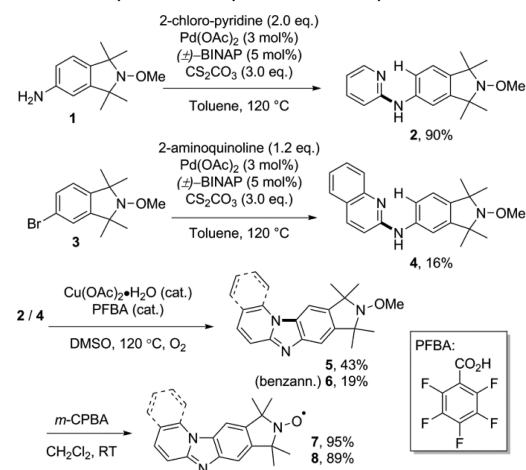


probe would retain the features of each of the individual progenitor compounds: the (pro)fluorescence, notable Stokes shift, nucleobase isosterism/intercalation, and detection by electron paramagnetic resonance (EPR). To facilitate the development of this project, direct and modular methods for the synthesis of the “PyrImid” core via C–H functionalization have been developed by the research groups of Zhu²⁴ and Maes.²⁵

The synthesis of an array of π -extended and rigid nitroxides may be readily achieved through the application of Buchwald–Hartwig coupling to form *N*-arylamidines²⁶ and copper-catalyzed C–H amination to cyclize the subsequent methyl-protected TMIO derivatives; these has recently benefitted from the use of a methoxyamine protecting group strategy.²⁷ Beginning from known TMIO derivatives, the methoxyamines **1**²⁵ and **3**²⁷ (Scheme 2) can be generated in high yields via Fenton chemistry. Subsequent coupling of either 2-chloropyridine (with **1**) or 2-aminoquinoline (with **3**) can be achieved through Buchwald–Hartwig amination under the conditions of Maes and co-workers^{26b,c} to yield amidines **2** and **4** in yields which varied depending upon the substrates (90–16%, with 2-chloroquinoline failing to deliver **4**).

Cyclizations of *N*-aryl-*N*-pyridylamine **2** and *N*-aryl-*N*-quinylamine **4** were performed with conditions developed by

Scheme 2. Synthesis of PyrImid-TMIO Hybrids 7 and 8



Maes and co-workers.²⁵ Catalytic amounts of cupric acetate monohydrate and a fluorinated benzoic acid ligand, 2,3,4,5,6-pentafluorobenzoic acid (PFBA, Scheme 2), were applied to the amidines in DMSO under an atmosphere of oxygen to effect Cu-mediated C–H amination/oxidative cyclization to the aromatic products **5** and **6**, which were isolated in workable yields (19–43%) following purification. The existing procedure was notably improved by the use of diethyl ether as eluent to quickly deliver the TMIOme–PyrImid derivative as a sharp band (cf. NH₃ in methanol/CH₂Cl₂ in the reported method). The subsequent *m*-CPBA deprotection, which proceeds via *N*-oxidation and Cope-like elimination,²⁷ delivered the spin-labeled targets in high yields (89–95%).

In line with previously characterized PyrImid derivatives, TMIOme–Pyrimid hybrid **5** was discovered to produce a significant Stokes shift (165 nm, Figure 2). In the case of π -

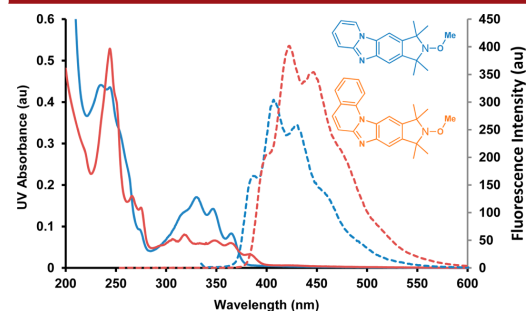


Figure 2. UV (solid line) and fluorescence (dashed line) spectra for Compounds **5** and **6**.

extended **6**, this was even greater (179 nm). Alkoxyamines **5** and **6**, once deprotected to the nitroxide radicals **7** and **8**, exhibited a decreased fluorescence, particularly in the case of **8** (see the Supporting Information). These properties provide supporting evidence for the potential application of compounds related to **7** and **8** as a profluorescent nitroxide (PFN) probes. Structural confirmation and crystal packing analysis for the

novel structures of **5** and **6** were achieved by X-ray diffractometry (see the Supporting Information).

Using EPR spectroscopy, nitroxide radicals **7** and **8** were evaluated as spin labels for noncovalent binding (see the Supporting Information) to an abasic site in DNA and RNA duplexes at temperatures ranging from 0 to $-30\text{ }^{\circ}\text{C}$ (Figure 3

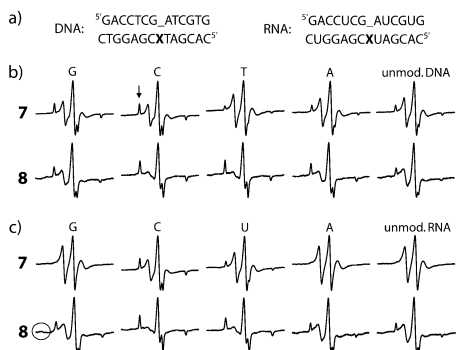


Figure 3. (a) DNA and RNA duplexes used for EPR binding studies where “_” denotes an abasic site and X the complementary base. EPR spectra showing the extent of binding of **7** and **8** to DNA (b) and RNA (c), respectively, at $-30\text{ }^{\circ}\text{C}$. Letters above each spectrum denote the base opposite to the abasic site. For unmodified duplexes, “_” and X stand for C and G, respectively. Binding studies were performed in phosphate buffer (pH = 7.0) containing 2% DMSO and 30% ethylene glycol at $-30\text{ }^{\circ}\text{C}$. The arrow indicates the slow moving (bound) component and the circle shows signs of aggregation.

and Figures S11–S14, Supporting Information). A spin label bound to a nucleic acid duplex moves slower and results in a wider EPR spectrum that reflects a shorter rotational correlation time.^{16b} Prior to recording EPR data, it was confirmed by thermal denaturation experiments and circular dichroism (CD) that the DNA and RNA oligonucleotides were in duplex form under the conditions used for ligand binding (see the Supporting Information). The EPR data revealed partial binding of nitroxide **7** to DNA as judged by the emergence of a slow moving component at low temperatures (denoted by an arrow in Figure 3b), which was also observed in the control experiment, indicating some nonspecific binding. However, there was slight, but noticeable, specific binding (ca. 10%) observed at $-30\text{ }^{\circ}\text{C}$ when G or C was the orphan base opposite to the abasic site. More substantial binding was observed when **7** was incubated with an RNA duplex containing an abasic site, in particular opposite C (ca. 40%) and U (ca. 25%). In addition, the binding was clearly specific since the unmodified RNA duplex showed no indication of binding to nitroxide **7** (Figure 3c).

In contrast to **7**, the EPR data for nitroxide **8** revealed significant and substantially increased binding to both DNA and RNA, presumably due to the extra aromatic ring that facilitates additional stacking interactions. For DNA, the highest affinity was observed for an abasic site complementary to C or T, where nearly all of the label was bound at $-30\text{ }^{\circ}\text{C}$; however, some nonspecific binding was also observed (Figure 3b). Although the extra aromatic character of **8** led to better binding, it also showed signs of aggregation in the EPR spectra (denoted by a circle in Figure 3c), especially for the sequences that had limited affinity for the spin label. The EPR data of

nitroxide **8** in the presence of RNA duplexes surprisingly resembled those for DNA (Figure 3c). However, close observation revealed less RNA binding, compared with DNA, when the abasic site was placed opposite to A and slightly more binding to C, the latter of which showed complete binding.

In summary, we have developed an expedient route for the synthesis of a promising new class of hybrid PyrImid–TMIO probes while retaining the useful properties of each of the parent compounds and may provide a mechanism for fluorescence/EPR detection. Nitroxide **8** provided complete binding to C as an orphan base in an abasic DNA or RNA duplex, previously inaccessible, target site. Further structural refinement of this exciting new class of probes in terms of nucleobase specificity, optical properties, and solubility under biological conditions is in progress, and the results will be reported in due course.

■ ASSOCIATED CONTENT

Supporting Information

Experimental procedures, NMR spectra and X-ray crystallographic data. This material is available free of charge via the Internet at <http://pubs.acs.org>.

■ AUTHOR INFORMATION

Corresponding Authors

*E-mail: snorrisi@hi.is.

*E-mail: s.bottle@qut.edu.au.

*E-mail: kye.masters@qut.edu.au.

Notes

The authors declare no competing financial interest.

■ ACKNOWLEDGMENTS

B.A.C. acknowledges a fellowship from the Australian Research Council Centre of Excellence for Free Radical Chemistry and Biotechnology, Grant No. CE0561607. K.-S.M. acknowledges the generous support of a Vice-Chancellor’s Research Fellowship from QUT. This work was also supported by the Icelandic Research Fund (141062051, S.Th.S.) and by a doctoral fellowship from the University of Iceland Research Fund (S.S.). We thank Mr. N. Kamble for assistance in collecting thermal denaturation data for the RNA oligonucleotide duplexes.

■ REFERENCES

- (1) Stryer, L.; Griffith, H. O. *Proc. Natl. Acad. Sci. U.S.A.* **1965**, *54*, 1785–1791.
- (2) Tebben, L.; Studer, A. *Angew. Chem., Int. Ed.* **2011**, *50*, 5034–5068.
- (3) Soule, B. P.; Hyodo, F.; Matsumo, K.-I.; Simone, N. L.; Cook, J. A.; Krishna, M. C.; Mitchell, J. B. *Free Radical Biol. & Med.* **2007**, *42*, 1632–1650.
- (4) Samunis, A.; Krishna, C. M.; Riesz, P.; Finkelstein, E.; Rusw, A. *Biol. Chem.* **1988**, *263* (43), 17921–17924.
- (5) Fairfull-Smith, K. E.; Blinco, J. P.; Keddle, D. J.; George, G. A.; Bottle, S. E. *Macromolecules* **2008**, *41*, 1577–1580.
- (6) Beckwith, A. L. J.; Bowry, V. W. *J. Org. Chem.* **1988**, *53*, 1632–1641.
- (7) (a) Swartz, H. M.; Chen, K.; Pals, M.; Sentjurc, M.; Morse, P. D., II. *Magn. Reson. Med.* **1986**, *3*, 169–174. (b) Morrow, B. J.; Keddle, D. J.; Gueven, N.; Lavin, M. F.; Bottle, S. E. *Free Radical Biol. Med.* **2010**, *40*, 67–76.
- (8) (a) Walker, J. R.; Fairfull-Smith, K. E.; Anzai, K.; Lau, S. P.; White, J.; Scammells, P. J.; Bottle, S. E. *Med. Chem. Commun.* **2011**, *2*,

- 436–441. (c) Hosokawa, K.; Chen, P.; Lavin, M. F.; Bottle, S. E. *Free Radicals Biol. Med.* **2004**, *37*, 946–952.
- (9) Shelke, S. A.; Sigurdsson, S. Th. *Eur. J. Org. Chem.* **2012**, 2291–2301.
- (10) Shelke, S. A.; Sigurdsson, S. Th. *Struct. Bonding (Berlin)* **2013**, *152*, 121–162.
- (11) (a) Kim, N. K.; Murali, A.; DeRose, V. J. *J. Am. Chem. Soc.* **2005**, *127*, 14134–14135. (b) Zang, X.; Cekan, P.; Sigurdsson, S. Th.; Qin, P. Z. In *Methods in Enzymology*; Herschlag, D., Ed.; Academic Press: New York, 2009; Vol. 469, pp 303–328.
- (12) Edwards, T. E.; Okonogi, T. M.; Sigurdsson, S. Th. *Biochemistry* **2002**, *41*, 14843–7. (b) Jacobsen, U.; Shelke, S. A.; Vogel, S.; Sigurdsson, S. Th. *J. Am. Chem. Soc.* **2010**, *132*, 10424–8. (c) Edwards, T. E.; Robinson, B. H.; Sigurdsson, S. Th. *Chem. Biol.* **2005**, *12*, 329–337.
- (13) Shelke, S. A.; Sigurdsson, S. Th. *Nucleic Acids Res.* **2012**, *40* (8), 3732–3740.
- (14) Gannett, P. M.; Darian, E.; Powell, J.; Johnson, E. M., II; Mundoma, C.; Greenbaum, N. L.; Ramsey, C. M.; Dalal, N. S.; Budil, D. E. *Nucleic Acids Res.* **2002**, *30* (23), 5328–5337.
- (15) (a) Schiemann, O.; Piton, N.; Plackmeyer, J.; Bode, B. E.; Prinsner, T. F.; Engels, J. W. *Nat. Protoc.* **2007**, *2*, 904–923. (b) Sowa, G. Z.; Qin, P. Z. *Prog. Nucleic Acid Res. Mol. Biol.* **2008**, *82*, 147–197. (c) J. Zhang, X.; Cekan, P.; Sigurdsson, S. Th.; Qin, P. Z. *Methods Enzymol.* **2009**, *469*, 303–328.
- (16) (a) Barhate, N.; Cekan, P.; Massey, A. P.; Sigurdsson, S. Th. *Angew. Chem., Int. Ed.* **2007**, *46*, 2655–2658. (b) Shelke, S. A.; Sigurdsson, S. Th. *Angew. Chem., Int. Ed.* **2010**, *49*, 7984–7986.
- (17) Benner, K.; Ihmels, H.; Kölsch, S.; Pithan, P. M. *Org. Biomol. Chem.* **2014**, *12*, 1725–1734.
- (18) Prostakov, N. S.; Varlamov, A. V.; Shendrik, I. V.; Anisimov, B. N.; Krapivko, A. P.; Lavani-Edogivierie, S.; Fomichev, A. A. *Khim. Geterotsikl. Soedin.* **1983**, *10*, 1384–1386.
- (19) Rifaximin: Koo, H. L.; Dupont, H. L. *Curr. Opin. Gastroenterol.* **2010**, *26*, 17–25.
- (20) (a) Brana, M. F.; Castellano, J. M.; Keilhauer, G.; Machuca, A.; Martin, Y.; Redondo, C.; Schlick, E.; Walker, N. *Anti-Cancer Drug Des.* **1994**, *9*, 527–538. (b) Deady, L. W.; Rodemann, T.; Finlay, G. J.; Baguley, B. C.; Denny, W. A. *Anti-Cancer Drug Des.* **2000**, *15*, 339–346. (c) Weinkauff, R. L.; Chen, A. Y.; Yu, C.; Liu, L.; Barrows, L.; LaVoie, E. J. *Bioorg. Med. Chem.* **1994**, *2* (8), 781–786. (d) Cox, O.; Jackson, H.; Vargas, V. A.; Bæz, A.; Colón, J. I.; Gonzalez, B. C.; De León, M. J. *Med. Chem.* **1982**, *25*, 1378–1381. (e) Muir, M. M.; Cox, O.; Rivera, L. A. *Inorg. Chim. Acta* **1992**, *191*, 131–139. (f) Alegria, A. A.; Cox, O.; Santiago, V.; Colon, M.; Reyes, Z.; Zayas, L.; Rivera, L. A.; Dumas, J. A. *Free Radical Biol. Med.* **1993**, *15*, 49–56. (g) Vivas-Mejía, P.; Rodríguez-Cabán, J. L.; Díaz-Velázquez, M.; Hernández-Pérez, M. G.; Cox, O.; Gonzalez, F. A. *Mol. Cell. Biochem.* **1997**, *177*, 69–77. (h) Vivas-Mejía, P.; Cox, O.; Gonzalez, F. A. *Mol. Cell. Biochem.* **1998**, *178*, 203–212.
- (21) (a) Hranjec, M.; Kralj, M.; Piantanida, I.; Sedić, M.; Šuman, L.; Pavelić, K.; Karminski-Zamola, G. *J. Med. Chem.* **2007**, *50*, 5696. (b) Sedić, M.; Poznic, M.; Gehrig, P.; Scott, M.; Schlapbach, R.; Hranjec, M.; Karminski-Zamola, G.; Pavelić, K.; Kraljevic, S. *Mol. Cancer Ther.* **2008**, *7*, 2121. (c) Hranjec, M.; Piantanida, I.; Kralj, M.; Šuman, L.; Pavelić, K.; Karminski-Zamola, G. *J. Med. Chem.* **2008**, *51*, 4899. (d) Hranjec, M.; Lučić, B.; Ratkaj, I.; Pavelić, S. K.; Piantanida, I.; Pavelić, K.; Karminski-Zamola, G. *Eur. J. Med. Chem.* **2011**, *46*, 2748–2758.
- (22) Fluorescence: (a) Smirnova, E. N.; Onshenskaya, T. V.; Zvolinskii, V. P.; Nnde, D. L. *Fiz. Khim. Poverkh.* **1988**, 65–72. (b) Bae, J.-S.; Lee, D.-W.; Lee, D.-H.; Jeong D.-S., WO2007011163A1, 2007. (c) Erckel, R.; Gnther, D.; Frhbeis H. DE2640760A1, 1978. (d) Schefczik, E. DE2701659A1, 1978. (e) Denhert, J.; Lamm, G., DE2022817, 1972.
- (23) (a) Ahn, H.-Y.; Fairfull-Smith, K. E.; Morrow, B. J.; Lussini, V.; Kim, B.; Bondar, M. V.; Bottle, S. E.; Belfield, K. D. *J. Am. Chem. Soc.* **2012**, *134*, 4721–4730. (b) Blinco, J.; Fairfull-Smith, K.; Morrow, B.; Bottle, S. *Aust. J. Chem.* **2011**, *64*, 373–389.
- (24) (a) Wang, H.; Wang, Y.; Peng, C.; Zhang, J.; Zhu, Q. *J. Am. Chem. Soc.* **2010**, *132*, 13217. (b) He, Y.; Huang, J.; Liang, D.; Liu, L.; Zhu, Q. *Chem. Commun.* **2013**, *49*, 7352–7354.
- (25) Masters, K.-S.; Rauws, T. R. M.; Yadav, A. K.; Herrebout, W. A.; Van der Veken, B.; Maes, B. U. W. *Chem.—Eur. J.* **2011**, *17*, 6315–6320.
- (26) (a) Meyers, C.; Maes, B. U. W.; Loones, K. T. J.; Bal, G.; Lemière, G. L. F.; Dommissie, R. A. *J. Org. Chem.* **2004**, *69*, 6010. (b) Anderson, K. W.; Tundel, R. E.; Ikawa, T.; Altman, R. A.; Buchwald, S. L. *Angew. Chem., Int. Ed.* **2006**, *45*, 6523. (c) Hostyn, S.; Van Baelen, G.; Lemière, G. L. F.; Maes, B. U. W. *Adv. Synth. Catal.* **2008**, *350*, 2653. (d) Shen, Q.; Ogata, T.; Hartwig, J. F. *J. Am. Chem. Soc.* **2008**, *130*, 6586.
- (27) Chalmers, B. A.; Morris, J. C.; Fairfull-Smith, K. E.; Grainger, R. S.; Bottle, S. E. *Chem. Commun.* **2013**, *49*, 10382.

TMIO-Pyrimid Hybrids are Profluorescent, Site-Directed Spin Labels for Nucleic Acids

Benjamin A. Chalmers,[†] Subham Saha,[‡] Tri Nguyen,[†] John McMurtrie,[†] Snorri Th. Sigurdsson,^{‡*} Steven E. Bottle,^{†*} Kye-Simeon Masters^{†*}

[†] Faculty of Science and Engineering, Queensland University of Technology, PO Box 2434, 2 George St, Brisbane, QLD 4001, Australia.

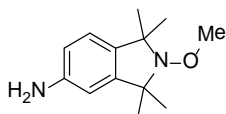
[‡] University of Iceland, Department of Chemistry, Science Institute, Dunhaga 3, 107 Reykjavik, Iceland.

Supporting Information

General Experimental

All chemicals and solvents were used as commercially supplied without further purification, unless otherwise noted. 2-Methoxy-1,1,3,3-tetramethylisoindolin-2-amine (**1**) was synthesised according to the procedure of Bottle and co-workers,ⁱ likewise 5-bromo-2-methoxy-1,1,3,3-tetramethylisoindoline (**3**) was prepared by the method of Bottle and co-workers.ⁱⁱ 2-Chloropyridine (99%), 2-chloroquinoline (99%), cupric acetate monohydrate (≥99%), palladium diacetate (98%), (±)-2,2'-bis(diphenylphosphino)-1,1'-binaphthyl [(±)-BINAP] (97%) and pentafluorobenzoic acid (99%) were supplied by Aldrich. Toluene (analytical reagent grade, obtained from Chemsupply Australia) was dried over freshly-pressed sodium wire prior to use. Both anhydrous powdered cesium carbonate (99%) and dimethylsulfoxide (Reagentplus ≥99.5% purity) were obtained from Aldrich. Buchwald-Hartwig coupling and Cu-catalysed C–H amination were adapted from the methodology of Maes and co-workers.ⁱⁱⁱ Column chromatography was performed on Davisil (LC60A, 40-63µm Grace). NMR data were recorded on a Varian Infinity-Plus 400 spectrometer (¹H at 400 MHz; ¹³C at 100 MHz), and resonances are reported in terms of chemical shift (δ) in parts per million (ppm) referenced to the solvent peak; coupling constants (*J*) are given in Hertz (Hz) and the number of protons per signal as *n*H. Splitting is reported as br. = broad, s = singlet, d = doublet, dd = doublet of doublets and m = multiplet.

Preparation and Characterisation of Compounds

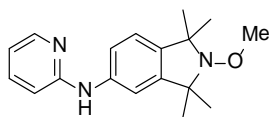


2-Methoxy-1,1,3,3-tetramethylisoindolin-5-amine (**1**)

Prepared by the method of Bottle, Belfield and co-workers.ⁱ

¹H NMR (400 MHz, CDCl₃): δ = 6.88 (d, *J* = 7.83 Hz, 1H), 6.56 (dd, *J* = 8.22, 1.96 Hz, 1H), 6.42 (d, *J* = 1.96 Hz, 1H), 3.77 (s, 3H), 3.60 (br. s, 2H), 1.39 (br. s, 12H); ¹³C NMR (101 MHz, CDCl₃): 146.3, 145.2,

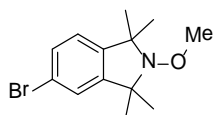
135.8, 122.2, 114.7, 108.4, 67.1, 66.7, 65.4 (isoindoline methyl peaks not visible due to rapid ring flipping on the NMR time-scale); **HRMS (+ESI)**: Calculated ($C_{13}H_{21}N_2O^+$): 221.1654; Found: 221.1696



2-Methoxy-1,1,3,3-tetramethyl-N-(pyridin-2-yl)isoindolin-5-amine (**2**)

To a 5 mL microwave vial (Biotage) were added palladium acetate (3 mol%), (\pm)-2,2'-bis(diphenylphosphino)-1,1'-binaphthyl [(\pm)-BINAP] (5 mol%) and toluene (anhydrous, 2.0 mL, 0.10 M relative to the limiting reagent), and the resulting mixture then stirred under a shower of argon for 10 minutes. After this time, 2-methoxy-1,1,3,3-tetramethylisoindolin-5-amine, **1**, (limiting reagent, 44.0 mg, 0.20 mmol) and 2-chloropyridine (45.0 mg, 0.40 mmol) were added alongside cesium carbonate (195 mg, 0.60 mmol, 3.00 eq.). The reaction vial was capped under argon and heated to 115 °C with vigorous stirring for 48 hours. After this time the crude reaction mixture was diluted with CH_2Cl_2 , silica gel added, the volatiles removed by rotary evaporation under diaphragm pump vacuum (to 30 MBar) and the amidine compound was isolated by column chromatography on silica gel with ethyl acetate/hexanes (1:9, 1:4, then 1:1), which gave the title compound **2** as a beige wax; 53.3 mg, 0.18 mmol, 90% yield.

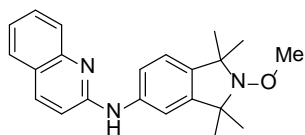
1H NMR (400 MHz, $CDCl_3$): δ = 8.18 (d, J = 3.91 Hz, 1H) 7.40–7.54 (m, 1H) 7.18 (dd, J = 7.83, 1.57 Hz, 1H) 6.99–7.08 (m, 2H) 6.83 (d, J = 8.22 Hz, 1H) 6.65–6.78 (m, 2H) 3.72–3.86 (m, 3H) 1.44 (br. s, 12 H); **^{13}C NMR (101 MHz, $CDCl_3$)**: δ = 156.4, 148.4, 146.4, 140.2, 139.5, 137.7, 122.3, 120.4, 114.7, 114.2, 107.8, 67.1, 66.9, 65.5. (isoindoline methyl peaks not visible due to rapid ring flipping on the NMR time-scale). **HRMS (+ESI)**: Calculated ($C_{18}H_{25}N_3O^+$): 298.1919; Found: 298.1969.



5-Bromo-2-methoxy-1,1,3,3-tetramethylisoindoline (**3**)

Prepared by the method of Bottle and co-workers.ⁱⁱ

1H NMR (400 MHz, $CDCl_3$): δ = 7.35 (dd, J = 8.05, 1.87 Hz, 1H), 7.23 (d, J = 1.84 Hz, 1H), 6.98 (d, J = 8.05 Hz, 1H), 3.78 (s, 3H), 1.42 (br. s, 12H); **HRMS (+ESI)**: Calculated ($C_{13}H_{19}NBrO^+$): 284.0650; Found: 284.0697.

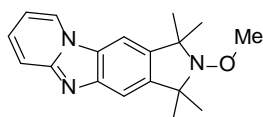


N-(2-Methoxy-1,1,3,3-tetramethylisoindolin-5-yl)quinolin-2-amine (**4**)

To a 5 mL microwave vial (Biotage) were added palladium acetate (7.5 mg, 0.033 mmol, 3 mol%), (\pm)-2,2'-bis(diphenylphosphino)-1,1'-binaphthyl [(\pm)-BINAP] (28.3 mg, 0.045 mmol, 4 mol%) and toluene (anhydrous, 11.0 mL, 0.10 M relative to the limiting reagent), and the resulting mixture then stirred under a shower of argon for 10 minutes. After this time 5-bromo-2-methoxy-1,1,3,3-

tetramethylisoindoline, **3**, (limiting reagent, 320 mg, 1.13 mmol) and 2-aminoquinoline (195.0 mg, 1.35 mmol) were added alongside cesium carbonate (1.10 g, 3.38 mmol, 3.00 eq.). The reaction vial was capped under argon and heated to 115 °C with vigorous stirring for 48 hours. After this time the crude reaction mixture was diluted with CH₂Cl₂, silica gel added, the volatiles removed by rotary evaporation under diaphragm pump vacuum (to 30 MBar) and the amidine compound was isolated by column chromatography eluting with CH₂Cl₂, then gradient methanol/CH₂Cl₂ (1:199, 1:99, 1:49, 1:32 and 1:16), which gave the title compound **4** as a beige wax; 61.0 mg, 0.18 mmol, 16% yield.

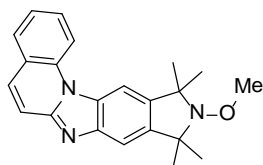
¹H NMR (400 MHz, CDCl₃): δ = 7.85 (d, *J* = 9.00 Hz, 1 H), 7.69 (dd, *J* = 7.83 Hz, 1 H), 7.59 (d, *J* = 7.83, 1H), 7.53 (t, *J* = 7.63 Hz, 1 H), 7.32 (d, *J* = 7.83 Hz, 1 H), 7.18 - 7.29 (m, 2 H), 7.04 (d, *J* = 7.83 Hz, 1 H), 6.92 (d, *J* = 9.00 Hz, 1 H), 3.76 (s, 3 H), 1.42 (br. s, 12 H); **¹³C NMR (101 MHz, CDCl₃):** δ = 154.7, 147.6, 146.3, 140.4, 139.2, 137.8, 129.8, 127.4, 126.5, 124.1, 123.0, 122.2, 120.4, 114.4, 111.5, 67.1, 66.9, 65.5 (isoindoline methyl peaks not visible due to rapid ring flipping on the NMR time-scale). **HRMS (+ESI):** Calculated (C₂₂H₂₆N₃O⁺): 348.2076; Found: 348.2264.



2-Methoxy-1,1,3,3-tetramethyl-2,3,4a,10a-tetrahydro-1H-pyrido[1',2':1,2]imidazo[4,5-f]isoindole (5**)**

2-Methoxy-1,1,3,3-tetramethyl-*N*-(pyridin-2-yl)isoindolin-5-amine, **2**, (67.5 mg, 0.25 mmol), catalytic cupric acetate monohydrate (6.8 mg, 0.034 mmol, 15 mol%), 2,3,4,5,6-pentafluorobenzoic acid (7.2 mg, 0.034 mmol, 15 mol%) and DMSO (1.00 mL) were added to a 10 mL microwave vial. The resulting reaction mixture was stirred under a flow of oxygen for 5 minutes, during which time all the copper salt dissolved, prior to sealing under oxygen with a pressure cap. The reaction vessel was then supplied with additional oxygen balloon by a needle through the cap septum and heated by a temperature-calibrated aluminium hotplate at 122 °C for 24 h. After this time, the vial was unsealed and the reaction mixture taken up in ethyl acetate (10 mL), then washed with concentrated NH₄OH(aq)/water (1:9, 50 mL). The organic phase was then washed with H₂O (2 x 10 mL), dried over Na₂SO₄ and the volatiles removed by rotary evaporation under diaphragm pump vacuum (to 30 MBar). The resulting residue was isolated by column chromatography on silica gel eluting with diethyl ether - the products location on the column can be visualised in a dark fume-hood using a UV light wand (336 nm) - to deliver the title compound **5** as a brown wax, 31.9 mg, 0.108 mmol, 43% yield.

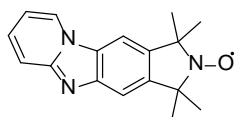
¹H NMR (400 MHz, CDCl₃): δ = 8.44 (d, *J* = 7.0 Hz, 1 H), 7.66 (d, *J* = 9.4 Hz, 1 H), 7.62 (s, 1 H), 7.59 (s, 1 H), 7.39 (ddd, *J* = 0.8, 5.9, 7.8 Hz, 1 H), 6.83 (t, *J* = 6.7 Hz, 1 H), 3.83 (s, 3 H), 1.55 (br. s, 12 H); **¹³C NMR (101 MHz, CDCl₃):** δ = 148.4, 144.3, 144.2, 139.7, 128.8, 128.2, 124.9, 117.9, 112.3, 110.1, 103.2, 67.0, 66.9, 65.5 (isoindoline methyl peaks not visible due to rapid ring flipping on the NMR time-scale). **HRMS (+ESI):** Calculated (C₁₈H₂₃N₃O⁺): 296.1763; Found: 296.1790.



10-Methoxy-9,9,11,11-tetramethyl-10,11-dihydro-9H-isoindolo[5',6':4,5]imidazo[1,2-a]quinolone (6)

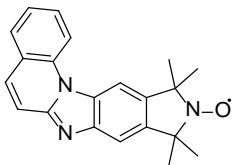
N-(2-Methoxy-1,1,3,3-tetramethylisoindolin-5-yl)quinolin-2-amine, **4**, (45.0 mg, 0.13 mmol), catalytic cupric acetate monohydrate (6.5 mg, 0.033 mmol, 25 mol%) and 2,3,4,5,6-pentafluorobenzoic acid (6.9 mg, 0.033 mmol, 15 mol%) and DMSO (2.00 mL) were added to a 10 mL microwave vial. The resulting reaction mixture was stirred under a flow of oxygen for 5 minutes, during which time all the copper salt dissolved, prior to sealing under oxygen with a pressure cap. The reaction vessel was then supplied with additional oxygen balloon by a needle through the cap septum and heated by a temperature-calibrated aluminium hotplate at 145 °C for 36 h. After this time, the vial was unsealed and the reaction mixture taken up in ethyl acetate (10 mL), then washed with concentrated NH₄OH(aq)/water (1:9, 50 mL). The organic phase was then washed with H₂O (2 x 10 mL), dried over Na₂SO₄ and the volatiles removed by rotary evaporation under diaphragm pump vacuum (to 30 MBar). The resulting residue was isolated by column chromatography on silica gel eluting with diethyl ether /hexanes (3:2)- the products location on the column can be visualised in a dark fume-hood using a UV light wand (336 nm) - to deliver the title compound **6** as a brown oil which formed a wax upon standing, 8.5 mg, 0.025 mmol, 19% yield.

¹H NMR (400 MHz, CDCl₃): δ = 8.58 (d, *J* = 8.61 Hz, 1H), 8.06 (s, 1 H), 7.85 (d, *J* = 7.83 Hz, 1 H), 7.80 (t, *J* = 7.83 Hz, 1 H), 7.71 (s, 1 H), 7.67 (d, *J* = 8.0 Hz, 1 H), 7.62 (d, *J* = 8.0 Hz, 1 H), 7.50 (t, *J* = 7.43 Hz, 1 H), 3.85 (s, 3 H), 1.34 - 1.91 (m, 12 H); ¹³C NMR (101 MHz, CDCl₃) δ = 148.3, 144.7, 142.7, 141.2, 135.7, 130.7, 130.6, 129.6, 124.1, 123.5, 117.9, 115.2, 113.1, 106.8, 67.3, 67.0, 65.6 (isoindoline methyl peaks not visible due to rapid ring flipping on the NMR time-scale). HRMS (+ESI): Calculated (C₂₂H₂₄N₃O⁺): 346.1919; Found: 346.1957.



10,11-Dihydro-[5',6':4,5]imidazo[1,2-a]quinolon-9H-9,9,11,11-tetramethylisoindolin-2-yloxy (7)

To a stirred solution of 2-methoxy-1,1,3,3-tetramethyl-2,3,4a,10a-tetrahydro-1H-pyrido[1',2':1,2]imidazo[4,5-f]isoindole, **5**, (4.9 mg, 0.16 mmol) in CH₂Cl₂ (1.00 mL) was added *meta*-chloroperbenzoic acid (*m*-CPBA, 77% by weight, 5.0 mg, 0.050 mmol, 3.0 eq.). The reaction was monitored by TLC and a second portion of *m*-CPBA was added after 0.5 h. After 1 h, the reaction mixture was diluted with CH₂Cl₂ (10 mL) and washed with H₂O (2 x 5 mL), dried over Na₂SO₄ and the volatiles removed by rotary evaporation under diaphragm pump vacuum (to 30 MBar). There were several components in the reaction mixture (as determined by TLC). The product was isolated by planar chromatography on silica with MeOH/CH₂Cl₂ (1:8) to furnish the product as a pale-yellow powder; 1.8 mg, 6.4 x 10⁻³ mmol, 40% yield. HRMS (+ESI): Calculated (C₁₇H₁₉N₃O⁺): 281.1523; Found: 281.1633.

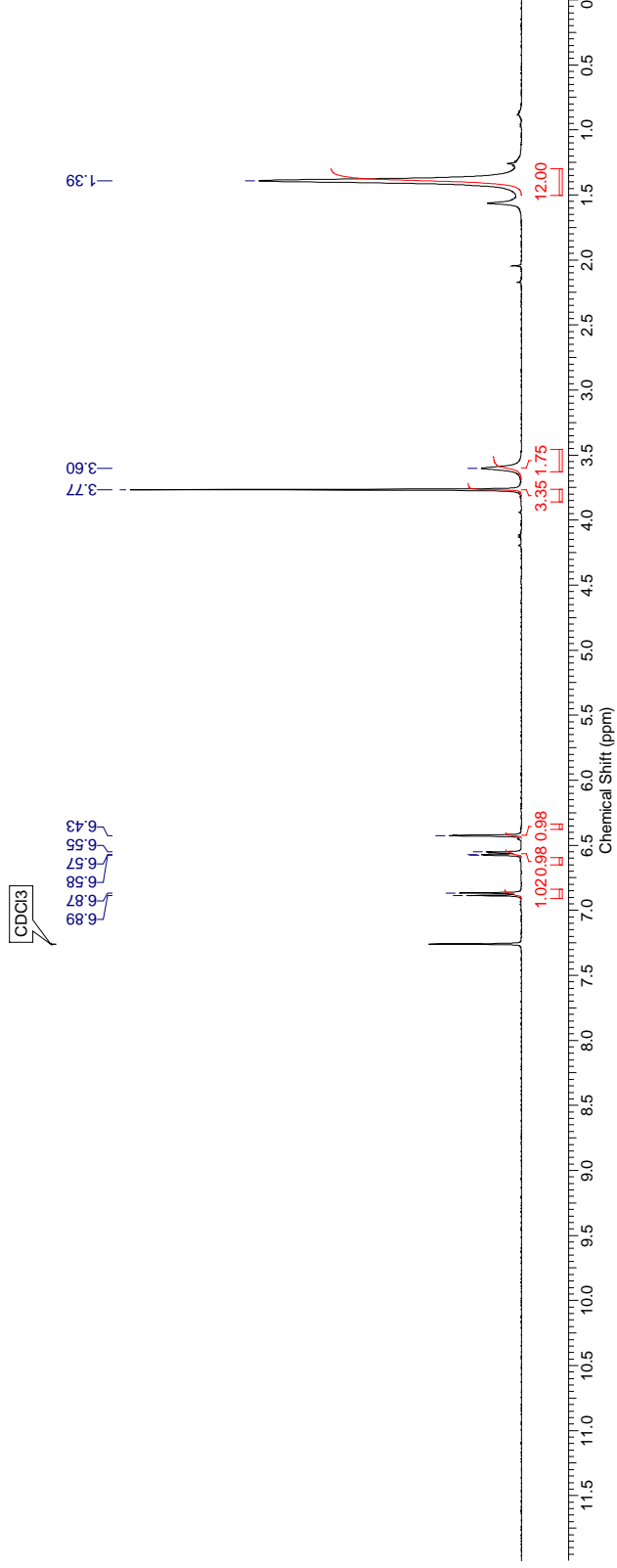
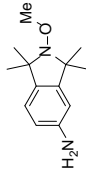


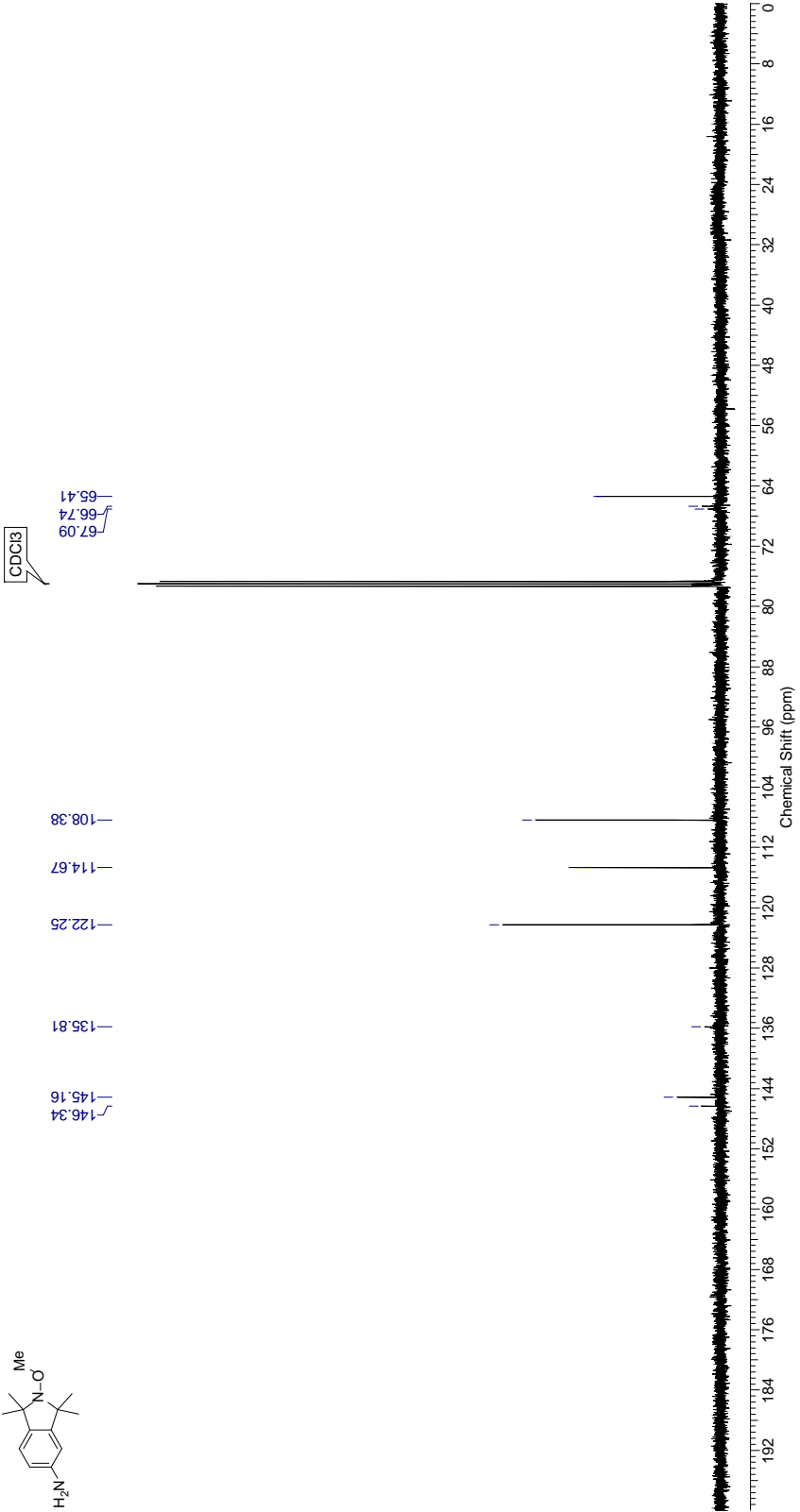
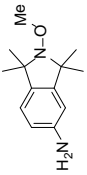
10,11-Dihydro-[5',6':4,5]imidazo[1,2-a]quinolon-9H-9,9,11,11-tetramethylisoindolin-2-yloxy (8)

[[Note-care was taken with stoichiometry and reaction duration in this step in order to prevent formation of aromatic *N*-oxides]] To a stirred solution of 10-methoxy-9,9,11,11-tetramethyl-10,11-dihydro-9H-isoindolo[5',6':4,5]imidazo[1,2-*a*]quinolone, **6**, (2.7 mg, 7.8 x 10⁻³ mmol) in CH₂Cl₂ was added *meta*-chloroperbenzoic acid (*m*-CPBA, 77% by weight, 1.8 mg, 7.8 x 10⁻³ mmol, 1.00 eq.). The reaction was monitored by TLC and two more equally-sized portions of *m*-CPBA were added after 6 h and 12 h. After 24 h, the reaction mixture was passed through a short silica plug with ethyl acetate/hexane (3:2) and the volatiles removed by rotary evaporation under diaphragm pump vacuum (to 30 MBar) to furnish the title compound **8** as a pale-yellow crystalline solid; 2.3 mg, 7.0 x 10⁻³ mmol, 89% yield. **HRMS (+ESI)**: Calculated (C₂₁H₂₁N₃O⁺): 331.1679; Found: 331.1733.

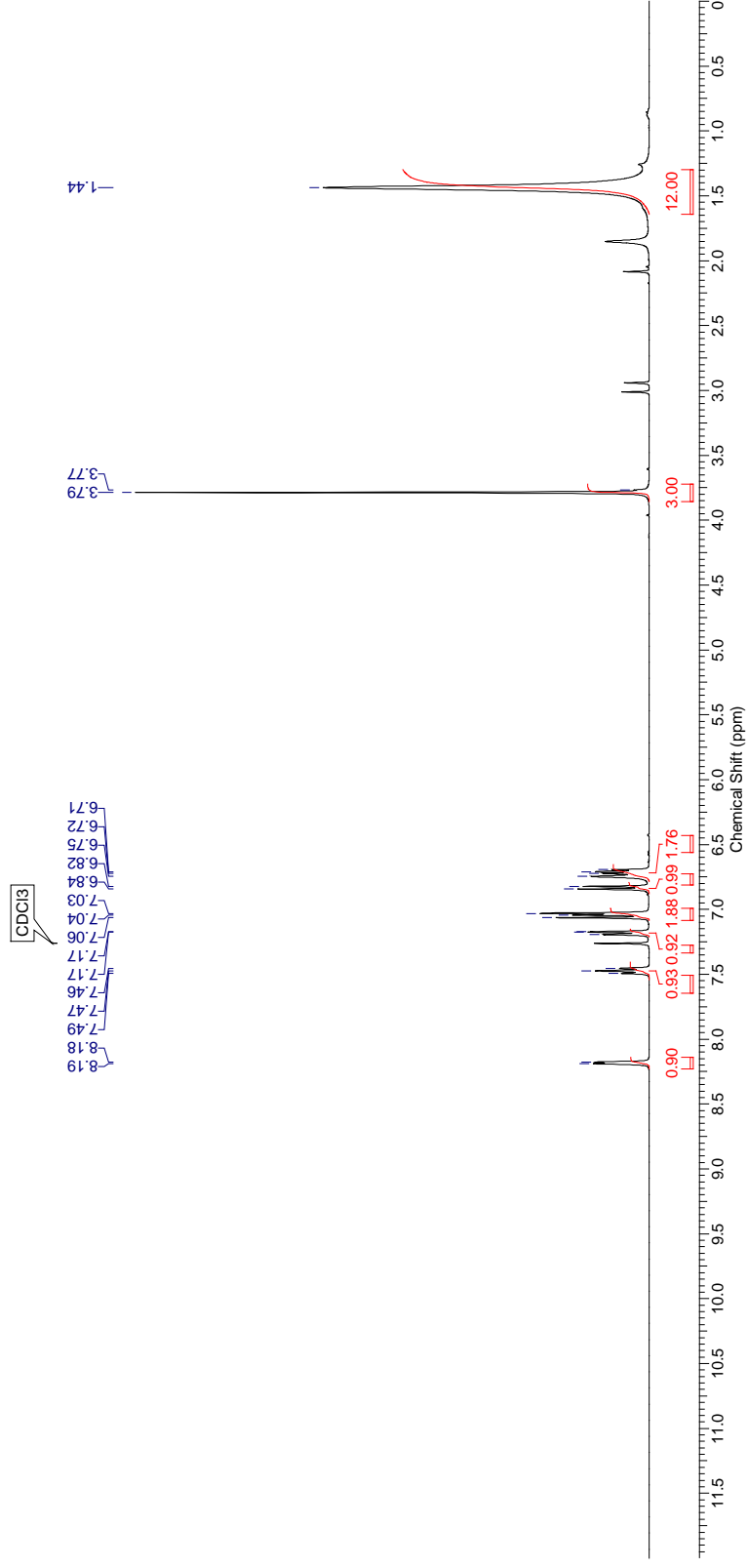
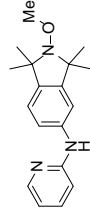
Nuclear Magnetic Resonance Spectra

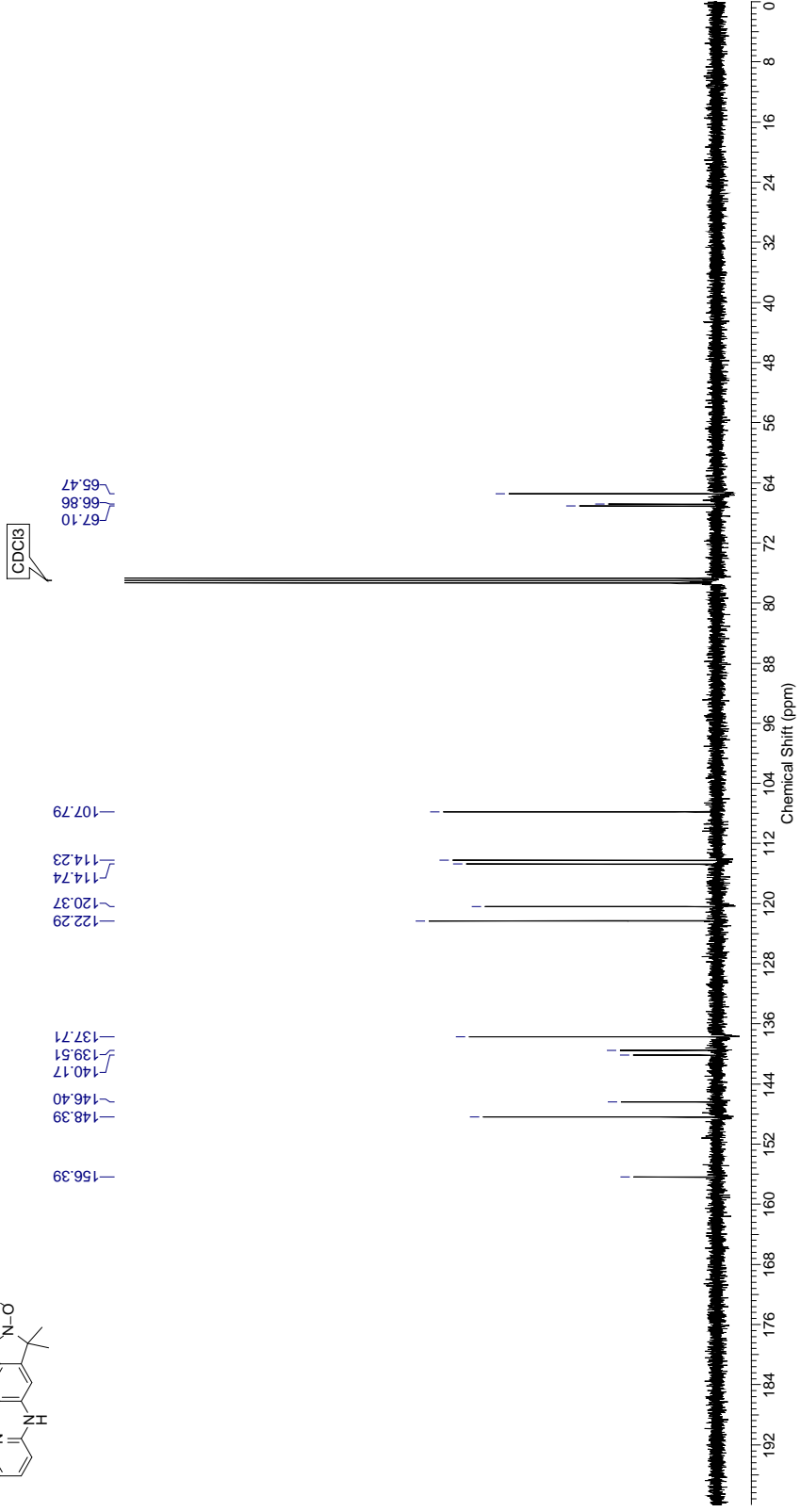
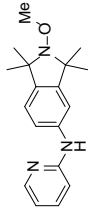
2-Methoxy-1,1,3,3-tetramethylisoindolin-5-amine (1)



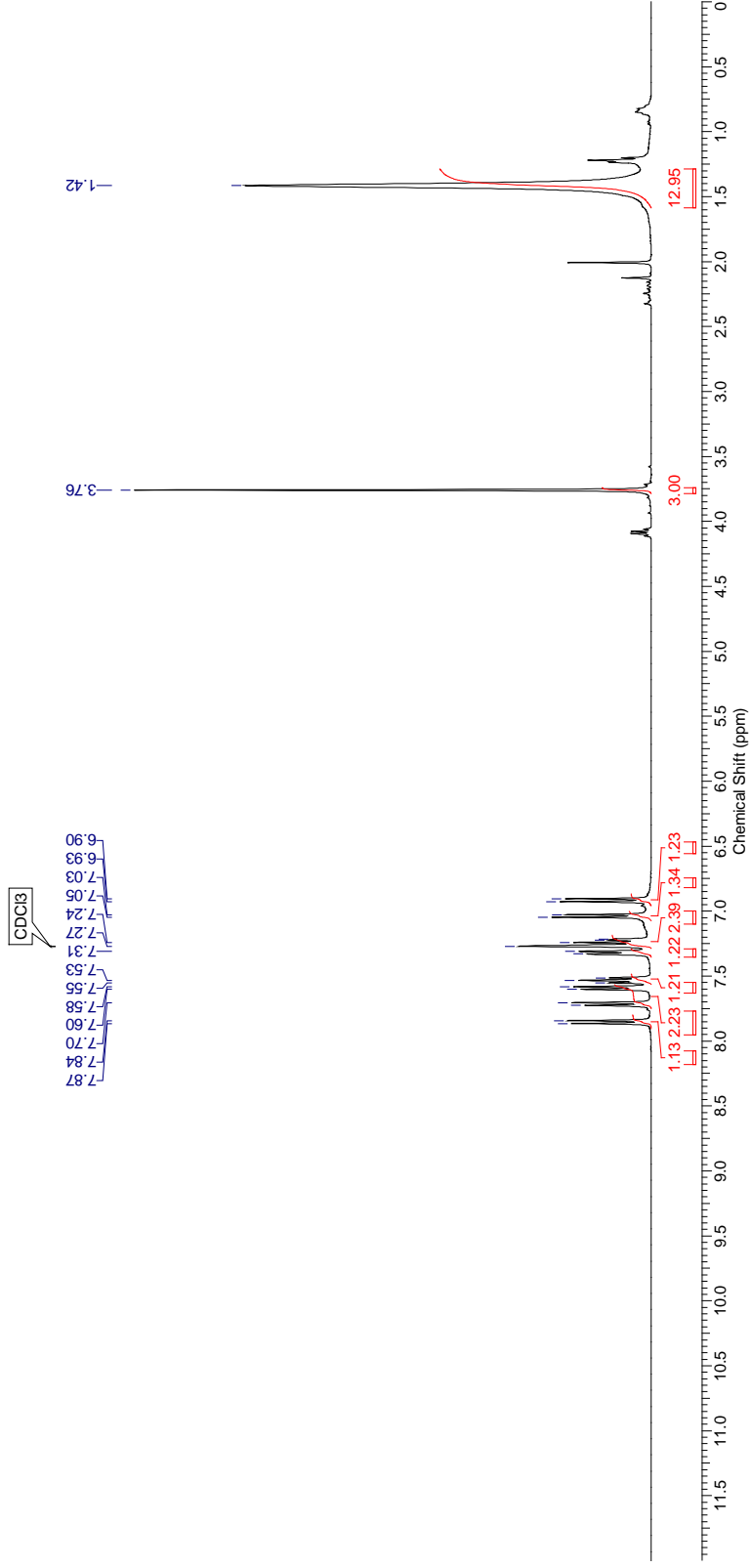
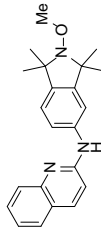


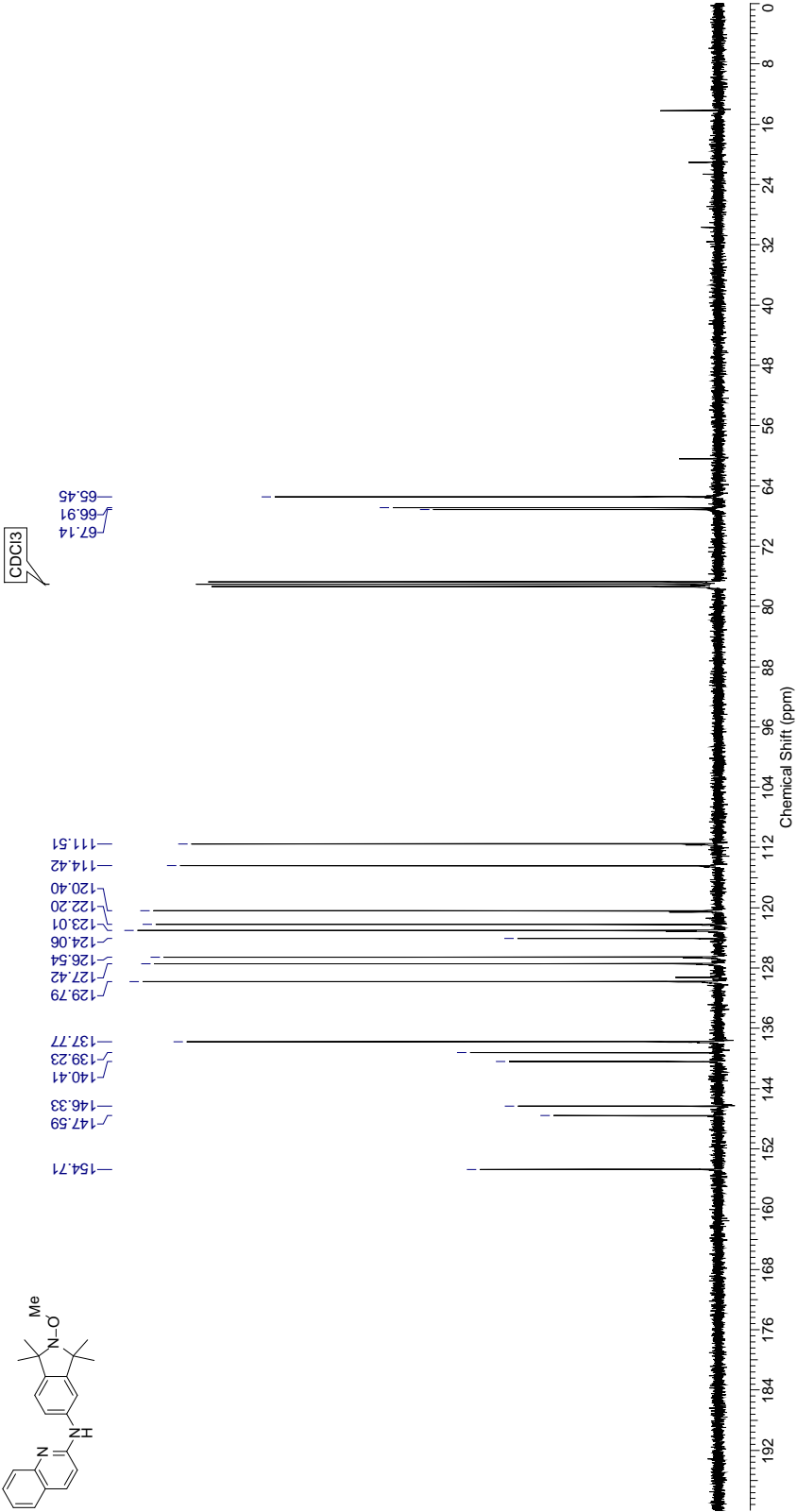
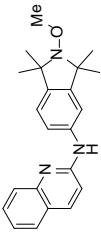
2-Methoxy-1,1,3,3-tetramethyl-N-(pyridin-2-yl)isoindolin-5-amine (2)



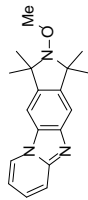


N-(2-Methoxy-1,1,3,3-tetramethylisoindolin-5-yl)quinolin-2-amine (4)

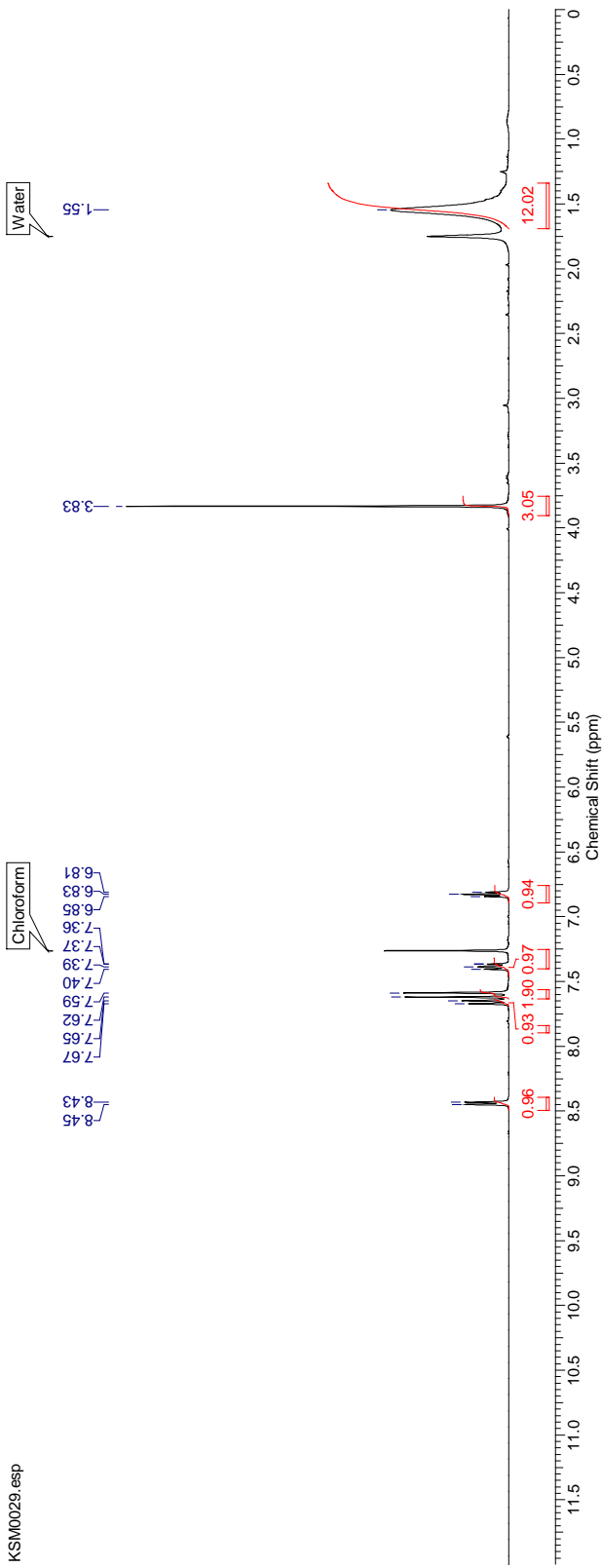


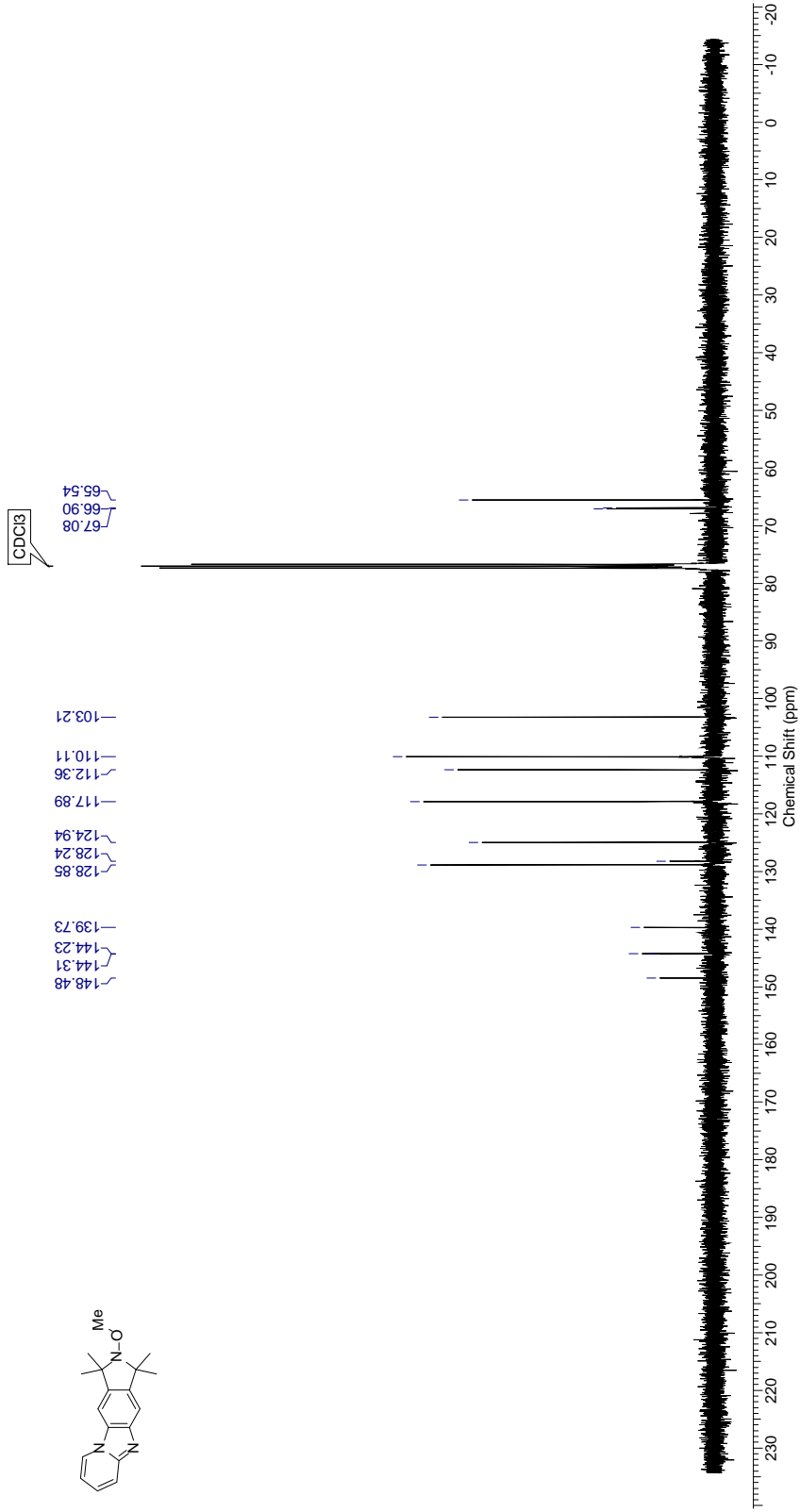
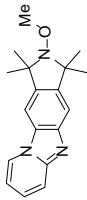


2-Methoxy-1,1,3,3-tetramethyl-2,3,4a,10a-tetrahydro-1H-pyrido[1,2'-1,2]imidazo[4,5-f]isoindole (5)

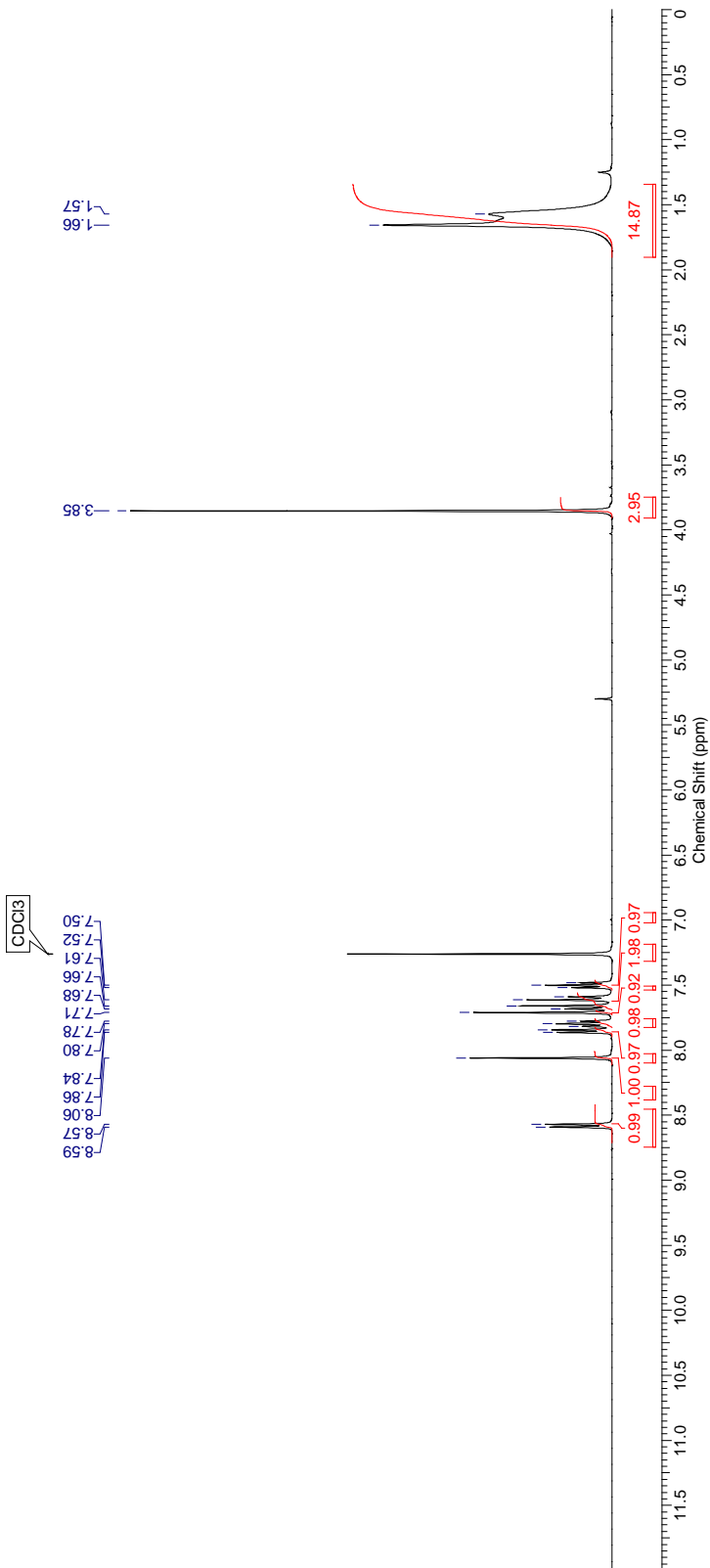
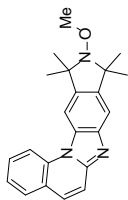


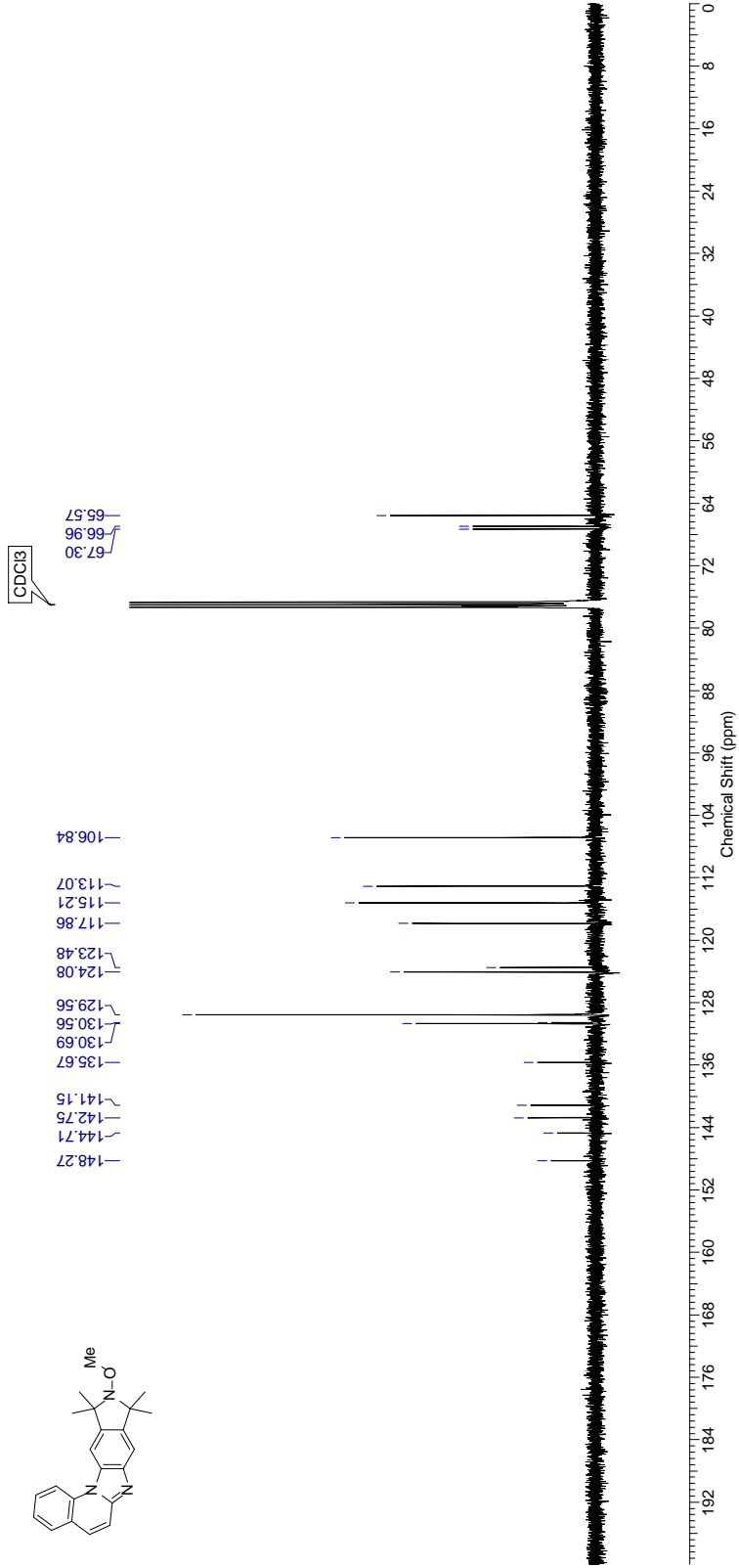
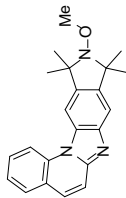
KSM0029.esp





10-Methoxy-9,11,11-tetramethyl-10,11-dihydro-9H-isoindolo[5',6':4,5]imidazo[1,2-a]quinolone (6)



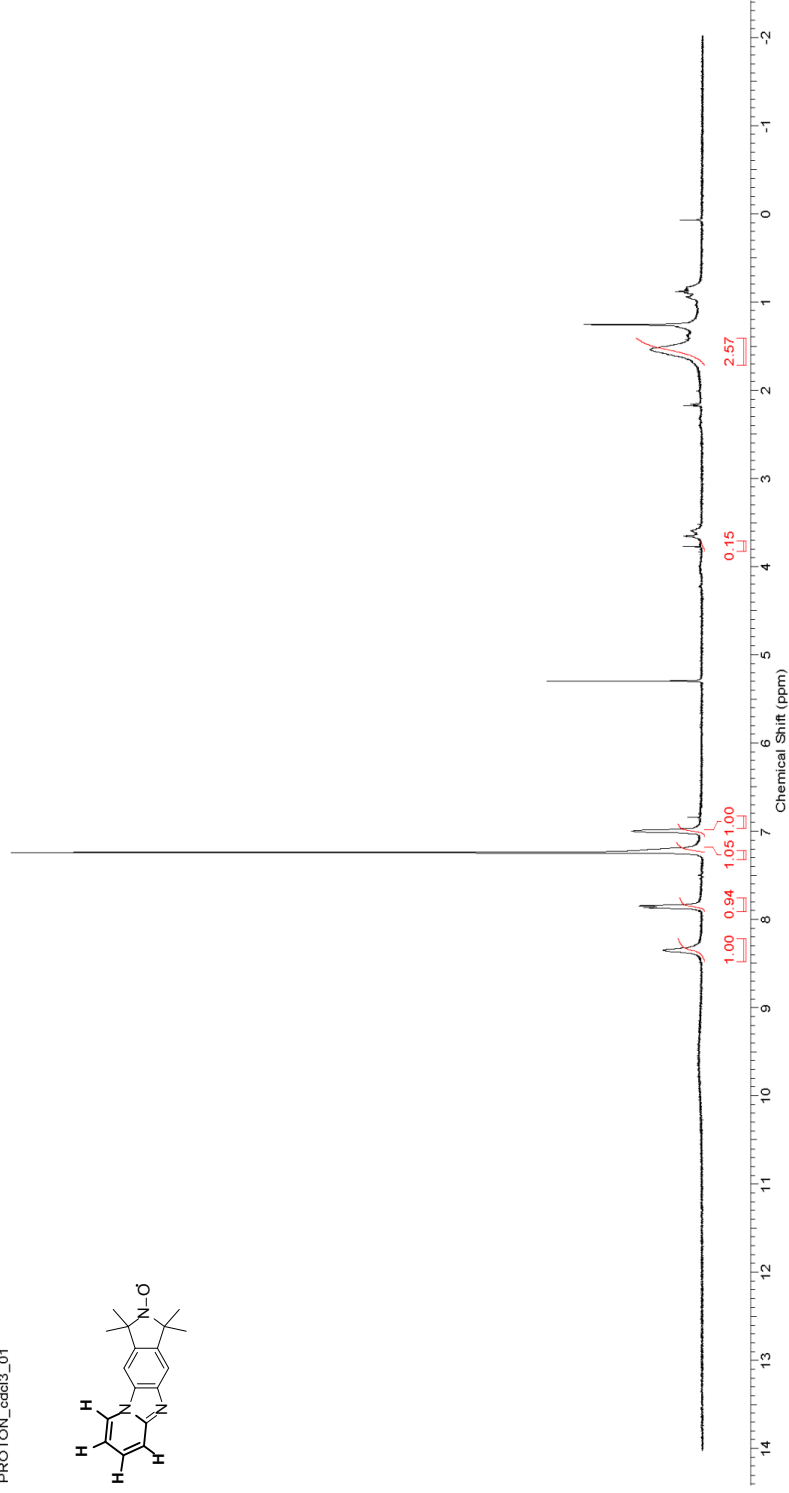
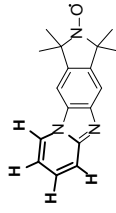


10,11-Dihydro-[5',6':4,5]imidazo[1,2-a]quinolon-9H-9,11,11-tetramethylisoindolin-2-yl oxy (7)

This report was created by ACD/NMR Processor Academic Edition. For more information go to www.acdlabs.com/nmrprocl/

¹H NMR (400MHz, CHLOROFORM-d) δ = 8.35 (br. s., 1 H), 7.86 (d, J = 7.8 Hz, 14 H), 7.00 (br. s., 15 H), 1.55 (br. s., 38 H)

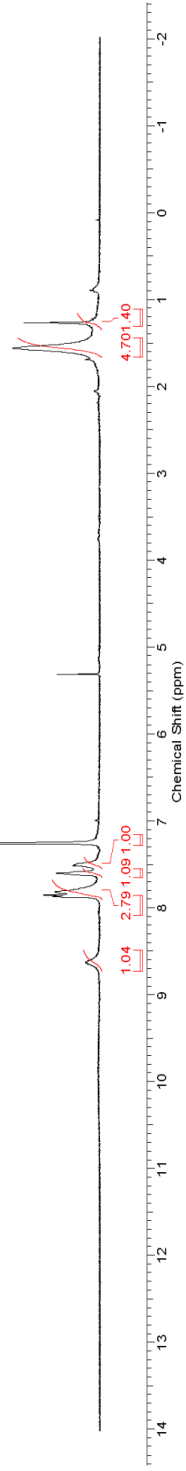
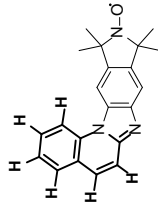
PROTON_gddis_01



10,11-Dihydro-[5',6':4,5]imidazo[1,2-a]quinolon-9H-9,9,11,11-tetramethylisoindolin-2-ylloxy (8)

This report was created by ACD/NMR Processor Academic Edition. For more information go to www.acdlabs.com/nmrproc/

¹H NMR (400MHz, CHLOROFORM-d) δ = 8.63 (br. s., 9 H), 7.91 - 7.68 (m, 23 H), 7.60 (br. s., 9 H), 7.51 (br. s., 1 H), 1.56 (br. s., 39 H), 1.27 (s, 12 H)
PROTON_cddB_01



UV/Vis and Fluorescence Spectra

Spectrofluorimetry was undertaken with a Varian Cary Eclipse fluorescence spectrophotometer. UV/Vis spectroscopy was performed with a Varian Cary 50 spectrophotometer. Samples were prepared at concentrations of 1.0 μM in acetonitrile (UV Spec Grade).

Colour-coded lines for each methoxylamine compounds **5** and **6** show the UV absorbance (solid line, **Figure SI1**) and the fluorescence (dashed line). Excitation was performed at the corresponding wavelength of maximum measured absorbance.

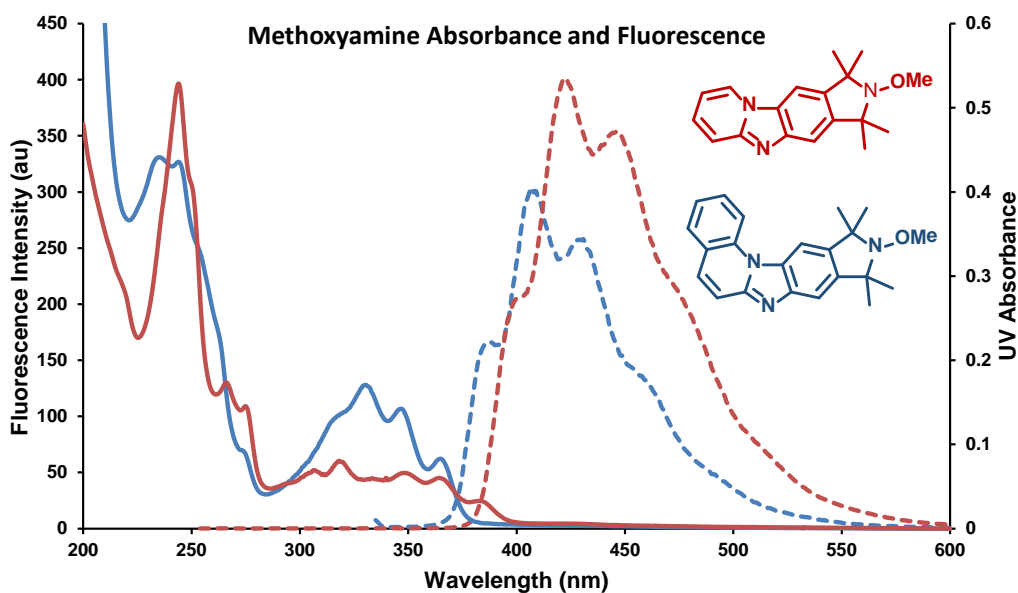


Figure SI1: Compounds 5 and 6

Colour-coded lines for each nitroxyl radicals **7** and **8** show the UV absorbance (solid line, **Figure S12**) and the fluorescence (dashed line). Excitation was performed at the corresponding wavelength of maximum measured absorbance. (A possible cause for the decreased fluorescence of **8** is that aggregation is occurring (as seen in EPR studies, possibly via p-stacking effects related of the kind observed in the solid state, see below).

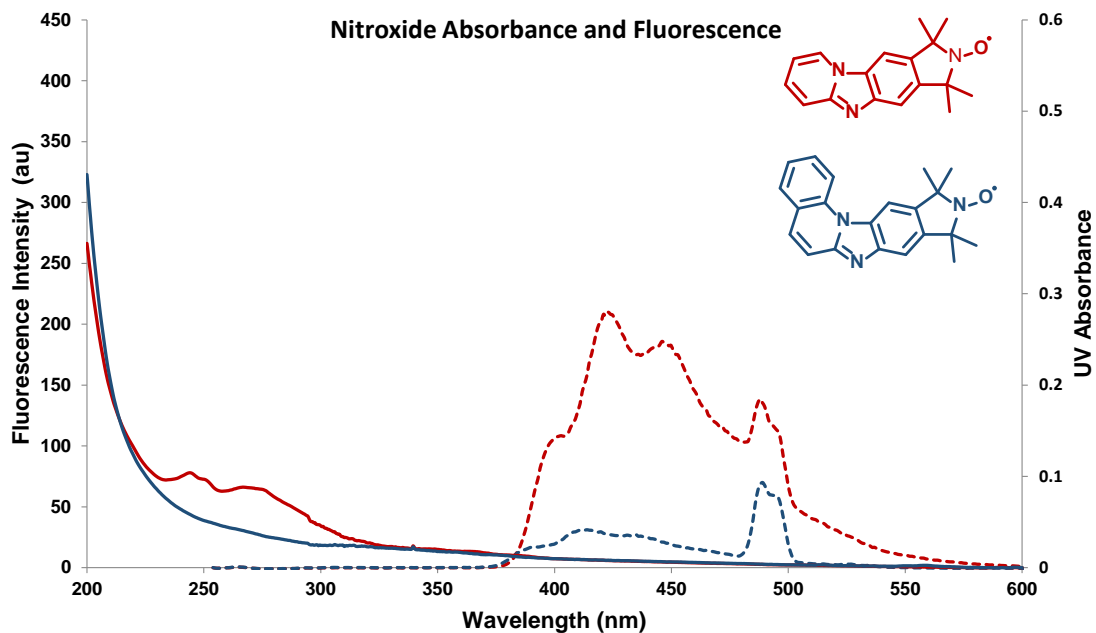


Figure S12: Compounds 7 and 8

DNA/RNA synthesis and purification

All DNA and RNA oligonucleotides were synthesized in-house on an automated ASM800 DNA synthesizer (BIOSSET Ltd.) using phosphoramidite chemistry. All phosphoramidites and CPG columns were purchased from ChemGenes Corp., USA. Reagents and solvents were purchased from Sigma-Aldrich Co. Acetonitrile for oligomer synthesis was purchased from Tedia®, USA. Syntheses were performed on 1 μmol scale on 1000 Å CPG columns. The DNAs were deprotected using a concentrated aqueous ammonia solution at 55 °C for 8 h. For RNAs, general deprotection was done using a 1:1 solution of methylamine and ammonia heated for 40 minutes at 65 °C whereas TBDMS deprotection was performed using triethylamine trihydrofluoride, heated at 55 °C for 90 minutes, followed by precipitation in 1-butanol. All oligonucleotides were subsequently purified by 20 % denaturing polyacrylamide gel electrophoresis (DPAGE) and extracted from the gel slices using “crush and soak” with Tris buffer containing 250 mM NaCl, 10 mM Tris, 1 mM Na₂EDTA, pH 7.5. The solutions were filtered through 0.45 μm , 25 mm diameter GD/X syringe filters (Whatman®, USA) and were subsequently desalted using Sep-Pak cartridges (Waters, USA), following instructions provided by the manufacturer. Dried oligonucleotides were dissolved in sterilized and de-ionised water (200 μL for each oligonucleotide). Concentrations of the oligonucleotides were determined by UV absorbance at 260 nm using a Perkin Elmer™ Inc. Lambda 25 UV/Vis spectrometer.

Protocol for Evaluating Binding of TMIO-Pyrimid Hybrids with Abasic Nucleic Acids by EPR

Stock solutions of TMIO-Pyrimids **7** and **8** were prepared in absolute ethanol. 1 nmol of TMIO-Pyrimid **7** or **8**, 2 nmol of abasic DNA/RNA and 2.4 nmol of the desired complementary strand were taken from their respective stock solutions, mixed and concentrated to dryness on a Thermo Scientific™ Speedvac™. The residue was dissolved in phosphate buffer (10 μL) [10 mM Na₂HPO₄, 100 mM NaCl, 0.1 mM Na₂EDTA, pH 7.0] and the strands were annealed in an MJ Research PTC 200 Thermal Cycler using the following protocol: 90 °C for 2 mins, 60 °C for 5 mins, 50 °C for 5 mins followed by 40 °C for 5 mins and 22 °C for 15 mins. Prior to EPR measurements, the solvent was evaporated on the Speedvac and the residue dissolved in a solution of 2% DMSO, 30% ethylene glycol and 68% sterile water (10 μL) yielding a final TMIO-Pyrimid concentration of 100 μM . This solution was transferred into a quartz EPR capillary tube (BLAUBRAND®-intraMARK) and EPR measurements were performed over a range of temperatures from 0 °C to -30 °C with intervals of 10 °C on an X-band EPR spectrometer (Miniscope MS 200, Magnettech, Germany) with 100 kHz modulation frequency, 1.0 G modulation amplitude and 2.0 mW microwave power and using 50 to 60 scans for each sample. The temperature was regulated by a Magnettech temperature controller M01. Oligonucleotide sequences are shown in Figure 3a and Figures SI1-SI4.

Duplex stability

To ascertain the stability of DNA/RNA duplexes, thermal denaturation curves of select oligonucleotides were determined using a Perkin Elmer™ PTP-1 and PCB 150 Water Peltier System.

DNA/RNA samples (3.0 nmol of each strand) were dissolved in phosphate buffer (100 μ L) (10 mM phosphate, 100 mM NaCl, 0.1 mM Na₂EDTA, pH 7.0), annealed using the following protocol: 90 °C for 2 mins, 60 °C for 5 mins, 50 °C for 5 mins, 40 °C for 5 mins and 22 °C for 15 mins. Samples that were prepared in this manner and to be measured in 2% DMSO and 30% ethylene glycol were dried on a Speedvac and the aforementioned solution was then added. Prior to recording T_M data, the samples were diluted to 1.0 mL with the desired solvent and degassed using argon. The samples were heated up from 10 °C to 90 °C (1.0 °C/min) while recording the absorbance at 260 nm.

Melting temperatures ($T_{M,s}$) of the RNA duplexes **I** (abasic) and **II** (unmodified) (**Table S11**) in aqueous phosphate buffer showed a difference in $T_{M,s}$ of ca. 20 °C, indicating that introduction of an abasic site in an RNA duplex substantially destabilizes the duplex. When 2% DMSO and 30% ethylene glycol were used, RNA duplexes **I** and **II** showed a drop in $T_{M,s}$ of ca. 11-12 °C. However, despite the destabilization caused by the abasic site and the organic cosolvent, the results clearly demonstrate that the RNA oligonucleotides exist as duplexes in the ligand binding experiments.

Duplex	RNA sequence	Buffered solution*	T_M
I	5'-GAC CUC G_A UCG UG 3'-CUG GAG CCU AGC AC	H ₂ O	52 °C
		2% DMSO + 30% ethylene glycol	41 °C
II	5'-GAC CUC GCA UCG UG 3'-CUG GAG CGU AGC AC	H ₂ O	73 °C
		2% DMSO + 30% ethylene glycol	61 °C

*10 mM phosphate, 100 mM NaCl, 0.1 mM Na₂EDTA, pH 7.0; RNA concentration 3 μ M.

Table S11: Melting temperatures ($T_{M,s}$) of RNA duplexes. ' _ ' denotes an abasic site.

Table S12 shows the melting temperatures ($T_{M,s}$) of the DNA duplexes, which are ca. 10 °C lower than for the RNA duplexes, as expected. In aqueous phosphate buffer, duplex **III** (abasic) showed lower T_M of ca. 20 °C than duplex **IV** (unmodified), echoing the trend observed with RNA, where introduction of an abasic site lowered the T_M of the duplexes. When 2% DMSO and 30% ethylene glycol were used, DNA duplex **III** and **IV** caused a further decrease in $T_{M,s}$ of ca. 12-14 °C, as observed with the RNA duplexes, indicating that including the organic cosolvents destabilized the RNA duplexes. However, all results indicate that the DNA oligonucleotides exist as duplexes under the conditions used for evaluation of ligand binding.

Duplex	DNA Sequence	Buffered solution*	Spin label	T_M
III	5'-GAC CTC G_A TCG TG 3'-CTG GAG CCT AGC AC	H ₂ O	-	43 °C
		2 % DMSO + 30 % ethylene glycol		31 °C
III	5'-GAC CTC G_A TCG TG 3'-CTG GAG CCT AGC AC	2 % DMSO + 30 % ethylene glycol	Nitroxide 7	31 °C
			Nitroxide 8	31 °C
IV	5'-GAC CTC GCA TCG TG 3'-CTG GAG CGT AGC AC	H ₂ O	-	63.5 °C
		2 % DMSO + 30 % ethylene glycol		49 °C

*10 mM phosphate, 100 mM NaCl, 0.1 mM Na₂EDTA, pH 7.0; DNA concentration 3 μ M.

Table S12: Melting temperatures ($T_{M,s}$) of DNA duplexes. ' _ ' denotes an abasic site.

In two separate experiments, TMIO-Pyrlmid **7** in one case and **8** in the other (3.0 nmol each) were added along with DNA duplex **III** in 2% DMSO and 30% ethylene glycol (EPR-binding conditions) to check whether introduction of a ligand capable of binding to an abasic site stabilized the duplex.^{1iv} However, a T_M of 31 °C was obtained in both cases, indicating no change in duplex stability, which

was not unexpected because both TMIO-PyrImid **7** and **8** only displays noncovalent binding at much lower temperatures.

To further confirm formation of duplexes in our EPR-binding conditions, circular dichroism (CD) spectra of DNA duplexes were recorded in a Jasco J-810 spectropolarimeter. DNA samples (3.0 nmol of each strand) were mixed, annealed and dried as per the protocol stated in the T_M measurement section. Prior to recording CD spectra, the samples were dissolved in a 200 μ L aqueous solution of 2% DMSO, 30% ethylene glycol containing phosphate buffer ingredients yielding a concentration of 15 μ M for each strand. Cuvette with 1 mm path length was used for the CD measurements and data were recorded from 350 nm to 225 nm at 5 $^{\circ}$ C (**Figure S13**).

The spectra of DNA duplex **III** (abasic) displayed negative and positive molar ellipticities at ca. 245 nm and 273 nm respectively whereas duplex **IV** (unmodified) showed negative and positive molar ellipticities at ca. 250 nm and 274 nm respectively; both in excellent agreement with the characteristic B-DNA duplex values,^{2v} thus confirming formation of duplexes under the experimental conditions used to evaluate binding of **7** and **8** to an abasic site.

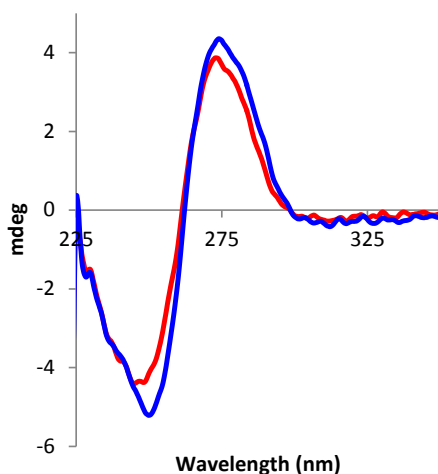
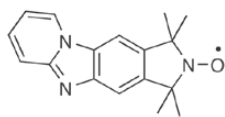


Figure S13: CD spectra of 14-mer DNA duplex **III** (red line) and **IV** (blue line) recorded at 5 $^{\circ}$ C in an aqueous solution containing 2% DMSO, 30% ethylene glycol, 10 mM phosphate, 100 mM NaCl and 0.1 mM Na₂EDTA at pH 7.0.



Nitroxide **7**

⁵GACCTCG_ATCGTG
CTGGAGCXTAGCAC³

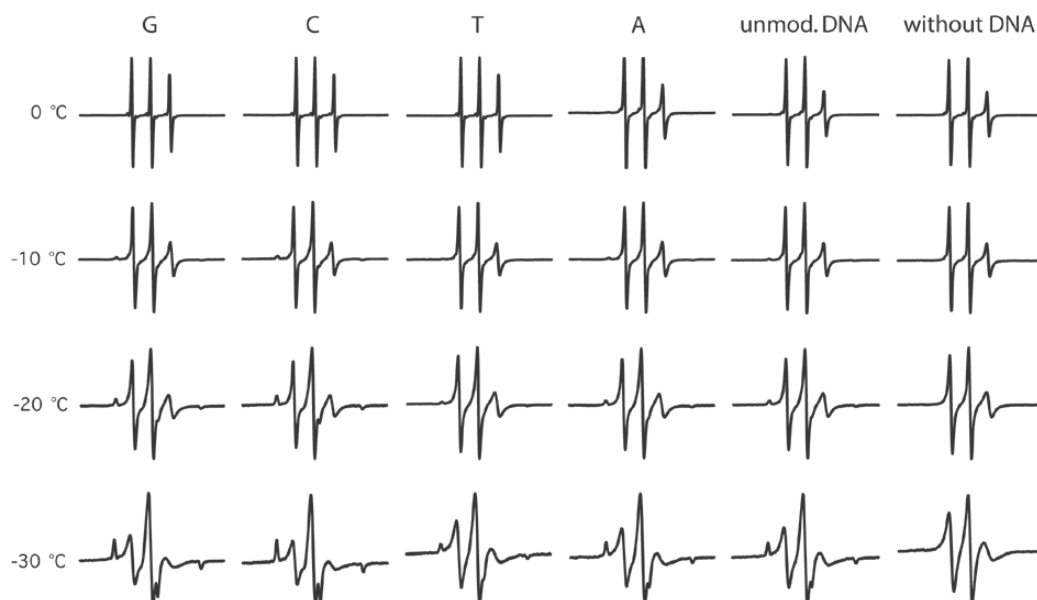
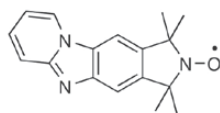


Figure S14: EPR binding data of nitroxide **7** with 14-mer DNA duplex containing an abasic site. EPR spectra are plotted from left to right as a function of base opposite the abasic site (the orphan base) and done as a function of decreased temperatures. All spectra were phase corrected and aligned with respect to the central peak.



Nitroxide **7**

⁵GACCUCG_AUCGUG
CUGGAGCXUAGCAC³

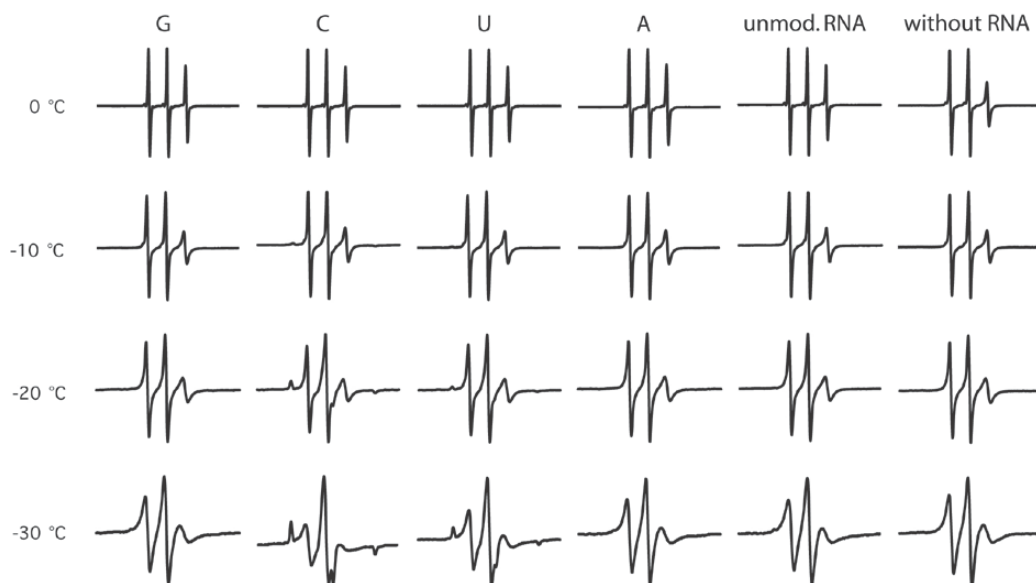
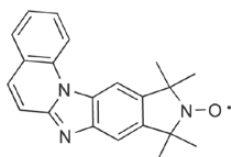


Figure S15: EPR binding data of nitroxide **7** with 14-mer RNA duplex containing an abasic site. EPR spectra are plotted from left to right as a function of base opposite the abasic site (the orphan base) and done as a function of decreased temperatures. All spectra were phase corrected and aligned with respect to the central peak.



Nitroxide **8**

5'GACCTCG_ATCGTG
CTGGAGCXTAGCAC5'

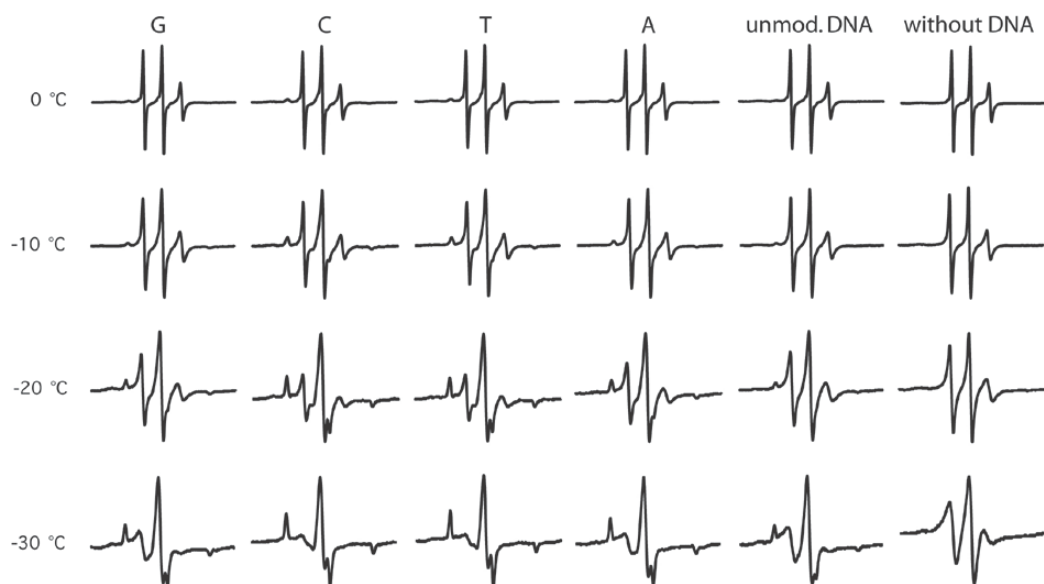
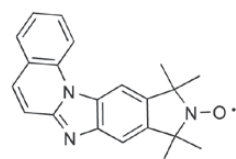


Figure S16: EPR binding data of nitroxide **8** with 14-mer DNA duplex containing an abasic site. EPR spectra are plotted from left to right as a function of base opposite the abasic site (the orphan base) and done as a function of decreased temperatures. All spectra were phase corrected and aligned with respect to the central peak.



Nitroxide **8**

5'GACCUCG_AUCGUG
CUGGAGCXUAGCAC5'

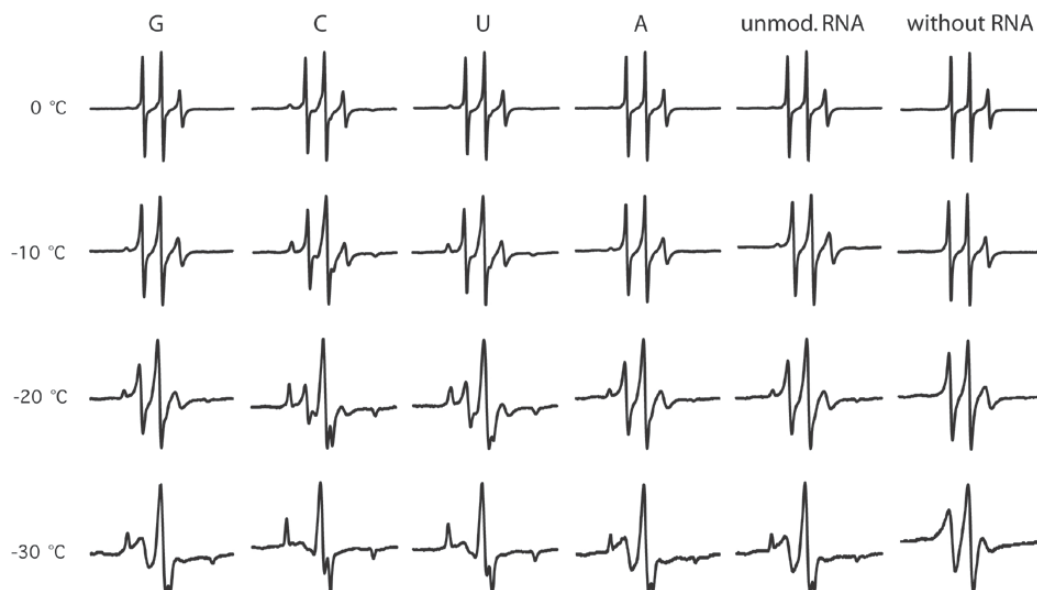
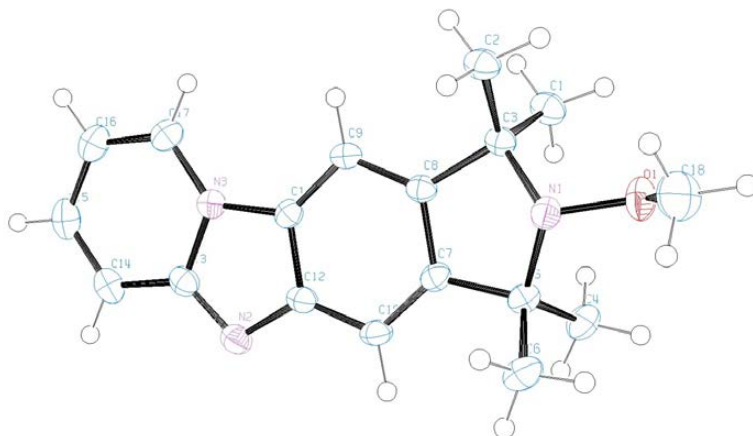


Figure S17: EPR binding data of nitroxide **8** with 14-mer RNA duplex containing an abasic site. EPR spectra are plotted from left to right as a function of base opposite the abasic site (the orphan base) and done as a function of decreased temperatures. All spectra were phase corrected and aligned with respect to the central peak.

Crystallographic Data 1: Structure

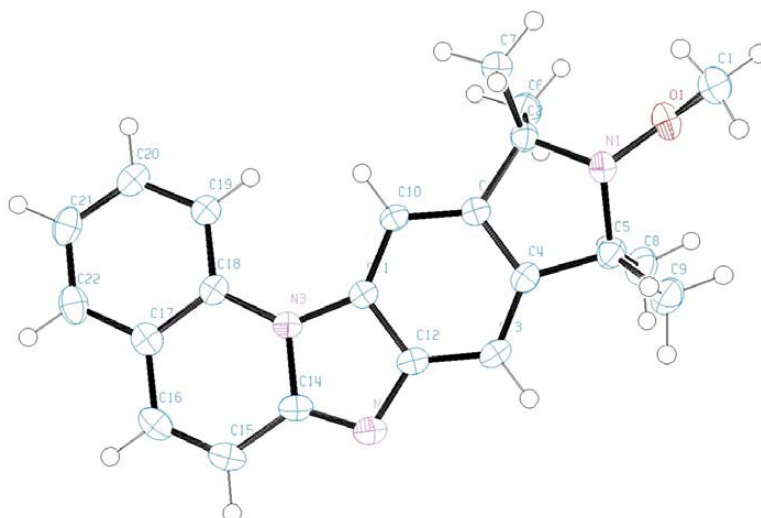
Data were collected for both compounds **5** and **6** at 173(2) K under the software control of CrysAlis CCDx on an Oxford Diffraction Gemini Ultra diffractometer using Mo K α radiation generated from a sealed tube. Data reduction was performed using CrysAlis REDx. Multiscan empirical absorption corrections were applied using spherical harmonics, implemented in the SCALE3 ABSPACK scaling algorithm, within CrysAlis REDx, and subsequent computations were carried out using the WinGX-32x graphical user interface. The structures were refined with SHELXL-97x. Full occupancy non-hydrogen atoms were refined with anisotropic thermal parameters. C–H hydrogen atoms were included in idealized positions, and a riding model was used for their refinement.



2-Methoxy-1,1,3,3-tetramethyl-2,3,4a,10a-tetrahydro-1H-pyrido[1',2':1,2]imidazo[4,5-f]isoindole (Compound 5)

Formula C₁₈H₂₁N₃O

M = 295.38, monoclinic, space group $P2_1/c$ (#14), $a = 9.6129(5)$ Å, $b = 12.3517(6)$ Å, $c = 13.4019(6)$ Å, $\alpha = 90.00$, $\beta = 100.539(5)$, $\gamma = 90.00^\circ$, $V = 1564.44(13)$ Å³, $Z = 4$, crystal size $0.30 \times 0.29 \times 0.27$ mm, colourless, habit block, temperature 173.00(2) K, $\lambda(\text{Mo-K}\alpha) = 0.71073$, $\mu(\text{Mo-K}\alpha) = 0.08$ mm⁻¹, $T(\text{Empirical})_{\text{min,max}} = 0.889, 1.000$, $\theta_{\text{max}} = 28.72$, $\theta_{\text{min}} = 3.30$, hkl range -12 to 11 , -15 to 16 , -17 to 17 , $N = 11015$, $N_{\text{ind}} = 3670$ ($R_{\text{int}} = 0.019$), $N_{\text{obs}} = 3178$ ($I \geq 2\sigma(I)$), residuals $R1(F, 2\sigma) = 0.043$, $wR2(F^2, \text{all}) = 0.111$, $\text{GoF}(\text{all}) = 0.95$, $\Delta\rho_{\text{min,max}} = -0.20, 0.30$ e Å⁻³.



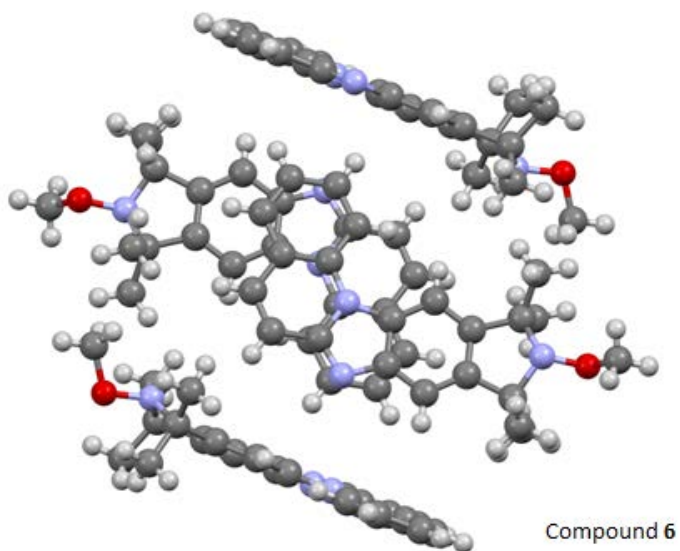
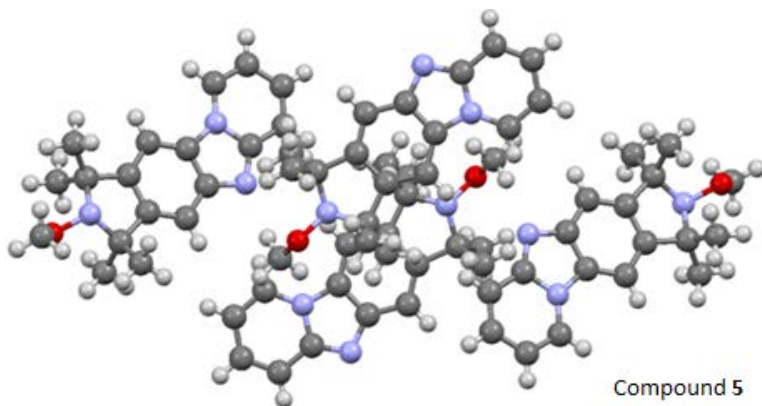
10-Methoxy-9,9,11,11-tetramethyl-10,11-dihydro-9H-isindolo[5',6':4,5]imidazo[1,2-a]quinolone (Compound 6)

Formula $C_{22}H_{23}N_3O$

$M = 345.43$, monoclinic, space group $P2_1/c$ (#14), $a = 15.0277(8) \text{ \AA}$, $b = 7.7067(4) \text{ \AA}$, $c = 16.0253(7) \text{ \AA}$, $\alpha = 90.00$, $\beta = 104.035(5)$, $\gamma = 90.00^\circ$, $V = 1800.55(14) \text{ \AA}^3$, $Z = 4$, crystal size $0.44 \times 0.14 \times 0.03 \text{ mm}$, colourless, habit plate, temperature $173.00(2) \text{ K}$, $\lambda(\text{Mo-K}\alpha) = 0.71073$, $\mu(\text{Mo-K}\alpha) = 0.08 \text{ mm}^{-1}$, $T(\text{Empirical})_{\text{min,max}} = 0.959, 1.000$, $\theta_{\text{max}} = 28.93$, $\theta_{\text{min}} = 3.34$, hkl range -18 to 19 , -10 to 8 , -10 to 21 , $N = 13347$, $N_{\text{ind}} = 4177$ ($R_{\text{int}} = 0.026$), $N_{\text{obs}} = 3367$ ($I \geq 2\sigma(I)$), residuals $R1(F, 2\sigma) = 0.045$, $wR2(F^2, \text{all}) = 0.105$, $\text{GoF}(\text{all}) = 1.02$, $\Delta\rho_{\text{min,max}} = -0.22, 0.25 \text{ e \AA}^{-3}$.

Crystallographic Data 2: Packing

The crystal packing of **5** consists only of hydrogen bonding between the 'tetramethyl' C–H hydrogens and the C₆ ring of a neighbour molecule, whereas **6** has this same form of hydrogen bonding in addition to one form of π -stacking, offset face-to-face interaction. In both structures, the crystal packing shows that the methoxyamine groups are at opposite ends for each pair of molecule. The intermolecular distance between these moieties in **5** is shorter than in **6**.



References

ⁱ Ahn, Hyo-Yang; Fairfull-Smith, Kathryn E.; Morrow, Benjamin J.; Lussini, Vanessa; Kim, Bosung; Bondar, Mykhailo V.; Bottle, Steven E.; Belfield, Kevin D. *J. Am. Chem. Soc.* **2012**, *134*, 4721-4730.

ⁱⁱ Chalmers, B. A.; Morris, J. C.; Fairfull-Smith, K. E.; Grainger, R. S.; Bottle, S. E. *Chem. Commun.* **2013**, *49*, 10382.

ⁱⁱⁱ Masters, Kye-Simeon; Rauws, Tom R. M.; Yadav, Ashok K.; Herrebout, Wouter A.; Van der Veken, Benjamin; Maes, Bert U. W. *Chemistry – Eur. J.* **2011**, *17*, 6315-6320, S6315/1-S6315/38.

^{iv} Yoshimoto, K.; Nishizawa, S.; Minagawa, M.; Teramae, N., Use of abasic site-containing DNA strands for nucleobase recognition in water. *Journal of the American Chemical Society* **2003**, *125*, 8982-8983.

^v Chang, Y.-M.; Chen, C. K.-M.; Hou, M.-H., Conformational changes in DNA upon ligand binding monitored by circular dichroism. *International journal of molecular sciences* **2012**, *13*, 3394-3413.

Paper II



Cite this: *Chem. Commun.*, 2015, 51, 13142

Received 17th June 2015,
Accepted 8th July 2015

DOI: 10.1039/c5cc05014f

www.rsc.org/chemcomm

Site-directed spin labeling of 2'-amino groups in RNA with isoindoline nitroxides that are resistant to reduction†

Subham Saha,‡ Anil P. Jagtap‡ and Snorri Th. Sigurdsson*

Two aromatic isothiocyanates, derived from isoindoline nitroxides, were synthesized and selectively reacted with 2'-amino groups in RNA. The spin labels displayed limited mobility in RNA, making them promising candidates for distance measurements by pulsed EPR. After conjugation to RNA, a tetraethyl isoindoline derivative showed significant stability under reducing conditions.

Electron paramagnetic resonance (EPR) spectroscopy is a biophysical technique that is routinely applied for the study of the structure and dynamics of nucleic acids in order to gain insights into their mechanism of action.¹ Structural information is usually derived from distance measurements, in particular using pulsed techniques, such as pulsed electron–electron double resonance (PELDOR),² also known as double electron–electron resonance (DEER). Information about dynamics can be derived from line-shape analysis of continuous wave (CW) EPR spectra,³ from the width of distance distributions⁴ and by analysis of orientation-dependent PELDOR measurements.^{1d,5}

Most EPR studies of nucleic acids require incorporation of paramagnetic reporter groups at specific sites, a technique referred to as site-directed spin labeling (SDSL).^{1a,e,6} Aminoxyl radicals, usually called nitroxides, are common spin labels that can be attached to the desired site in the nucleic acid of interest with a covalent bond, although there are examples of noncovalent labeling.⁷ Two main approaches have been used for covalent spin-labeling of nucleic acids.⁸ The phosphoramidite method utilizes spin-labeled phosphoramidites as building blocks for automated chemical synthesis of the spin-labeled oligonucleotide.⁹ This strategy usually involves significant synthetic effort¹⁰ and the spin label is exposed to reagents used in nucleic acid synthesis that can partially reduce the nitroxide.¹¹ The other covalent SDSL approach involves a post-synthetic modification of the nucleic acid, wherein

a spin-labeling reagent reacts with a specific reactive functional group within the nucleic acid.¹² Post-synthetic spin-labeling usually requires less effort than the classical phosphoramidite approach and can often be performed with commercially available reagents.

Post-synthetic modification of 2'-amino groups in RNA is an efficient method for site-directed spin labeling of oligonucleotides.¹³ 2'-Amino-modified RNAs are commercially available or can alternately be prepared using commercially available phosphoramidites. This 2'-labeling method has been used to incorporate the paramagnetic 2'-ureido-TEMPO [(2,2,6,6-tetramethylpiperidin-1-yl)oxyl] at specific sites by reaction of 2'-amino groups with 4-isocyanato-TEMPO.^{12c} However, isocyanates are relatively reactive and, therefore, prone to hydrolysis and can react with other functional groups of the nucleic acid.¹⁴ Thus, special care is required while handling this reagent and when carrying out the spin-labeling reaction.^{13b} In addition, incomplete labeling has been observed for some long RNAs, presumably due to the formation of secondary structures under the spin-labeling conditions (−8 °C), which may slow down the spin-labeling reaction relative to the competing hydrolysis of the isocyanate. Therefore, it is of interest to find more suitable reagents to react with 2'-amino groups in oligonucleotides, which would make this spin-labeling strategy even more useful.

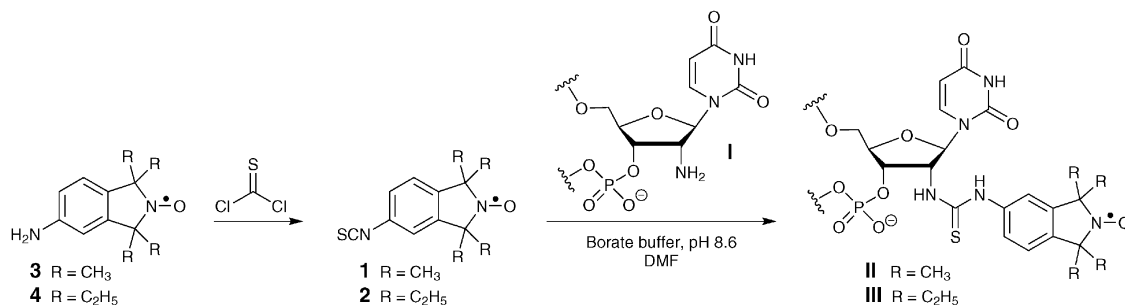
This report describes the spin-labeling of 2'-amino groups in RNA using isoindoline-derived aromatic isothiocyanates. Aromatic isothiocyanates are more stable than isocyanates and yet reactive enough to modify 2'-amino groups in RNA.¹⁵ We show here that the isothiocyanate spin labels react very efficiently with 2'-amino uridine in RNA, forming a stable thiourea linkage. Moreover, the spin-labeling reactions were carried out at 37 °C in the presence of a denaturing agent (DMF), which minimizes the formation of secondary structures that might reduce the efficiency of 2'-amino labeling.

Two spin-labeling reagents were prepared, isothiocyanates **1** and **2** (Scheme 1), in a single step using readily accessible starting materials. When isoindolines are utilized for spin-labeling, tetramethyl derivatives are normally used,^{10b,c,16} but isoindoline **2** was included because tetraethyl derivatives have

University of Iceland, Department of Chemistry, Science Institute, Dunhaga 3, 107 Reykjavik, Iceland. E-mail: snorrisi@hi.is

† Electronic supplementary information (ESI) available. See DOI: 10.1039/c5cc05014f

‡ These authors contributed equally to this work.



Scheme 1 Preparation of spin-labeling reagents **1** and **2** and their reaction with the 2'-amino modified RNA oligonucleotide **I** [5'-GAC CUC G(2'-NH₂)U A UCG UG] to yield spin-labeled oligonucleotides **II** and **III**.

been shown to be more resistant towards reduction.¹⁷ 1,1,3,3-Tetramethylisoinidolin-5-amine-2-oxyl (**3**)^{17b,18} and its corresponding tetraethyl derivative (**4**)^{17b} were treated with thiophosgene to obtain the isothiocyanate spin-labeling reagents **1** and **2** in 82% and 57% yields, respectively (Scheme 1). Unlike 4-isocyanato-TEMPO, aromatic isothiocyanates **1** and **2** were found to be stable solids and did not require special precautions when prepared or handled.

Spin-labeling reagents **1** and **2** were reacted with the 2'-amino modified RNA oligonucleotide 5'-GAC CUC G(2'-NH₂)U A UCG UG (**I**) at 37 °C, in borate buffer (pH 8.6) containing 50% DMF. Samples were removed at specific intervals of time and analyzed by denaturing polyacrylamide gel electrophoresis (DPAGE) analysis (Fig. 1). A new product was formed in each reaction that migrated slower than the parent oligonucleotide, thus indicating successful covalent attachment of the spin labels to the RNA. Tetramethyl-derivative **1** reacted faster than **2**; the former fully converted RNA **I** within 4 h and the latter in 8 h, to the corresponding spin-labeled derivatives. Selective reaction at the 2'-amino group was verified by the lack of reaction between **1** and an unmodified RNA, even after heating at 60 °C for 48 h (Fig. S3, ESI[†]).

The spin-labeled oligonucleotides **II** and **III** were purified by DPAGE to give **II** and **III** in ca. 75–80% yields. It is noteworthy that ethanol precipitation of RNA **II** gave material of the same purity, as judged by EPR and DPAGE, (Page S7, ESI[†]), making it a very rapid spin-labeling method. MALDI-TOF analysis of the oligonucleotides showed the mass expected for the spin-labeled oligomers (Fig. S4, ESI[†]). Circular dichroism (CD) spectroscopy

of the corresponding spin-labeled RNA duplexes **IV** and **V** showed negative and positive molar ellipticities at ca. 210 nm and 262–264 nm, respectively (Fig. S5, ESI[†]), values that are characteristic of A-form RNA duplexes.¹⁹ The thermodynamic stabilities of the spin-labeled RNA duplexes were determined by thermal denaturation (*T_M*) experiments (Table S3 and Fig. S6, ESI[†]). Only minor destabilization of 1.2 °C and 2.0 °C were observed for the tetramethyl- and the tetraethyl-derivative, respectively, relative to an unmodified duplex. The corresponding TEMPO-labeled RNA duplex **VII**, prepared by reaction of 4-isocyanato-TEMPO with oligonucleotide **I**,^{13b} was considerably less stable ($\Delta T_M = -5.3$ °C).

The EPR spectra of **II** and **III** (Fig. 2) show broadening of the EPR spectral lines relative to spin labels **1** and **2** (Fig. S1 and S2, ESI[†]), which is consistent with their covalent attachment to the RNA. The EPR spectra of single stranded oligonucleotides **II** and **III** were also compared with the corresponding TEMPO-derived oligonucleotide **VI**, which had a noticeably narrower spectrum. The narrow spectrum of **VI** presumably reflects in part the inherent flexibility of TEMPO, in which the six-membered ring can sample different conformations. The EPR spectra of the corresponding RNA duplexes (Fig. 2, **IV**, **V**, **VII**) were considerably broader than for

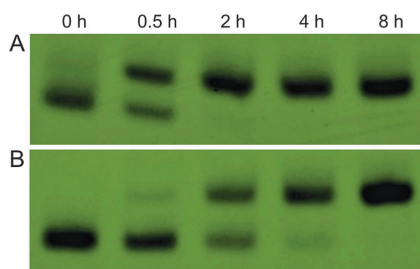


Fig. 1 A time-course of the spin-labeling reactions between the 2'-amino oligonucleotide **I** and the aromatic isothiocyanates **1** (A) and **2** (B). Reaction conditions: 1 mM RNA, 50 mM **1**, 50 mM borate buffer (pH 8.6), 50% DMF.

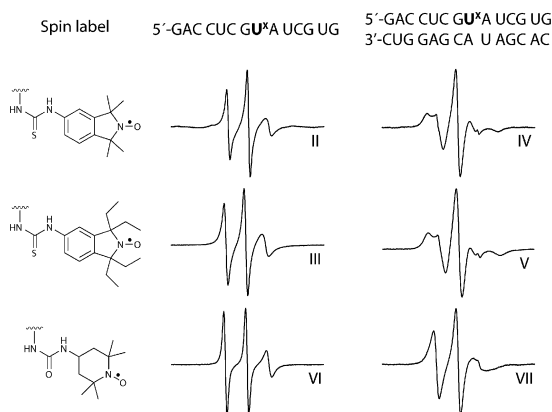


Fig. 2 EPR spectra of the spin-labeled oligonucleotides at 10 °C (10 mM phosphate, 100 mM NaCl, 0.1 mM Na₂EDTA, pH 7.0). U^x indicates the position of the spin-labeled uridine and roman numerals under the spectra identify the oligonucleotides (see Table S1, ESI[†]).

the single strand and again, the EPR spectra of the isoindoline-derived duplexes (**IV** and **V**) were broader than that of the TEMPO-modified duplex (**VII**). It was somewhat surprising to see how broad the spectra for isoindoline nitroxide-labeled duplexes **IV** and **V** were, with both the high- and low-field peaks splitting at 10 °C (see Fig. S7, ESI† for other temperatures), given the fact that rotation is possible around bonds in the linker. Since the thiourea can be regarded as a stiff tether, flexibility is restricted to rotation between two single bonds, namely the one connecting the 2'-C and the 2'-N as well as the bond between the urea and the isoindoline. Molecular modeling (Fig. 3) showed that there is only one low-energy rotamer for the C–N bond, in which the large sulfur atom is lodged between two oxygen atoms on the spin-labeled nucleotide: the 3'-oxygen and the oxygen of the tetrahydrofuran ring, resulting in a snug fit for the sulfur atom. Otherwise, the label is projected away from the nucleic acid; the limited mobility indicates that there is restricted rotation around the bond connecting the isoindoline to the urea, as might be expected because of conjugation.

In-cell EPR spectroscopy has emerged as a promising technique to study nucleic acids *in vivo*.²⁰ Pyrrolidine- and piperidine-based nitroxides have very limited stabilities in reductive environments²¹ and are thus considered to be ineffective spin labels for in-cell EPR studies. On the other hand, isoindolines have shown higher stability towards reduction, especially tetraethyl derivatives.¹⁷ The stabilities of the spin-labeled duplexes **IV**, **V** and **VII** were tested in the presence of ascorbic acid, which is a known cellular reducing agent and often used to evaluate the stability of nitroxides.^{17b,21a,22} Fig. 4 shows a normalized EPR signal as a function of time. There was a striking difference in the stability of the different spin labels: the TEMPO label was fully reduced within 10 min and the tetraethyl isoindoline within an hour, while ca. 90% of the tetraethyl isoindoline label still remained intact after 10 h (Fig. 4, inset). It is

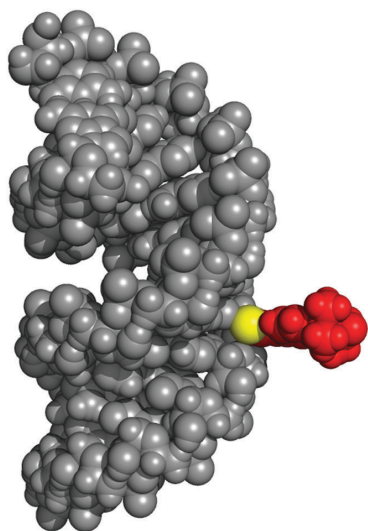


Fig. 3 A space-filling molecular model of spin-labeled oligonucleotide duplex **IV**. The RNA constituents are shown in grey and covalently attached spin label **1** in red, except for the sulfur (yellow) in the thiourea linker.

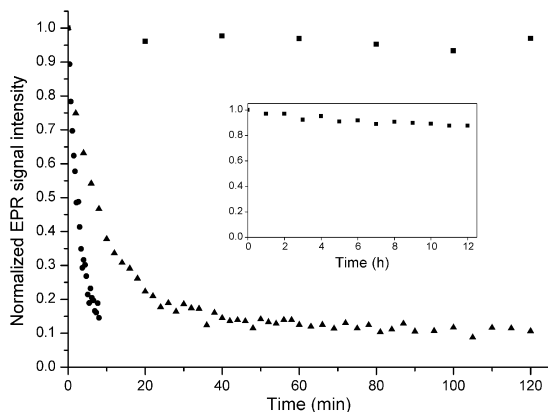


Fig. 4 Stabilities of the spin-labeled RNA duplexes **IV** (triangle), **V** (square) and **VII** (circle) towards reduction (5 mM ascorbic acid, 10 mM phosphate, 100 mM NaCl, 0.1 mM Na₂EDTA, pH 7.0). Inset shows a longer time course (12 h) for duplex **V**.

also noteworthy that the stabilities of the nitroxide radicals were slightly higher after being conjugated to the RNA oligonucleotides. For example, under identical conditions, 5% of simple tetraethyl isoindoline derivatives remained after 2 h,^{17b} while 12% of RNA duplex **IV** (Fig. S9, ESI†) still had an intact spin label. Taken together, these ascorbate experiments indicate that the tetraethyl derivative is a promising spin label for in-cell EPR studies. However, a more detailed study of spin-label stability under cellular conditions, where other reducing agents (*e.g.* glutathione) are present, will be conducted and reported in due course.

In summary, we have described an efficient method for post-synthetic spin-labeling of 2'-amino groups with aromatic isothiocyanates using two new isoindoline-derived spin labels. This divergent synthetic approach can be used for a variety of isoindoline spin labels and has three major advantages over the previously described 2'-TEMPO derivative. First, the new spin labels have only a minor effect on the thermal stability of RNA duplexes. Second, the isoindoline labels have limited mobility independent of the nucleic acid duplex to which they are attached, which should make them useful for distance measurements. Third, the tetraethyl isoindoline conjugated to RNA exhibits high stability towards reduction, making it a promising candidate for in-cell EPR studies. This spin-labeling strategy should also be useful for spin-labeling long RNAs, either through direct derivatization of 2'-amino groups or by ligation of oligonucleotides containing the tetraethyl spin label, which is carried out in the presence of a reducing agent.

This work was supported by the Icelandic Research Fund (141062-051). S. S. and A. P. J. gratefully acknowledge doctoral fellowships provided by the University of Iceland. The authors thank Dr S. Jonsdottir for assistance with collecting analytical data for structural characterization of compounds prepared and members of the Sigurdsson research group for critical reading of the manuscript.

References

- (a) G. Z. Sowa and P. Z. Qin, *Prog. Nucleic Acid Res. Mol. Biol.*, 2008, **82**, 147–197; (b) O. Schiemann, *Methods Enzymol.*, 2009, **469**,

- 329–351; (c) P. Nguyen and P. Z. Qin, *Wiley Interdiscip. Rev.: RNA*, 2012, 3, 62–72; (d) T. F. Prisner, A. Marko and S. T. Sigurdsson, *J. Magn. Reson.*, 2015, 252, 187–198; (e) Y. Ding, P. Nguyen, N. S. Tangprasertchai, C. V. Reyes, X. Zhang and P. Z. Qin, *Electron Paramagnetic Resonance*, The Royal Society of Chemistry, 2015, vol. 24, pp. 122–147.
- 2 (a) A. Milov, K. Salikhov and M. Shirov, *Sov. Phys. Solid State*, 1981, 23, 565–569; (b) O. Schiemann, A. Weber, T. E. Edwards, T. F. Prisner and S. T. Sigurdsson, *J. Am. Chem. Soc.*, 2003, 125, 3434–3435; (c) O. Schiemann and T. F. Prisner, *Q. Rev. Biophys.*, 2007, 40, 1–53.
- 3 X. J. Zhang, P. Cekan, S. T. Sigurdsson and P. Z. Qin, *Methods Enzymol.*, 2009, 469, 303–328.
- 4 (a) A. D. Milov, Y. D. Tsvetkov, F. Formaggio, S. Oancea, C. Toniolo and J. Raap, *J. Phys. Chem. B*, 2003, 107, 13719–13727; (b) N. A. Kuznetsov, A. D. Milov, V. V. Koval, R. I. Samoilova, Y. A. Grishin, D. G. Knorre, Y. D. Tsvetkov, O. S. Fedorova and S. A. Dzuba, *Phys. Chem. Chem. Phys.*, 2009, 11, 6826–6832; (c) G. Y. Shevelev, O. A. Krumkacheva, A. A. Lomzov, A. A. Kuzhelev, D. V. Trukhin, O. Y. Rogozhnikova, V. M. Tormyshev, D. V. Pyshnyi, M. V. Fedin and E. G. Bagryanskaya, *J. Phys. Chem. B*, 2015, DOI: 10.1021/acs.jpcc.5b03026, ahead of print.
- 5 A. Marko, V. Denysenkov, D. Margraft, P. Cekan, O. Schiemann, S. T. Sigurdsson and T. F. Prisner, *J. Am. Chem. Soc.*, 2011, 133, 13375–13379.
- 6 (a) S. A. Shelke and S. T. Sigurdsson, in *Structural Information from Spin-Labels and Intrinsic Paramagnetic Centres in the Biosciences*, ed. C. R. Timmel and J. R. Harmer, Springer, Berlin, Heidelberg, 2013, vol. 152, ch. 62, pp. 121–162; (b) G. W. Reginsson and O. Schiemann, *Encyclopedia of Biophysics*, Springer, 2013, pp. 2429–2431.
- 7 (a) P. Belmont, C. Chapelle, M. Demeunynck, J. Michon, P. Michon and J. Lhomme, *Bioorg. Med. Chem. Lett.*, 1998, 8, 669–674; (b) K. Maekawa, S. Nakazawa, H. Atsumi, D. Shiomi, K. Sato, M. Kitagawa, T. Takui and K. Nakatani, *Chem. Commun.*, 2010, 46, 1247–1249; (c) S. A. Shelke and S. T. Sigurdsson, *Angew. Chem., Int. Ed.*, 2010, 49, 7984–7986; (d) S. A. Shelke, G. B. Sandholt and S. T. Sigurdsson, *Org. Biomol. Chem.*, 2014, 12, 7366–7374; (e) B. A. Chalmers, S. Saha, T. Nguyen, J. McMurtrie, S. T. Sigurdsson, S. E. Bottle and K. S. Masters, *Org. Lett.*, 2014, 16, 5528–5531.
- 8 S. A. Shelke and S. T. Sigurdsson, *Eur. J. Org. Chem.*, 2012, 2291–2301.
- 9 A. Spaltenstein, B. H. Robinson and P. B. Hopkins, *J. Am. Chem. Soc.*, 1988, 110, 1299–1301.
- 10 (a) T. R. Miller, S. C. Alley, A. W. Reese, M. S. Solomon, W. V. McCallister, C. Mailer, B. H. Robinson and P. B. Hopkins, *J. Am. Chem. Soc.*, 1995, 117, 9377–9378; (b) N. Barhate, P. Cekan, A. P. Massey and S. T. Sigurdsson, *Angew. Chem., Int. Ed.*, 2007, 46, 2655–2658; (c) D. B. Gophane and S. T. Sigurdsson, *Chem. Commun.*, 2013, 49, 999–1001.
- 11 (a) N. Piton, Y. Mu, G. Stock, T. F. Prisner, O. Schiemann and J. W. Engels, *Nucleic Acids Res.*, 2007, 35, 3128–3143; (b) P. Cekan, A. L. Smith, N. Barhate, B. H. Robinson and S. T. Sigurdsson, *Nucleic Acids Res.*, 2008, 36, 5946–5954.
- 12 (a) H. Hara, T. Horiuchi, M. Saneyoshi and S. Nishimura, *Biochem. Biophys. Res. Commun.*, 1970, 38, 305–311; (b) P. Z. Qin, S. E. Butcher, J. Feigon and W. L. Hubbell, *Biochemistry*, 2001, 40, 6929–6936; (c) T. E. Edwards, T. M. Okonogi, B. H. Robinson and S. T. Sigurdsson, *J. Am. Chem. Soc.*, 2001, 123, 1527–1528; (d) P. Z. Qin, K. Hideg, J. Feigon and W. L. Hubbell, *Biochemistry*, 2003, 42, 6772–6783; (e) P. Z. Qin, I. S. Haworth, Q. Cai, A. K. Kusnetzow, G. P. G. Grant, E. A. Price, G. Z. Sowa, A. Popova, B. Herreros and H. He, *Nat. Protoc.*, 2007, 2, 2354–2365; (f) G. P. G. Grant and P. Z. Qin, *Nucleic Acids Res.*, 2007, 35, e77; (g) P. Ding, D. Wunnicke, H. J. Steinhoff and F. Seela, *Chem. – Eur. J.*, 2010, 16, 14385–14396; (h) U. Jakobsen, S. A. Shelke, S. Vogel and S. T. Sigurdsson, *J. Am. Chem. Soc.*, 2010, 132, 10424–10428.
- 13 (a) N. K. Kim, A. Murali and V. J. DeRose, *Chem. Biol.*, 2004, 11, 939–948; (b) T. E. Edwards and S. T. Sigurdsson, *Nat. Protoc.*, 2007, 2, 1954–1962.
- 14 S. T. Sigurdsson and F. Eckstein, *Nucleic Acids Res.*, 1996, 24, 3129–3133.
- 15 (a) H. Aurup, T. Tuschl, F. Benseler, J. Ludwig and F. Eckstein, *Nucleic Acids Res.*, 1994, 22, 20–24; (b) S. T. Sigurdsson, T. Tuschl and F. Eckstein, *RNA*, 1995, 1, 575–583.
- 16 D. B. Gophane, B. Endeward, T. F. Prisner and S. T. Sigurdsson, *Chem. – Eur. J.*, 2014, 20, 15913–15919.
- 17 (a) L. Marx, R. Chiarelli, T. Guiberteau and A. Rassat, *J. Chem. Soc., Perkin Trans. 1*, 2000, 1181–1182; (b) A. P. Jagtap, I. Krstić, N. C. Kunjir, R. Hänsel, T. F. Prisner and S. T. Sigurdsson, *Free Radical Res.*, 2015, 49, 78–85.
- 18 (a) D. A. Reid, S. E. Bottle and A. S. Micallef, *Chem. Commun.*, 1998, 1907–1908; (b) E. Mileo, E. Etienne, M. Martinho, R. Lebrun, V. Roubaud, P. Tordo, B. Gontero, B. Guigliarelli, S. R. A. Marque and V. Belle, *Bioconjugate Chem.*, 2013, 24, 1110–1117.
- 19 H. T. Steely, D. M. Gray, D. Lang and M. F. Maestre, *Biopolymers*, 1986, 25, 91–117.
- 20 (a) I. Krstić, R. Hänsel, O. Romainczyk, J. W. Engels, V. Dötsch and T. F. Prisner, *Angew. Chem., Int. Ed.*, 2011, 50, 5070–5074; (b) M. Azarkh, O. Okle, V. Singh, I. T. Seemann, J. S. Hartig, D. R. Dietrich and M. Drescher, *ChemBioChem*, 2011, 12, 1992–1995; (c) I. T. Holder, M. Drescher and J. S. Hartig, *Bioorg. Med. Chem.*, 2013, 21, 6156–6161; (d) M. Azarkh, V. Singh, O. Okle, I. T. Seemann, D. R. Dietrich, J. S. Hartig and M. Drescher, *Nat. Protoc.*, 2013, 8, 131–147; (e) M. Qi, A. Groß, G. Jeschke, A. Godt and M. Drescher, *J. Am. Chem. Soc.*, 2014, 136, 15366–15378; (f) R. Hänsel, L. M. Luh, I. Corbeski, L. Trantirek and V. Dötsch, *Angew. Chem., Int. Ed.*, 2014, 53, 10300–10314.
- 21 (a) W. R. Couet, R. C. Brasch, G. Sosnovsky, J. Lukszo, I. Prakash, C. T. Gnewuch and T. N. Tozer, *Tetrahedron*, 1985, 41, 1165–1172; (b) J. P. Blinco, J. L. Hodgson, B. J. Morrow, J. R. Walker, G. D. Will, M. L. Coote and S. E. Bottle, *J. Org. Chem.*, 2008, 73, 6763–6771; (c) M. Azarkh, O. Okle, P. Eyring, D. R. Dietrich and M. Drescher, *J. Magn. Reson.*, 2011, 212, 450–454; (d) T. B. Kajer, K. E. Fairfull-Smith, T. Yamasaki, K. Yamada, S. Fu, S. E. Bottle, C. L. Hawkins and M. J. Davies, *Free Radical Biol. Med.*, 2014, 70, 96–105.
- 22 (a) Y. Kinoshita, K. Yamada, T. Yamasaki, H. Sadasue, K. Sakai and H. Utsumi, *Free Radical Res.*, 2009, 43, 565–571; (b) Y. Kinoshita, K. Yamada, T. Yamasaki, F. Mito, M. Yamato, N. Kosem, H. Deguchi, C. Shirahama, Y. Ito, K. Kitagawa, N. Okukado, K. Sakai and H. Utsumi, *Free Radical Biol. Med.*, 2010, 49, 1703–1709.

Site-directed spin-labeling of 2'-amino groups in RNA with isoindoline nitroxides that are resistant to reduction

Subham Saha[†], Anil P. Jagtap[†] and Snorri Th. Sigurdsson*

University of Iceland, Department of Chemistry, Science Institute, Dunhaga 3, 107 Reykjavik, Iceland. E-mail: snorrisi@hi.is

Table of contents

List of abbreviations	S2
Synthetic procedures	S2
General materials and methods	S2
1,1,3,3-Tetramethylisoindolin-5-isothiocyanate-2-oxyl (1)	S3
1,1,3,3-Tetraethylisoindolin-5-isothiocyanate-2-oxyl (2)	S4
RNA synthesis and purification	S5
General procedure for RNA spin-labeling with 1 and 2	S7
Investigating if reaction of 1 with RNA results in non-specific labeling	S8
Analyses of spin-labeled oligonucleotides	S9
Instruments and methods	S9
MALDI-TOF analyses	S10
Circular dichroism (CD) spectra	S11
Thermal denaturation experiments	S12
Electron paramagnetic resonance (EPR) spectra	S13
Molecular modeling	S14
Stability of spin-labeled RNAs towards ascorbate reduction	S15
References	S16

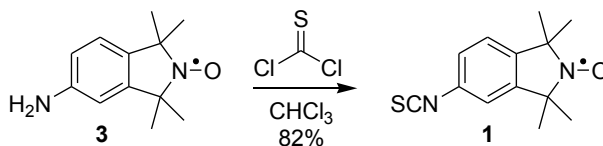
List of abbreviations

DPAGE	Denaturing polyacrylamide gel electrophoresis
EPR	Electron paramagnetic resonance
DMF	<i>N,N</i> -Dimethylformamide
MALDI-TOF	Matrix-assisted laser desorption/ionization - time of flight
HR-ESI-MS	High-resolution electrospray ionization mass spectrometry
TLC	Thin layer chromatography
IR	Infrared spectroscopy
CD	Circular dichroism
TBDMS	<i>tert</i> -butyldimethylsilyl
UV	Ultraviolet
CW	Continuous wave
MMFF	Merck Molecular Force Field

Synthetic procedures

General materials and methods

All reagents and CHCl_3 , used as a solvent for reactions, were purchased from Sigma Aldrich and used without further purification. Water was purified on a MILLI-Q water purification system. TLC was carried out using glass plates pre-coated with silica gel (0.25 mm, F-254) from Silicycle, Canada. All synthesized compounds were visualized by UV light. Flash column chromatography was performed using ultra pure flash silica gel (Silicycle, 230-400 mesh size, 60 Å). All moisture and air-sensitive reactions were carried out in oven-dried glassware under an inert argon atmosphere. Nitroxide radicals show broadening and loss of NMR signals due to their paramagnetic nature,^{1, 2} and therefore, the NMR data for the isoindoline spin labels have not been shown. Mass spectrometric analyses of all organic compounds were performed on an HR-ESI-MS (Bruker, MicrOTOF-Q) in a positive ion mode.



1,1,3,3-Tetramethylisindolin-5-isothiocyanate-2-oxyl (**1**)

A solution of thiophosgene (0.041 mL, 0.54 mmol) in CHCl_3 (1 mL) was added dropwise to a solution of 1,1,3,3-tetramethylisindolin-5-amine-2-oxyl³ (**3**) (0.100 g, 0.49 mmol) in CHCl_3 (3.5 mL). The reaction mixture was stirred at 24 °C for 2 h, diluted with CH_2Cl_2 (5 mL) and the organic layer was washed successively with NaOH solution (4 mL, 1 M), water (2 x 5 mL) and brine (5 mL). The organic layer was dried over anhydrous Na_2SO_4 , filtered and concentrated *in vacuo* to obtain the crude product, which was purified by flash column chromatography (silica) using a gradient elution (EtOAc:pet. ether; 0:100 to 5:95) to give **1** (0.098 g, 82%) as a yellowish solid.

TLC: (Silica gel, 20% EtOAc in pet. ether), R_f (**3**) = 0.2, R_f (**1**) = 0.5.

EPR: Compound **1** shows characteristic EPR triplet of a nitroxide radical (**Fig. S1**).

HRMS: Calculated for $\text{C}_{13}\text{H}_{15}\text{N}_2\text{OS}$: 247.09, found 270.0802 ($\text{M}+\text{Na}^+$).

IR: Shows the characteristic isothiocyanato (-NCS) stretching frequency at 2120 cm^{-1} .

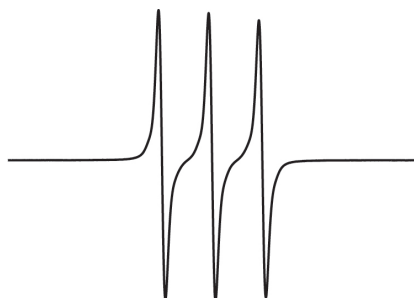
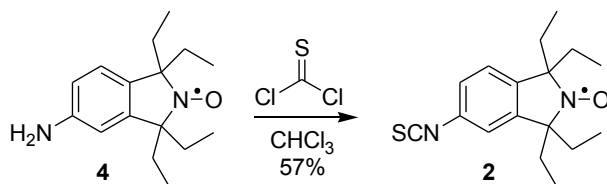


Fig. S1. EPR spectrum of 1,1,3,3-tetramethylisindolin-5-isothiocyanate-2-oxyl (**1**) recorded in EtOH at 25 °C.



1,1,3,3-Tetraethylisindolin-5-isothiocyanate-2-oxyl (**2**)

A solution of thiophosgene (0.032 mL, 0.42 mmol) in CHCl_3 (1 mL) was added dropwise to a solution of 1,1,3,3-tetraethylisindolin-5-amine-2-oxyl³ (**4**) (0.100 g, 0.38 mmol) in CHCl_3 (3.5 mL). The reaction mixture was stirred at 24 °C for 2 h, diluted with CH_2Cl_2 (5 mL) and the organic layer was washed successively with NaOH solution (4 mL, 1 M), water (2 x 5 mL) and brine (5 mL). The organic layer was dried over anhydrous Na_2SO_4 , filtered and concentrated *in vacuo* to obtain the crude product, which was purified by flash column chromatography (silica) using a gradient elution (EtOAc:pet. ether; 0:100 to 5:95) to give 1,1,3,3-tetraethylisindolin-5-isothiocyanate-2-oxyl (**2**) (0.066 g, 57%) as a yellowish solid.

TLC: (Silica gel, 20% EtOAc in pet. ether), R_f (**4**) = 0.2, R_f (**2**) = 0.8.

EPR: Compound **2** shows characteristic EPR triplet of a nitroxide radical (**Fig. S2**).

HRMS: Calculated for $\text{C}_{17}\text{H}_{23}\text{N}_2\text{OS}$: 303.15, found 326.1426 ($\text{M}+\text{Na}^+$).

IR: Shows the characteristic isothiocyanato (-NCS) stretching frequency at 2120 cm^{-1} .

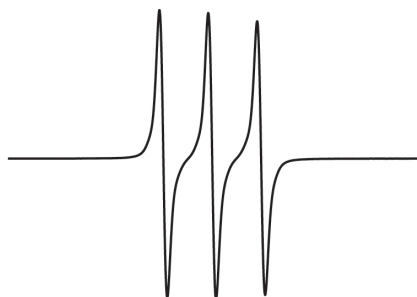

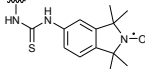
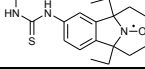
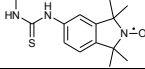
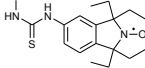
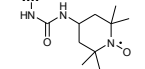
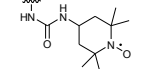



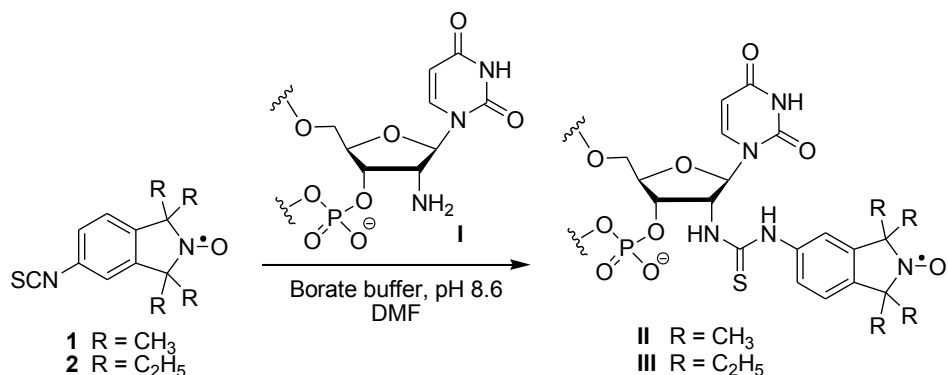
Fig. S2. EPR spectrum of 1,1,3,3-tetraethylisindolin-5-isothiocyanate-2-oxyl (**2**) recorded in EtOH at 25 °C.

RNA synthesis and purification

All unmodified RNA oligonucleotides and 2'-amino uridine-modified oligonucleotide **I** were synthesized in-house on an automated ASM800 DNA synthesizer (BIOSSET Ltd., Russia) using phosphoramidite chemistry. All phosphoramidites, the activator 5-benzylthiotetrazole, acetonitrile for oligomer synthesis and controlled pore glass (CPG) columns (1000 Å) were purchased from ChemGenes Corp., USA. All other reagents and solvents were purchased from Sigma-Aldrich Co. Syntheses were performed on a 1 µmol scale by trityl-off synthesis. After completion of RNA synthesis, the oligonucleotides were deprotected and cleaved from the resin by adding a 1:1 solution (2 mL) of CH₃NH₂ (8 M in EtOH) and NH₃ (33% w/w in H₂O) and heating for 40 min at 65 °C. The solvent was removed *in vacuo* and the TBDMS-protection groups were removed by incubation in NEt₃:3HF (600 µL) for 90 min at 55 °C in DMF (200 µL), followed by addition of water (200 µL). The resulting solution was transferred into a 50 mL Falcon tube and the RNA was precipitated by adding 1-butanol (20 mL, 12 h at -80 °C). All oligonucleotides were subsequently purified by 20% DPAGE and extracted from the gel slices using the “crush and soak method” with Tris buffer containing 250 mM NaCl, 10 mM Tris, 1 mM Na₂EDTA, pH 7.5. The solutions were filtered through 0.45 µm, 25 mm diameter GD/X syringe filters (Whatman, USA) and were subsequently desalted using Sep-Pak cartridges (Waters, USA), following the instructions provided by the manufacturer. Dried oligonucleotides were dissolved in sterilized and deionized water (200 µL for each oligonucleotide). Concentrations of the oligonucleotides were determined by UV absorbance at 260 nm using a Perkin Elmer Inc. Lambda 25 UV/Vis spectrometer and calculated by Beer's law. Isocyanato-TEMPO-modified RNA oligonucleotide **VI** was prepared following a previously reported procedure.⁴ **Table S1** shows the complete list of all the modified and unmodified RNA oligonucleotides along with the structure of the modifications.

Table S1. List of all RNA oligonucleotides.

Modification (U ^X)	RNA	Sequence
	I	5'-GAC CUC G (2'-NH ₂ U) A UCG UG-3'
	II	5'-GAC CUC GU ^X A UCG UG-3'
	III	5'-GAC CUC GU ^X A UCG UG-3'
	IV	5'-GAC CUC GU ^X A UCG UG-3' 3'-CUG GAG CA U AGC AC-5'
	V	5'-GAC CUC GU ^X A UCG UG-3' 3'-CUG GAG CA U AGC AC-5'
	VI	5'-GAC CUC GU ^X A UCG UG-3'
	VII	5'-GAC CUC GU ^X A UCG UG-3' 3'-CUG GAG CA U AGC AC-5'
	VIII	5'-GAC CUC G (2'-NH ₂ U) A UCG UG-3' 3'-CUG GAG C A U AGC AC-5'
-	IX	5'-GAC CUC GUA UCG UG-3'
-	X	5'-GAC CUC GUA UCG UG-3' 3'-CUG GAG CAU AGC AC-5'



General procedure for RNA spin-labeling with **1** and **2**

A solution of RNA oligonucleotide **I** (40 nmol) in 100 mM borate buffer, pH 8.6 (20 μ L) was added to a solution of **1** or **2** (2 μ mol) in DMF (20 μ L). The reaction mixture was heated at 37 $^{\circ}$ C for 8 h, followed by addition of sterile water (200 μ L) and extraction with EtOAc (6 x 500 μ L) to remove any unreacted spin label. For RNA **II**, an EtOH precipitation was performed [5 μ L of 3M sodium acetate (pH 4.6), 300 μ L of cold (-20 $^{\circ}$ C) absolute ethanol and storing at -80 $^{\circ}$ C for 4 h] to remove the rest of the free-spin contaminant. RNA **II** obtained by precipitation was of similar purity (as judged by EPR and DPAGE), as observed for **II** that was purified further by 20% DPAGE, to obtain 32 nmol of RNA oligonucleotide **II** (76%). DPAGE purification of RNA oligonucleotide **III** yielded 34 nmol (80%) after the EtOAc extraction.

Investigating if reaction of **1** with RNA results in non-specific labeling

To test the selectivity of the spin labeling strategy, a solution of RNA oligonucleotide **IX** (40 nmol) in borate buffer (20 μ L, 100 mM, pH 8.6) was added to a solution of **1** (2 μ mol) in DMF (20 μ L) and heated at 60 $^{\circ}$ C. Aliquots were collected at specific time points (described in **Table S2**) and analyzed by DPAGE (**Fig. S3**). No change was observed in the mobility of the unmodified oligonucleotide, even after heating for 48 h (**Fig. S3**, lane D), proving that the spin labeling procedure is highly specific to 2'-amino groups in RNA. Spin-labeled RNA **II** was used as a marker for modified RNA.

Table S2. Table describing the control reactions (showed in **Fig. S7**).

Lane	RNA	Temperature	Duration
A	5' -GAC CUC GUA UCG UG	---	0 h
B	5' -GAC CUC GUA UCG UG	60 $^{\circ}$ C	12 h
C	5' -GAC CUC GUA UCG UG	60 $^{\circ}$ C	24 h
D	5' -GAC CUC GUA UCG UG	60 $^{\circ}$ C	48 h

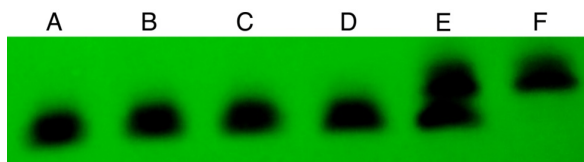


Fig. S3. DPAGE analysis of reaction of **1** and **I**. Lanes A-D are described in **Table S2**, Lane F contains spin-labeled RNA **II** and lane E is an equimolar mixture of lanes D and F.

Analyses of spin-labeled oligonucleotides

Instruments and methods

MALDI-TOF analyses of the RNA oligonucleotides were performed on a Bruker Daltonics Autoflex III. The instrument was calibrated with external standards prior to measuring the mass of the spin-labeled oligonucleotides and 3-hydroxypicolinic acid was used as the matrix. Prior to analysis by CD, thermal denaturation and EPR, an appropriate quantity of each RNA stock solution was dried on a Thermo Scientific ISS 110 Speedvac and dissolved in phosphate buffer (10 mM phosphate, 100 mM NaCl, 0.1 mM Na₂EDTA, pH 7.0). RNA duplexes were formed by annealing in an MJ Research PTC 200 Thermal Cycler using the following protocol: 90 °C for 2 min, 60 °C for 5 min, 50 °C for 5 min, 40 °C for 5 min and 22 °C for 15 min. CD spectra of RNA duplexes were recorded in a Jasco J-810 spectropolarimeter. Cuvettes with 1 mm path length were used and the CD data were recorded from 350 nm to 200 nm at 25 °C. Thermal denaturation curves of the oligonucleotides were obtained using a Perkin Elmer PTP-1 and PCB 150 Water Peltier System. Prior to recording T_M data, the samples were diluted to 1.0 mL with phosphate buffer, making the final concentration 3 μ M and degassed using argon. The samples were heated up from 10 °C to 90 °C (1.0 °C/min) while recording the absorbance at 260 nm. EPR spectroscopy was performed to judge the mobilities of the spin-labeled oligonucleotides and measured over a range of temperatures from 30 °C to -10 °C, with intervals of 10 °C on an X-band EPR spectrometer (Miniscope MS 200, Magnettech, Germany) with 100 kHz modulation frequency, 1.0 G modulation amplitude and 2.0 mW microwave power and using 60 to 100 scans for each sample after placing them into a quartz capillary tube (BLAUBRAND®-intraMARK). The temperature was regulated by a Magnettech temperature controller M01.

MALDI-TOF analyses

To verify incorporation of the spin labels into the oligonucleotides, they were analyzed by MALDI-TOF experiments. **Fig. S4** shows the MALDI-TOF spectra of spin-labeled oligonucleotides **II** (5'-GAC CUC GU¹A UCG UG-3') (4667.121, calcd. 4666.711) and **III** (5'-GAC CUC GU²A UCG UG-3') (4722.435, calcd. 4722.771).

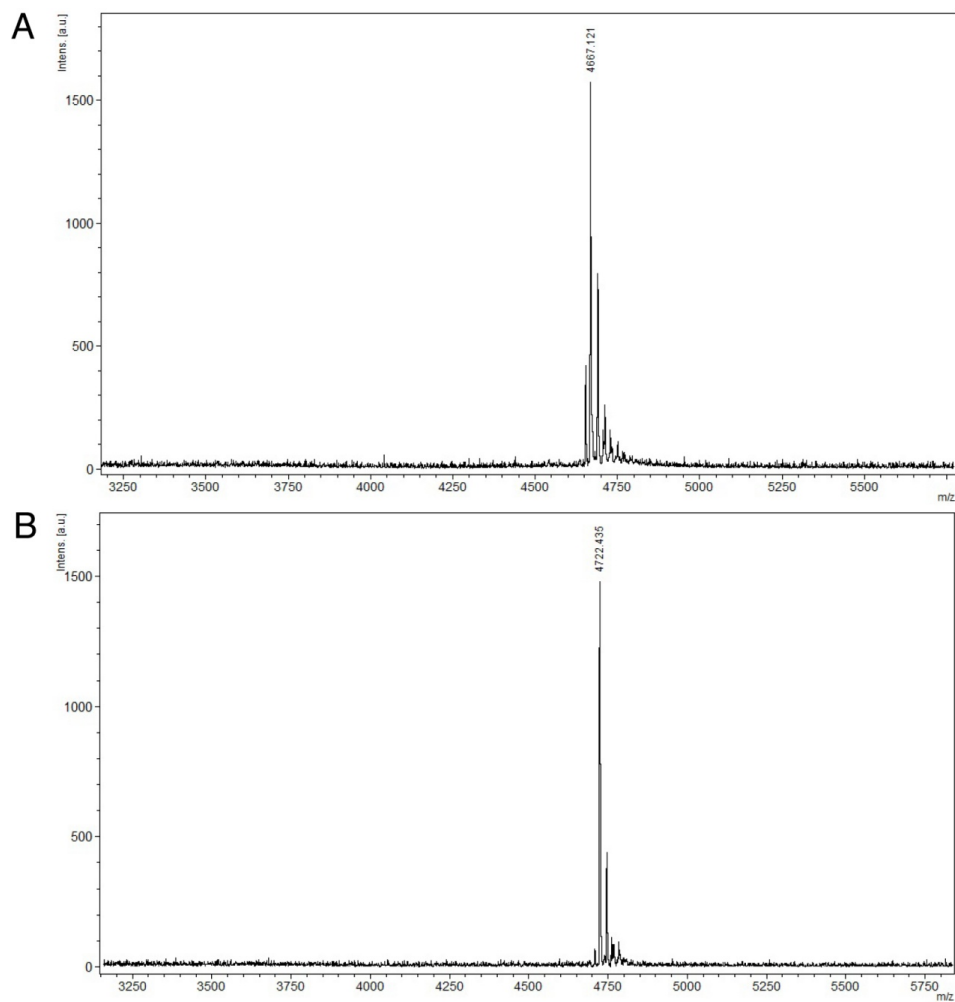


Fig. S4. MALDI-TOF spectra of spin-labeled oligonucleotides **II** (A) and **III** (B).

Circular dichroism (CD) spectra

CD spectra were recorded to determine if modifications on the oligonucleotides altered the RNA duplex conformation. **Fig. S5** shows the CD spectra of RNA duplexes **IV**, **V**, **VIII** and **X**. All the RNA duplexes showed negative and positive molar ellipticities at ca. 210 nm and 262-264 nm, respectively.

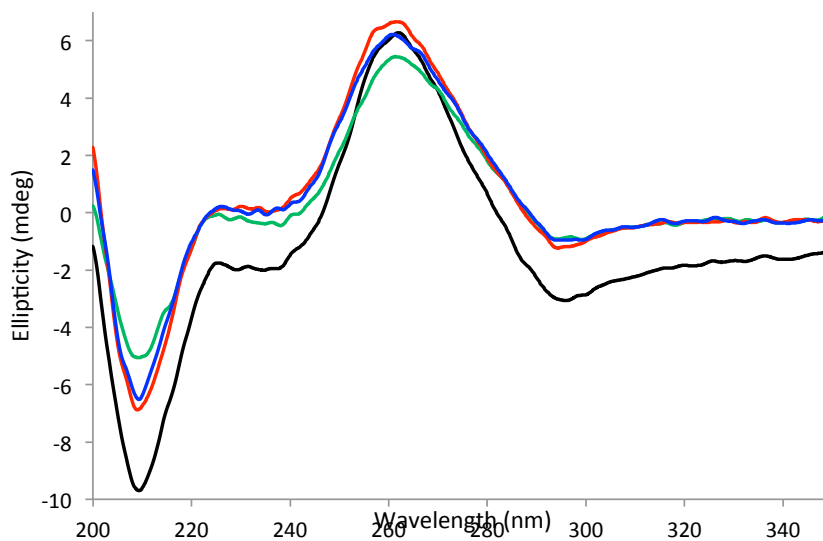


Fig. S5. CD spectra of 14-mer RNA duplex **IV** (red), **V** (blue), **VIII** (green) and **X** (black) (12.5 μ M each) recorded at 25 $^{\circ}$ C in phosphate buffer (10 mM phosphate, 100 mM NaCl, 0.1 mM Na₂EDTA, pH 7.0).

Thermal denaturation experiments

To investigate if the spin labels affect RNA duplex stability, thermal denaturation experiments were performed. **Fig. S6** shows representative melting curves for RNA duplexes, showing cooperative melting transitions. The T_M values were determined from the first derivatives of the melting curves and summarized in **Table S3**.

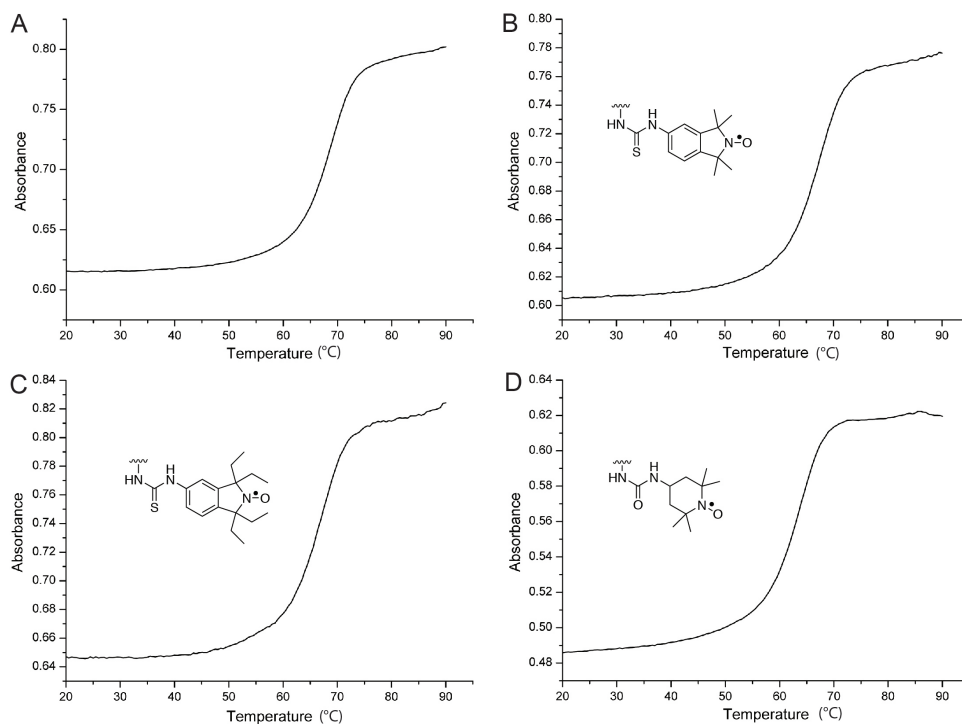
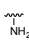
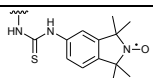
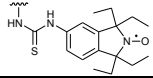
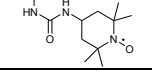


Fig. S6. Thermal denaturation curves of unmodified duplex **X** (A), as well as spin-labeled duplexes **IV** (B), **V** (C) and **VII** (D).

Table S3. Melting temperatures (T_M) of the RNA duplexes.

Modification	RNA	Duplex sequences	T_M (°C)	ΔT_M (°C)
—	X	5' -GAC CUC GUA UCG UG-3' 3' -CUG GAG CAU AGC AC-5'	68.5 ± 0.5	—
	VIII	5' -GAC CUC G (2'-NH ₂ U) A UCG UG-3' 3' -CUG GAG C A U AGC AC-5'	66.3 ± 0.5	-2.2
	IV	5' -GAC CUC GU ^x A UCG UG-3' 3' -CUG GAG CA U AGC AC-5'	67.3 ± 0.7	-1.2
	V	5' -GAC CUC GU ^x A UCG UG-3' 3' -CUG GAG CA U AGC AC-5'	66.5 ± 0.9	-2.0
	VII	5' -GAC CUC GU ^x A UCG UG-3' 3' -CUG GAG CA U AGC AC-5'	63.2 ± 0.5	-5.3

Electron paramagnetic resonance (EPR) spectra

Fig. S7 shows EPR spectra of single strands (A) and duplexes (B) at different temperatures. As expected, the spectra become broader upon cooling. Furthermore, the spectral width for duplexes **IV** and **V** were significantly wider than for the single-stranded counterparts, indicating that duplex formation severely restricted the mobility of the spin labels. Therefore, molecular modeling was performed on the spin-labeled duplexes (See **Page S14**).

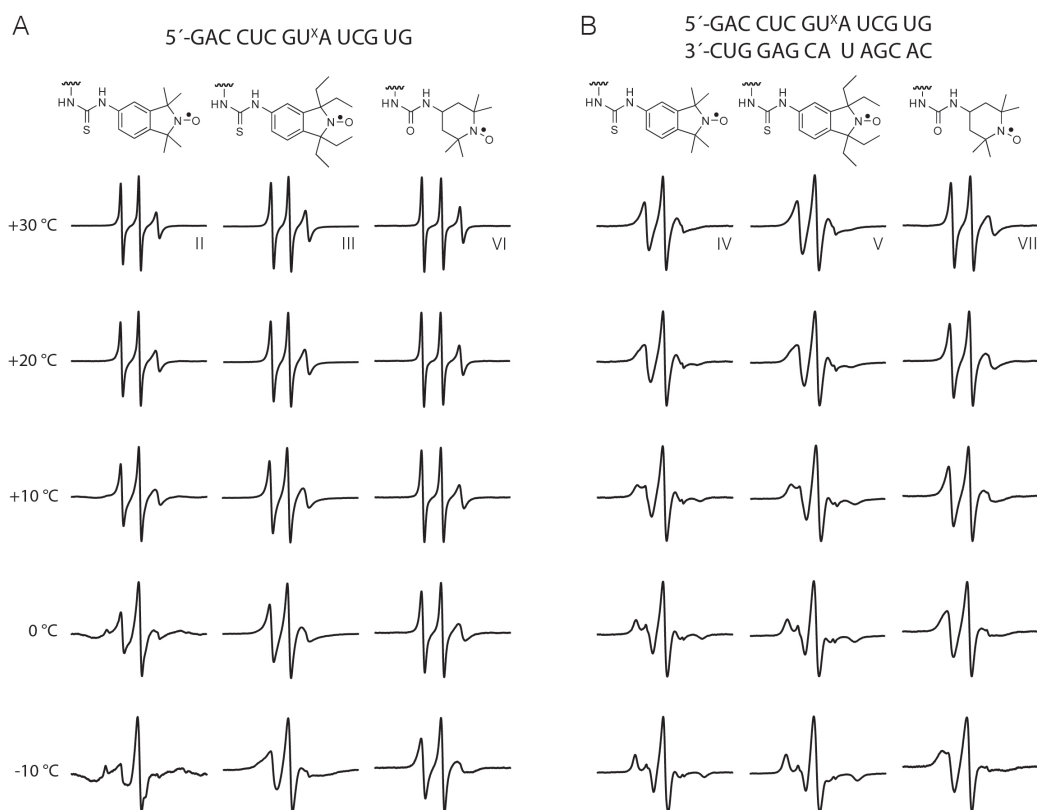


Fig. S7. CW EPR data of spin-labeled RNA single strands **II**, **III**, **VI** (A) and duplexes **IV**, **V** and **VII** (B) plotted as a function of decreased temperature. All spectra were phase corrected and aligned with respect to the central peak.

Molecular modeling

A molecular model for an RNA duplex was generated in Spartan'10 using the “nucleotide” constructing feature and the spin label was constructed using the “organic” construction tool. Energy of the spin label was minimized using the minimizer built into Spartan, which is based on the MMFF force field. The spin label was then connected to the desired position in the RNA using the “make bond” tool. **Fig. S8A** shows the resulting structure as obtained from PyMOL, in a space-filling display. The sulfur atom (yellow) nestled snugly between two oxygen atoms of the spin-labeled nucleotide, the 3'-oxygen and the oxygen within the corresponding ribose sugar ring (**Fig. S8B-C**), restricting its motion.

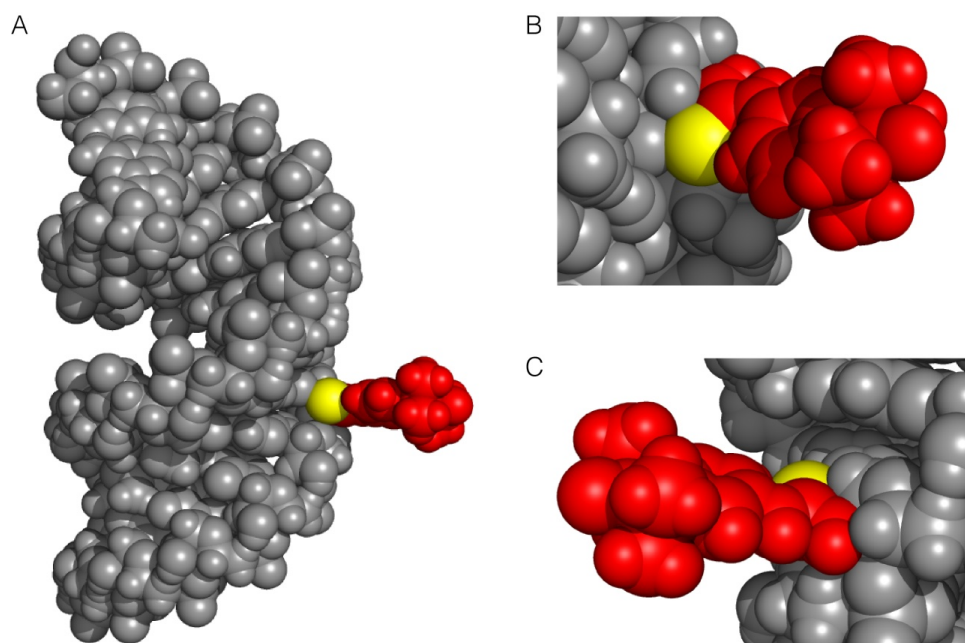


Fig. S8. Molecular model of the RNA duplex **IV** (grey) shown in entirety (A) and as close-ups from two different dimensions (B) and (C). Conjugated spin label **1** has been shown in red except for the sulfur atom that has been coloured yellow.

Stability of spin-labeled RNAs towards ascorbate reduction

To check the stability of the spin labels in RNA under reducing conditions, the spin-labeled RNAs were reacted with ascorbic acid (5 mM ascorbic acid, 200 μ M spin-labeled RNA, 10 mM phosphate, 100 mM NaCl, 0.1 mM Na₂EDTA, pH 7.0) and the EPR signal decay was plotted as a function of time (**Fig. S9**). Ethyl isoindoline-derived oligonucleotides **III** and **V** were found to be highly stable and thus, their decay curves have been plotted up to 12 h. Methyl isoindoline-derived RNAs **II** and **IV** were moderately stable (2 h plots) whereas isocyanato-TEMPO-labeled oligonucleotides **VI** and **VII** were found to be rapidly reduced.

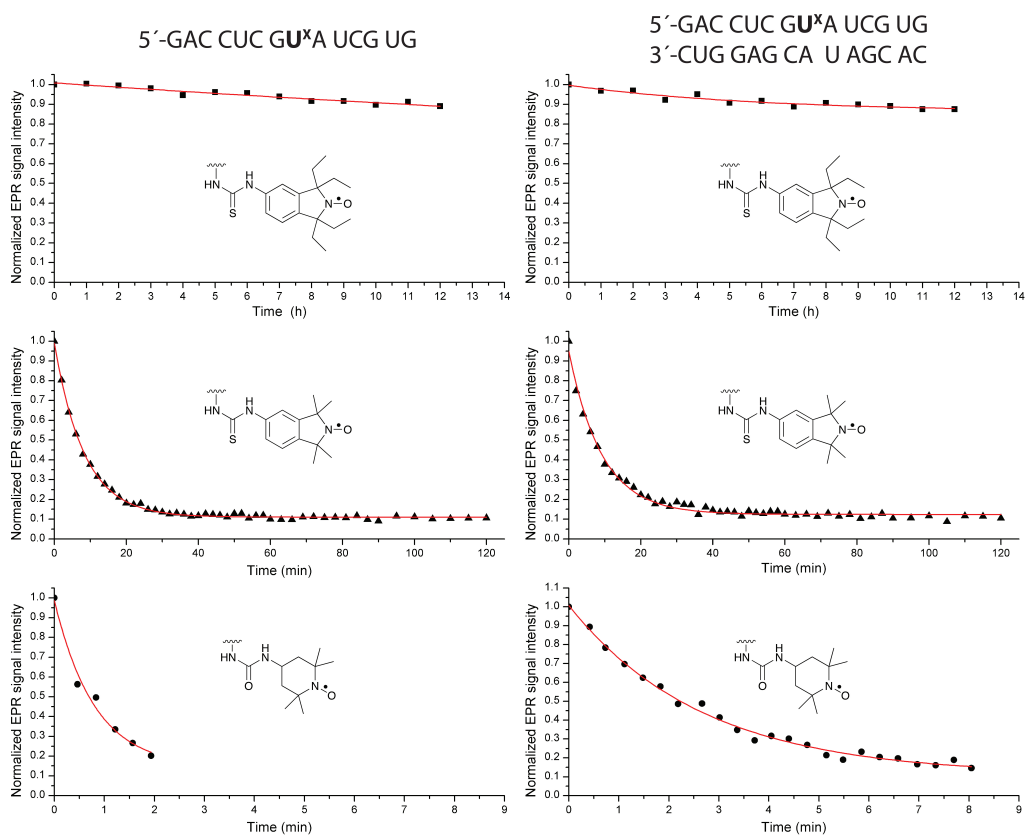
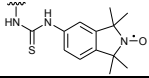
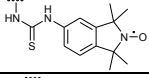
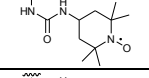
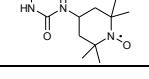


Fig. S9. Ascorbic acid reduction curves for single-stranded RNA oligonucleotides **III**, **II**, **VI** (left column) and their corresponding duplexes **V**, **IV** and **VII** (right column). All curves were fitted with their exponential functions (red line).

Due to the large excess of ascorbic acid, reduction of the radicals followed (pseudo) first order kinetics. The EPR signal decay curves were fitted with a first order exponential function and their half-lives ($t_{1/2}$) were calculated accordingly. **Table S4** shows the half-lives of the tetramethyl isoindoline- and 4-isocyanato TEMPO-labeled oligonucleotides. Single-

stranded tetramethyl isoindoline-labeled RNA **II** showed a $t_{1/2}$ of 6.7 min whereas it increased slightly to 7.2 min as duplex **IV**. The TEMPO label was the least stable one with the single strand **VI** and duplex **VII** showing half-lives of 0.7 min and 2.2 min, respectively. Reduction kinetics of the tetraethyl isoindoline-labeled RNAs **III** and **V** did not follow exponential decay, but ca. 90% was still intact after 12 h.

Table S4. Half-lives ($t_{1/2}$) of select RNA sequences.

Modification	RNA	Sequence	$t_{1/2}$
	II	5'-GAC CUC GU ^X A UCG UG-3'	6.7 min
	IV	5'-GAC CUC GU ^X A UCG UG-3' 3'-CUG GAG CA U AGC AC-5'	7.2 min
	VI	5'-GAC CUC GU ^X A UCG UG-3'	0.7 min
	VII	5'-GAC CUC GU ^X A UCG UG-3' 3'-CUG GAG CA U AGC AC-5'	2.2 min

References

1. T. D. Lee and J. F. Keana, *J. Org. Chem.*, 1975, **40**, 3145-3147.
2. Y. Li, X. Lei, X. Li, R. G. Lawler, Y. Murata, K. Komatsu and N. J. Turro, *Chem. Commun.*, 2011, **47**, 12527-12529.
3. A. P. Jagtap, I. Krstić, N. C. Kunjir, R. Hänsel, T. F. Prisner and S. T. Sigurdsson, *Free Radical Res.*, 2014, **49**, 1-25.
4. T. E. Edwards and S. T. Sigurdsson, *Nat. Protoc.*, 2007, **2**, 1954-1962.

Paper III



Site-Directed Spin Labeling of RNA by Postsynthetic Modification of 2'-Amino Groups

Subham Saha, Anil P. Jagtap, Snorri Th. Sigurdsson¹

Department of Chemistry, Science Institute, University of Iceland, Reykjavik, Iceland

¹Corresponding author: e-mail address: snorrisi@hi.is

Contents

1. Introduction	398
1.1 The Phosphoramidite Method for SDSL	400
1.2 Postsynthetic Spin-Labeling	401
2. 2'-Amino Spin-Labeling with Aliphatic Isocyanates and Aromatic Isothiocyanates	404
2.1 Spin-Labeling of 2'-Amino Groups in RNA with 4-Isocyanato-TEMPO	405
2.2 Synthesis of Isothiocyanate-Containing Spin Labels	406
2.3 Spin Labeling of 2'-Amino Groups in RNA with Isothiocyanates	407
2.4 Analysis of Spin-Labeled Oligonucleotides	409
3. Summary and Conclusions	410
Acknowledgments	411
References	411

Abstract

To elucidate mechanisms that govern functions of nucleic acids, it is essential to understand their structure and dynamics. Electron paramagnetic resonance (EPR) spectroscopy is a valuable technique that is routinely used to study those aspects of nucleic acids. A prerequisite for most EPR studies of nucleic acids is incorporation of spin labels at specific sites, known as site-directed spin labeling (SDSL). There are two main strategies for SDSL through formation of covalent bonds, i.e., the phosphoramidite approach and postsynthetic spin-labeling. After describing briefly the advantages and disadvantages of these two strategies, postsynthetic labeling of 2'-amino groups in RNA is delineated. Postsynthetic labeling of 2'-amino groups in RNA using 4-isocyanato-TEMPO has long been established as a useful approach. However, this method has some drawbacks, both with regard to the spin-labeling protocol and the flexibility of the spin label itself. Recently reported isothiocyanate-substituted aromatic isoindoline-derived nitroxides can be used to quantitatively and selectively modify 2'-amino groups in RNA and do not have the drawbacks associated with 4-isocyanato-TEMPO. This chapter provides a detailed description of the postsynthetic spin-labeling methods of 2'-amino groups in RNA with a special focus on using the aromatic isothiocyanate spin labels.



1. INTRODUCTION

Nucleic acids are essential molecules for sustaining life. DNA and RNA are responsible for storage, expression, and transmission of genetic information—DNA carries the genetic information, whereas RNA has varied functions, such as transferring genetic information and acting as a chief constituent of ribonucleoprotein complexes involved with mRNA processing and translation. RNA can also catalyze reactions; a prominent example is formation of peptide bonds by the ribosome (Nissen, Hansen, Ban, Moore, & Steitz, 2000). RNA has also been implied in the catalytic function of the spliceosome (Fica et al., 2013). Recently discovered siRNAs play a notable role in RNA interference, where they inhibit particular gene expressions (Brummelkamp, Bernards, & Agami, 2002). Moreover, riboswitches have an important role in regulating gene expression (Mandal & Breaker, 2004).

It is of interest to know the structure and dynamics of nucleic acids, because these properties govern their functions. There are several biochemical and biophysical techniques that have been applied for the study of the structure and function of nucleic acids. The most powerful technique is undoubtedly X-ray crystallography, which is capable of providing a “photographic” representation of the three-dimensional molecular structure. However, this highly informative technique requires a sufficiently large and regular single crystal, which can be a daunting task to obtain for nucleic acids. In addition, a crystal structure might not represent a biologically active conformation. Moreover, an X-ray structure provides a static view, whereas conformational changes are usually required to carry out specific functions. Another high-resolution technique to study nucleic acid structure is nuclear magnetic resonance (NMR) spectroscopy, which provides structural information of the nucleic acid in solution, thus revealing their conformation under biologically relevant conditions. However, NMR of nucleic acids often requires relatively large amounts of isotopically labeled samples. Furthermore, NMR studies are usually restricted to nucleic acids that are smaller than 50 kDa (Xu & Matthews, 2013), because the increased anisotropy associated with slower tumbling of large molecules in solution causes peak broadening. Another common technique for studying nucleic acids is Förster resonance energy transfer, which is capable of measuring distances in the nanometer range. This technique can also be used to study nucleic acids under biologically relevant conditions, in addition to enabling

single-molecule studies (Roy, Hohng, & Ha, 2008; Sisamakis, Valeri, Kalinin, Rothwell, & Seidel, 2010). However, since natural nucleic acids do not possess any fluorescent chromophores, a prerequisite for this technique is the incorporation of a pair of rather bulky fluorophores.

The technique that will be addressed here is electron paramagnetic resonance (EPR) spectroscopy, which is applicable for the study of paramagnetic centers. EPR can provide structural information for biomolecules through measurement of distances between paramagnetic centers, using continuous wave (CW)- or pulsed EPR. CW EPR can be used to measure distances up to 25 Å through analysis of peak broadening (Kim, Murali, & DeRose, 2004; Macosko, Pio, Tinoco, & Shin, 1999). Pulsed EPR, such as pulsed electron–electron double resonance, also called double electron–electron resonance, can yield distances of 15–100 Å (Duss, Yulikov, Jeschke, & Allain, 2014; Jeschke, 2012; Milov, Salikhov, & Shirov, 1981; Reginsson & Schiemann, 2011; Schiemann & Prisner, 2007). EPR is also capable of probing the orientation of paramagnetic centers, which can provide information about both structure and dynamics (Denysenkov, Prisner, Stubbe, & Bennati, 2006; Marko et al., 2011; Schiemann, Cekan, Margraf, Prisner, & Sigurdsson, 2009). EPR is valuable for studying dynamics on a range of timescales (Marko et al., 2011; Nguyen & Qin, 2012; Sowa & Qin, 2008). Thus, EPR is a multifaceted tool that can provide valuable insights into both structure and dynamics of nucleic acids.

Nucleic acids are not inherently paramagnetic and, therefore, it is necessary to modify them with paramagnetic atoms or groups, referred to as spin labels. Although there are some examples of paramagnetic metal ions that have been used as spin probes (Goldfarb, 2014; Hunsicker-Wang, Vogt, & DeRose, 2009; Schiemann, Fritscher, Kisseleva, Sigurdsson, & Prisner, 2003), the most commonly used spin labels are aminoxyl radicals, usually called nitroxides. Many of these nitroxide radicals are commercially available or can be readily synthesized using standard techniques of organic synthesis. Therefore, nitroxides have found extensive use as spin labels. Although there are examples of noncovalent spin labeling of nucleic acids with nitroxides (Belmont et al., 1998; Chalmers et al., 2014; Maekawa et al., 2010; Shelke, Sandholt, & Sigurdsson, 2014; Shelke & Sigurdsson, 2010), the most common spin-labeling approach for nucleic acids is attachment of spin labels through covalent bonds.

There are several methods available for incorporation of spin labels at the end of nucleic acids (Shelke & Sigurdsson, 2012, 2013), but end-labeling has limited applicability for EPR studies. Therefore, this text focuses on

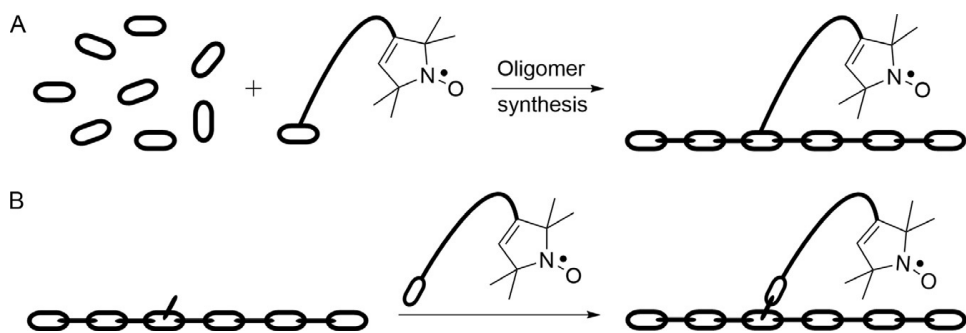


Figure 1 Strategies for site-directed spin labeling through covalent bonding. (A) The phosphoramidite approach. (B) Postsynthetic spin-labeling. A pyrrolidine-based spin label is used as a representative nitroxide spin label. Nucleotides are represented by links that form oligonucleotide chains.

methods for incorporation of spin labels at internal sites. Moreover, it will address how spin labels can be incorporated at specific sites of choice, referred to as site-directed spin labeling (SDSL). There are two main strategies that have been applied for covalent SDSL (Fig. 1). The first one utilizes spin-labeled phosphoramidites that are incorporated at specific positions during automated chemical synthesis of the nucleic acid (Shelke & Sigurdsson, 2012), shown schematically in Fig. 1A, and sometimes referred to as the phosphoramidite method. The second SDSL strategy is postsynthetic spin labeling, where spin labels are incorporated after the synthesis of the oligonucleotide, by either chemical or enzymatic methods (Fig. 1B).

The main features of these two spin-labeling strategies, the phosphoramidite method and postsynthetic labeling, will be described briefly below. Both of these SDSL routes are useful and complement each other. A facile approach for postsynthetic labeling of 2'-amino groups in RNA will subsequently be described in detail.

1.1 The Phosphoramidite Method for SDSL

Nucleoside phosphoramidites are derivatives of natural nucleosides and serve as building blocks in solid-phase synthesis of nucleic acids. A generic structure of a phosphoramidite is shown in Fig. 2A, where the 5'-hydroxyl group of a ribonucleoside is protected as a 5'-dimethoxytrityl (DMT) ether, while the phosphoramidite group is at the 3'-position. The 2'-position also needs to be protected when synthesizing RNA. The main advantage of the phosphoramidite method is that spin labels with specific and desired structural features can be inserted at chosen sites, which might not be possible using postsynthetic labeling.

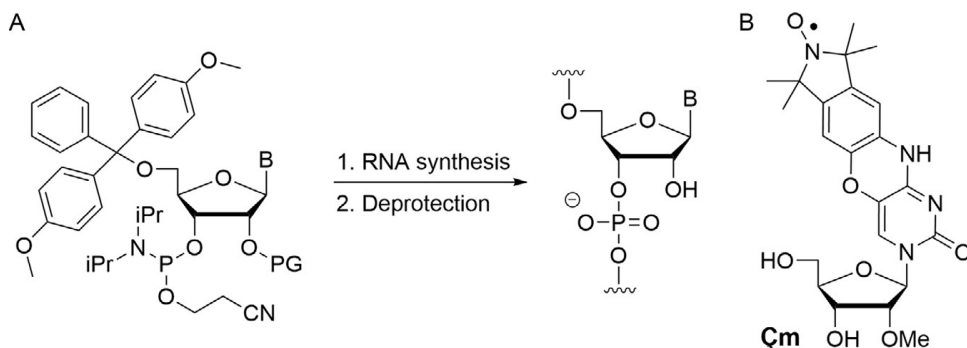


Figure 2 (A) Phosphoramidite monomer building block. PG is a protecting group for the 2'-hydroxy group. B is a nucleobase. (B) The rigid spin label **Çm** that has been incorporated into RNA by the phosphoramidite method.

There are several examples of spin labels that have been incorporated into DNA by the phosphoramidite method (Shelke & Sigurdsson, 2012). However, there is only one example of a spin-labeled nucleoside that has been incorporated into RNA by this method, the nucleoside **Çm** (Fig. 2B). **Çm** is a rigid spin label containing a nitroxide that has been fused to a nucleobase (Höbartner, Sicoli, Wachowius, Gophane, & Sigurdsson, 2012). Synthesis of spin-labeled phosphoramidites usually requires a substantial effort and involves a high degree of expertise in synthetic organic chemistry. Another drawback is the exposure of the spin labels to the reagents used during the oligonucleotide synthesis, which may result in partial reduction of the nitroxide radical. For example, iodine/water, which has traditionally been used to oxidize the phosphorous atoms from P(III) to P(V), needs to be replaced by *tert*-butyl hydroperoxide to avoid degradation of the radical (Cekan, Smith, Barhate, Robinson, & Sigurdsson, 2008; Piton et al., 2007). Moreover, the acid treatment, which removes the DMT groups from the 5'-end of the growing chain during elongation, can also result in decomposition of nitroxide spin labels, depending on their stability.

1.2 Postsynthetic Spin-Labeling

Postsynthetic spin labeling is the other main method of choice for incorporation of spin labels at specific sites (Fig. 1B). This strategy requires oligonucleotides that have uniquely reactive groups at specific sites where the spin label is to be incorporated. Such oligomers are normally prepared by the phosphoramidite method, often using commercially available reagents. This is a useful feature of this method, because both the modified oligonucleotide and a suitable spin label can often be either purchased or readily prepared. The other merit of this method is that the spin label does not get exposed

to the reagents used in the chemical synthesis of oligonucleotides. However, a drawback of this method is the possibility of nonspecific labeling due to the nucleophilic groups present in the nucleic acids, such as the exocyclic amino groups of the nucleobases, the N7 of purines, and nonbridging oxygen atoms of the phosphodiester. In addition, incomplete spin labeling is also a well-known drawback of this method.

There are a number of sites on a nucleotide in RNA that can in principle be spin labeled postsynthetically, namely the nucleobase, the sugar, and the phosphodiester backbone. Postsynthetic spin labeling of a nucleobase can, for example, be performed by the reaction of 4-thiouridine with a suitable spin-labeling reagent. **Figure 3A** shows such examples, where thiol-specific methane-thiosulfonate spin-labeling reagents have been reacted with 4-thiouridine in RNA to yield a variety of spin-labeled oligomers (Qin, Hideg, Feigon, & Hubbell, 2003; Qin, Iseri, & Oki, 2006). 4-Thiouridine can also be spin labeled through alkylation (Ramos & Varani, 1998). Another facile postsynthetic method is the reaction of phosphorothioates, in which one of the nonbridging oxygen atoms has been replaced with sulfur by oxidation with a sulfurizing agent during oligonucleotide synthesis, with alkylating agents (**Fig. 3B**; Grant, Boyd, Herschlag, & Qin, 2009; Qin, Butcher, Feigon, & Hubbell, 2001). This method requires the use of a deoxynucleotide at the phosphorothioate site to prevent cleavage of the RNA strand. Exocyclic amino groups in RNA have also been modified with a spin label (Sicoli, Wachowius, Bennati, & Höbartner, 2010) using the “convertible nucleoside” approach (Macmillan & Verdine, 1990). In this method, a derivative of a nucleoside possessing a leaving group on its nucleobase (the convertible nucleoside) is

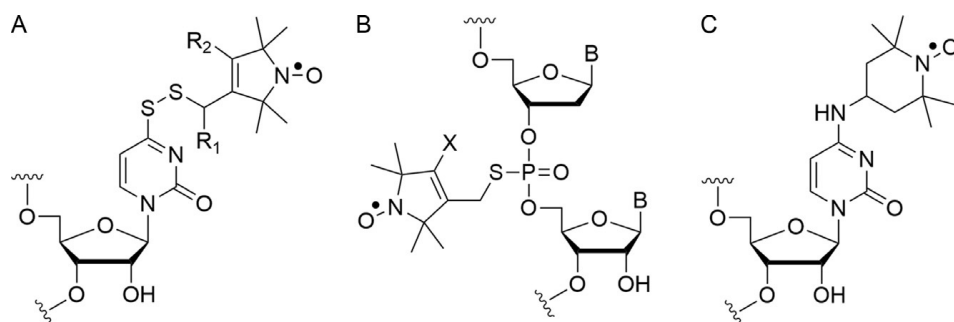


Figure 3 Representative examples of postsynthetic spin-labeling of nucleobases and phosphodiester backbones. (A) Attachment of spin labels at 4-thiouridine. (B) Spin-labeling at phosphate backbone. (C) Labeling of exocyclic amino groups of cytosine through the convertible nucleoside approach. R_1 and $R_2 = \text{H}$ or CH_3 , $X = \text{H}$ or Br , and B is a nucleobase.

incorporated into RNA through solid-phase synthesis. After the synthesis of the full-length oligomer, it is treated with an amine-based nucleophile, which substitutes the leaving group on the nucleobase, and becomes covalently attached. [Figure 3C](#) shows an example, where TEMPO was utilized as the nucleophile ([Sicoli et al., 2010](#)).

Spin labels have also been incorporated at the 2'-position of sugars in oligonucleotides using postsynthetic methods ([Fig. 4](#)). The 2'-position is the only site that is readily available for labeling of sugars at internal positions of nucleic acids. Moreover, a spin label attached at the 2'-position gets projected out of the minor groove, causing minimal structural perturbation of the labeled RNA. Spin labels have been incorporated into 2'-positions of RNA using the Cu(I)-catalyzed Huisgen–Meldal–Sharpless [3+2] cycloaddition reaction (click chemistry), yielding triazole-linked spin labels ([Büttner, Javadi-Zarnaghi, & Höbartner, 2014](#); [Flaender et al., 2008](#); [Fig. 4A](#)).

Postsynthetic labeling of 2'-amino groups is another particularly facile and selective approach for labeling the 2'-position; the aliphatic 2'-amino group is more nucleophilic than the aromatic amines on the nucleobases or the hydroxyl groups on the phosphodiester and can be converted to ureas and esters ([Fig. 4B](#)). Moreover, RNA oligonucleotides having 2'-amino modification(s) are commercially available or can be synthesized in-house on an automated synthesizer using commercially available 2'-amino-modified phosphoramidites. Thus, easy availability of 2'-amino-modified RNAs makes this approach attractive. The 2'-amino group has been spin labeled through reaction with a succinimidyl ester of a pyrrolidine-derived

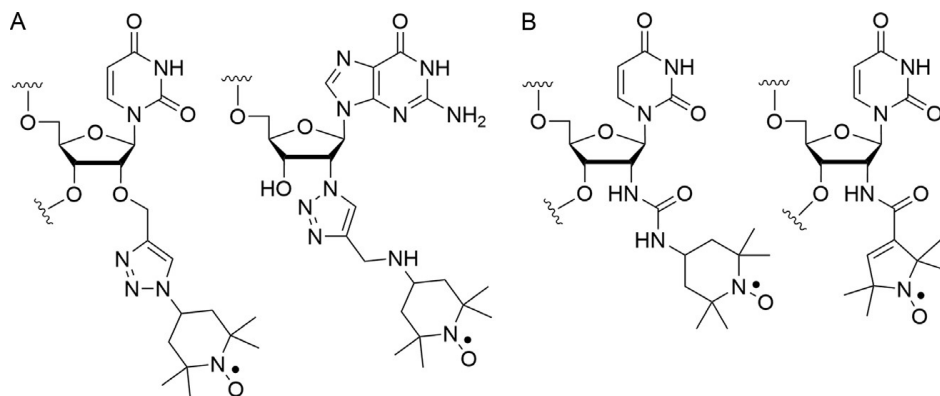


Figure 4 (A) Postsynthetic spin labeling of RNA at the 2'-position by using cycloaddition reaction between an azide and an alkyne. (B) Postsynthetic spin labeling at 2'-amino position through formation of urea or amide linkage.

nitroxide spin label to yield amide-modified spin label (Fig. 4B); however, this modification was found to cause considerable destabilization of RNA duplexes (Kim et al., 2004). Spin labeling of 2'-amino groups through reactions with aliphatic isocyanates and aromatic isothiocyanates is a more useful route than amide formation and is described in detail below.

2. 2'-AMINO SPIN-LABELING WITH ALIPHATIC ISOCYANATES AND AROMATIC ISOTHIOCYANATES

The first example of spin labeling of the 2'-position in RNA was the reaction of 4-isocyanato-TEMPO (**1**) with 2'-amino groups in RNA, forming a urea linkage (Fig. 5; Edwards, Okonogi, Robinson, & Sigurdsson, 2001). Spin-labeled oligonucleotides, prepared by this method, were used to study the structure-dependent dynamics of the transactivation response RNA (Edwards, Okonogi, & Sigurdsson, 2002; Edwards, Robinson, & Sigurdsson, 2005; Edwards & Sigurdsson, 2002, 2003) and the hammerhead ribozyme by EPR spectroscopy (Edwards & Sigurdsson, 2005). This spin-labeling method has been used by several other research groups and has the advantage that the starting materials are commercially available. However, it also has a few drawbacks. First, the isocyanate functional group is highly reactive and can lead to incomplete labeling in RNA due to a competing hydrolysis reaction, requiring a careful control of the reaction conditions. Second, at the low temperatures under which the spin-labeling reaction is performed, long RNAs sometimes form secondary structures that reduce

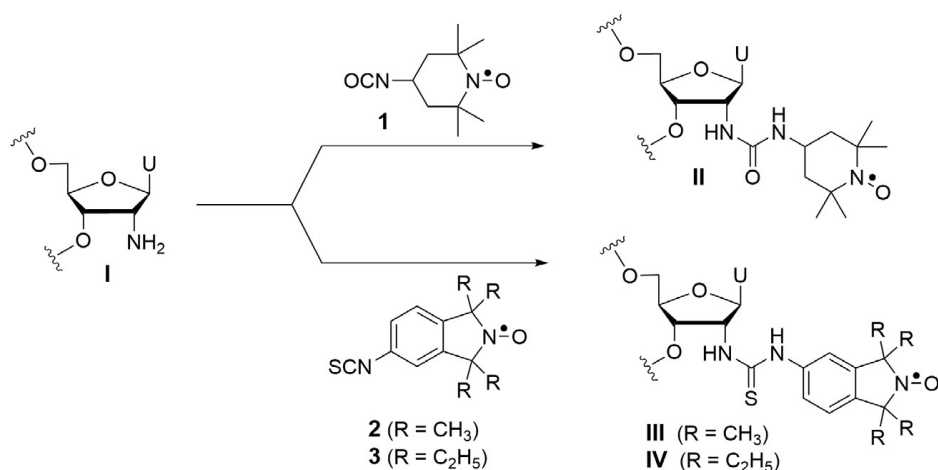


Figure 5 Spin labeling at the 2'-amino position of the oligonucleotide **I** by isocyanate **1** and isothiocyanate spin-labeling reagents **2** and **3**. U, uracil.

the reactivity of 2'-amino groups and result in low yields. In addition, TEMPO is not the optimal spin label for EPR studies due to its inherent flexibility.

To overcome these shortcomings of 4-isocyanato-TEMPO, a new class of spin labels for 2'-amino labeling has recently been introduced: isoindoline-derived nitroxides **2** and **3** have an aromatic isothiocyanate functional group, which forms a stable thiourea linker upon reaction with 2'-amino groups (Fig. 5; Saha, Jagtap, & Sigurdsson, 2015). Aromatic isothiocyanates are less reactive than aliphatic isocyanates, which allows the reaction to be carried out at a higher temperature without any nonspecific labeling. Performing these reactions at higher temperature in the presence of an organic cosolvent reduces RNA secondary structure and thus avoids potential reduced reactivity of the 2'-amino group. The detailed protocols of the preparation of these spin-labeling reagents and their incorporation into 2'-amino sites in RNA will be described in the latter part of this chapter.

2.1 Spin-Labeling of 2'-Amino Groups in RNA with 4-Isocyanato-TEMPO

Isocyanate **1**, the spin-labeling reagent for this protocol, can be either purchased (Toronto Research Chemicals) or synthesized using a previously reported protocol (Edwards et al., 2001; Edwards & Sigurdsson, 2007). As previously mentioned, the 2'-amino-modified oligonucleotides are also commercially available. A representative 2'-amino spin-labeling protocol (Edwards et al., 2001; Edwards & Sigurdsson, 2007, 2014) using isocyanate **1** is as follows:

- (1) To a solution of 2'-amino-modified RNA **I** (i.e., 5'-GACCUCG (2'-NH₂U)AUCGUG-3') (30 nmol), previously precipitated to exchange ammonium ions with sodium ions, in boric acid buffer (15 μL, 70 mM, pH 8.6) was added formamide (9 μL). The resulting solution was cooled in a rock salt/ice water bath (−8 °C). It is recommended to perform this reaction in a cold room (4 °C), which helps keeping the temperature low during transfer of reagents. The low temperature minimizes the competing isocyanate hydrolysis reaction and ensures the specificity of the labeling reaction toward the 2'-amino groups.
- (2) The solution was treated with freshly prepared **1** (9 μL) in anhydrous *N,N*-dimethylformamide (DMF) and incubated for 1 h at −8 °C. The solution of **1** was prepared by dissolving **1** (1 mg) in anhydrous DMF (67.6 μL) to a final concentration 75 mM. Isocyanates are electrophilic functional groups and as such they are reactive toward a variety of

- nucleophiles, including amines and water. Therefore, anhydrous and amine-free DMF should be used.
- (3) To ensure complete spin labeling, it is advisable to add a second aliquot of freshly prepared **1** in DMF (9 μL) after 1 h and a third aliquot after 2 h.
 - (4) The extent of the spin-labeling reaction can be determined by a denaturing polyacrylamide gel electrophoresis (DPAGE) analysis. An aliquot from the reaction mixture (1 μL) was run on 20% DPAGE gel along with the starting RNA **I**; one lane contained an equimolar mixture of the starting RNA and the RNA present in the reaction. The spin-labeled RNA displays reduced mobility on DPAGE (see [Section 2.3](#) for an example of DPAGE analysis of 2'-amino spin labeling). DPAGE can be readily used to monitor the extent of spin labeling of oligonucleotides of up to ca. 20 nt long; for longer RNA sequences, it may be a challenge to gauge the difference in the mobilities of spin-labeled and unlabeled material. A quantitative conversion to spin-labeled RNA is usually observed. Non- or partial spin labeling indicates decomposition of isocyanate **1**. The purity of **1** can be examined by thin-layer chromatography (TLC) (silica gel, 5% MeOH:CH₂Cl₂, R_f (**1**) = 0.7) and IR spectroscopy (RNCO stretching at 2100–2270 cm^{-1}).
 - (5) On completion of the reaction, H₂O (100 μL) was added to the reaction mixture, the solution was washed with CHCl₃ (4 \times 300 μL), and the solvent was removed *in vacuo*.
 - (6) The spin-labeled RNA was precipitated in EtOH (NaOAc (5 μL , 3 M, pH 4.6) and EtOH (300 μL), -80°C , 4 h) and purified by 20% DPAGE. The gel slices containing spin-labeled material were excised, extracted using the “crush and soak method” with Tris buffer (250 mM NaCl, 10 mM Tris, 1 mM Na₂EDTA, pH 7.5), and subsequently desalted using Sep-pak C18 cartridges following the manufacturer’s instructions, to obtain the final product (28 nmol).

2.2 Synthesis of Isothiocyanate-Containing Spin Labels

Spin labeling with **2** and **3** is a newly published method at the time of this writing and thus, these reagents are not yet commercially available. Therefore, the protocol for their preparation has been included. In short, **2** and **3** were prepared by reaction of their corresponding amino derivatives **4** and **5** with thiophosgene ([Fig. 6](#)), according to the following representative protocol for the synthesis of **2**:

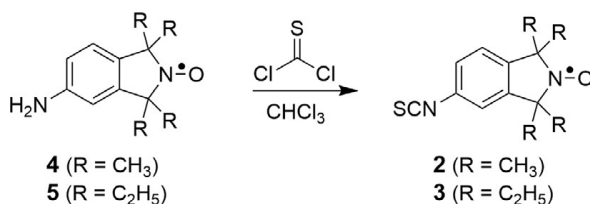


Figure 6 Synthesis of isothiocyanate spin-labeling reagents **2** and **3**.

- (1) A solution of 1,1,3,3-tetramethylisindoline-5-amine-2-oxyl (**4**) (Jagtap et al., 2015; Mileo et al., 2013) (100 mg, 0.49 mmol) in CHCl_3 (3.5 mL) was treated dropwise with a solution of thiophosgene (0.041 mL, 0.54 mmol) in CHCl_3 (1 mL) at 24 °C. (Note: Thiophosgene is a toxic reagent and it is strongly recommended to perform the reaction in an efficiently ventilated fume hood.) The progress of the reaction was monitored by TLC (20% EtOAc:pet. ether, $R_f(\mathbf{4})=0.2$, $R_f(\mathbf{2})=0.8$).
- (2) After stirring for 2 h at 24 °C, the reaction mixture was washed successively with aq. NaOH (4 mL, 1 M), H_2O (2×5 mL) and brine (5 mL).
- (3) The organic layer was dried over anhydrous sodium sulfate, filtered, and concentrated *in vacuo*. The crude product was purified by flash column chromatography using a gradient elution (EtOAc:pet. ether from 0:100 to 5:95) to give **2** as a yellow solid (98 mg, 82%).

Spin-labeling reagent **3** was prepared from its corresponding amino derivative **5** (1,1,3,3-tetraethylisindoline-5-amine-2-oxyl) (Jagtap et al., 2015) in the same manner. Isothiocyanates **2** and **3** are stable solids that have not shown any detectable decomposition after storing at -20 °C for several months.

2.3 Spin Labeling of 2'-Amino Groups in RNA with Isothiocyanates

The main difference between the protocols for spin labeling with isothiocyanates **2** and **3** and isocyanate **1** is that the spin-labeling reactions were performed at 37 °C for **2** and **3**, compared with -8 °C for **1**. A detailed representative protocol for this spin-labeling method is as follows:

- (1) A solution of an isothiocyanate spin label (**2** or **3**) (2 μmol) in DMF (20 μL) was added to a solution of RNA oligonucleotide **I** (40 nmol) in borate buffer (20 μL , 100 mM, pH 8.6) and heated at 37 °C for 8 h. For isothiocyanate **2**, we observed a precipitate at the end of the reaction which was extracted into an organic solvent (see next step).

- (2) Sterile water was added (200 μL) and the excess labeling reagent was removed by extracting the aqueous reaction mixture with EtOAc ($6 \times 500 \mu\text{L}$). Each of the EtOAc washings was collected separately, and the presence of excess unreacted spin label was monitored. TLC (silica gel, 20% EtOAc:pet. ether, R_f (**2** or **3**) = 0.8) could only be used to detect the presence of spin label in the first two rounds of extraction. In addition, EPR spectroscopy could be used to monitor the whole extraction process; the last EtOAc washing should not show any EPR activity.
- (3) In spite of the washings in step 2, we have observed traces of unattached spin contaminants in the spin-labeled RNA (especially using **2**), which were removed by EtOH precipitation: (NaOAc (5 μL , 3 M, pH 4.6) and EtOH (300 μL), -80°C , 4 h) to yield 30–34 nmol of spin-labeled RNA. Note: Further purification of the spin-labeled RNA from the precipitation by DPAGE yielded a product which was of similar purity as the precipitated RNA as judged by EPR and DPAGE.

As mentioned in the spin-labeling protocol of **1**, DPAGE is a useful method to ascertain the extent of RNA spin labeling with **1**, **2**, and **3**. It is also useful for determining the time course of a spin-labeling reaction, just as TLC is useful for monitoring the extent of chemical reactions. Figure 7 shows a DPAGE analysis of samples taken from the spin-labeling reaction mixtures (1 μL) after specific intervals of time. The spin-labeled oligonucleotide showed reduced mobility as compared to the starting 2'-amino RNA, owing to its increased mass. For example, the sample containing **2**, which

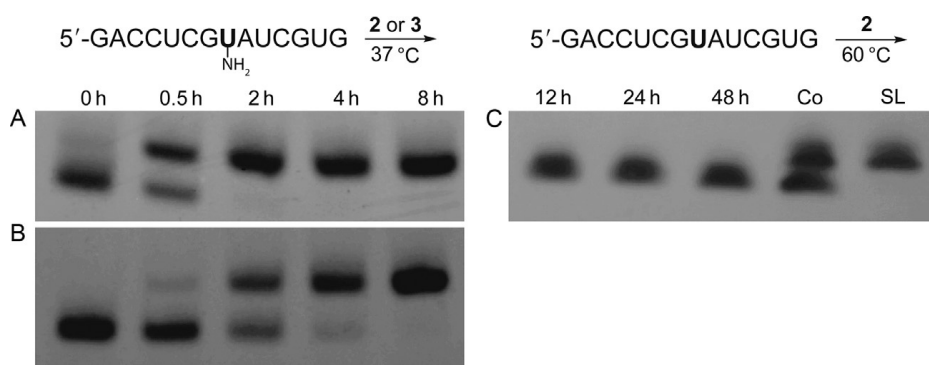


Figure 7 (A) Time course of spin-labeling reaction of RNA sequence **I** with **2**. (B) Time course of spin-labeling reaction of RNA sequence **I** with **3**. (C) Control reaction on unmodified sequence for checking out specificity of the labeling reaction with isothiocyanate spin label **2**. Lane SL contains spin-labeled RNA **III**, and Co is an equimolar mixture of SL and reaction mixture after 48 h.

was removed from the reaction mixture after 0.5 h, clearly showed two bands (Fig. 7A), indicating that the reaction was still not complete. However, the band corresponding to the starting oligonucleotide had disappeared after 2 h, showing that RNA **I** had been converted to its spin-labeled derivative **III**. In contrast, when tetraethyl-derivative **3** was used as the labeling reagent, 90% of the same RNA **I** was converted to **IV** in 4 h (Fig. 7B), showing that **2** was more reactive than **3**. All of the RNA for both reagents had fully reacted after 8 h.

One of the potential drawbacks of postsynthetic labeling is nonspecific reaction of reagents at unwanted sites in RNA. For example, reacting aliphatic isocyanates with unmodified RNA at 37 °C yields modified RNA (Sigurdsson & Eckstein, 1996). To determine specificity of the 2'-amino spin labeling with aromatic isothiocyanates, isothiocyanate **2** was reacted with an unmodified RNA oligonucleotide of the same sequence as 2'-amino-labeled oligomer **I**. Although the spin-labeling reactions of **I** were performed at 37 °C, the unmodified RNA was heated with **2** at 60 °C and reacted for 48 h to assess the degree of potential nonspecific labeling. Figure 7C shows no detectable conversion of the unlabeled RNA to slower moving products, demonstrating the selectivity of **2** for 2'-amino groups in RNA.

2.4 Analysis of Spin-Labeled Oligonucleotides

After the reaction of a 2'-amino-modified oligonucleotide with a spin-labeling reagent and isolation of the product, incorporation of the spin label into the RNA should be verified. Several techniques are routinely used for this purpose. Analysis by DPAGE and HPLC can be used to verify that the oligonucleotide has been modified, but other methods must be used to verify incorporation of an intact spin label (Edwards & Sigurdsson, 2014). Even mass spectrometry (MALDI-TOF) cannot distinguish between a nitroxide and its hydroxylamine derivative, which may result from an unlikely reduction of the spin label. Digestion of the oligonucleotide, followed by HPLC analysis and coinjection with an authentic sample of the spin label lesion, is a useful technique for that purpose (Edwards & Sigurdsson, 2014). However, the most direct method for detecting radicals is EPR spectroscopy.

Oligonucleotides labeled with a nitroxide radical show a characteristic three-peak pattern by EPR. EPR can also be used to detect and quantify free spin label contaminants. A free spin label tumbles rapidly in solution, giving a narrow EPR spectrum, but after attachment to RNA, the EPR lines

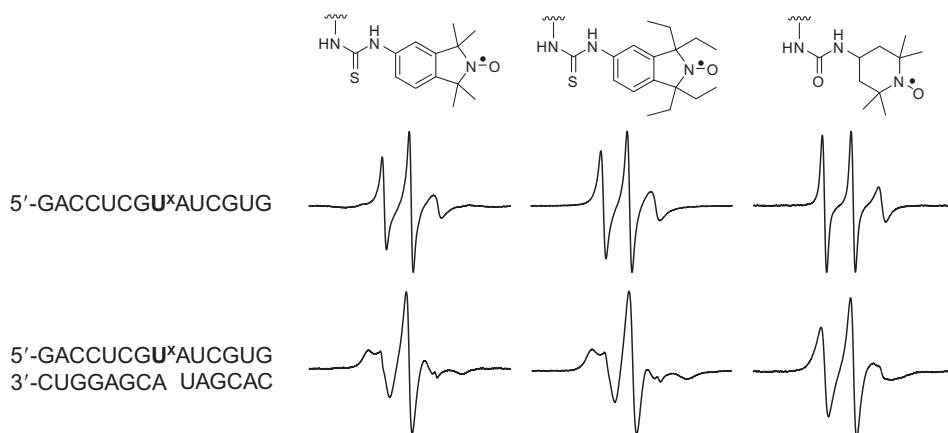


Figure 8 EPR spectra of the spin-labeled oligonucleotides at 10 °C (10 mM phosphate, 100 mM NaCl, 0.1 mM Na₂EDTA, pH 7.0). **U^x** indicates the position of the spin-labeled uridine.

become broader due to slower tumbling in solution. In the spin-labeling reaction with **2**, we detected the presence of an importunate unattached spin contaminant by EPR, which was still present after DPAGE purification. This impurity was removed by performing repeated ethyl acetate washes after the spin-labeling reaction, followed by ethanol precipitation. EPR can also be used to perform a spin-count experiment that quantifies the amount of nitroxide, which can be compared to the amount of oligonucleotides determined by UV spectroscopy.

In addition to verifying spin label incorporation, EPR spectroscopy gives valuable information about the mobility of the spin label, independent of the nucleic acid. **Figure 8** shows the EPR spectra of oligonucleotides labeled with **1**, **2**, and **3**. It is noteworthy that the spectra of the isoindoline-derived spin labels are broader, compared to the TEMPO derivative, especially for the RNA duplexes. This shows that the isoindoline spin labels are less mobile and should, therefore, be more useful for studies of the structure and dynamics of nucleic acids.

3. SUMMARY AND CONCLUSIONS

Gaining understanding of RNA function through studies of structure and dynamics is an active area of research. SDSL, in combination with EPR spectroscopy, is fast turning out to be a valuable method for such studies. There are two main approaches for spin labeling, the phosphoramidite method and postsynthetic spin labeling. Among these, the latter strategy

requires minimal effort and is less time consuming. In this chapter, we have described postsynthetic spin labeling of 2'-amino groups in RNA using two classes of spin labels, aliphatic isocyanates and aromatic isothiocyanates. The aromatic isothiocyanates are particularly useful and do not suffer from any of the potential drawbacks associated with the postsynthetic labeling strategy, for example, incomplete and/or nonspecific labeling. Spin labeling with isothiocyanates is easy to perform and gives quantitative yields in a short period of time, with no detectable nonspecific labeling. These isoindoline-based spin labels are promising candidates for use in distance measurement with pulsed EPR as they showed reduced mobility by EPR, compared to a TEMPO-based spin label. Moreover, the isoindoline-derived spin labels are stable under reducing conditions (Saha et al., 2015), which makes them promising candidates for in-cell EPR spectroscopy.

ACKNOWLEDGMENTS

This research was supported by the Icelandic Research Fund. S.S. and A.P.J. gratefully acknowledge their doctoral fellowships provided by the University of Iceland. The authors would also like to thank members of the Sigurdsson research group for helpful discussions.

REFERENCES

- Belmont, P., Chapelle, C., Demeunynck, M., Michon, J., Michon, P., & Lhomme, J. (1998). Introduction of a nitroxide group on position 2 of 9-phenoxyacridine: Easy access to spin labelled DNA-binding conjugates. *Bioorganic and Medicinal Chemistry Letters*, 8(6), 669–674.
- Brummelkamp, T. R., Bernards, R., & Agami, R. (2002). A system for stable expression of short interfering RNAs in mammalian cells. *Science*, 296(5567), 550–553.
- Büttner, L., Javadi-Zarnaghi, F., & Höbartner, C. (2014). Site-specific labeling of RNA at internal ribose hydroxyl groups: Terbium-assisted deoxyribozymes at work. *Journal of the American Chemical Society*, 136(22), 8131–8137.
- Cekan, P., Smith, A. L., Barhate, N., Robinson, B. H., & Sigurdsson, S. T. (2008). Rigid spin-labeled nucleoside Ç: A nonperturbing EPR probe of nucleic acid conformation. *Nucleic Acids Research*, 36(18), 5946–5954.
- Chalmers, B. A., Saha, S., Nguyen, T., McMurtrie, J., Sigurdsson, S. T., Bottle, S. E., et al. (2014). TMIO-Pyrimid hybrids are profluorescent, site-directed spin labels for nucleic acids. *Organic Letters*, 16(21), 5528–5531.
- Denysenkov, V. P., Prisner, T. F., Stubbe, J., & Bennati, M. (2006). High-field pulsed electron-electron double resonance spectroscopy to determine the orientation of the tyrosyl radicals in ribonucleotide reductase. *Proceedings of the National Academy of Sciences of the United States of America*, 103(36), 13386–13390.
- Duss, O., Yulikov, M., Jeschke, G., & Allain, F. H. T. (2014). EPR-aided approach for solution structure determination of large RNAs or protein-RNA complexes. *Nature Communications*, 5, 3669.

- Edwards, T. E., Okonogi, T. M., Robinson, B. H., & Sigurdsson, S. T. (2001). Site-specific incorporation of nitroxide spin-labels into internal sites of the TAR RNA; structure-dependent dynamics of RNA by EPR spectroscopy. *Journal of the American Chemical Society*, *123*(7), 1527–1528.
- Edwards, T. E., Okonogi, T. M., & Sigurdsson, S. T. (2002). Investigation of RNA-protein and RNA-metal ion interactions by electron paramagnetic resonance spectroscopy: The HIV TAR-Tat motif. *Chemistry and Biology*, *9*(6), 699–706.
- Edwards, T. E., Robinson, B. H., & Sigurdsson, S. T. (2005). Identification of amino acids that promote specific and rigid TAR RNA-tat protein complex formation. *Chemistry and Biology*, *12*(3), 329–337.
- Edwards, T. E., & Sigurdsson, S. T. (2002). Electron paramagnetic resonance dynamic signatures of TAR RNA—Small molecule complexes provide insight into RNA structure and recognition. *Biochemistry*, *41*(50), 14843–14847.
- Edwards, T. E., & Sigurdsson, S. T. (2003). EPR spectroscopic analysis of TAR RNA-metal ion interactions. *Biochemical and Biophysical Research Communications*, *303*(2), 721–725.
- Edwards, T. E., & Sigurdsson, S. T. (2005). EPR spectroscopic analysis of U7 hammerhead ribozyme dynamics during metal ion induced folding. *Biochemistry*, *44*(38), 12870–12878.
- Edwards, T. E., & Sigurdsson, S. T. (2007). Site-specific incorporation of nitroxide spin-labels into 2'-positions of nucleic acids. *Nature Protocols*, *2*(8), 1954–1962.
- Edwards, T. E., & Sigurdsson, S. T. (2014). Modified RNAs as tools in RNA biochemistry. In R. K. Hartmann, A. Bindereif, A. Schön, & E. Westhof (Eds.), *Handbook of RNA biochemistry* (pp. 151–172). Germany: Wiley: Wiley-VCH Verlag GmbH & Co. KGaA.
- Fica, S. M., Tuttle, N., Novak, T., Li, N. S., Lu, J., Koodathingal, P., et al. (2013). RNA catalyses nuclear pre-mRNA splicing. *Nature*, *503*(7475), 229–234.
- Flaender, M., Sicoli, G., Fontecave, T., Mathis, G., Saint-Pierre, C., Boulard, Y., et al. (2008). Site-specific insertion of nitroxide-spin labels into DNA probes by click chemistry for structural analyses by ELDOR spectroscopy. *Nucleic Acids Symposium Series (Oxford)*, *52*(1), 147–148.
- Goldfarb, D. (2014). Gd³⁺ spin labeling for distance measurements by pulse EPR spectroscopy. *Physical Chemical Physics*, *16*(21), 9685–9699.
- Grant, G. P. G., Boyd, N., Herschlag, D., & Qin, P. Z. (2009). Motions of the substrate recognition duplex in a group I intron assessed by site-directed spin labeling. *Journal of the American Chemical Society*, *131*(9), 3136–3137.
- Höbartner, C., Sicoli, G., Wachowius, F., Gophane, D. B., & Sigurdsson, S. T. (2012). Synthesis and characterization of RNA containing a rigid and nonperturbing cytidine-derived spin label. *Journal of Organic Chemistry*, *77*(17), 7749–7754.
- Hunsicker-Wang, L., Vogt, M., & DeRose, V. J. (2009). EPR methods to study specific metal-ion binding sites in RNA. *Methods in Enzymology*, *468*, 335–367.
- Jagtap, A. P., Krstić, I., Kunjir, N. C., Hänsel, R., Prisner, T. F., & Sigurdsson, S. T. (2015). Sterically shielded spin labels for in-cell EPR spectroscopy: Analysis of stability in reducing environment. *Free Radical Research*, *49*(1), 78–85.
- Jeschke, G. (2012). DEER distance measurements on proteins. *Annual Review of Physical Chemistry*, *63*, 419–446.
- Kim, N. K., Murali, A., & DeRose, V. J. (2004). A distance ruler for RNA using EPR and site-directed spin labeling. *Chemistry and Biology*, *11*(7), 939–948.
- Macmillan, A. M., & Verdine, G. L. (1990). Synthesis of functionally tethered oligodeoxynucleotides by the convertible nucleoside approach. *Journal of Organic Chemistry*, *55*(24), 5931–5933.
- Macosko, J. C., Pio, M. S., Tinoco, I., & Shin, Y. K. (1999). A novel 5' displacement spin-labeling technique for electron paramagnetic resonance spectroscopy of RNA. *RNA*, *5*(9), 1158–1166.

- Maekawa, K., Nakazawa, S., Atsumi, H., Shiomi, D., Sato, K., Kitagawa, M., et al. (2010). Programmed assembly of organic radicals on DNA. *Chemical Communications*, 46(8), 1247–1249.
- Mandal, M., & Breaker, R. R. (2004). Gene regulation by riboswitches. *Nature Reviews. Molecular Cell Biology*, 5(6), 451–463.
- Marko, A., Denysenkov, V., Margraft, D., Cekan, P., Schiemann, O., Sigurdsson, S. T., et al. (2011). Conformational flexibility of DNA. *Journal of the American Chemical Society*, 133(34), 13375–13379.
- Mileo, E., Etienne, E., Martinho, M., Lebrun, R., Roubaud, V., Tordo, P., et al. (2013). Enlarging the panoply of site-directed spin labeling electron paramagnetic resonance (SDSL-EPR): Sensitive and selective spin-labeling of tyrosine using an isoindoline-based nitroxide. *Bioconjugate Chemistry*, 24(6), 1110–1117.
- Milov, A., Salikhov, K., & Shirov, M. (1981). Application of the double resonance method to electron spin echo in a study of the spatial distribution of paramagnetic centers in solids. *Soviet Physics—Solid State*, 23, 565–569.
- Nguyen, P., & Qin, P. Z. (2012). RNA dynamics: Perspectives from spin labels. *Wiley Interdisciplinary Reviews RNA*, 3(1), 62–72.
- Nissen, P., Hansen, J., Ban, N., Moore, P. B., & Steitz, T. A. (2000). The structural basis of ribosome activity in peptide bond synthesis. *Science*, 289(5481), 920–930.
- Piton, N., Mu, Y., Stock, G., Prisner, T. F., Schiemann, O., & Engels, J. W. (2007). Base-specific spin-labeling of RNA for structure determination. *Nucleic Acids Research*, 35(9), 3128–3143.
- Qin, P. Z., Butcher, S. E., Feigon, J., & Hubbell, W. L. (2001). Quantitative analysis of the isolated GAAA tetraloop/receptor interaction in solution: A site-directed spin labeling study. *Biochemistry*, 40(23), 6929–6936.
- Qin, P. Z., Hideg, K., Feigon, J., & Hubbell, W. L. (2003). Monitoring RNA base structure and dynamics using site-directed spin labeling. *Biochemistry*, 42(22), 6772–6783.
- Qin, P. Z., Iseri, J., & Oki, A. (2006). A model system for investigating lineshape/structure correlations in RNA site-directed spin labeling. *Biochemical and Biophysical Research Communications*, 343(1), 117–124.
- Ramos, A., & Varani, G. (1998). A new method to detect long-range protein-RNA contacts: NMR detection of electron-proton relaxation induced by nitroxide spin-labeled RNA. *Journal of the American Chemical Society*, 120(42), 10992–10993.
- Reginsson, G. W., & Schiemann, O. (2011). Studying bimolecular complexes with pulsed electron-electron double resonance spectroscopy. *Biochemical Society Transactions*, 39, 128–139.
- Roy, R., Hohng, S., & Ha, T. (2008). A practical guide to single-molecule FRET. *Nature Methods*, 5(6), 507–516.
- Saha, S., Jagtap, A. P., & Sigurdsson, S. T. (2015). Site-directed spin labeling of 2'-amino groups in RNA with isoindoline nitroxides that are resistant to reduction. *Chemical Communications*, 51, 13142–13145.
- Schiemann, O., Cekan, P., Margraf, D., Prisner, T. F., & Sigurdsson, S. T. (2009). Relative orientation of rigid nitroxides by PELDOR: Beyond distance measurements in nucleic acids. *Angewandte Chemie, International Edition*, 48(18), 3292–3295.
- Schiemann, O., Fritscher, J., Kisseleva, N., Sigurdsson, S. T., & Prisner, T. F. (2003). Structural investigation of a high-affinity Mn-II binding site in the hammerhead ribozyme by EPR spectroscopy and DFT calculations. Effects of neomycin B on metal-ion binding. *ChemBioChem*, 4(10), 1057–1065.
- Schiemann, O., & Prisner, T. F. (2007). Long-range distance determinations in biomacromolecules by EPR spectroscopy. *Quarterly Reviews of Biophysics*, 40(1), 1–53.
- Shelke, S. A., Sandholt, G. B., & Sigurdsson, S. T. (2014). Nitroxide-labeled pyrimidines for non-covalent spin-labeling of abasic sites in DNA and RNA duplexes. *Organic & Biomolecular Chemistry*, 12(37), 7366–7374.

- Shelke, S. A., & Sigurdsson, S. T. (2010). Noncovalent and site-directed spin labeling of nucleic acids. *Angewandte Chemie, International Edition*, 49(43), 7984–7986.
- Shelke, S. A., & Sigurdsson, S. T. (2012). Site-directed spin labelling of nucleic acids. *European Journal of Organic Chemistry*, 2012(12), 2291–2301.
- Shelke, S. A., & Sigurdsson, S. T. (2013). Site-directed nitroxide spin labeling of biopolymers. In C. R. Timmel & J. R. Harmer (Eds.), *Structural information from spin-labels and intrinsic paramagnetic centres in the biosciences*, (pp. 121–162). Germany: Springer.
- Sicoli, G., Wachowius, F., Bennati, M., & Höbartner, C. (2010). Probing secondary structures of spin-labeled RNA by pulsed EPR spectroscopy. *Angewandte Chemie, International Edition*, 49(36), 6443–6447.
- Sigurdsson, S. T., & Eckstein, F. (1996). Site specific labelling of sugar residues in oligoribonucleotides: Reactions of aliphatic isocyanates with 2' amino groups. *Nucleic Acids Research*, 24(16), 3129–3133.
- Sisamakris, E., Valeri, A., Kalinin, S., Rothwell, P. J., & Seidel, C. A. M. (2010). Accurate single-molecule FRET studies using multiparameter fluorescence detection. *Methods in Enzymology*, 475, 455–514.
- Sowa, G. Z., & Qin, P. Z. (2008). Site-directed spin labeling studies on nucleic acid structure and dynamics. *Progress in Nucleic Acid Research and Molecular Biology*, 82, 147–197.
- Xu, Y., & Matthews, S. (2013). TROSY NMR spectroscopy of large soluble proteins. *Topics in Current Chemistry*, 335, 97–119.

Paper IV

Noncovalent Spin-Labeling of RNA: The Aptamer Approach

Subham Saha¹, Thilo Hetzke², Thomas F. Prisner² and Snorri Th. Sigurdsson^{1*}

¹University of Iceland, Department of Chemistry, Science Institute, Dunhaga 3, 107 Reykjavik, Iceland. E-mail: snorrisi@hi.is

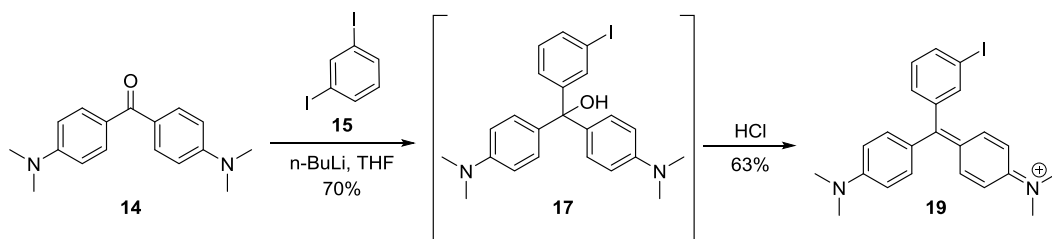
²Institute of Physical and Theoretical Chemistry, J. W. Goethe University, Max-von-Laue-Str. 7, 60438 Frankfurt (Germany)

Draft, 2nd June 2017

Experimental Section

Chemical specifications:

Chemicals were purchased from Sigma-Aldrich Chemical Company and Acros, Belgium, and were used without further purification. All solvents were distilled from calcium hydride before use and stored over activated 4 Å molecular sieves under nitrogen. TLC was carried out using glass plates pre-coated with silica gel (Kieselgel 60 F₂₅₄, 0.2 mm, Merck). Visualisation was done by UV light. Silica gel was purchased from Silicycle, and used for medium pressure chromatography ('flash'-chromatography). ¹H and ¹³C NMR spectra were recorded at the frequencies stated, using deuterated solvents as internal standards. 400 MHz spectra were recorded on a Bruker Avance 400 spectrometer. Residual proton signals from the deuterated solvents were used as references [D₂O (4.81 ppm), *d*₆-DMSO (2.50 ppm), chloroform (7.26 ppm), *d*₄-MeOH (4.84 and 3.31 ppm)] for ¹H spectra. The residual ¹³C signals from the deuterated solvents being used as references [*d*₆-DMSO (39.7 ppm), chloroform (77.0 ppm), *d*₄-MeOH (49.05 ppm)] for ¹³C spectra. All coupling constants were measured in Hertz. All moisture sensitive reactions were carried out in flame-dried glassware using nitrogen or argon from standard industrial cylinders, dried through an activated silica column.



Synthesis of 19. 2M *n*-BuLi (3.64 mL, 1.2 equivalents) was added dropwise under argon to a solution of 1,3-diiodobenzene **15** (2 g, 0.00607 mol) in freshly dried THF (24.3 mL) at -78 °C. This was allowed to stir for 2 hours at -78°C. Following this, a solution of Michler's ketone **14** (1.62 g, 0.00607 mol) in THF (36.4 mL) was added drop wise. The reaction mixture was allowed to reach room temperature and was left to stir for 18 hours. After completion of the reaction (TLC), the reaction mixture was quenched by adding water and extracted with ethyl acetate and washed with water and brine to obtain 2 g (70%) crude of **17**. TLC analysis revealed this compound to be highly unstable and therefore, the crude material was immediately used for the next step. This was dissolved in methanol (84.7 mL) and hydrochloric acid (1.2 equiv.) was added to it dropwise and immediately the colour changed to dark green. This was refluxed at 90 °C for 2 hours following which all solvents were evaporated out under reduced pressure and the crude reaction mixture was extracted in 10% methanol in dichloromethane and washed with water and brine. This was purified using 60-200 mesh size silica gel column chromatography and pure compound **19** was eluted in 6% methanol-dichloromethane to obtain 1.2 g (63%) as a dark green solid.

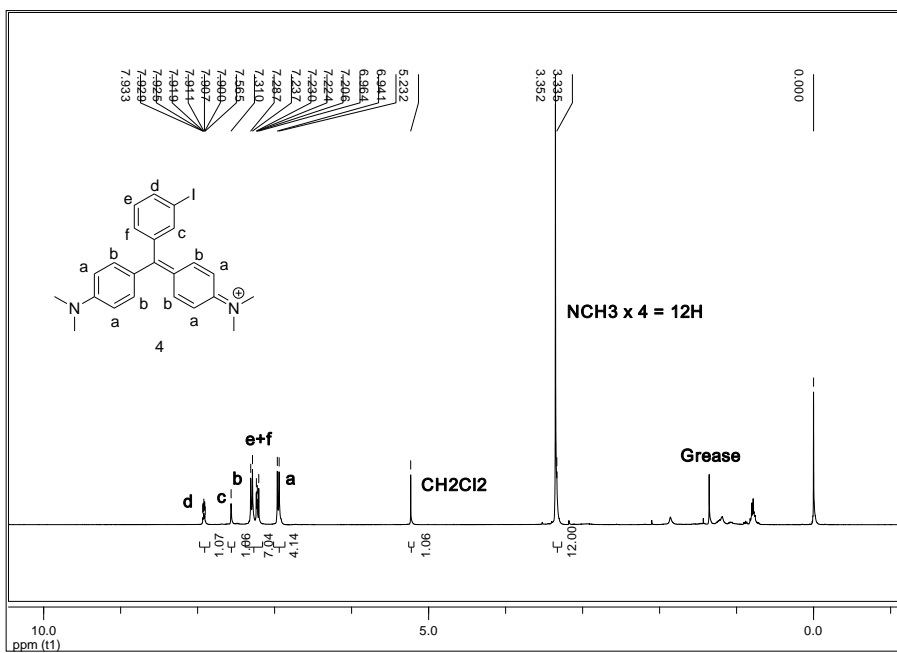
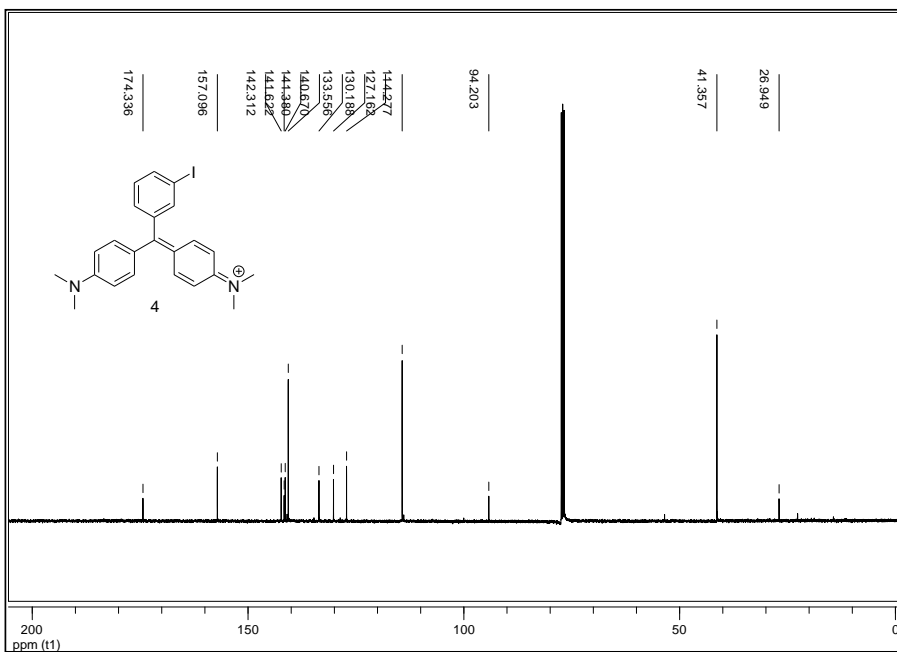
TLC (Silica gel, 40% EtOAc in petroleum ether), R_f (**17**) = 0.6

TLC (Silica gel, 10% methanol in dichloromethane), R_f (**19**) = 0.2

$^1\text{H-NMR}$ (400MHz, CDCl_3): δ 3.35 (s, 12H, $\text{NH}_3 X 4$), 6.95 (d, 4H, *a*, $J = 9.2$ Hz), 7.23-7.22 (m, 2H, *e+f*), 7.29 (d, 2H, *b*, $J = 9.2$ Hz), 7.56 (s, 1H, *c*), 7.93-7.90 (m, 1H, *d*).

Mass spectrometry: Calculated mass = 455.1

Observed mass = 455.09

Figure 1: ¹H NMR spectrum of 19.Figure 2: ¹³C NMR spectrum of 19.

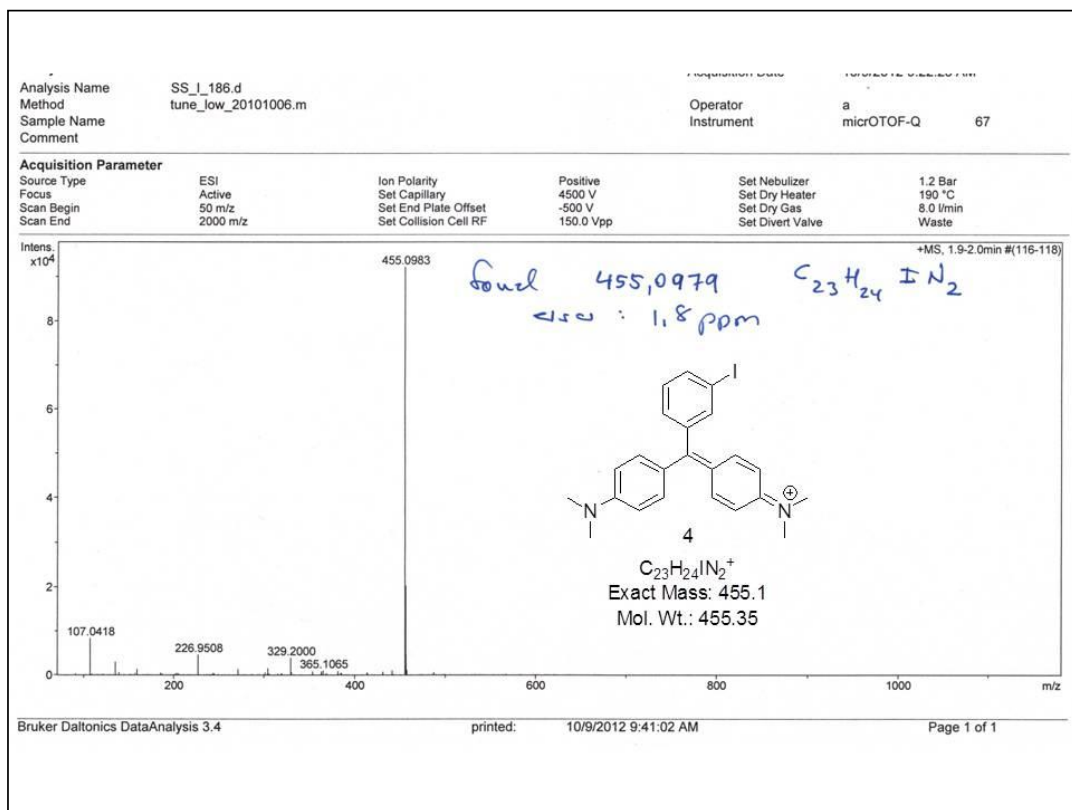
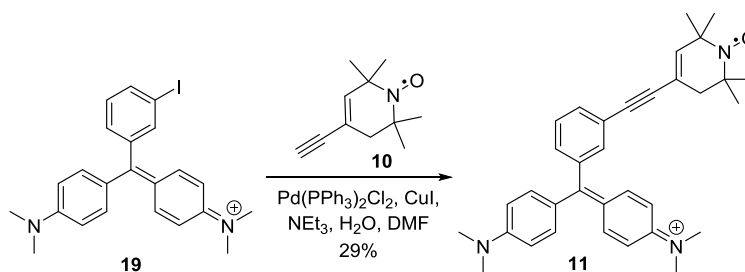


Figure 3: Mass spectrum for 19.



Synthesis of 11. To a stirred solution of **19** (0.050 g, 0.109 mmol) and nitroxide **10** (0.058 g, 0.329 mmol) in DMF (1 mL), copper iodide (0.002 g, 0.0109 mmol) was added, followed by triethylamine (0.5 mL, 0.274 mmol) was added to the reaction mixture. After degassing with argon for a couple of minutes, bis(triphenylphosphine)palladium(II) chloride (0.0077 g, 0.0109 mmol) was added and this reaction mixture was heated at 70 °C for 18 h. After completion of the reaction (TLC), the reaction mixture was washed with water and brine and extracted in ethyl acetate. The crude reaction mixture was purified by preparative TLC. The plate was run thrice in 35% ethyl acetate in petroleum ether and eluted in 5% methanol in dichloromethane. 8 mg of the spin probe **6** was obtained in 29% yield.

TLC (Silica gel, 30% ethyl acetate in petroleum ether), R_f (**6**) = 0.5

$^1\text{H-NMR}$ (400 MHz, Methanol- d_4) δ = 7.38 (s, 1H), 7.06 (s, 1H), 6.94 (s, 2H), 6.59 (s, 2H), 3.03 (d, $J=7.1$, 1H), 2.80 (s, 6H), 1.18 (t, $J=6.9$, 3H), 0.78 (s, 2H).

Mass spectrometry: Calculated mass = 505.31

Observed mass = 505.309

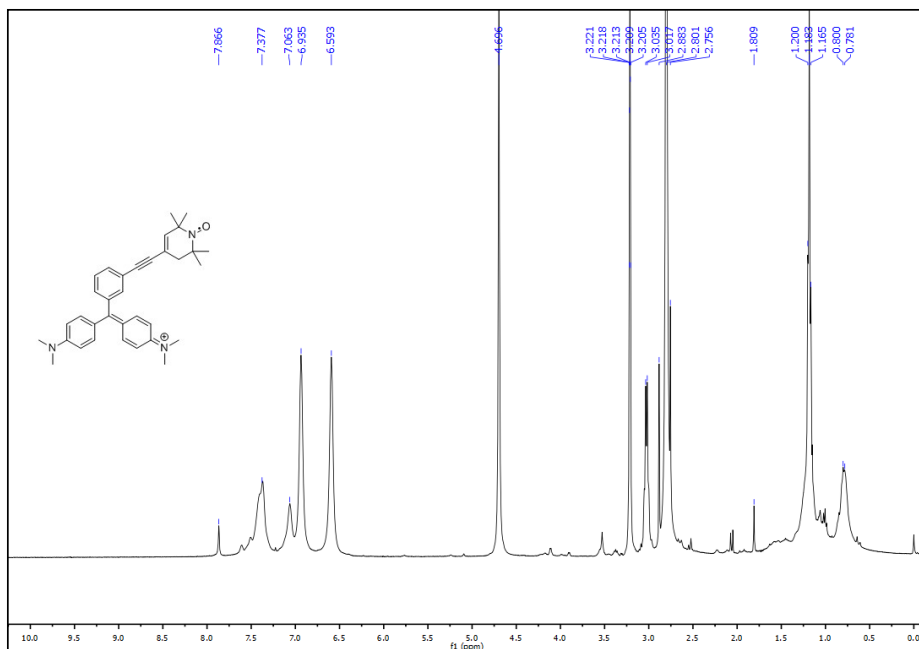
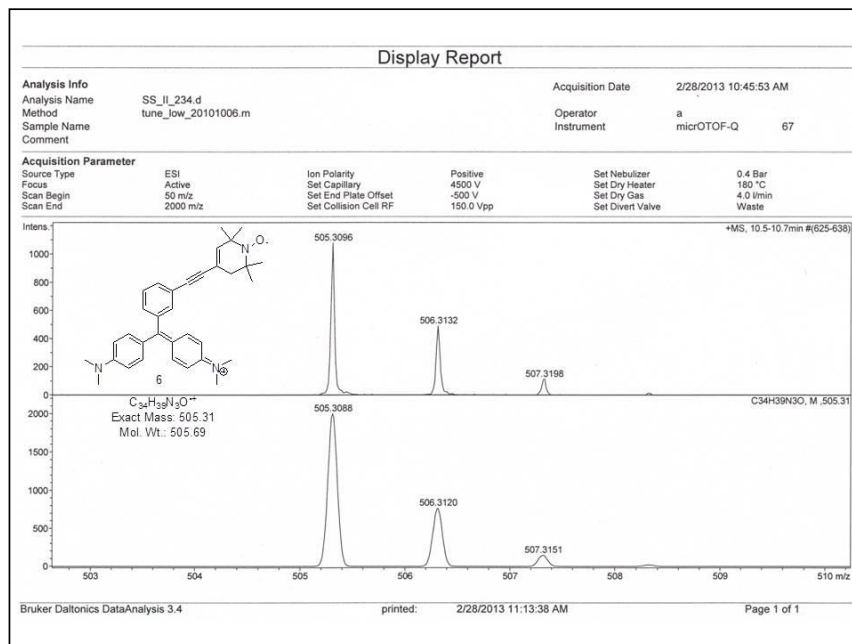
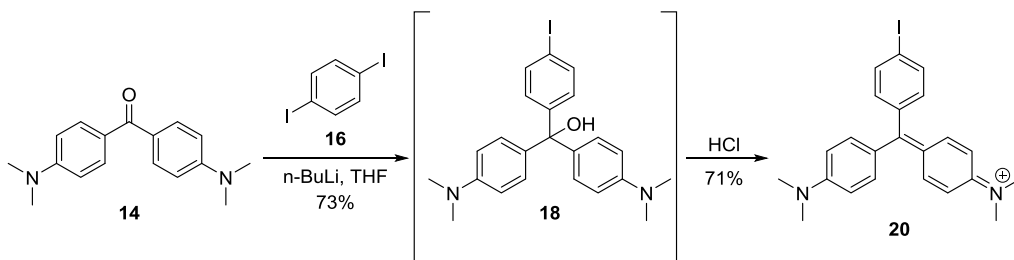
Figure 4: $^1\text{H NMR}$ spectrum for 11.

Figure 5: Mass spectrum for 11.



Synthesis of 20. 2M *n*-BuLi (3.64 mL, 1.2 equivalents) was added dropwise under argon to a solution of 1,4-diiodobenzene **16** (2 g, 0.00607 mol) in freshly dried THF (24.3 mL) at $-78\text{ }^{\circ}\text{C}$. This was allowed to stir for 2 hours at $-78\text{ }^{\circ}\text{C}$. This was followed by dropwise addition of a solution of Michler's ketone **14** (1.62 g, 0.00607 mol) in THF (36.4 mL). The reaction mixture was allowed to reach room temperature and was left to stir for 18 hours. The reaction mixture was quenched by adding water after completion of the reaction (TLC). This was extracted with ethyl acetate and washed with water and brine to obtain 1.6 g (73%) crude of **18**. TLC analysis revealed this compound to be highly unstable and therefore, the crude material was immediately used for the next step. This bis(4-(dimethylamino)phenyl)(4-iodophenyl)methanol **18** (1.6 g, 0.00388 mol) was dissolved in methanol (67.7 mL) and hydrochloric acid (1.2 equivalents) was added to it dropwise and immediately the colour changed to dark green. This was refluxed at $90\text{ }^{\circ}\text{C}$ for 2 hours following which all solvents were evaporated out under reduced pressure and the crude reaction mixture was extracted in 10% methanol in dichloromethane and washed with water and brine. This was purified using 60-200 mesh size silica gel column chromatography and pure compound **20** was eluted in 6% methanol-dichloromethane to obtain 1.23 g (71%) as a dark green solid.

TLC (Silica gel, 40% EtOAc in petroleum ether), R_f (**18**) = 0.6

TLC (Silica gel, 10% methanol in dichloromethane), R_f (**20**) = 0.2

$^1\text{H-NMR}$ (400MHz, CDCl_3): δ 3.43 (s, 12H, $\text{NH}_3 \times 4$), 7.07-7.01 (m, 6H, *a+c*), 7.40-7.38 (d, 4H, *b*, $J = 9.2\text{ Hz}$), 7.93-7.91 (dd, 2H, *d*).

Mass spectrometry: Calculated mass = 455.1

Observed mass = 455.09

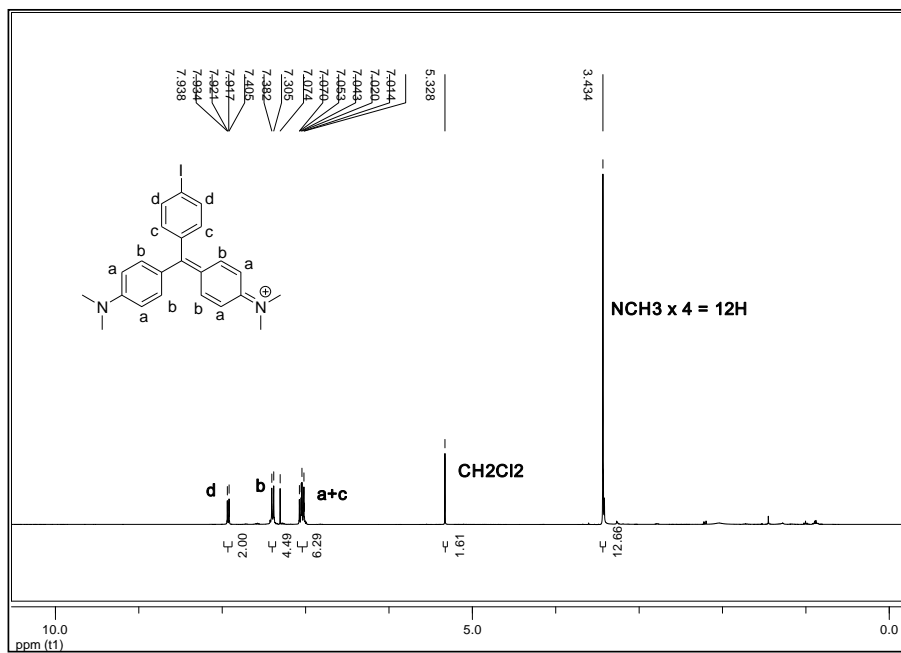


Figure 6: ^1H NMR spectrum of 20.

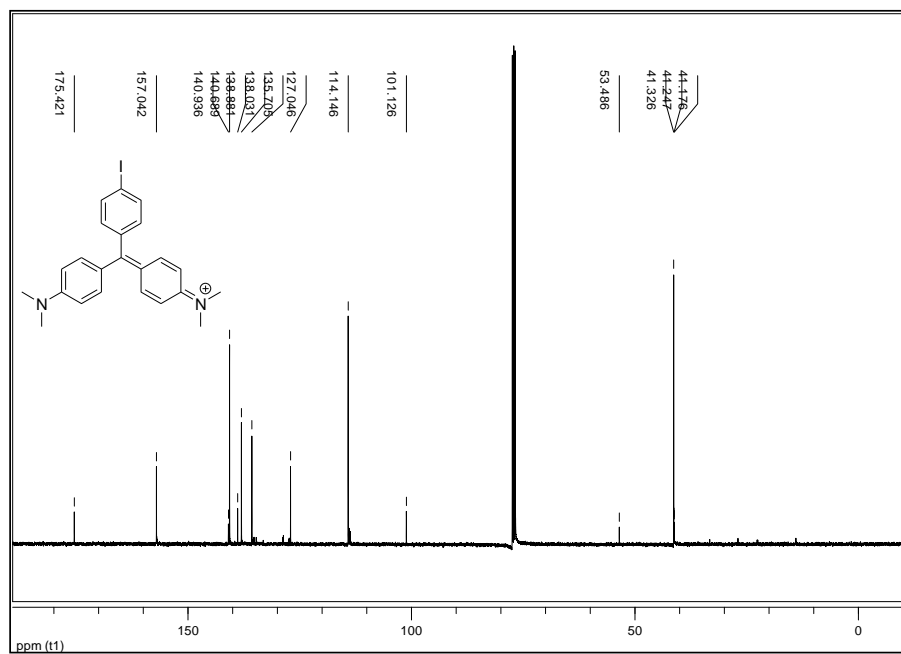


Figure 7: ^{13}C NMR spectrum of 20.

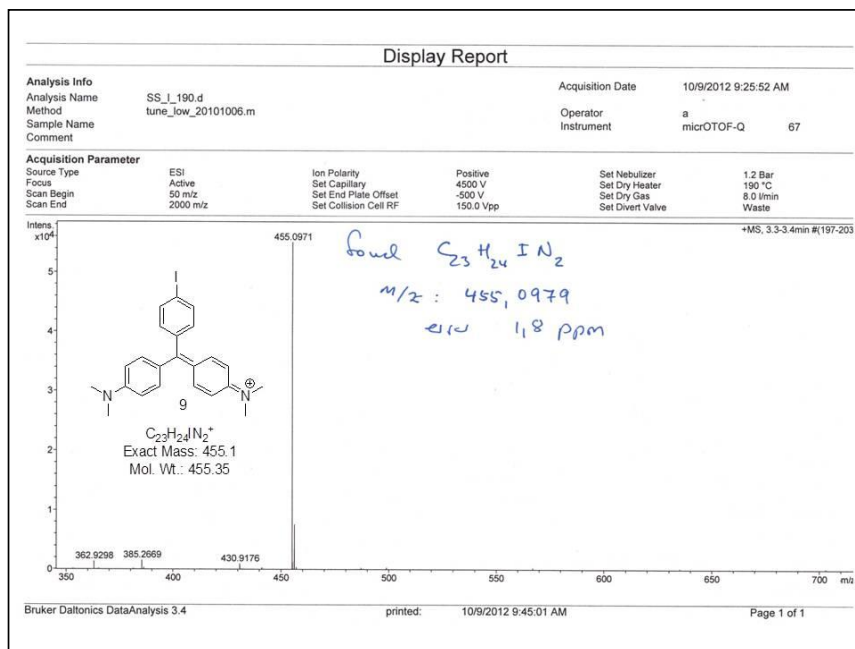
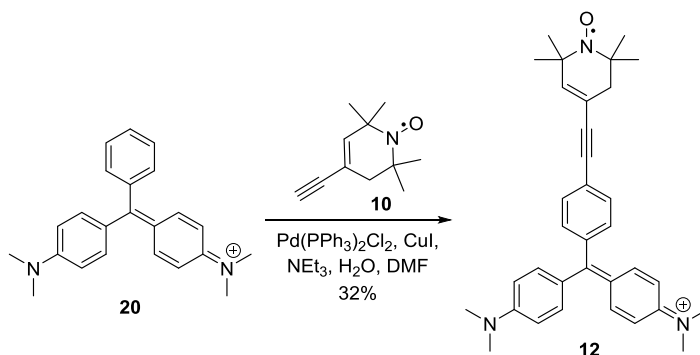


Figure 8: Mass spectrum for 20.



Synthesis of 12. To a stirred solution of **20** (0.050 g, 0.109 mmol) and **10** (0.058 g, 0.329 mmol) in DMF (1 mL), copper iodide (0.002 g, 0.0109 mmol) was added, followed by triethylamine (0.5 mL, 0.274 mmol). Bis(triphenylphosphine)palladium(II) chloride (0.0077 g, 0.0109 mmol) was added after degassing with argon for a 5 minutes and this reaction mixture was heated at 70 °C for 18 h. After completion of the reaction (TLC), the reaction mixture was washed with water and brine and extracted in ethyl acetate. The crude reaction mixture was purified thrice by preparative TLC. The plates were run in 35% ethyl acetate in petroleum ether and eluted in 5% methanol in dichloromethane. 8.5 mg of the final spin probe **12** was obtained in 32% yield.

TLC (Silica gel, 30% ethyl acetate in petroleum ether), R_f (**12**) = 0.5

^1H NMR (400 MHz, Methanol- d_4) δ = 7.34 (d, $J=8.2$, 1H), 7.08 (dd, $J=12.9$, 5.7, 1H), 6.95 (dd, $J=15.5$, 7.9, 1H), 6.60 (d, $J=7.7$, 1H), 3.23 (s, 2H), 3.10 (q, $J=7.3$, 6H), 2.81 (d, $J=2.8$, 3H), 1.21 (t, $J=7.3$, 11H), 0.83 – 0.75 (m, 1H).

Mass spectrometry: Calculated mass = 505.31

Observed mass = 505.309

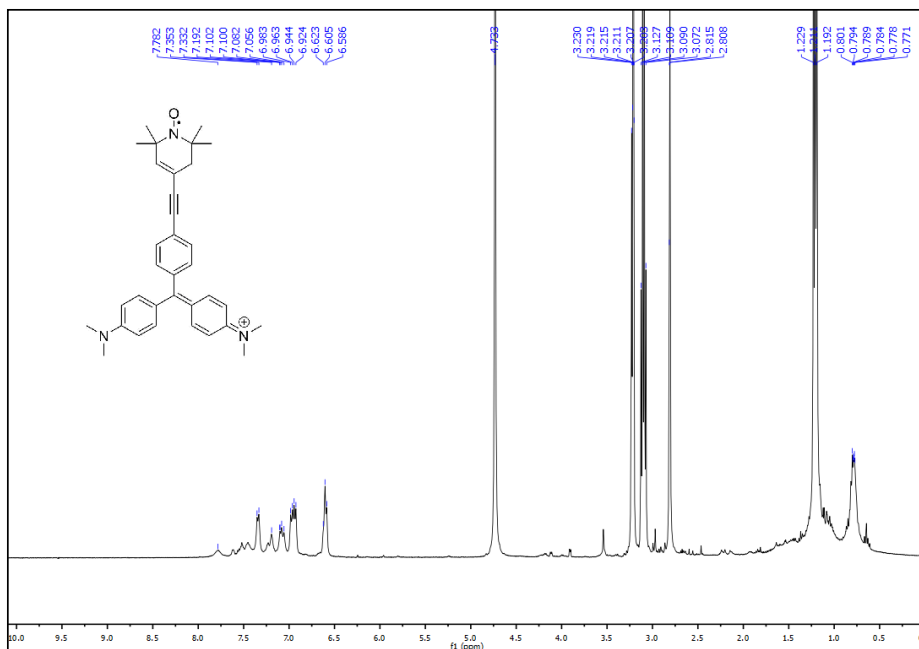
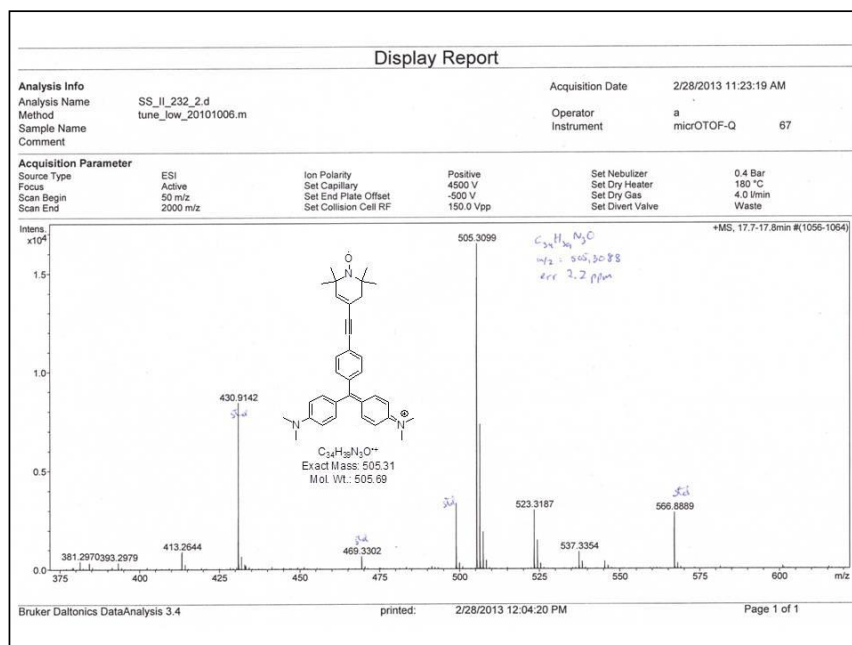
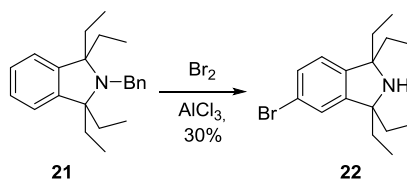
Figure 9: ^1H NMR spectrum of 20.

Figure 10: Mass spectrum for 12



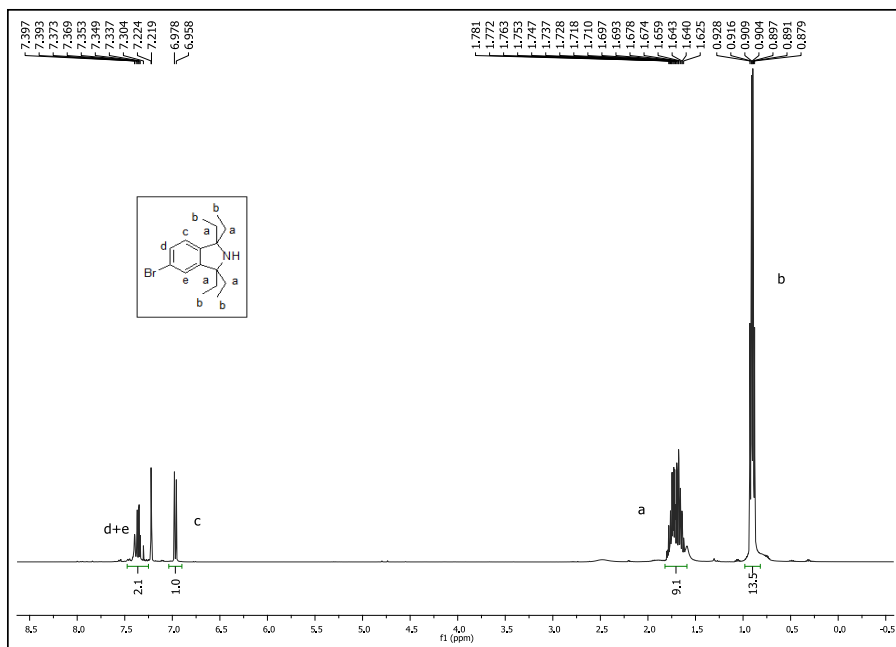
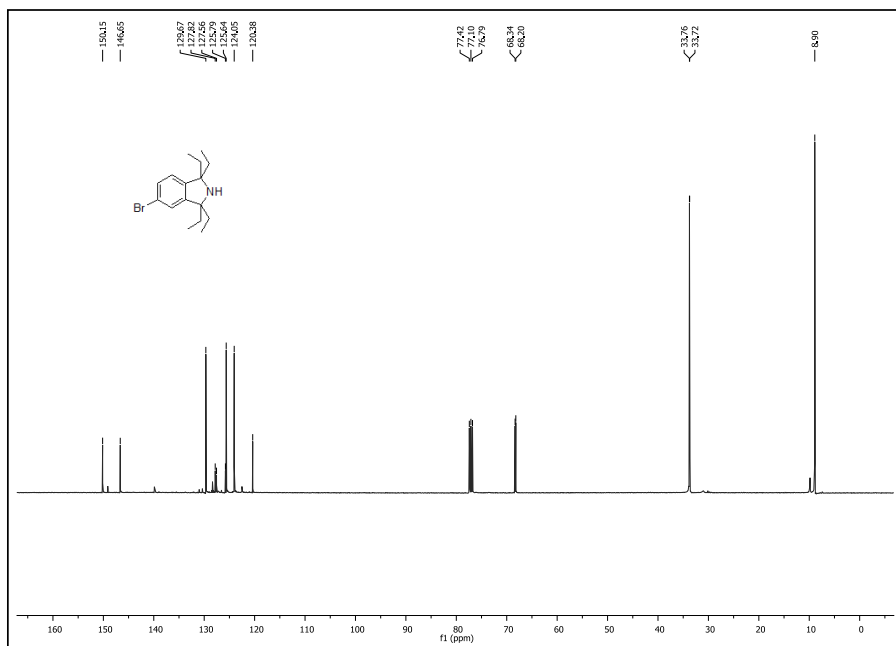
Synthesis of 22. To a solution of 2-benzyl-1,1,3,3-tetraethylisindoline **21** (0.5 g, 0.00155 mol) in freshly dried CH_2Cl_2 (4.7 mL) was added a solution of Br_2 (0.088 mL, 0.00342 mol) in CH_2Cl_2 (3.11 mL) at 0°C . AlCl_3 (0.726 g, 0.00545 mol) was added immediately and this was stirred at 0°C for 1 hour. After completion of the reaction (TLC), the reaction mixture was poured into a glass beaker with 15 g of ice. The aqueous layer was basified with 10N NaOH and extracted in CH_2Cl_2 twice. The combined CH_2Cl_2 layers were washed with brine. The crude reaction mixture was purified by 60-200 silica gel column chromatography. Pure compound was eluted in 1.5% methanol in dichloromethane to obtain 166 mg (30 %) of compound **22**.

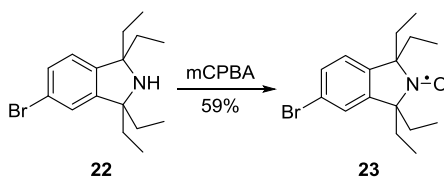
TLC (Silica gel, 10% MeOH in CH_2Cl_2), R_f (compound **22**) = 0.5

$^1\text{H-NMR}$ (400MHz, CDCl_3): δ = 7.36 (ddd, $J=19.7, 13.7, 7.5$, 2H, d+e), 6.97 (d, $J=8.1$, 1H, c), 1.82 – 1.59 (m, 9H, a), 0.98 – 0.82 (m, 14H, b).

$^{13}\text{C NMR}$: δ 150.15, 146.65, 129.67, 127.82, 127.56, 125.79, 125.64, 124.05, 120.38, 77.42, 77.10, 76.79, 68.34, 68.20, 33.76, 33.72, 8.90.

Mass spectrometry: For $\text{C}_{16}\text{H}_{24}\text{BrN}$, calculated mass: 309.11, observed mass: 310.11

Figure 11: ^1H NMR spectrum of compound 22Figure 12: ^{13}C NMR spectrum of compound 22



Synthesis of 23. To a stirred solution of compound **22** (0.50 g, 0.00161 mol) in dry CH_2Cl_2 , mCPBA (0.556g, 0.00322 mol) was added at 0 °C and the reaction mixture was allowed to stir at room temperature overnight. After completion of the reaction (TLC), this was washed with water and extracted in dichloromethane and washed with brine. The crude reaction mixture was purified by 60-200 silica gel column chromatography. Pure compound was eluted in 5% ethyl acetate in petroleum ether to obtain 450 mg (59%) of compound **23**.

TLC (Silica gel, 20% ethyl acetate in petroleum ether), R_f (compound **23**) = 0.8

$^1\text{H-NMR}$ (400MHz, CDCl_3): δ = 7.25 (dd, $J=8.1, 1.5$, 1H), 7.11 (d, $J=1.4$, 1H), 6.84 (d, $J=8.1$, 1H), 1.90 (ddd, $J=14.1, 7.4, 2.2$, 4H), 1.63 (ddd, $J=14.0, 7.3, 2.7$, 4H), 0.75 (dd, $J=16.2, 7.6$, 12H).

$^{13}\text{C NMR}$: δ 151.32, 145.33, 141.82, 129.38, 129.29, 129.15, 128.41, 126.63, 125.32, 120.19, 119.52, 112.21, 77.57, 77.26, 76.94, 72.36, 72.26, 28.65, 28.61, 9.17, 9.12.

Mass spectrometry: For $\text{C}_{16}\text{H}_{23}\text{BrNO}$, calculated mass: 324.1, observed mass: 347 (sodium adduct)

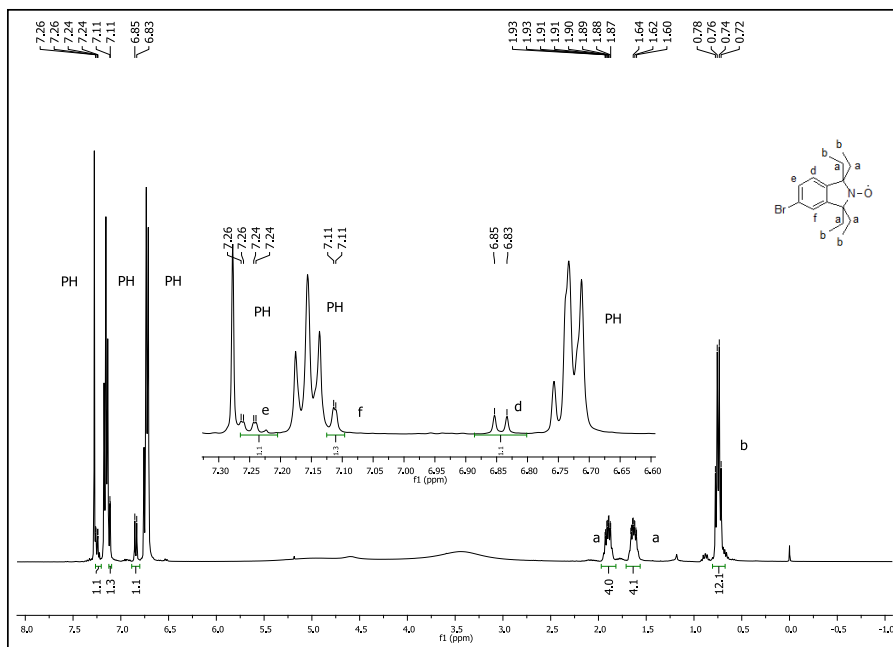


Figure 13: ^1H NMR spectrum of compound **23**. PH stands for phenyl hydrazine.

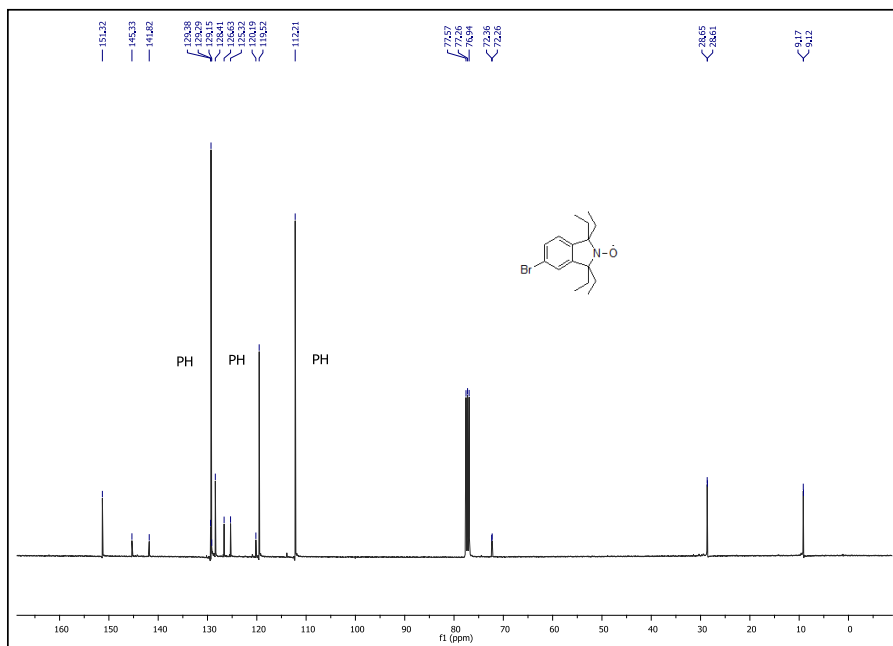
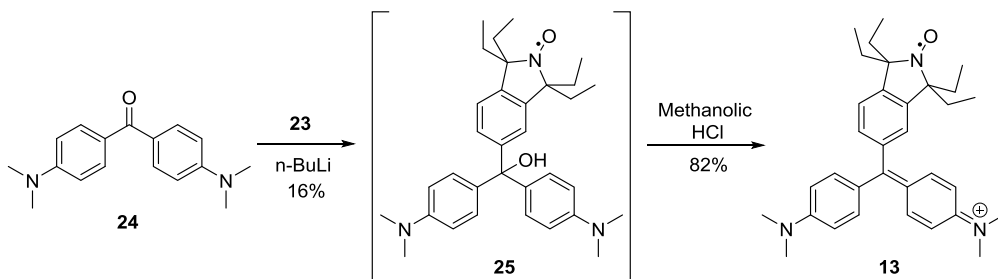


Figure 14: ^{13}C NMR spectrum of compound **23**. PH stands for phenyl hydrazine.



Synthesis of 13. To a solution of compound **23** (0.038 g, 0.000116 mol) in freshly dried THF (0.467 mL), 2M n-BuLi (0.064 mL, 0.000128 mol) was added dropwise under argon at $-78\text{ }^{\circ}\text{C}$. This was stirred for 35 minutes at $-78\text{ }^{\circ}\text{C}$ following which a solution of **24** (0.031 g, 0.000116 mol) in THF (0.701 mL) was added. This was allowed stir at $-78\text{ }^{\circ}\text{C}$ for 30 minutes and then left at room temperature for 18 hours. After completion of the reaction (TLC), the reaction mixture was quenched by adding water at $0\text{ }^{\circ}\text{C}$. The reaction mixture was extracted with ethyl acetate and washed with water and brine to obtain 10 mg (16%) crude of (**25**). TLC analysis revealed this compound to be highly unstable and therefore, the crude material was immediately used for the next step. 1.25M methanolic HCl (0.012 mol, 0.8 equiv.) was added at room temperature to compound **25** (0.010g, 0.0000194 mol) dissolved in methanol (0.291 mL). This was stirred at ambient temperature for 5 minutes, followed which, it was concentrated to dryness and azeotroped with toluene. The crude compound was purified in thrice using preparative TLC which was run in 10% methanol in dichloromethane and eluted in 250 mL 8% methanol in dichloromethane to afford 10 mg (82%) of compound **13**.

TLC (Basified silica gel, 40% EtOAc in petroleum ether), R_f (compound **25**) = 0.4

TLC (Silica gel, 10% methanol in dichloromethane), R_f (**13**) = 0.2

$^1\text{H NMR}$ (400 MHz, Methanol- d_4) δ = 7.39 (s, 2H), 6.98 (s, 2H), 3.26 (s, 6H), 2.82 (s, 1H), 1.94 (s, 1H), 1.20 (d, $J=9.3$, 14H), 0.83 – 0.75 (m, 3H).

Mass spectrometry: For $\text{C}_{33}\text{H}_{43}\text{N}_3\text{O}^{\bullet+}$, calculated mass = 497.34,

Found = 497.3443

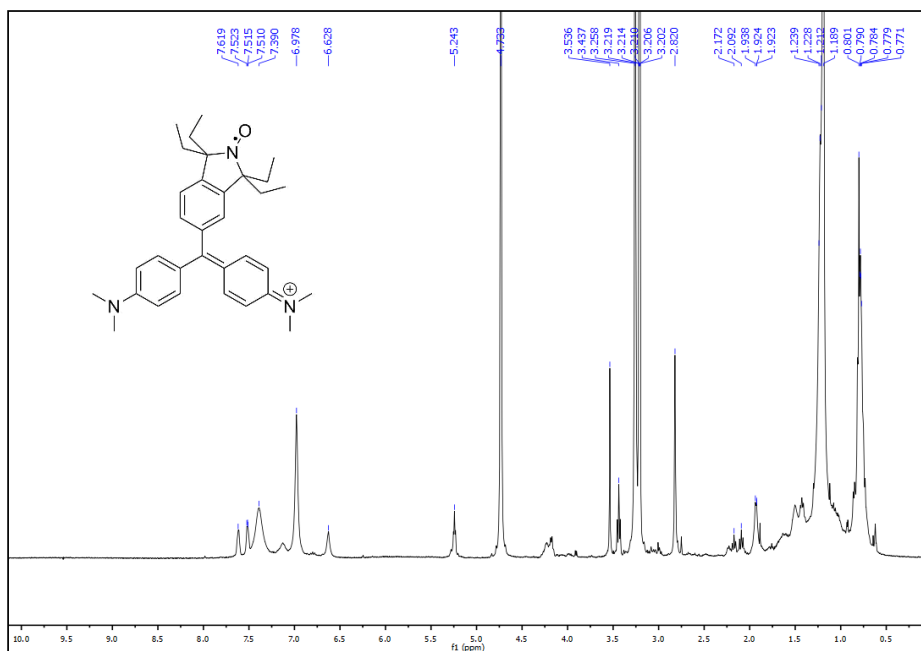


Figure 15: ^1H NMR spectrum of compound 13.

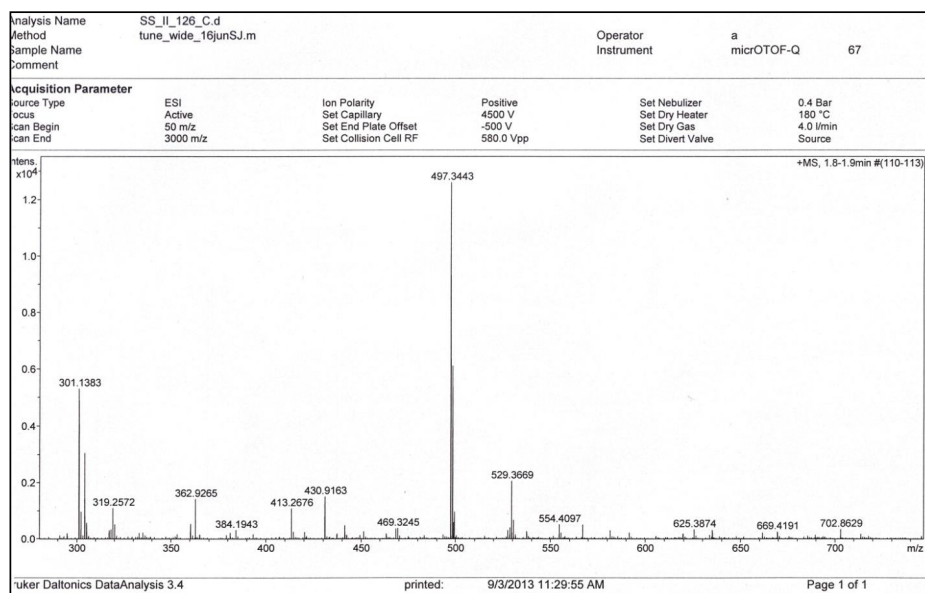
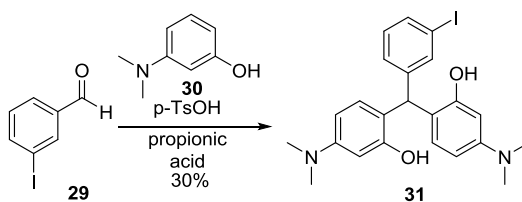


Figure 16: Mass spectrum of spin label 13



Synthesis of 31. 3-Iodobenzaldehyde **29** (0.170 g, 0.732 mmol) was added to a stirred solution of 3-dimethylaminophenol **30** (0.200 g, 1.46 mmol) in propionic acid (1.5 mL). p-TsOH (0.016 g, 0.0975 mmol) was added to it and this was heated for 16 hours at 80 °C., following which, the reaction mixture was diluted with ethyl acetate and water. The aqueous layer was basified using 90% KOH (aq.). The crude product was then extracted in ethyl acetate and washed with water. The organic layer was separated and dried under anhydrous Na₂SO₄, decanted and concentrated under reduced pressure. The crude product was purified by flash column chromatography (60-200 mesh size silica gel). Pure compound was eluted in 40% EtOAc-petroleum ether. Furthermore, the product was concentrated and recrystallized in dichloromethane-petroleum ether to obtain light brown coloured solid product **31** (0.110 g, 30 % yield).

TLC (Silica gel, 70% Ethyl acetate in Petroleum ether), R_f (**31**) = 0.4

¹H NMR (400 MHz, DMSO-d₆) δ = 8.95 (s, 2H), 7.58 – 7.37 (m, 1H), 7.26 (s, 1H), 7.09 – 6.91 (m, 2H), 6.45 (d, J=8.4, 2H), 6.18 (d, J=2.5, 2H), 6.10 (dd, J=8.5, 2.5, 2H), 5.73 (s, 1H), 2.81 (s, 12H).

Mass spectrometry: Mass calculated for C₂₃H₂₅IN₂O₂ = 488.1

Mass observed for C₂₃H₂₅IN₂O₂ = 489.1

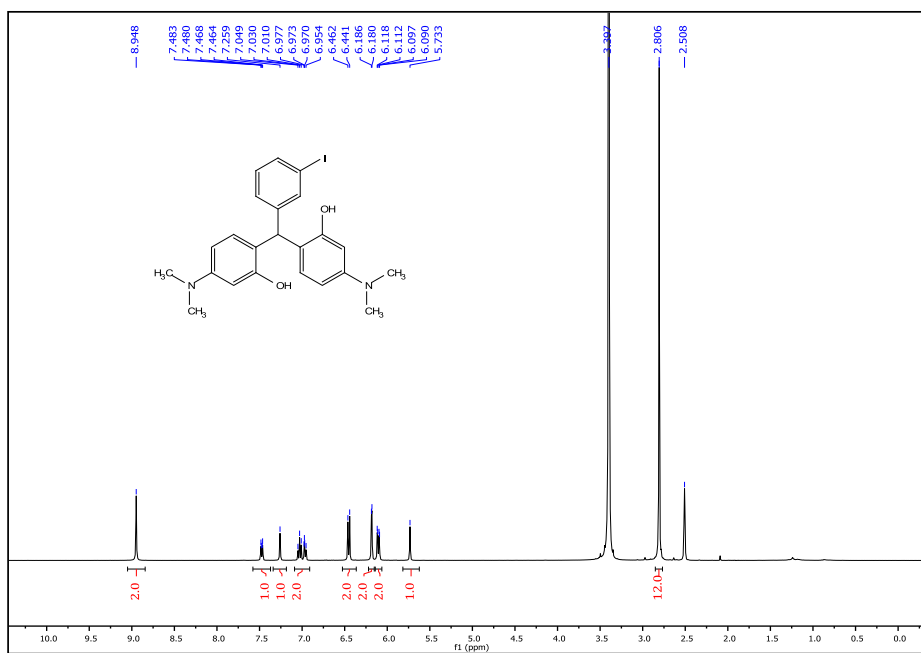


Figure 17: ¹H NMR spectrum of compound 31.

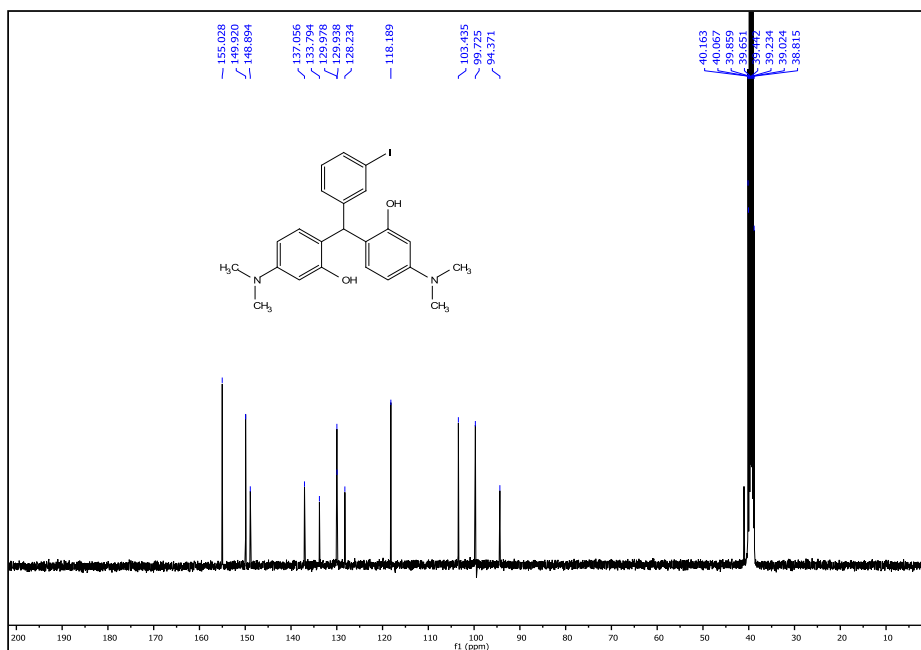
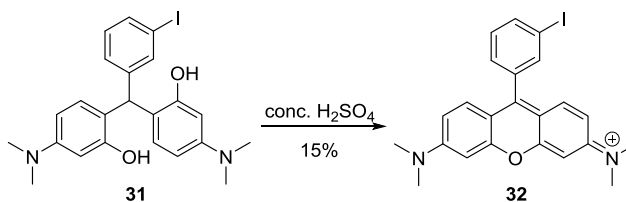


Figure 18: ¹³C NMR spectrum of compound 31.



Synthesis of 32. Concentrated sulphuric acid (6.76 mL, 5mL/mmol) was added at 0°C to compound **31** (0.660 g, 1.35 mmol) in a vial. The vial was sealed and the reaction was stirred at room temperature for 48 hours. The work up was done in dark as the product **32** is sensitive to light. The reaction mixture poured into 100 g of ice. It was then washed with water and extracted in 9% methanol in dichloromethane and dried using Na₂SO₄. The crude product was purified in 60-200 mesh size silica gel column chromatography and the pure fractions were eluted in 8% methanol in dichloromethane. The purified product obtained was concentrated in a rotavapour under dark conditions (covered appropriately with aluminium foil) and dried under high vacuum to obtain a dark purple product. This was further purified twice using preparative TLC under darkness to obtain 99 mg (15%) of compound **32**.

TLC (Silica gel, 10% methanol in dichloromethane), R_f (**32**) = 0.1

¹H NMR (400 MHz, Methanol-d₄) δ = 8.07 (dt, J=7.9, 1.4, 1H), 7.91 (t, J=1.7, 1H), 7.55 (dt, J=7.6, 1.4, 1H), 7.47 (t, J=7.8, 1H), 7.33 (d, J=9.5, 2H), 7.10 (dd, J=9.5, 2.5, 2H), 6.93 (d, J=2.5, 2H), 3.34 (d, J=0.9, 12H).

Mass spectrometry: Calculated for C₂₃H₂₂IN₂O⁺ = 469.0771

Found = 469.0773

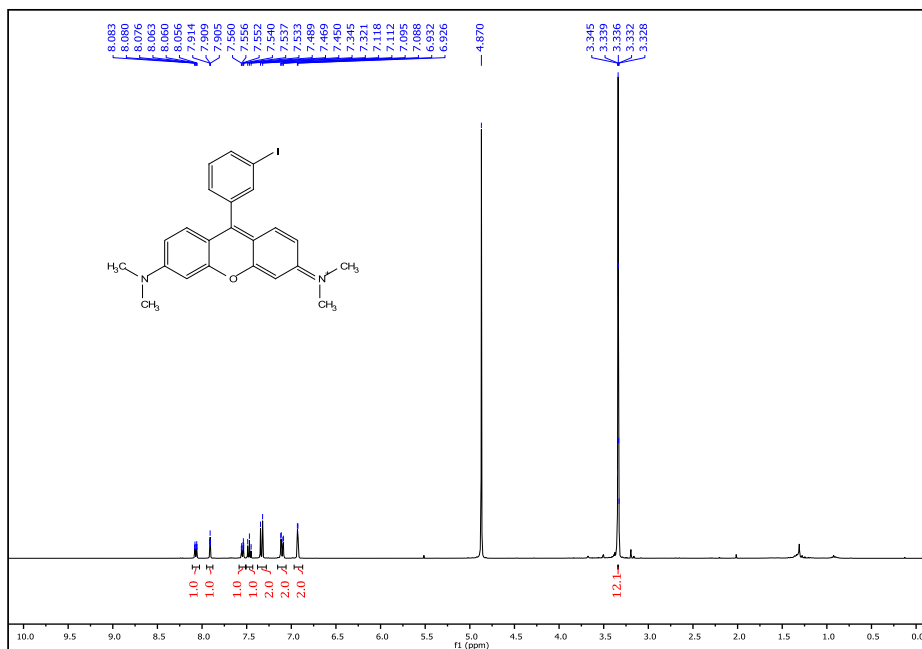


Figure 19. ¹H NMR spectrum of 32.

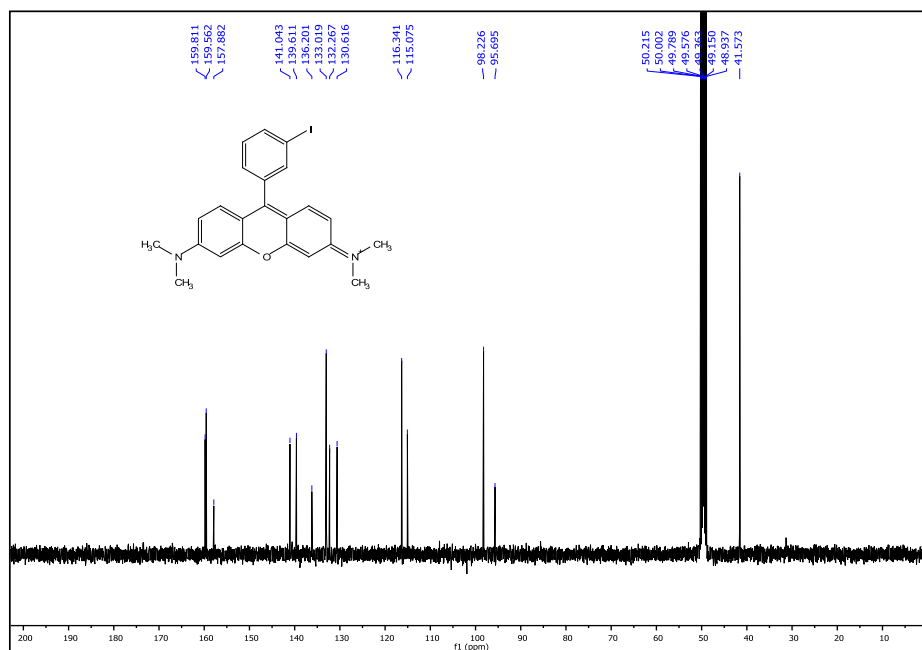
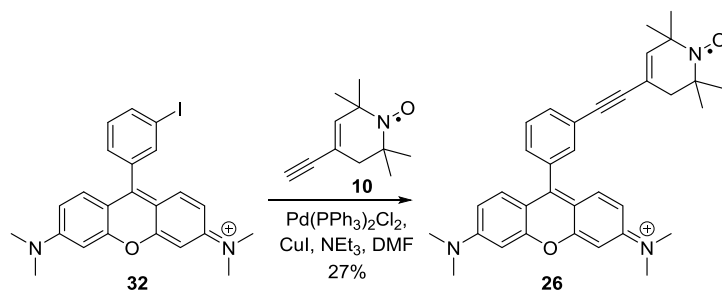


Figure 20: ¹³C NMR spectrum of compound 32.



Compound 26. Iodo- intermediate **32** (0.027 g, 0.0575 mmol) and nitroxide **10** (0.030 g, 0.172 mmol) were dissolved in 0.5 mL of dimethylformamide and 0.5 mL of triethylamine. Copper iodide (0.001 g, 0.00575 mmol) was added and this was degassed with argon for 5 minutes. Under argon, bis(triphenylphosphine)palladium(II) chloride (0.004 g, 0.00575 mmol) was added and this was heated at 60 °C overnight. The crude reaction mixture was passed through a filtration column (60-200 mesh size silica gel) and eluted in 10% methanol in dichloromethane. This was concentrated and extracted in ethyl acetate and washed with excess of water and purified in 60-200 mesh size silica gel column chromatography where the desired spot was obtained in 4% methanol in dichloromethane. To obtain purer compound, preparative TLC was done twice to obtain 8 mg of **26** with 27% yield.

TLC (Silica gel, 20% methanol in dichloromethane), R_f (**26**) = 0.4

$^1\text{H NMR}$ (400 MHz, Methanol- d_4) δ = 7.59 – 7.43 (m, 2H), 3.23 (s, 2H), 2.83 (s, 1H), 1.19 (s, 3H), 0.84 – 0.75 (m, 1H), 0.79 (s, 1H).

Mass spectrometry: Mass calculated for $\text{C}_{34}\text{H}_{37}\text{N}_3\text{O}_2^{+\circ}$ = 519.29

Mass obtained for $\text{C}_{34}\text{H}_{37}\text{N}_3\text{O}_2^{+\circ}$ = 519.2834

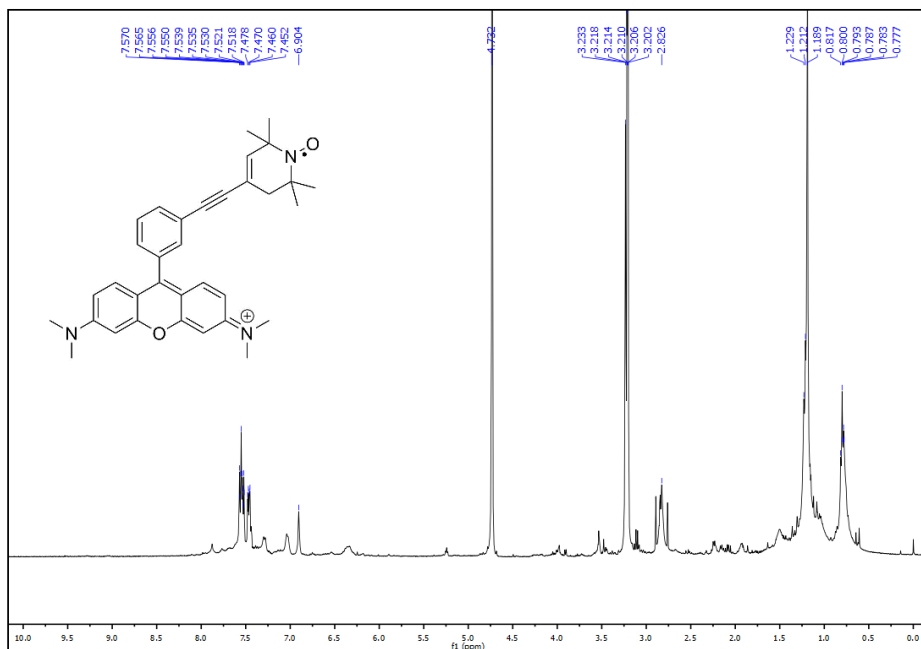
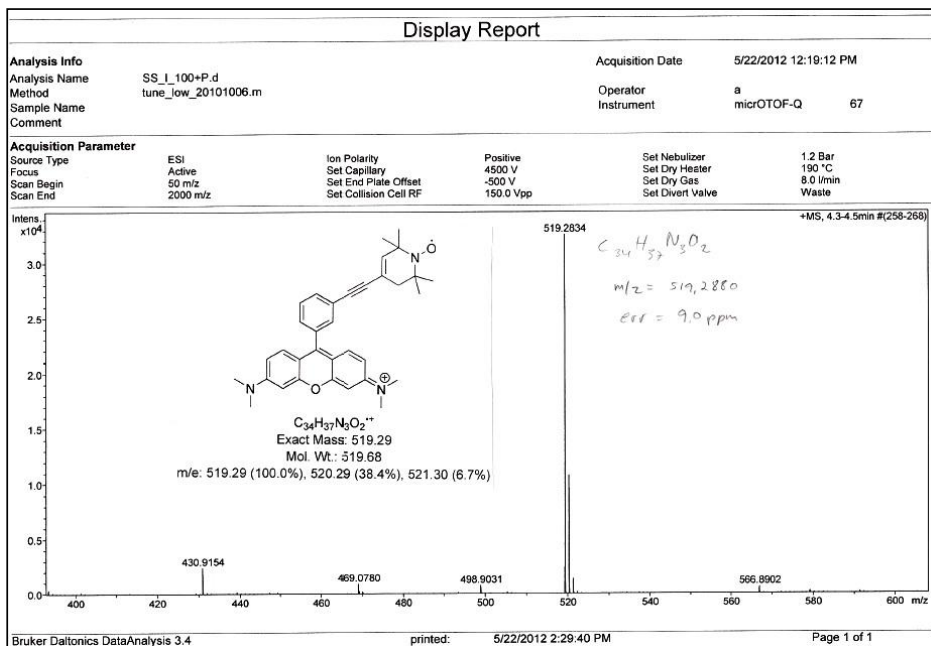
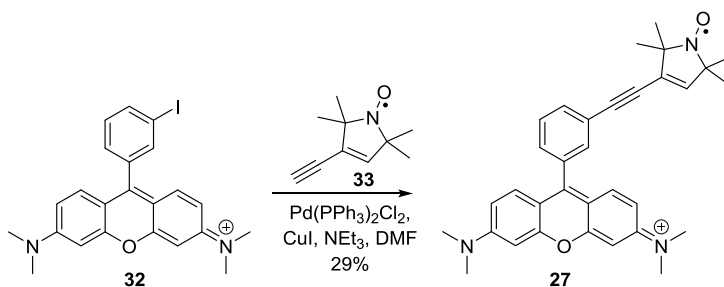
Figure 21. $^1\text{H NMR}$ spectrum of 26.

Figure 22. Mass spectrum of spin probe 26.



Compound 27. Iodo- intermediate **32** (0.030 g, 0.0639 mmol) and nitroxide **33** (0.031 g, 0.191 mmol) were dissolved in 0.5 mL of dimethylformamide and 0.5 mL of triethylamine. Copper iodide (0.0012 g, 0.00639 mmol) was added and this was degassed with argon for 5 minutes. Under argon, bis(triphenylphosphine)palladium(II) chloride (0.0044 g, 0.00639 mmol) was added and this was heated at 60°C overnight. The crude reaction mixture was passed through a filtration column (60-200 mesh size silica gel) and eluted in 10% methanol in dichloromethane. This was concentrated and extracted in ethyl acetate and washed with excess of water and purified in 60-200 mesh size silica gel column chromatography where the desired spot was obtained in 4% methanol in dichloromethane. To obtain purer compound, preparative TLC was done twice to obtain 8.3 mg of **27** with 29% yield.

TLC (Silica gel, 20% methanol in dichloromethane), R_f (**27**) = 0.3

¹H NMR (400 MHz, Methanol-d₄) δ = 7.29 (d, J=8.5, 1H), 7.05 (s, 1H), 6.92 (s, 1H), 3.24 (s, 4H), 1.19 (s, 4H), 0.78 (s, 2H).

Mass spectrometry: Mass calculated for C₃₃H₃₅N₃O₂⁺ = 505.2724

Mass obtained for C₃₃H₃₅N₃O₂⁺ = 505.2710

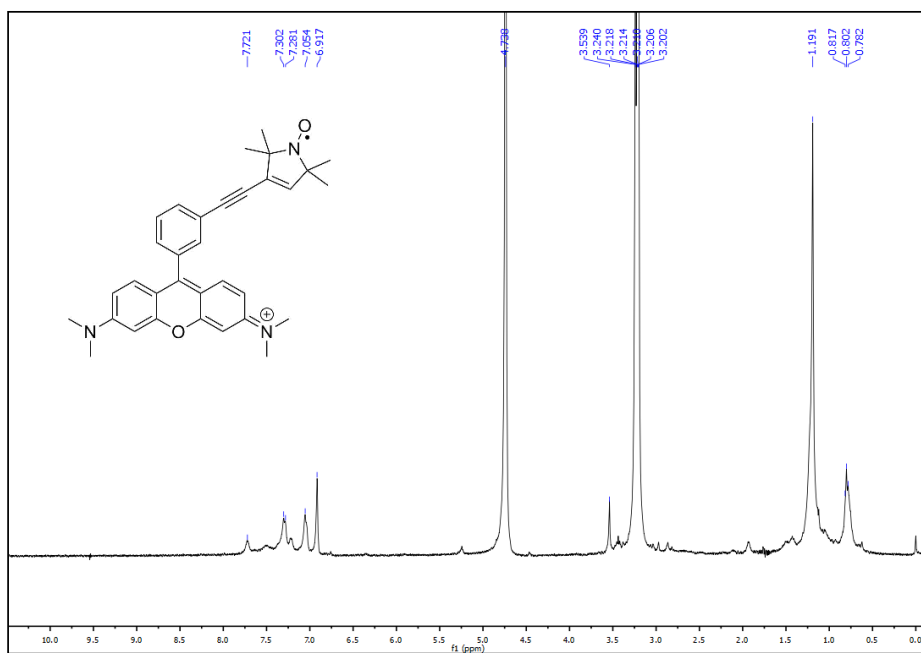
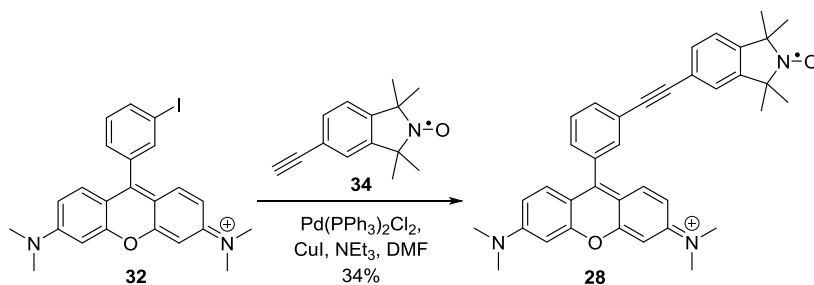


Figure 23. ^1H NMR spectrum of 27.



Compound 28. Iodo- intermediate **32** (0.035 g, 0.0745 mmol) and nitroxide **34** (0.047 g, 0.223 mmol) were dissolved in 0.5 mL of dimethylformamide and 0.5 mL of triethylamine. Copper iodide (0.0014 g, 0.00745 mmol) was added and this was degassed with argon for 5 minutes. Under argon, bis(triphenylphosphine)palladium(II) chloride (0.0052 g, 0.00745 mmol) was added and this was heated at 60°C overnight. The crude reaction mixture was passed through a filtration column (60-200 mesh size silica gel) and eluted in 10% methanol in dichloromethane. This was concentrated and extracted in ethyl acetate and washed with excess of water and purified in 60-200 mesh size silica gel column chromatography where the desired spot was obtained in 6% methanol in dichloromethane. To obtain purer compound, preparative TLC was done twice to obtain 7.8 mg of **28** with 34% yield.

TLC (Silica gel, 20% methanol in dichloromethane), R_f (**28**) = 0.2

^1H NMR (400 MHz, Methanol- d_4) δ = 7.64 (s, 0H), 7.55 (s, 0H), 7.32 (d, $J=8.4$, 1H), 7.05 (d, $J=9.0$, 1H), 6.93 (d, $J=8.5$, 1H), 3.24 (d, $J=2.8$, 8H), 2.05 (d, $J=1.0$, 0H), 1.49 (s, 2H), 1.34 – 1.26 (m, 4H), 1.19 (s, 1H).

Mass spectrometry: Mass calculated for $\text{C}_{37}\text{H}_{37}\text{N}_3\text{O}_2^+$ = 555.2880

Mass obtained for $\text{C}_{37}\text{H}_{37}\text{N}_3\text{O}_2^+$ = 555.2833

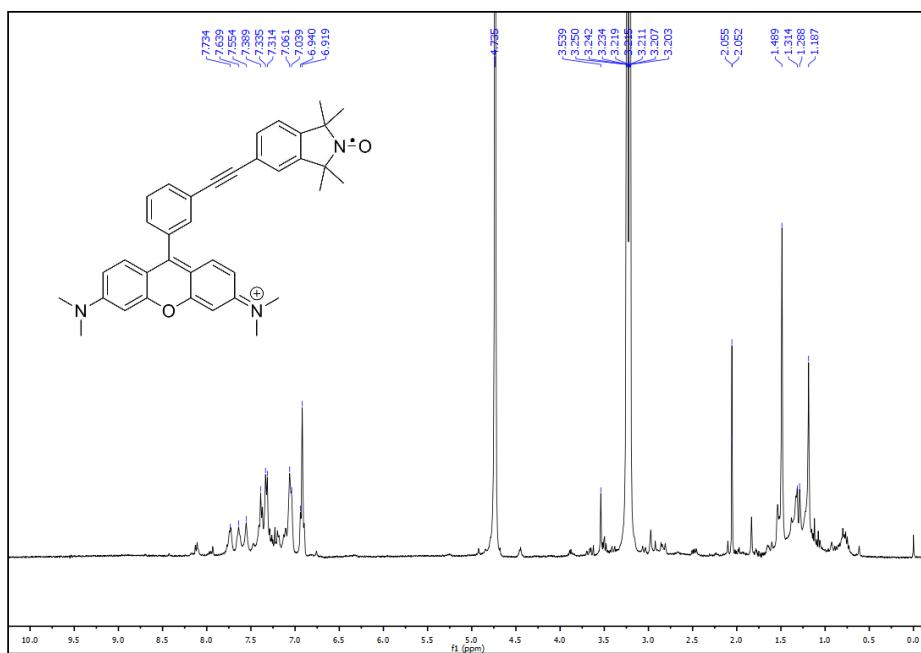


Figure 24. ^1H NMR spectrum of **28**.

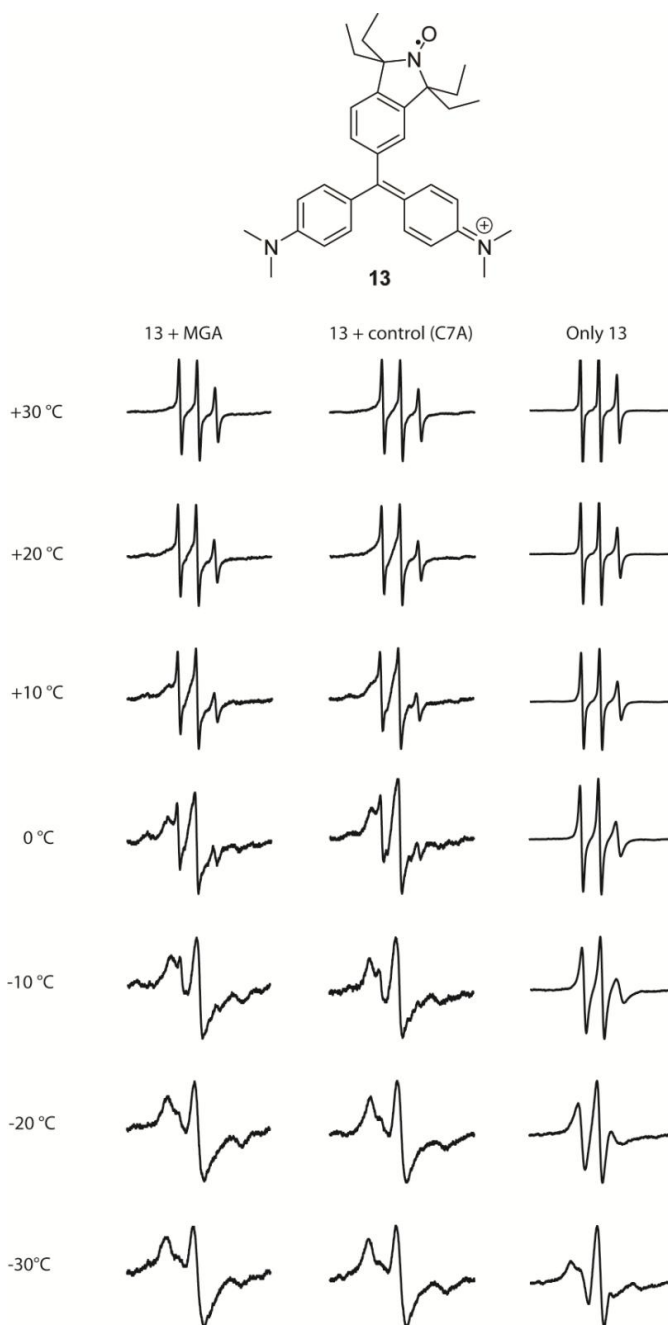


Figure 25: EPR spectra of nitroxide **13** with MG aptamer (left column), with non-binding mutant (middle column) and without any RNA (right column). EPR spectra have been shown as a function of decreased temperature. All spectra were phase corrected and aligned with respect to the central peak. Data recorded in a phosphate buffer [10 mM Na₂HPO₄, 100 mM NaCl, 0.1 mM Na₂EDTA, pH 7.0] dissolved in 2% DMSO, 30% ethylene glycol and 68% sterile water.

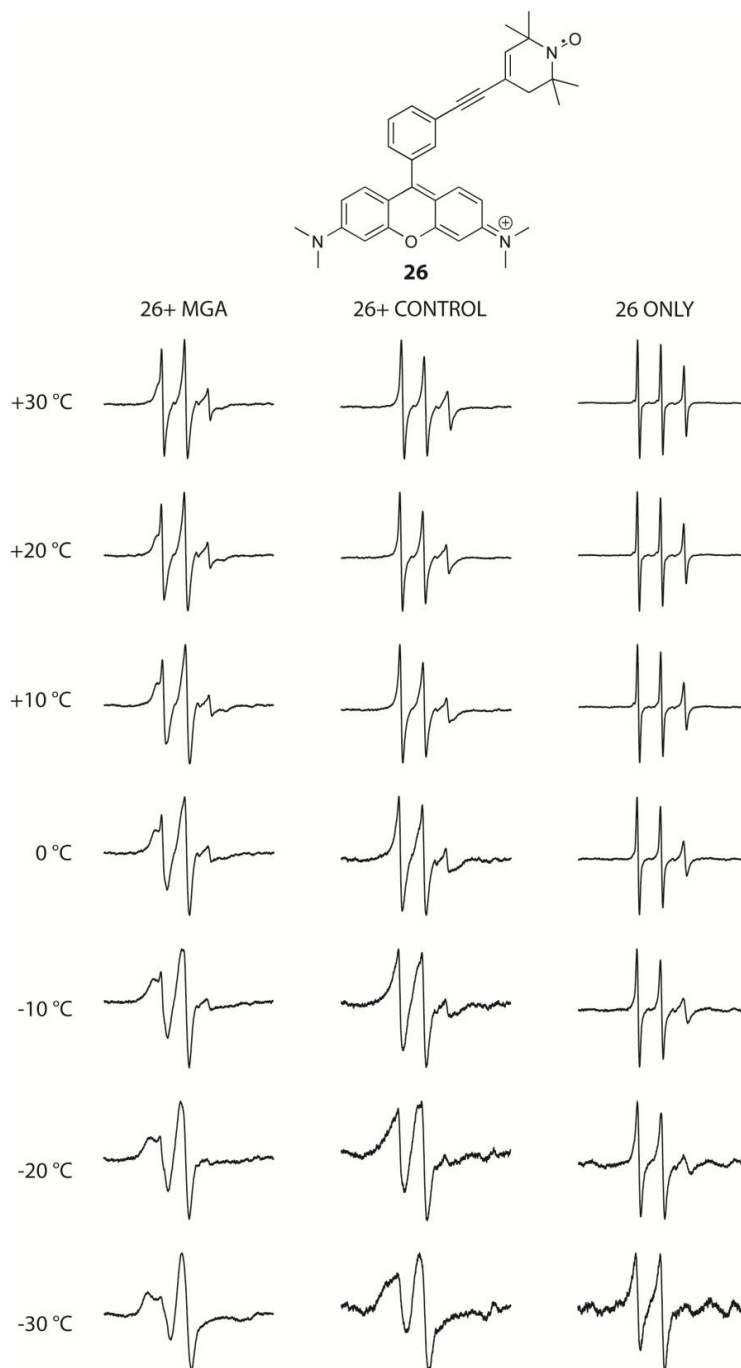


Figure 26: EPR spectra of nitroxide **26** with MG aptamer (left column), with non-binding mutant (middle column) and without any RNA (right column). EPR spectra have been shown as a function of decreased temperature. All spectra were phase corrected and aligned with respect to the central peak. Data recorded in a phosphate buffer [10 mM Na₂HPO₄, 100 mM NaCl, 0.1 mM Na₂EDTA, pH 7.0] dissolved in 2% DMSO, 30% ethylene glycol and 68% sterile water.

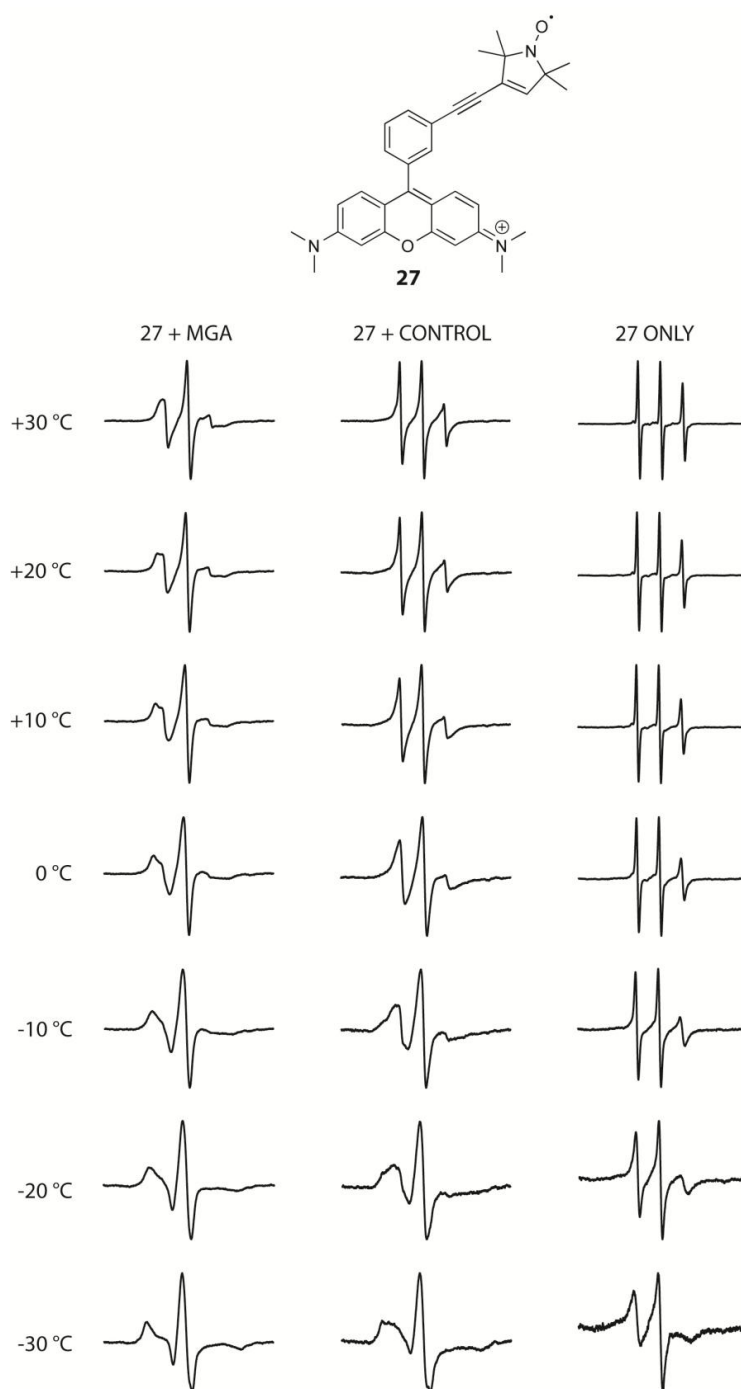


Figure 27: EPR spectra of nitroxide **28** with MG aptamer (left column), with non-binding mutant (middle column) and without any RNA (right column). EPR spectra have been shown as a function of decreased temperature. All spectra were phase corrected and aligned with respect to the central peak. Data recorded in a phosphate buffer [10 mM Na₂HPO₄, 100 mM NaCl, 0.1 mM Na₂EDTA, pH 7.0] dissolved in 2% DMSO, 30% ethylene glycol and 68% sterile water.

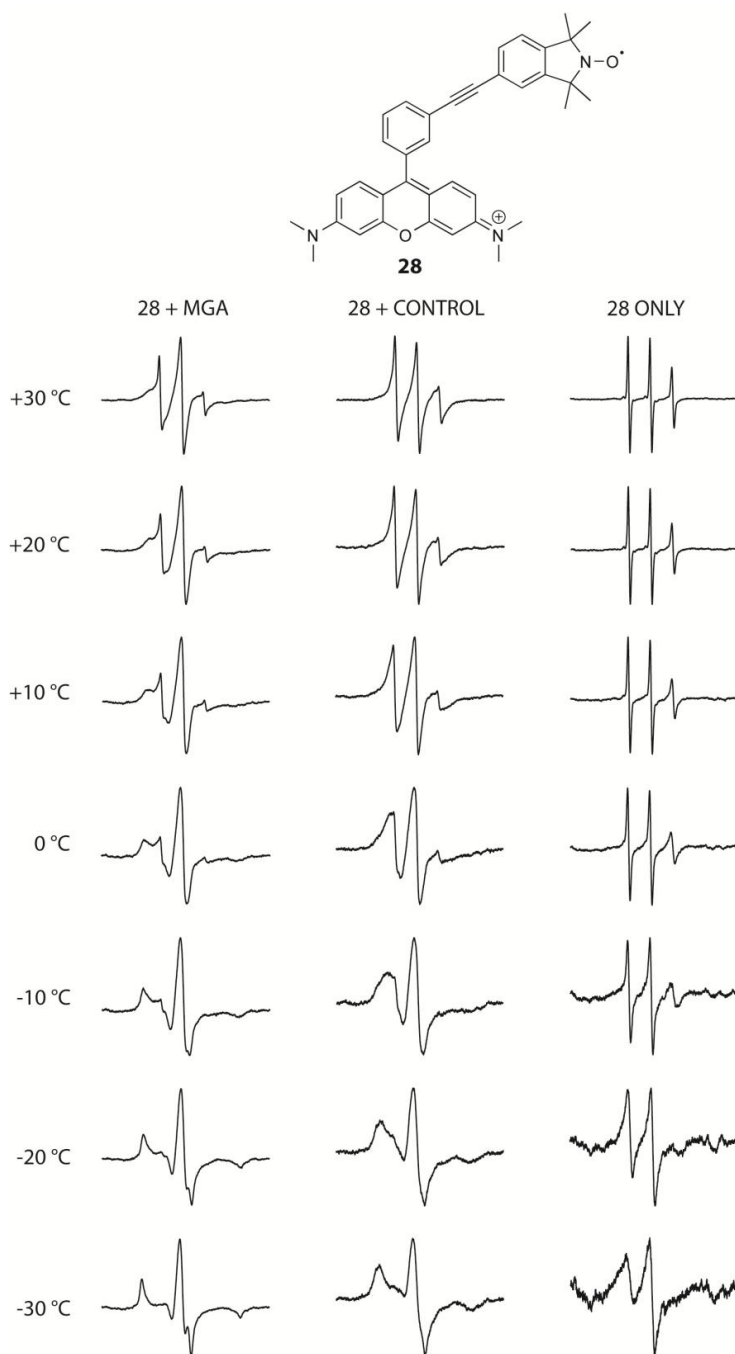


Figure 28: EPR spectra of nitroxide **28** with MG aptamer (left column), with non-binding mutant (middle column) and without any RNA (right column). EPR spectra have been shown as a function of decreased temperature. All spectra were phase corrected and aligned with respect to the central peak. Data recorded in a phosphate buffer [10 mM Na₂HPO₄, 100 mM NaCl, 0.1 mM Na₂EDTA, pH 7.0] dissolved in 2% DMSO, 30% ethylene glycol and 68% sterile water.

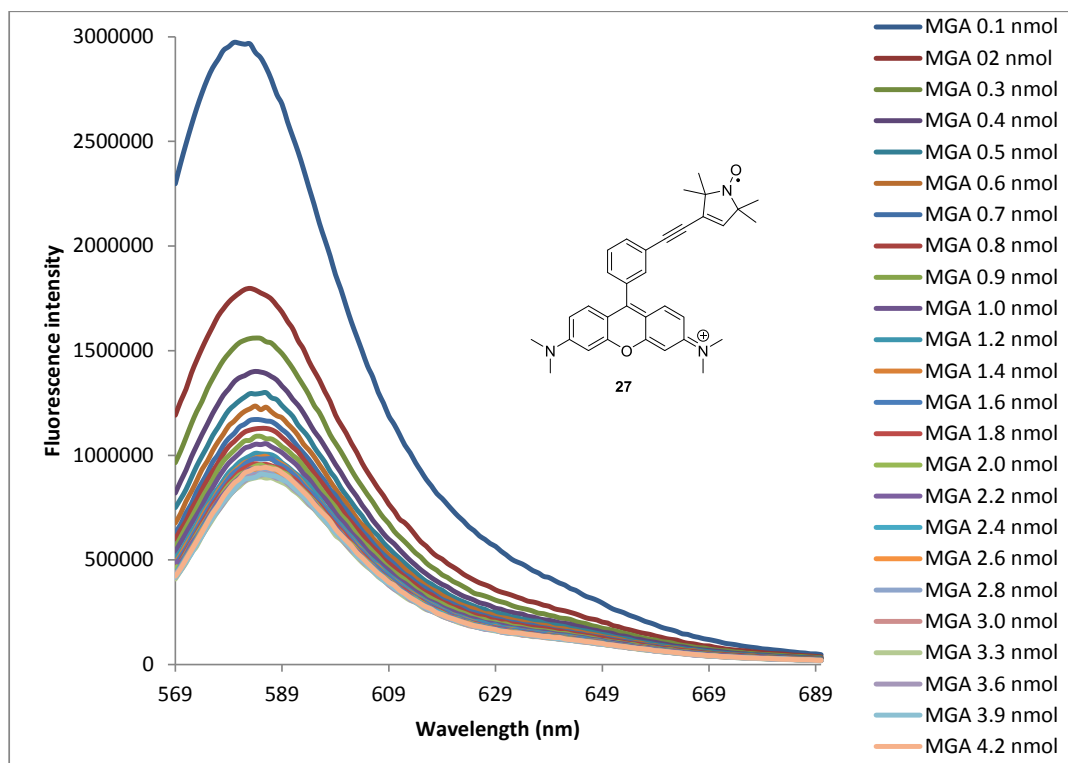


Figure 29: Fluorescence titration spectra of binding of nitroxide **27** (0.45 nmol in 3000 μ L) with increasing amounts of MGA aptamer. Data recorded in a phosphate buffer (10 mM Na_2HPO_4 , 100 mM NaCl, 0.1 mM Na_2EDTA , pH 7.0).

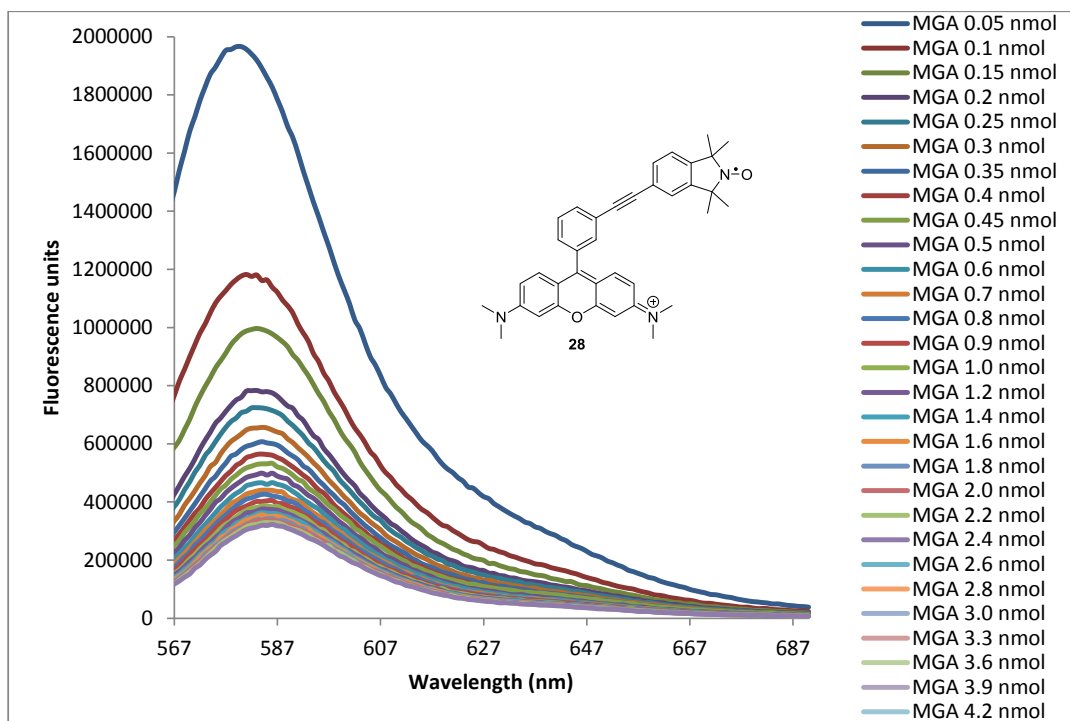


Figure 30: Fluorescence titration spectra of binding of nitroside **28** (0.45 nmol in 3000 μ L) with increasing amounts of MG aptamer. Data recorded in a phosphate buffer (10 mM Na_2HPO_4 , 100 mM NaCl, 0.1 mM Na_2EDTA , pH 7.0).

